Development of an RFID approach to monitoring bedload sediment transport and a field case study

by

Christina Jane Bright

A thesis
presented to the University of Waterloo
in fulfillment of the
thesis requirement for the degree of
Master of Applied Science
in
Civil Engineering

Waterloo, Ontario, Canada, 2014

I hereby declare that I am the sole author of this thesis. This is a true copy of the thesis, including any required final revisions, as accepted by my examiners.

I understand that my thesis may be made electronically available to the public.

ABSTRACT

Bedload transport studies are essential in the understanding of river forms, functions and processes. These studies have been done using various methods over the past century. In recent years Radio Frequency Identification Technology (RFID) has become popular with researchers to track bedload particles. However, no standard operating procedures are used in the implementation of this technology. Methods used for tagging, seeding and tracking RFID tracers (RFID transponders inserted into a bedload particle) can introduce variability in their detection.

In this study, RFID tracers were used to study four sites in Laurel Creek in Waterloo, Ontario. Two hundred RFID tracers were seeded in each of the four sites. Following three major storm events, the tracers were tracked with an antenna and their locations surveyed. The tracers were able to be detected to a precision of 1 m as a transponder used can be detected at a maximum of this distance.

Practical tracking in the field highlighted the need for the understanding of how precisely the tag location can be identified. Laboratory experiments were designed and carried out to determine the effects of factors (tracer orientation, antenna orientation, tracer size, clustering of multiple tracers, burial depth, saturation and submergence of the soil matrix) that possibly confounded detection. Of these factors, tracer orientation, clustering and burial depths were determined to be the ones that affected detection distances the most. A transponder in a vertical orientation was found to have as much as 40% larger range of detection than a transponder in a horizontal orientation (i.e., they could be detected from further away). Additionally, "skip zones" were identified during laboratory and field experiments. These are zones of gaps in the electromagnetic field of the transponder that occur directly over the transponder. These zones were experimentally determined to extend to approximately 10 cm on each side of the transponder. Therefore, by identifying the skip zones, the tracers can be located to a precision of 10 cm; this is an order of magnitude smaller than the published detection limit of the transponder. The precision of detection can also be improved by the reduction of the effects of confounding factors. However, the improvement in the precision of detection is a tradeoff with the ease of detection. A tagging, seeding and tracking protocol is recommended to counter the effects of confounding factors.

ACKNOWLEDGEMENTS

I would like to thank my supervisor Dr. Bruce MacVicar for providing me with guidance and support through the process of research work and writing the thesis. This work was supported by NSERC IPS in partnership with Water's Edge Environmental Solutions Team Ltd. Thanks Ed, for employing me, and also for supporting me through the IPS grant.

Thanks to the research group for all those fun filled fluvial and non-fluvial discussions and for support with lab and field work. Thanks especially to Vernon Bevan, and Scott Dilling who spent, what then seemed like, endless hours in the lab with me. My special shout-outs go to Michael McIsaac and Johnathan Nault for being excellent co-op and URA students.

There is also a host of other undergraduate and fellow graduate students that helped me out with field and lab work. Without you (Jarryd Buck, Amr Farag, Jessica Friesen, Nasim Hosseini, John Hufnagel, Anthony Lui, Cailey McCutcheon, Lana Obach, Wayne Park, Joe Simonji, and Mark Spanjers), this project would have been very difficult! Thanks also to my friends, Jane Ho, Jeffrey Ng, and Agatha Wong who spent some quality field time with me!

Thanks to Terry Ridgway for helping out with the various field set ups and with the sandbox construction. Thanks to my thesis reviewers (Dr. Bill Annable and Dr. Jeff Casello) whose comments have helped me to make this document a better one.

Thanks to Margot Chapuis for the pasta night. It was so much fun and much required. Talking and supping with you always lifts my spirit!

Mark Spanjers, thanks for pebble counting with me on the hottest day of 2011, for proof reading my thesis with me and best of all, for the beautiful thesis completion gift!

Mummy and Papa, thanks for believing in me, for praying for me and supporting me.

Thank you to all my friends who kept me motivated through the thesis writing.

TABLE OF CONTENTS

LIST OF FIGURES

LIST OF TABLES

1 INTRODUCTION

"Contemplating the lace-like fabric of streams outspread over the mountains we are reminded that everything is flowing." – John Muir in My First Summer in the Sierra (1911)

From time immemorial, rivers have played an important role in the development of human civilization. The earliest societies were formed along river floodplains so that the resources of the rivers could be harnessed. Building on floodplains forced these societies to manage and engineer the rivers. As populations grew and the demand for land increased, so did the management and engineering of rivers.

Natural rivers in unaltered watersheds are usually in the state of "quasi-equilibrium" and are "graded". Davis (1902) describes graded rivers as mature rivers in a condition of balance between erosion and deposition. Rivers in quasi-equilibrium exhibit continuity from their headwaters to their mouths and have a hydraulic relationship between stream power (rate at which a stream dissipates its energy on bed and banks) and sediment load (Langbein & Leopold, 1964). Leopold and Maddock (1953) suggest that the interactions between the variables of slope, channel velocity, depth and width, bed roughness and bed size particles enable a channel to achieve the state of quasi-equilibrium. At this state there is a long-term continuity and a dynamic balance between water and sediment loads. Natural rivers maintain this state of dynamic balance, readjusting their morphology with time to mitigate natural changes that occur within the watershed. However, when engineering works alter these river systems, they can potentially cause channel instability and negatively impact the riverine environment (Hey, 1996). The negative impacts are a result of changes in hydrologic, sediment and morphological variables which largely depend on water and sediment made available from upstream sources. Perturbations to the natural rivers in the state of quasi-equilibrium through means of disturbances to the water (flood or drought conditions) and sediment supply (causing erosion or aggradation) caused by deforestation, dam building, gravel mining, and climate change not only affect the local abiotic conditions, but also the riverine ecology and the rich life that is linked to the river corridor.

River engineering and other anthropogenic changes to the river channel and watersheds have caused urban streams to respond with channel incision, widening and even narrowing due to aggradation (Annable, Watson, & Thompson, 2012; Booth, 1990; Hammer, 1972; Surian & Rinaldi, 2004). These changes can cause a destabilization of the stream network, and hence increase the risk posed to urban infrastructure situated on or in proximity to the watercourses. However, these urban streams do have the ability to adjust themselves to conditions of quasi-equilibrium over long periods of time.

In a review of sedimentation engineering, MacArthur et al (2007) noted that “human settlements have increasingly occupied areas more vulnerable to erosion and sedimentation, thus aggravating runoff, soil erosion and gullying [sharp erosion on hillsides]”. In order to minimize the effects of human activities such as construction of dams and reservoirs, channelization of rivers, and landuse developments on the rivers, efforts have been directed to the application of scientific principles to the development of environmentally sensitive approaches for managing rivers (Petts & Calow, 1996). River restoration approaches are taken to manage rivers and encourage them on the path to quasi-equilibrium. Management of rivers also includes the management and monitoring of sedimentation processes such as erosion, transport and deposition. The management of urban rivers poses a challenge to river practitioners due to the lack of clear understanding of the processes that govern channel changes and sediment transport.

Sediment in rivers can be primarily divided into two categories: wash load and bed material load. The wash load is a finer material (fine silts and clay) that remains in suspension during floods. Bed material load represents the particulate load present in the channel bed and banks (Dingman, 2009). The bed material sediment load includes suspended sediment and bedload sediment. According to one definition, bedload is the portion of total sediment load that travels within a few grain diameters above the channel bed (Einstein, 1950).

Acquiring sediment data is essential for the management of river systems and the study of sediment transport in river systems. Sediment load data, when coupled with erosion studies, enables one to quantify upstream erosion, study the effectiveness of channel restoration measures used and investigate the stability of channel bed and banks. Since the morphology of a river is determined by the hydraulic conditions in a river channel and the sediment in the channel bed and banks, it becomes imperative to study bedload sediment to comprehend the changing morphology of a river in response to perturbations such as the changing land-use of a catchment, changing flow regimes due to climate change and the change in upstream sediment supply. From an ecological perspective, it is essential to study sediment transport as it enables researchers to develop their understanding of the interplay of the abiotic (sediment, channel form, etc) and the biotic factors (aquatic organisms) in a riverine system.

Bedload sediment transport is known to be an intermittent process with high variability in time and space. Given the variability, obtaining reliable and representative bedload transport data through measurement using sampling devices can be challenging. The lack of a sampling scheme that can accurately quantify bedload transport makes teasing out long term and large scale changes from the available data very difficult.

In addition to sampling devices, tracers are used to study and quantify bedload transport. The location of the tracers used are recorded prior to and after a large flow event. The intrinsic properties of the tracers and the change in the location of the tracers with respect to the surrounding channel morphology can provide valuable information concerning tracer path lengths, the flow events required to the trigger movement and the effect of the tracer properties on path lengths. However, most tracers (painted tracers and magnetically tagged tracers) have low recovery rates due to their burial in the channel bed (Nichols, 2004). Radio transmitter tracers are expensive and need an internal power source which limits the maximum size of the tagged particle and the duration of the experiment due to the battery's lifetime (Lamarre, MacVicar, & Roy, 2005).

In this thesis, a more recent tracer method of Radio Frequency Identification (RFID) tracking is studied and employed in an urban stream (Laurel Creek in Waterloo, ON). RFID tracers or Passive Integrated Transponder (PIT) tags have a much higher recovery rate than many other tracers currently used. They are relatively inexpensive and have a long operational life due to the absence of an internal power source. Each tag can be assigned a unique identification code. The size of the particle tagged is only limited by the size of the RFID tag. In spite of the obvious advantages of RFID tracers, the technology is limited in its use in that it only enables the tracker to detect the location of the tracer particle within 1 m. This large range of detection is due to the confounding effects of factors such as orientation of the antenna used to identify the tag, orientation of the tag itself, depth of burial, submergence of the tag, and its proximity to other tags. Since the earliest use of this technology by Nichols (2004), there have been many researchers employing RFID tracking. However, no standard operating procedures for tagging and tracking have been developed.

The objectives of the thesis are to 1) use RFID tags to track sediment movement in an urban stream (Laurel Creek in Waterloo, Ontario); 2) identify and quantify confounding factors when identifying the location of tracer stones; and 3) recommend a standard tagging procedure to improve the precision of tracer detection. The second chapter is a literature review on sediment transport research and on the site selected for this study: Laurel Creek in Waterloo, Ontario. The methodologies used in the field and the laboratory are described in the third chapter. The fourth and fifth chapters are presentations of field and laboratory results, respectively. The sixth chapter is a discussion of the results. Finally, the thesis concludes with remarks and recommendations for further improvement of the methodologies.

2 BACKGROUND

In this section, the general concepts of bedload sediment transport are outlined, various bed-load monitoring practices, particularly the more recent RFID technology are discussed, and the fluvial geomorphological effects of urbanization are examined.

2.1 Sediment transport

Sediment transport occurs when fluvial forces exerted by water flowing over a bed of sediment causes the sediment to become entrained in the water. Local flow conditions, composition of bed material and composition and quantity of sediment supplied from local and upstream sources contribute to sediment transport at any point along the stream (Hassan & Woodsmith, 2004). The process of sediment transport is remarkably complex as motion of the particles not only depends on the magnitude of the fluvial process but also on the intrinsic characteristics of the sediment. These factors coupled with the uneven bed morphology, turbulence in the water, interaction of the sediment particles, and the amount of sediment and water available contribute to the complexity and non-linearity of the process. The interplaying of multiple factors also results in spatial and temporal variability in sediment transport in uncontrolled water systems (i.e., in rivers as opposed to flumes). Transport rate of sediments can be very sensitive beyond an initial threshold condition. Despite the complex nature of sediment transport, it has been studied by various researchers for over a century, and progress has been made in the field and some consensus established in the theory of the initiation of particle motion.

2.1.1 Incipient Motion

Incipient motion can be defined as the threshold condition between erosion and sedimentation of a single particle. For incipient motion to occur the hydrodynamic moment of forces acting on a particle must balance the resisting moment of force contrib uted to by the particle weight (Julien, 1995). Traditionally, Shields' theory has been used to identify threshold conditions for particle movement. Numerous flume experiments were conducted by Shields (Shields, 1936) to examine incipient motion in sub-angular to very angular sediments of densities varying from 1060 to 4300 kg/m^3. Shields expressed incipient grain motion as a dimensionless ratio of the bed-shear stress (τ_0) to submerged grain weight per unit area

$$\tau_* = \frac{\tau_0}{(\rho_s - \rho)gD}$$

where ρ_s is sediment density; ρ is the density of water; D is characteristic grain size; and τ_* is the dimensionless bed-shear stress known as Shields parameter. Bed-shear stress τ_0 can be defined by the DuBoys' equation ((DuBoys, 1879) *in* Dingman (2009))*:*

$$\tau_0 = \gamma_w RS$$

where γ_w is the unit weight of water; R is the hydraulic radius; and S is the slope of the channel. Shields used dimensional analysis and fluid mechanics to deduce that the Shields parameter τ_* is a function of particle Reynolds number Re_*. Shields regime diagram is shown in Figure 1. It illustrates the relationship between two dimensionless parameters: Shields Stress τ_* and Reynolds Number Re_*

$$Re_* = \frac{u_* d_s}{v_m}$$

where u_* is shear velocity; d_s is the median grain size of the surface substrate; and v_m is the kinematic viscosity.

$$u_* = \sqrt{Dg\left(\frac{\rho_s - \rho}{\rho}\right)}$$

The Shields' diagram presented here is a product of modifications by Yalin and Karahan (1979) and Julien (1995). A dimensionless particle diameter d_* is shown in the diagram.

$$d_* = d_{50}\left[\frac{(G-1)g}{v_m^2}\right]^{1/3}$$

where d_{50} is the median grain diameter and G is the specific gravity of the particle.

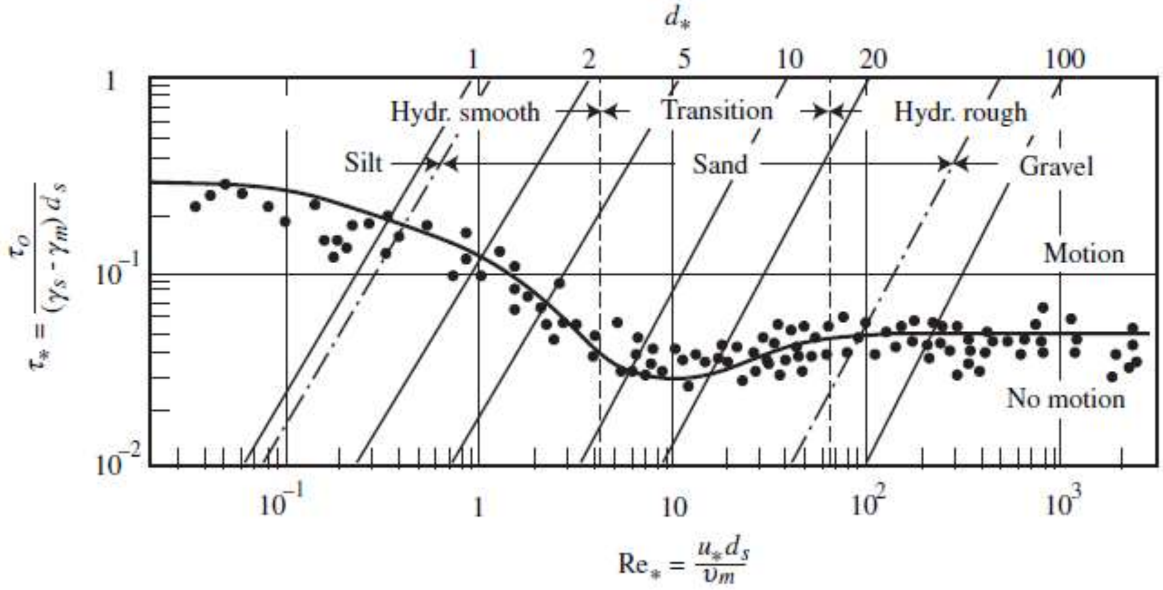

Figure 1: Modified Shields' Diagram (Julien, 1995)

The diagram offers an estimate of the threshold for particle movement (for non-cohesive and coarse sediment such as sands and larger). The curve proposed in the diagram defines the boundary above which transport is expected to occur.

Shields (1936) regarded average bed shear stress as the criterion that identifies conditions of flow required for incipient motion. However, this criterion does not account for turbulence in flow, i.e., velocity deviations from the average velocity that impart force impulses is regarded. Shields' theory presupposed that the critical shear stress τ_c responsible for inducing motion in non-turbulent flow is solely defined by the angle of internal friction or the angle of repose of single grains (Zanke, 2003). Experimental and theoretical analyses by Diplas et al (2008), conversely, support the hypothesis that impulse rather than force is the relevant parameter for the incipient motion of mobile sediment under limiting conditions of pure lift and pure drag. Thus, the inception of motion is largely dependent on fluid forces; however, the distribution of these forces is variable in time and space due to turbulence phenomenon such as coherent flow structures and macro-eddies. These turbulence phenomena contribute to fluctuations in bed-shear stress and enable initiation of motion of bed sediment particles.

2.1.2 Bedload Transport

Sediment load transported in rivers can be divided into bedload and suspended load on the basis of transport mechanisms. The component of the load that is transported closer to the stream bed through rolling, sliding, and saltating (leaping motions), as shown in Figure 2, is termed as bedload sediment. Suspended sediment is the portion of sediment load that is transported above the bedload layer and is typically composed of finer particles such as clays, silts and sands. This thesis focuses on bedload transport and hence this chapter only discusses the bed load component of sediment transport.

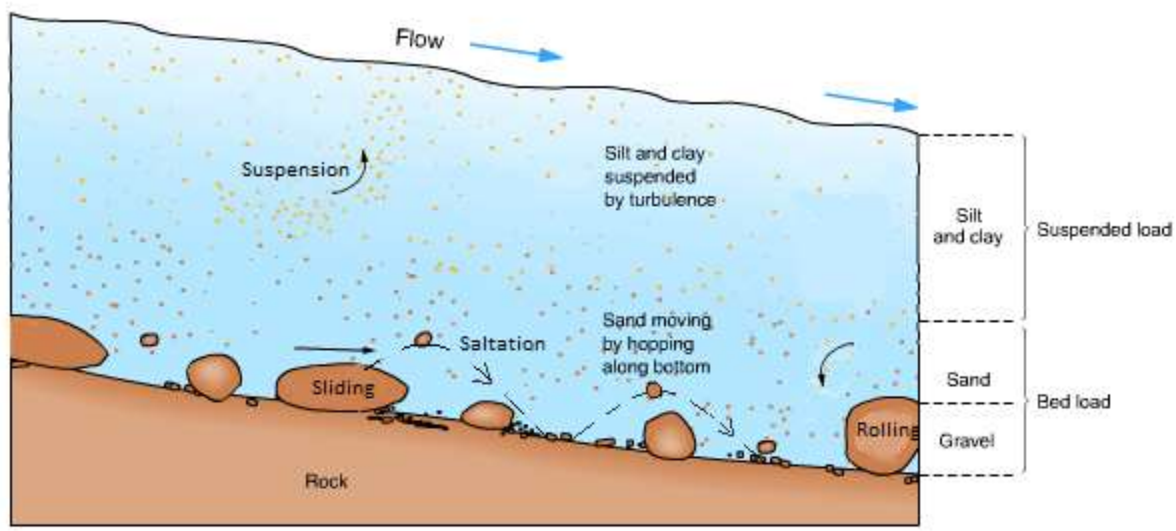

Figure 2: Mode of Sediment Transport (modified from Plummer et al, 2003)

2.1.2.1 Bedload Transport Mechanisms

There have been various views on mechanisms that govern bedload transport. Factors ranging from gravity to near bed turbulence have been considered to control bedload transport. A few seminal studies that spurred research into the process of bedload sediment transport are presented in this sub-section. Also presented are some of the newer perceptions of bedload transport mechanisms.

The action of tractive forces was one of the first identified causes of bedload transport as identified by one of the earliest studies in this field by DuBoys (1879). Though the basic approach of tractive forces is still used to compute bedload transport rates, there have been newer developments in the field. Over seven decades after DuBoys' initial work in this field, Einstein (1950) concluded that the motion of bed particles can be quantified by statistical laws and that the average distance travelled by a bed particle between consecutive depositional events is constant and is independent of the flow condition, rate of transport and the bed composition. For a grain of average sphericity, the transport distance was assumed to be 100 grain diameters. As a result, if the bed particles were to hop distances greater than a few diameters (vertically), the bed particle was no longer a part of the bedload. However, other researchers had a different interpretation on saltation. Bagnold (1973) also noted the statistical nature of bedload transport and attributed the variation in the movement of individual bed particles in the suspended and bedload phase to the randomness of turbulence effects and the contact conditions at the bed surface. However, unlike Einstein, Bagnold considered saltation as the primary mechanism of bedload transport and regarded rolling of particles over a rough bed to be incipient saltation. He also concluded that since saltation occurs in fluids under laminar flow (without turbulence), it must occur by means of a process that is independent of hydrodynamic lifts in a turbulent fluid. Saltation was thus thought to occur due to gravity (Figure 3 (a) and (c)) and due to successive contacts between the solid and the bed or other solids (Figure 3(b)) (Bagnold, 1956; Bagnold, 1973).

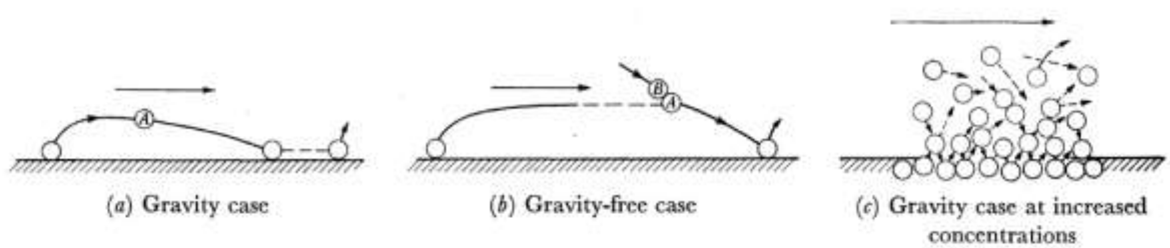

Figure 3: Saltation Mechanisms as postulated by Bagnold (Bagnold, 1956)

Einstein (1950) recognized that a bed particle was set in motion if the instantaneous hydrodynamic lift force overcame the particle weight. Though Bagnold (1956) did attribute the initial upward acceleration from the bed to the fluid-dynamic lift, he found this lift force insufficient to keep the particle in motion against gravity. More recent research by Niño and García (1998) attributes one of the causes of saltation to be the hydrodynamic lifts and vertical impulses due to flow turbulence. Once sediment starts moving and sliding along the bed, the prevalent mode for bedload transport will most likely be saltation for a range of bed shear stresses (García, 2007). Wilson (1987; 1989) found that high shear stresses can set a bed-layer thicker the diameter of bed particle or even several layers of the bed in motion as a sheet-flow layer. Therefore, bedload transport covers both the motion of individual bed material particles and also bed forms moving as a granular fluid flow sheet or a traction carpet. Traction carpets are highly concentrated bedload layers that are developed beneath and drive by turbulent overlying flows (Sohn, 1997).

Recently, researchers have also been examining the effects of turbulence on sediment transport. Nelson et al (1995) investigated the interaction between near-bed turbulence and sediment movement in a spatially non-uniform flow. They found that in non-uniform, and unsteady flow scenarios, considerable change in bedload transport processes could be seen with no variation of bed shear stress. Therefore, the theory provided by Shields (1936) did not sufficiently explain bedload transport in conditions of non-uniform unsteady flows with developing boundary layers. Zanke (2003) determined that initiation of motion can be simulated statistically by the random combination of an individual grain contact angle and a local instantaneous turbulence regime. Sumer et al (2003) performed plane and ripple-covered bed (sand bed) experiments to study the effect of turbulence on sediment transport. They found that with 20% increase in turbulence level in the bed shear stress of a plane bed, an increase of sediment transport by a factor of 6 was seen for a Shields parameter value of 0.085. For a ripple-covered bed, sediment transport rate was also noted to increase with the increase in near-bed turbulence. Valyrakis et al (2010) hypothesized that a series of impulses occurring at short (relative to their duration) temporal intervals, may act synergistically in completely dislodging a grain by rolling. Smart and Habersack (2010) measured the different pressures above and below a flat plate in the plane of a gravel riverbed and found that particle generated form-drag or lift forces are not necessary for entrainment of a particle. They suggested that future studies should also perform direct measurements of near-bed pressure as opposed to the measurement of the local shear stress and pressure measurements to investigate particle transport and entrainment. Such an investigation was done in a recent study by Paiement-Paradis et al (2011) who found that the turbulent variables of instantaneous fluid acceleration-deceleration (pressure fluctuations) and vertical normal stress affected the initiation of movement of individual bedload particles. The magnitude of streamwise velocity was found to affect particle transport by sliding; no relation was found between rolling movements and streamwise velocity. Vertical acceleration was also found to play an important role in the transport of particles by sliding.

2.1.2.2 Transport Equations

Various researchers have attempted to predict and quantify the capacity of a stream to transport sediment by formulating transport equations. Almost all transport models developed were based on flume studies and have not necessarily been tested in the field. Depending on the school of thought, the conceptualizations of the equations have resulted in different relations. Three such conceptualizations are presented below.

Meyer-Peter and Muller (1948) took an experimental approach to develop their bedload transport equation based on tractive force. They studied sediment sizes ranging from 0.4 mm to 30 mm in conditions of turbulent flows and developed the following equation for submerged bedload rate by weight per unit width (q'_{bw}):

$$q'_{bw} = 8(1/\rho)^{1/2}(\tau_o - \tau_c)^{2/3}$$

In the above equation, τ_o and τ_c are defined as follows:

$$\tau_c = \gamma d S$$

$$\tau_o = 0.047\gamma_s{}' D_m$$

where S is the slope which represents energy loss due to water and sediment transport; d is flow depth; γ is the specific weight of water; $\gamma_s{}'$is the bulk specific weight of the sediment; and, D_m is the representative grain size.

Einstein's (1950) hypothesis of bedload transport departed from the more common approach of expressing bedload transport as a function of excess shear stress and from the idea of formulation of a critical condition for the initiation of motion. He developed a transport rate equation and a probability function for transport to occur based on experimental results that led him to believe that bedload transport occurred in "steps" due to turbulent fluctuations caused when the hydrodynamic lift forces were higher than the particle's submerged weight. Brown (1950) presented a simplification of Einstein formula for bedload transport. The Einstein-Brown formula is presented below:

$$\phi = f\left(\frac{1}{\psi}\right) = f\left(\frac{\tau}{(\gamma_s - \gamma)D_s}\right)$$

where ϕ is the transport rate function defined as:

$$\phi = \frac{q_{bw}}{K\sqrt{g\gamma_s{}' D_s^3}}$$

where q_{bw} is the rate of movement of dry bedload weight per unit width, D_s is the representative sediment size for which the median grain size D_{50} is often used. K is defined as:

$$K = \sqrt{\frac{2}{3} + \frac{36\upsilon^2}{gD_s^3\left((\gamma_s - \gamma) - 1\right)}} - \sqrt{\frac{36\upsilon^2}{gD_s^3\left((\gamma_s - \gamma) - 1\right)}}$$

Data from flume experiments by other researchers suggest that for values of $1/\psi > 0.09$, the relationship between ϕ and ψ is :

$$\phi = 40\left(\frac{1}{\psi}\right)^3$$

Bagnold (1966) used a stream power approach to quantify the bedload transport. He defined bedload work rate as the product of available stream power (ω) and bedload transport efficiency(e_b). Available stream power is the product of mean boundary shear stress (τ) and mean flow velocity $(\bar{u})$. The bedload work rate is also defined as the product of the submerged weight per unit width per unit time and the ratio of tangential shear force to normal force $(\tan\alpha)$ where α is the angle of inclination. Equating the two definitions, he formulated the following equation for submerged bedload transport rate by weight per unit width (q'_{bw}):

$$q'_{bw} = \left(\frac{\rho}{\rho_s - \rho}\right)\frac{\omega e_b}{\tan\alpha}$$

Unfortunately, these equations are not without uncertainty. Predictions of bedload sediment through various transport models can vary by orders of magnitude, especially when used without proper calibration. These equations are only somewhat successful in natural rivers where the effects of topography, planform variability, mixed bed material sizes, and hydraulics are confounding factors. In order to improve the applicability of the transport equations, it is essential that the equations be calibrated using field measurements of sediment loads for a range of flows for the specific watercourse. Therefore, the usability of transport models largely depends on the availability of a large volume of field data which can be difficult to gather given that bedload transport does not always occur. Thus, developing a method to gather the essential field data in an expedient manner is imperative.

2.1.2.3 Size Selective Transport

All riverbeds are composed of a range of sediment sizes which reflect the range of sizes that they transport and sort in the process of deposition. This sorting can be observed in stream-wise, lateral and vertical directions. Stream-wise sorting can be observed in riffle-pool systems where the riffles tend to be composed of coarser substrate whereas the pools tend to be composed of finer substrate. Additionally, downstream fining observed in most streams is an example of stream-wise sorting. Lateral sorting in a stream cross section can be observed at bends. The inside of the bends tend to be finer than the outside of bends where the secondary flow velocities scour out the finer particles. Vertical sorting is observed in gravel-bed rivers where armouring (coarsening of the top most layer of the bed sediment) due to weaning with lower flow regimes is a common phenomenon in non-ephemeral streams. Sediment sorting is the result of the differential transport of different sediment sizes (Parker, 2007). A granular physics approach adopted by Frey & Church (2011) to categorize transport into three stages: (1) finer material pass over a static bed; (2) partial transport of local bed material; and (3) general motion of grains on the bed in which all grains are equally apt to move, suggests that the propensity for grains of similar size to block each other leads to accumulations of similarly sized grains in restricted areas of the channel bed.

Given the sediment sorting, it is easy to concede that equal mobility in rivers is unlikely. Sediment entrainment must be size-selective. Coarser grains are generally harder to move because they weigh more than the finer grains; however, because of their protrusion from the streambed, they are exposed to more drag than the finer grains and hence can move easily. However, these interplaying effects cause the coarser grains to tend to experience lesser mobility. This phenomenon is termed the “hiding effect”. A factor to account for this hiding effect is often included in equations featuring bedload transport of sediment mixtures.

Traditionally, absolute grain sizes that represented the channel substrate were used in excess shear stress type bedload equations. To account for selective transport, researchers tested the effect of relative grain sizes on the threshold of movement. One such research group of Ashworth and Kentworthy (1989) used mean and maximum particle sizes to quantify the threshold for particle entrainment in gravel-bed rivers and found that threshold shear stress for entrainment depended on relative grain sizes more than absolute grain sizes and that equal mobility of both small and large particles could be reached in conditions of high shear stress and transport rates.

Wilcock and McArdell (1993; 1997) defined a new threshold parameter for a region within which the condition of partial transport occurs (see Figure 4) to allow for the determination of surface-based fractional transport rates. According to their theory of partial transport, not all grains within the partially mobilized fraction experience entrainment; all sediments that show shear stresses above the newly defined threshold lie within a region of full mobility and are entrained on a regular basis. Their research (Wilcock & McArdell, 1993) suggests that the transport rate of specific sediment sizes is controlled by both their frequency and the fraction of sediments of the same size that remain immobile. They also suggest that partial transport determines the thickness of the active bed layer and hence influences the exchange of pavement and sub-pavement layers of the bed, armouring and other sediment sorting (Wilcock & McArdell, 1997).

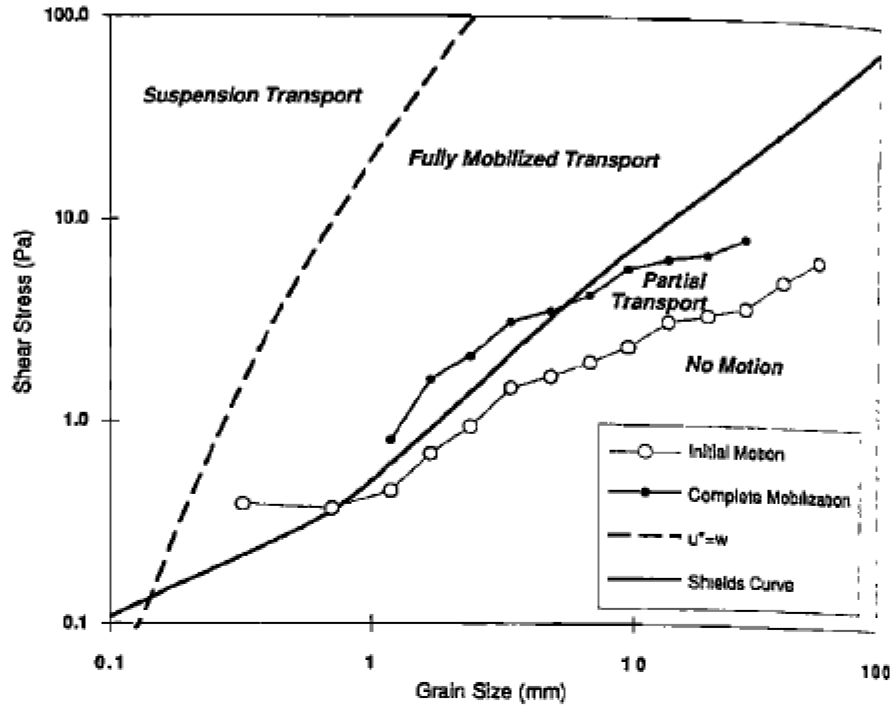

Figure 4: Regions of sediment transport (Wilcock & McArdell, 1993)

2.1.3 Bedload Measurements

It is essential to quantify bedload transport rates to design and evaluate stream restoration plans and to study the continuity of sediment to ensure that there is no accumulation or erosion. This knowledge enables engineers and practitioners to determine the net erosion (only with erosion studies) for upstream and local sources, and hence enables them to determine potential problems that can be caused by either an excess of sediment load (sedimentation of reservoirs and channels, flooding, obstructions in channel flow caused by deposition) or due to the lack of sufficient sediment supply (bank and bed erosion).

The idea of measuring bedload transport is a relatively old one. Various researchers (e.g., DuBoys (1879), Smart & Habersack (2010)) have been looking into this subject since the 19th century and still continue to do so in the 21st century. While the reasons to measure sediment loads have remained the same, the methods of measuring bedload have evolved. Bedload measurement methods can be divided into direct and indirect methods (Hubbell, 1964). Direct methods refer to methods that involve sampling of bed material while it is being transported, whereas the indirect methods refer to the use of tracers to monitor the transport of individual particles (Gomez, 1991). However, as noted by Diplas et al (2007), none of these techniques is suitable for a wide range of uses. Although bedload measuring techniques have been employed for over a century, they are not as widely measured as suspended sediments (Gray, Laronne, & Marr, 2010).

2.1.3.1 Direct Methods

Typically, bed-load samplers are deployed to determine and study sediment loads and transport rates, and data is collected, particularly during high flows. These samplers may be generalized into three types: samplers installed into the bed of a channel (pit and trough samplers), manually operated portable samplers, and non-intrusive samplers (Diplas, Kuhnle, Gray, Glysson, & Edwards, 2007). The latter category falls under the category of indirect method of sampling.

Hubbell (1964) classifies the sampling devices into the following types: box or basket, pan or tray, pressure difference and slot or pit. Box or basket types of samplers retain sediment deposited in due to reduction in flow velocity. This reduction in flow velocity causes sediment to be deposited at the entrance and hence reduces the efficiency of the sampler. Pressure-difference samplers alleviate this problem as they are designed such that the entrance velocity and the velocity of water adjacent to the sampler is approximately the same. Pan or tray samplers retain sediment that drops into a slot after it has rolled, slid or skipped up an entrance ramp. Slot or pit samplers are installed on the bottom of the bed such that they catch sediment as it moves along the streambed. A type of pressure-difference samplers called Helley-Smith samplers (Helley & Smith, 1971) developed for the calculation of sediment loads in sedimentation studies are a popular choice among researchers and practitioners for measuring bedload transport because they can be calibrated to achieve high hydraulic and sampling efficiencies.

2.1.3.2 Indirect Methods

Another method to study bed-load transport involves the use of tracers. This method can be particularly useful when the channel substrate is predominantly composed of gravels since the size of tracers limits the minimum size of particle tagged to the size of gravels. Tracers provide a way of characterizing transport parameters and the stochasticity of particle motion itself (Ganti, Meerschaert, Foufoula-Georgiou, Viparelli, & Parker, 2010) which was recognized by Einstein (1937). Painted rocks, radio transmitters, magnetic clasts, radio nuclides, and radio frequency identification (RFID) devices have been used as tracers to monitor and study sediment transport.

Bedload-surrogate monitoring technologies such as active sensors (e.g., acoustic Doppler current profilers (ADCPs), sonar, radar and smart sensors) and passive sensors (e.g., geophones and hydrophones) can be used to study both gravels and sand (Gray, Laronne, & Marr, 2010). Sediment transport in sand bed channels is estimated through the study of dimensions and speed of bedform movement using ultrasonic sounder data (Gomez, 1991).

2.1.3.3 Challenges

Bedload discharge is known to vary in an oscillatory manner such that the mean bedload discharge cannot be estimated by a single short-term measurement (Hubbell, 1964). This temporal and the spatial variability in the transport of bedload presents a challenge to the design of samplers and sampling strategies. Traditionally used direct methods also pose installation and retrieval problems especially in conditions of bankfull flows. Additionally, the type of sampler used and the placement of the sampler in the stream affect the sampling efficiency (Hubbell, 1964). Therefore, adequately capturing a representative sample becomes challenging.

2.2 RFID Technology

Radio Frequency Identification technology is an automatic (in that the reader is automated though it might have to be manually operated) data collection technology that uses wireless radio communications to uniquely identify objects and people without a line of sight (TI, 2012). This technology was employed as early as the 1940s by the allied forces to identify their WWII aircrafts. Later in the 1960s, the technology was then used in employee badges to enable automatic identification of people for security purposes (Want, 2006). In recent times, with the decrease in the cost of manufacturing and development of the technology, its application has varied from labeling airline luggage to tracking fish movements.

2.2.1 Theory

The RFID system consists of two parts: the transponder (or tag) located on the object to be identified and the reader (or interrogator or receiver) which contains both a transmitter and a receiver (Finkenzeller, 2003). There are two types of RFID tags (or transponders): active and passive. The passive tags are of interest to this research due to their small size and long operational life compared to active tags. A passive RFID tag is primarily comprised of a semiconductor chip which stores information, a capacitor and an antenna to send and receive signals, all of which are hermetically sealed in a glass vial (Figure 5). The RFID tags referred to henceforth in the thesis shall be passive tags unless mentioned otherwise. The power required to activate an RFID tag is supplied by the reader and the reader displays the data encoded on the tag. The structure of encapsulation of the transponder changes depending on its application. The transponder shown in Figure 5 specifically shows the schematic of a glass transponder which was used in this study.

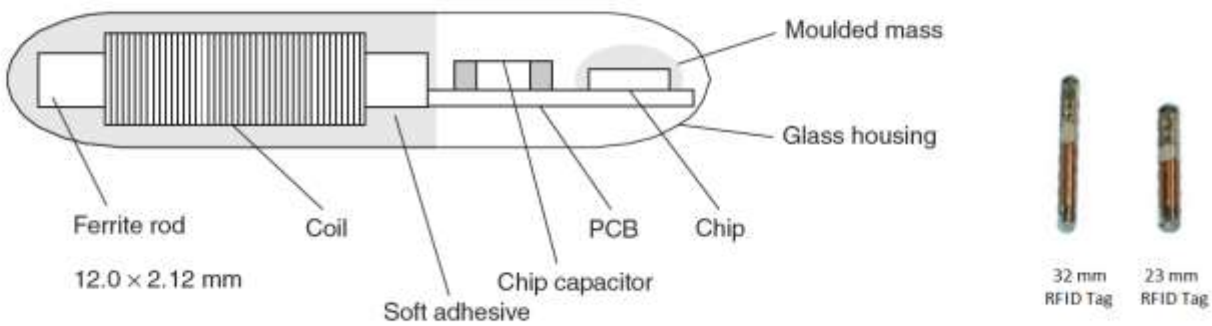

Figure 5: Schematic of a Glass Transponder (Finkenzeller, 2003) and TI RFID Tags used in the study

RFID tags can be further classified into Low Frequency (LF), High Frequency (HF), Ultra High Frequency (UHF) and Microwave based on the frequency of operation (Ranasinghe & Cole, 2008). LF RFID tags use a *near field* design approach in which power is delivered from the reader to the transponder through magnetic induction. They generally operate at a frequency less than 135 kHz. The tags used in this study operate at 134.2 kHz.

For a reader to be able to communicate with a tag, it is essential that the tag receive sufficient power for its activation (Finkenzeller, 2003). The zone within which the transfer of energy and information between tag and reader takes place is termed as the *interrogation zone*. The maximum linear distance between which the reader receives an interrogation signal (radio signal) from the tag is termed *read range* in this thesis. The dimensions of the 3-dimensional interrogation zone are governed by the power received by the tag from the reader. Though the power emitted by the reader is constant, its strength decays by a factor of the inverse cube of the distance between the reader and the tag (Lehpamer, 2012). Factors such as antenna diameter also play a role in the power of the antenna. For larger antennae, the power may stay constant for a certain distance before it starts to decay. The interrogation zone changes its shape depending on the orientation of the transponder with respect to the antenna.

Figure 6c and Figure 6d show the theoretical interrogation zone of the reader antenna in vertical and horizontal tag orientations (Figure 6a and Figure 6b), as provided by the manufacturers of the antenna (Aquartis, 2011) used in this study.

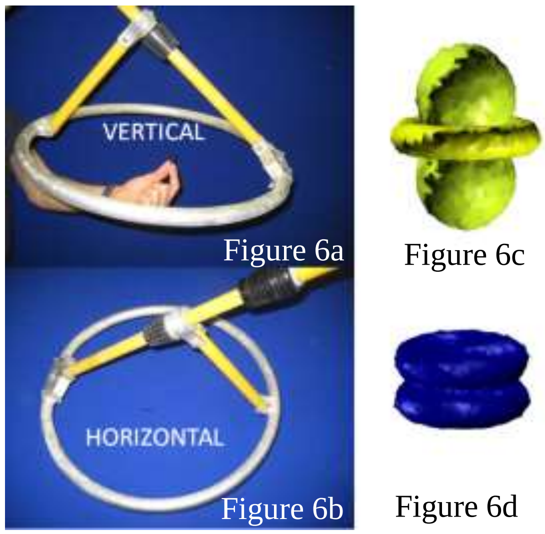

Figure 6: Theoretical Antenna Fields (interrogation zones modified from Aquartis, 2011)

2.2.2 RFID Application in Measuring Sediment Transport

Since the first use of RFID technology in tracking bedload sediment (Nichols, 2004), various researchers have used this technology to study sediment transport in various environments, as listed in Table 1. The use of passive RFID transponders in tracers has been favoured by these researchers since these tracers have high recovery rates and long life; they can be detected even when buried so long as the antenna is within the read range; they can be assigned unique identification codes; and, they are inexpensive compared to active radio transmitters. RFID tracers have been used to study bedload displacement distances, tracer frequency distributions and variability in tracer dispersions (Liébault, Bellot, Chapuis, Klotz, & Deschâtres, 2011), bedload transport around deflectors (Carre, Biron, & Gaskin, 2007), large woody debris in rivers (MacVicar, et al., 2009), sediment mobility in a specific morphology (MacVicar & Roy, 2011), effects of dams on sediment in river delta, (Miller, Warrick, & Morgan, 2011), and structures of active sediment layers (Miller & Warrick, 2012).

Table 1: List of previous RFID research papers

Reference	Environment	# of Tags
Nichols, M. H. (2004)	Rivers (Ephemeral)	124
Lamarre, H. et al (2005)	River (Gravel Bed)	204
Carre, D. M. et al (2007)	River	110
Lauth, T.J. & Papanicolaou, A.N. (2008)	Flume	-
Lauth, T.J. & Papanicolaou, A.N. (2009)	Flume	50
MacVicar, B. et al. (2009)	River (Large)	204
Schneider, J. et al (2010)	River (Mountain)	298 and 270
Liebault, F. et al (2011)	River (Mountain)	451
Miller, I. M. et al (2011)	River (Delta)	128
MacVicar, B.J. & Roy, A.G. (2011)	River (Gravel Bed)	299
Miller, I. M. & Warrick, J. A. (2012)	Mixed Beach (Littoral)	54
Bradley, N. D. & Tucker, G.E. (2012)	River (Mountain)	893
Papanicolaou, A.N. et al (2012)	Flume	-

Though all the researchers use the same technology, the method of usage is not necessarily the same. There are no standard operating procedures for tagging and tag detection. Confounding factors which influence tag detection present challenges in standardizing RFID bedload tracking, unlike the standardization of RFID identification of animals. ISO standards 11784, 11785 and 14223 contain the code structure of the radio-frequency identification code for animals. Similarly, there are ISO standards for freight containers. However, though they attempt at standardizing encoding of tags for a specific purpose, the ISO standards don't describe tagging and tag identification procedures. The standards also do not note performance standards for any RFID technology. Such standardization procedures, though far from being detailed standard operating procedures, are steps in the right direction. Unfortunately, there are no encoding, tagging, detection or performance standards in existence for bedload tracking. Given the use of the RFID technology by multiple research groups throughout the world, in the fields of sediment transport through fluvial and lacustrine systems, it would be beneficial for the procedures for tagging and tracking to be standardized. Standardization of these procedures can also enable new research groups to adopt the use of RFID technology with relative ease.

Lamarre, MacVicar and Roy (2005) determined a vertical detection distance of 0.5 m and a lateral detection range of 0.4 m ± 0.06 m. Based on controlled laboratory experiments, Schneider et al (2010) found that the read range of the mobile 50 cm diameter loop antenna varied depending on the sediment saturation condition. They also note that the stone material around the transponder can also affect the read range. Lamarre et al (2005) recognized that when multiple tagged articles were in the same interrogation range, interference in signal contributed to errors during detection. Lauth and Papanicolaou (2008) considered factors such as burial depth, proximity to other particles, and transponder orientation important while testing RFID systems in a flume. Background electromagnetic interference has also been identified as a factor that can affect the reading range (Lauth & Papanicolaou, 2009). Papanicolaou et al. (2012) also studied the effects of the medium between the transponder and antenna. They found that water and air were similar in their influence on signal strength; gravels did not cause large signal decay; sands caused the greatest signal decay. Benelli and Pozzebon (2013) examined a variety of low frequency RFID tags under water in conditions of varying conductivities and found that long glass tags could be read in a range of distances from 0.48 cm and 0.63 cm. Based on the available literature, it is safe to conclude that there are many factors that affect the precision of detection.

2.3 Urbanization

Lane (1955) established the following proportionality for channels that maintain dynamic equilibrium:

$$QS \propto Q_s d_{50}$$

where Q, S, Q_s, and d_{50} are the channel forming discharge, channel bed gradient, bed-material discharge and the median grain size of the bed material, respectively. Perturbations in the channel lead to changes in the equilibrium conditions that dictate Lane's equation. Urbanization has the potential to affect all four parameters in Lane's equation. Urban development has transformed river landscapes by changing hydrologic (dictated by Q in Lane's equation) and sedimentologic (dictated by Q_s and d_{50} in Lane's equation) regimes causing a range of morphologic adjustments (Chin, 2006) such as channel incisions and quasi-equilibrium channel expansions (Booth, 1990). Schumm (1969) studied morphological effects on rivers due to human activities and developed the following relationships between the controlling factors of channel discharge and bed-material discharge, and the channel dimension parameters such as channel width (w), depth (d), meander wavelength (λ), slope (S) and sinuosity (Ω):

$$Q^+ \approx \frac{w^+ d^+ \lambda^+}{S^-};\ Q^- \approx \frac{w^- d^- \lambda^-}{S^+};\ Q_s^+ \approx \frac{w^+ \lambda^+ S^+}{d^- \Omega^-};\ Q_s^- \approx \frac{w^- \lambda^- S^-}{d^+ \Omega^+}$$

The plus and minus exponents indicate an increase or decrease of the respective parameters. Thus, channel discharge is directly proportional to channel width, depth and meander wavelength, and inversely proportional to its slope. Similarly, bed-material discharge is directly proportional to channel width, meander wavelength and slope, and is inversely proportional to channel depth and sinuosity.

2.3.1 Effects of urbanization on hydrologic and sedimentologic regimes

Urbanization is known to increase the peak discharges of storm runoff due to the increase in impervious area. Uncontrolled urbanization can also increase the duration of flows (Pomeroy, Postel, O'Neill, & Roesner, 2008). The increase of peak discharge with increase in urbanization has been documented in studies by Leopold (1968) and Hollis (1975). Studies on rivers in the Philadelphia area by Hammer (1972) established that the duration for which the urban development has been in place is directly proportional to the channel size increases. The same study also suggested that impact of impervious development is positively related to the channel bed slope, hydraulic gradient and the slope of the developed land. Pizzuto, Hession & McBride (2000) defined the Hammer number H, in honour of Thomas Hammer's 1972 studies, as a function of bankfull discharge Q_{bf} and the basin area D_A:

$$H = Q_{bf}/D_A$$

They found that the Hammer number for urban stream channels is significantly larger than that of rural stream channels, which implies that the urban channels have adjusted their size and overall frictional characteristics in order to convey the increased peak discharges created by impervious surfaces,. Based on their research on two physically similar watersheds but with differing land-uses (urbanizing and rural/agricultural) in east-central Pennsylvania, Galaster et al (2006) determined that the relationship between the peak discharge and basin area is likely non-linear. The effects on the channel's morphological characteristics are further discussed in sub-section 2.3.2.

The sediment load available is influenced by the land-use of the upstream and headwater portions of the river. Urbanization of watersheds generally leads to a reduction of sediment supply from the watershed due to reduced availability of non-impervious area that could contribute overland erosion. Urbanization can also have indirect impacts on the sedimentologic regime of a watershed. Anthropogenic works of dam construction, channelization (hardening of channel bed and banks) and sediment mining that alter sediment flux (Surian & Rinaldi, 2004) typically increase with urbanization. Channel disturbances that cause excess stream power (a function of flow, slope and the specific weight of water) to occur in relation to the available sediment supply can cause the degradation of channel beds (Simon & Rinaldi, 2006).

Interestingly, Pizzuto, Hession & McBride (2000) found that urbanization did not significantly affect the simplified Shields parameters which are based on bankfull depth and median grain size (Chang, 1988); it is at bankfull discharge events that bed material is likely to be transported (Pizzuto, Hession, & McBride, 2000). This suggests that bedload transport occurs at bankfull stage in both urban and rural watersheds. However, Annable, Watson & Thompson (2012) found that the channel beds of urbanized gravel-bed rivers tended to be armoured and hence a reduction in the volume of bed material transported was observed. A study by Trimble (1997) shows that stream channels (that have not been hardened) contributed to the sediment yield of an arid urbanizing watershed as a result of increased storm runoff. In humid watersheds, according to a study by Bledsoe and Watson (Bledsoe & Watson, 2001), channel instability increases with increases in stream power associated with imperviousness as low as 10 to 20%. The effects of urbanization on the sedimentologic regime can be minimal depending on the type of existing native sediment substrate in the channel. One study found that the watersheds dominated by coarse or cohesive stream bed materials show less sensitivity to changes in erosion potential due to urbanization (Pomeroy, Postel, O'Neill, & Roesner, 2008).

2.3.2 Effects of urbanization on channel morphology

In combination with the changes in the hydrologic regime in the watershed, the sedimentologic changes to a system cause morphological impacts on a stream channel. Many recent studies have associated increased urban runoff with channel enlargement (Colosimo & Wilcock, 2007;

Galster, Pazzaglia, & Germanoski, 2008). Gregory (1987) found that the typical channel enlargement ratios range from 1.0 to 4.0 in the world's urbanizing rivers. Channel enlargement ratios are based on channel areas. Gregory, Davis & Downs (1992) observe that the channel enlargement downstream of a perturbation does not necessarily take place uniformly along the channel. One of the governing factors of channel enlargement is the sediment load being carried (Chin, 2006). An examination of the in-channel sediment storage characteristics can be used as indicators of the extent of channel adjustment due to urbanization (Colosimo & Wilcock, 2007).

The response to perturbations, especially anthropogenic, can develop over multiple stages of channel evolution leading to a stage of quasi-equilibrium (a dynamic state of re-stabilization). Simon (1989) outlined a six-stage model describing an incised channel evolution "characterized by six process-oriented stages of morphologic development for alluvial channels – pre-modified, constructed, degradation, threshold, aggradation and re-stabilization". He identified the period of bed-aggradation as the time during which top-bank widening and channel bed deposition occurs. A summary of a channel evolution model as described by Simon (1989), Schumm et al (1984) and Biedenharn et al (2007) is presented below (see Figure 7) using a space for time substitution which assumes that the changes to a particular location in a channel can be predicted based on observations of the changes in the channel as it progresses downstream.

Type I is located in the upper reaches and has not experienced significant bed or bank erosion or sediment deposition. Type II is immediately downstream of Type I; it is over steepened and has a sediment transport capacity which exceeds supply and causes active degradation. However, the bank height (h) does not exceed critical bank height (h_c) and hence there is no geotechnical instability. In a channel of Type III, $h > h_c$ and therefore, geotechnical instability occurs. There is a slight degradation, with channel widening being the dominating process in which the sediment transport capacity is reduced. This process initiates sediment deposition. In a Type IV channel, geotechnical instability and widening continue at a reduced rate. The increased aggradation causes the development of berms. In a Type V channel, dynamic equilibrium i.e., a balance between sediment transport supply and capacity is achieved. Berms are covered with riparian vegetation and a new compound channel forms within the incised channel which is bounded by a smaller floodplain. The older floodplain becomes a terrace.

Though the channel evolution model is widely used by river practitioners, it is not without defects. The model needs to be adapted to the catchment and stream type of the system under consideration.

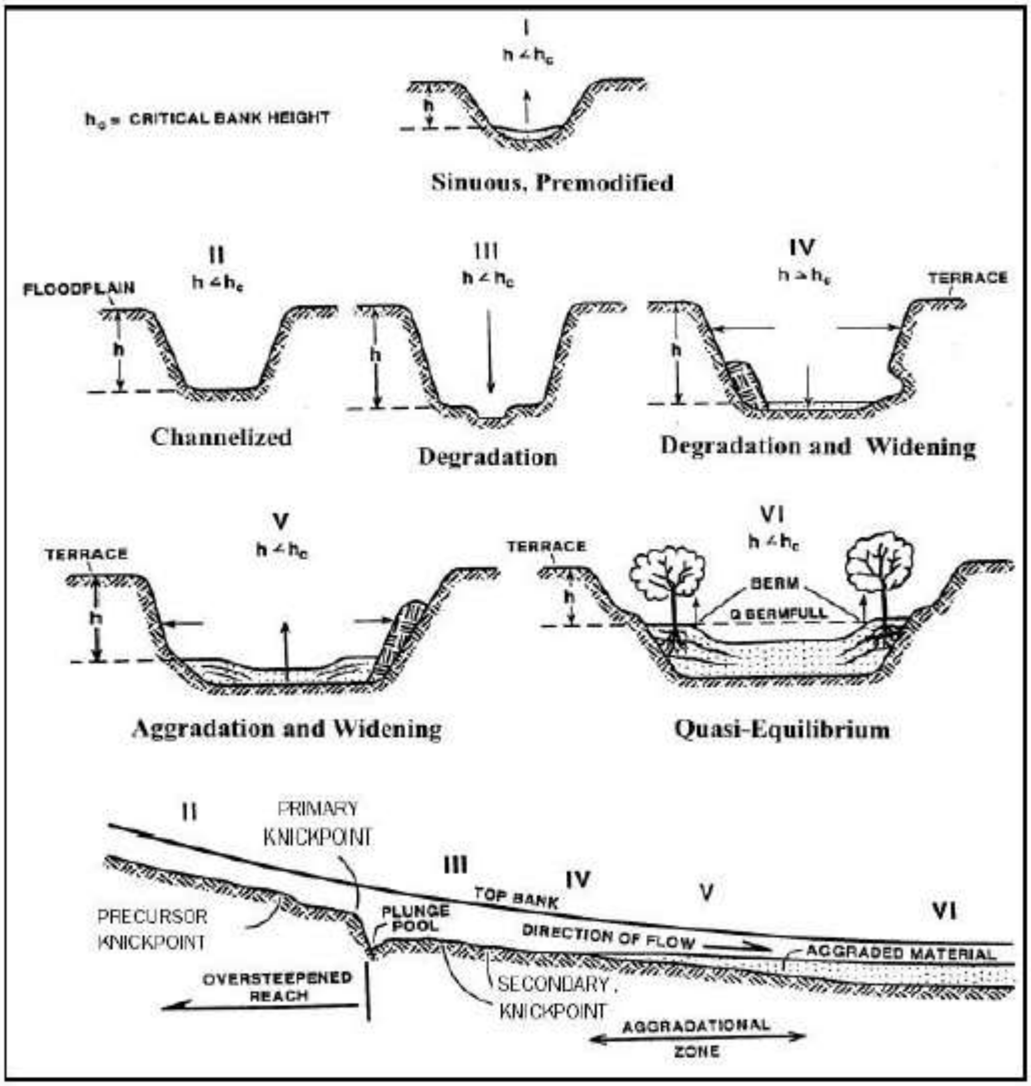

Figure 7: Channel Evolution Model (Schumm, Harvey, & Watson, 1984)

2.3.3 Implications for future research

Curtailing urbanization would effectively eliminate the ongoing adverse effects on a watercourse. However, where it is not possible to limit urbanization, development of a process based understanding of the effects of change in watershed land-uses on streams is required to ensure protection of streams from degradation (Booth & Jackson, 1997). Studies that document the increase in urbanization of watersheds over a long period of time, such as those by Leopold, Huppman & Miller (2005) spanning forty-one years, Cruise, Laymon & Al-Hamdan (2010) spanning twenty years, and Annable, Watson & Thompson (2012) spanning fifteen years enable practitioners to better understand the hydrologic and sedimentologic regimes in urban and urbanizing watersheds. Implementation of appropriately designed stream restoration measures and storm water management techniques can potentially mitigate the negative impacts of urbanization. The approaches taken to restoration can be broadly classified into form-based and process-based approaches to design and analyses (Bennett, et al., 2011). In order to create appropriate designs, it is imperative that they be based on experience of what works on a long term basis. The research project presented in this thesis attempts in part to supplement the current understanding of sediment processes in an urban creek with the hope that study will continue in the future years so as to establish a thorough understanding of the urban creek system; this will enable engineers and decision makers to develop appropriate mitigation measures in similar systems, as necessary.

2.4 Thesis Scope and Objectives

The aim of this research project is to improve methodologies for the investigation of bedload sediment movement through urban streams using RFID technology. The objectives were 1) to track sediment movement in an urban stream using RFID transponders; 2) to identify and quantify the factors that confound the detection of these tracers, and 3) to develop recommendations for a standardized RFID tagging procedure that will improve the precision and utility of the technique. Field studies were conducted to meet objective 1 and laboratory experiments were conducted to meet objective 2. It should be noted, for field studies, two study sites chosen were based on restoration plans by the City of Waterloo so that an evaluation of the restoration works could be undertaken. However, since the restoration through the creek was not completed within the timeframe of this research project, the evaluation of the restoration works is beyond the scope of this thesis. It is anticipated that the baseline data from this research project will contribute to a longer term comparative study on urbanization and sediment dynamics in rivers. The use of RFID technology made it very evident that the precision of tracking varied and often the detected location differed as much as one metre. Therefore, laboratory experiments were undertaken to study the factors that contributed to the variation in detection distances. Information from the field and laboratory studies was used to meet objective 3.

3 METHODOLOGY

This chapter outlines the field and laboratory methods undertaken to meet the objectives of the research project. The section on field methods describes the application of RFID technology in the study of sediment transport and the preliminary work required to undertake such a study. Background information pertaining to the study site is also presented in this section. The section on laboratory methods describes the process undertaken to identify and quantify the factors that confound the accurate detection and location of RFID tracers.

3.1 Field Methods

For the purpose of this study, four reaches of Laurel Creek (see Figure 8) were studied over a period of 18 months. Laurel Creek was chosen for its convenient location and its situation in an urbanized watershed (see Figure 9) that contains naturalized areas. The four reaches of the creek used in this study were chosen for their easy access, general channel morphology and locations with respect to a reach in which restoration works have been carried out by the City of Waterloo. In order to compare the sediment transport characteristics in urbanized sections as opposed to naturalized sections, two of the four reaches selected are situated in urban parks (Hillside Park and Bechtel Park – see Figure 10) where the creek has a greater access to the floodplain as compared to the other sites. Access to the sites was an important factor to consider. All the sites selected were easily accessible by foot; the sites situated in urban parks were accessible by an amphibious all-terrain vehicle for easy transport of RFID tracers. In order to ensure that the tracers would not get trapped in bends, it was necessary to seed the tracers in straight reaches. To eliminate the effects of changing channel morphology within the seeding section, it was essential for the reach to be straight both upstream and downstream of the seeding section. Therefore, three of the reaches selected were situated in straight sections. The fourth reach, which was located in Bechtel Park, was situated in a meandering section; this site was selected because it had been previously restored to a natural state.

Site reconnaissance of all four reaches (see Figure 11) was conducted in early Fall 2010. During reconnaissance, which site characteristics were noted and benchmarks were established. Thereafter, routine field work was carried out to collect substrate size information, seed the sites, i.e., introduce tagged sediment in the sites, and to track the tracers. Geomorphic surveys of each reach were also undertaken to characterize the morphology of the reaches. Substrate size information was collected through pebble counts (using the Wolman Pebble Count Method) and grain size analysis of bulk pavement and sub-pavement samples.

3.1.1 Laurel Creek Background

The water course chosen for this study, Laurel Creek, is a tributary of the Grand River located in the Regional Municipality of Waterloo (Figure 8). At the confluence with the Grand River, Laurel Creek has a drainage area of 74.4 km^2 (GRCA, 1993). The quaternary geology of the area is characterized by 45 to 100 metres of glacial deposits over a Salina bedrock formation which was deposited in the late Silurian and early Devonian Period (GRCA, 1993; GRCA, 2004). Forewell Creek, Beaver Creek, Monastery Creek, and Claire Creek are the main tributaries of Laurel Creek. The headwaters of the creek lie in a rural landscape consisting of woodlots and wetlands upstream of Laurel Creek Reservoir. Laurel Creek drains into the Grand River. Laurel Creek Reservoir is one of the largest storage facilities available within the system. Columbia Lake, Laurel Lake and Silver Lake are the other major storage areas located within the Laurel Creek drainage system. These three reservoirs are beneficial in regulating the streamflow and reducing sediment fluxes during intense storm events. However, the lakes also interrupt bedload transport in the creek. All lakes are man-made, built alternately for purposes of supporting sawmills (Silver Lake in 1808), flood control, low flow augmentation and pollution abatement (Laurel Creek Reservoir in 1966), and recreation and aesthetics (Columbia Lake and Laurel Lake).

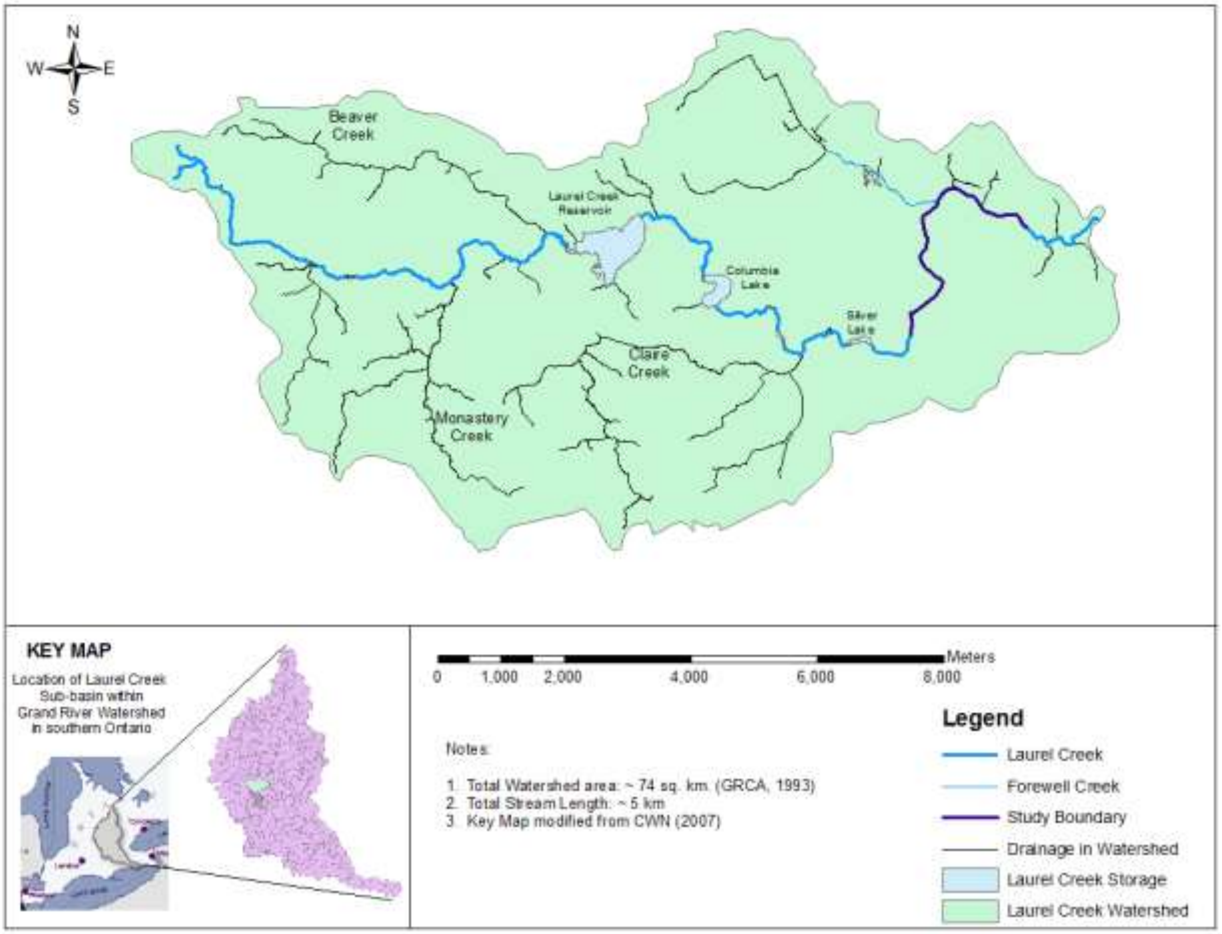

Figure 8: Laurel Creek Watershed Map

Most of the forested land in the watershed was cleared for agricultural use between the early 1800s and 1910. A number of mills and mill dams were constructed on the watercourses during the 1800s. Since 1910, the watercourses in the watershed underwent periods of change and channel stabilization to accommodate the changing flow conditions. Urbanization in the Laurel Creek Watershed has occurred primarily since 1946 (GRCA, 1993). As of 1999, almost the entire lower watershed is urbanized while the upper watershed is predominantly agricultural land as shown in Figure 9. The percent urbanization (as determined by total impervious area) in 1999 is 37.7%.

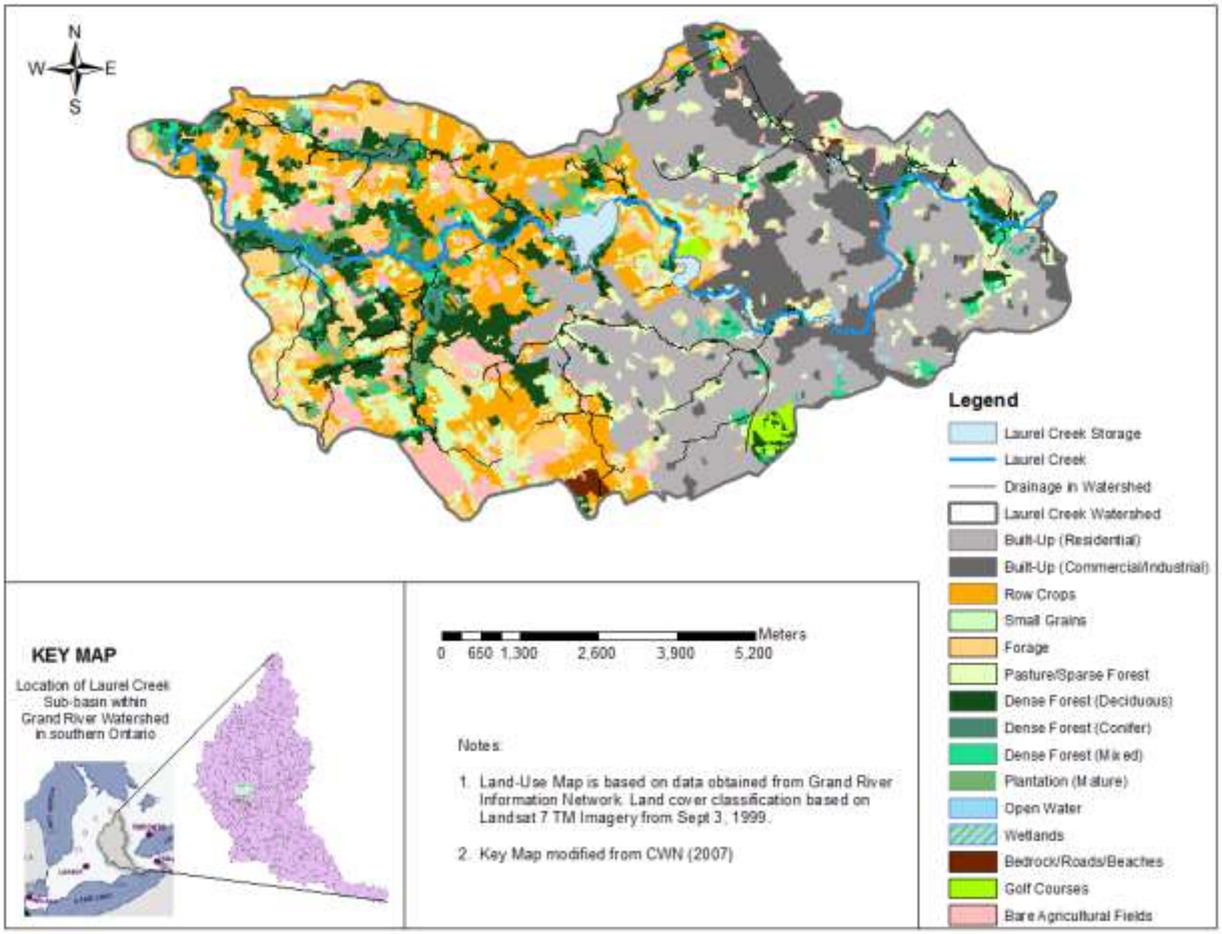

Figure 9: Laurel Creek Watershed Landuse

Many reaches of the creek were lined with concrete or gabion baskets as erosion control measures. A significant portion (~500 metres) of the watercourse downstream of Silver Lake has been channelized. Historically, the watercourse has undergone changes due to straightening and channelization, planform alterations, construction of lakes and crossing structures. Of particular interest to this study is the changes to channel made in the study reach through Bechtel Park. Also of interest are the historic and the proposed restoration works to be carried out in Hillside Park. Figure 10 shows the locations of these parks in the watershed.

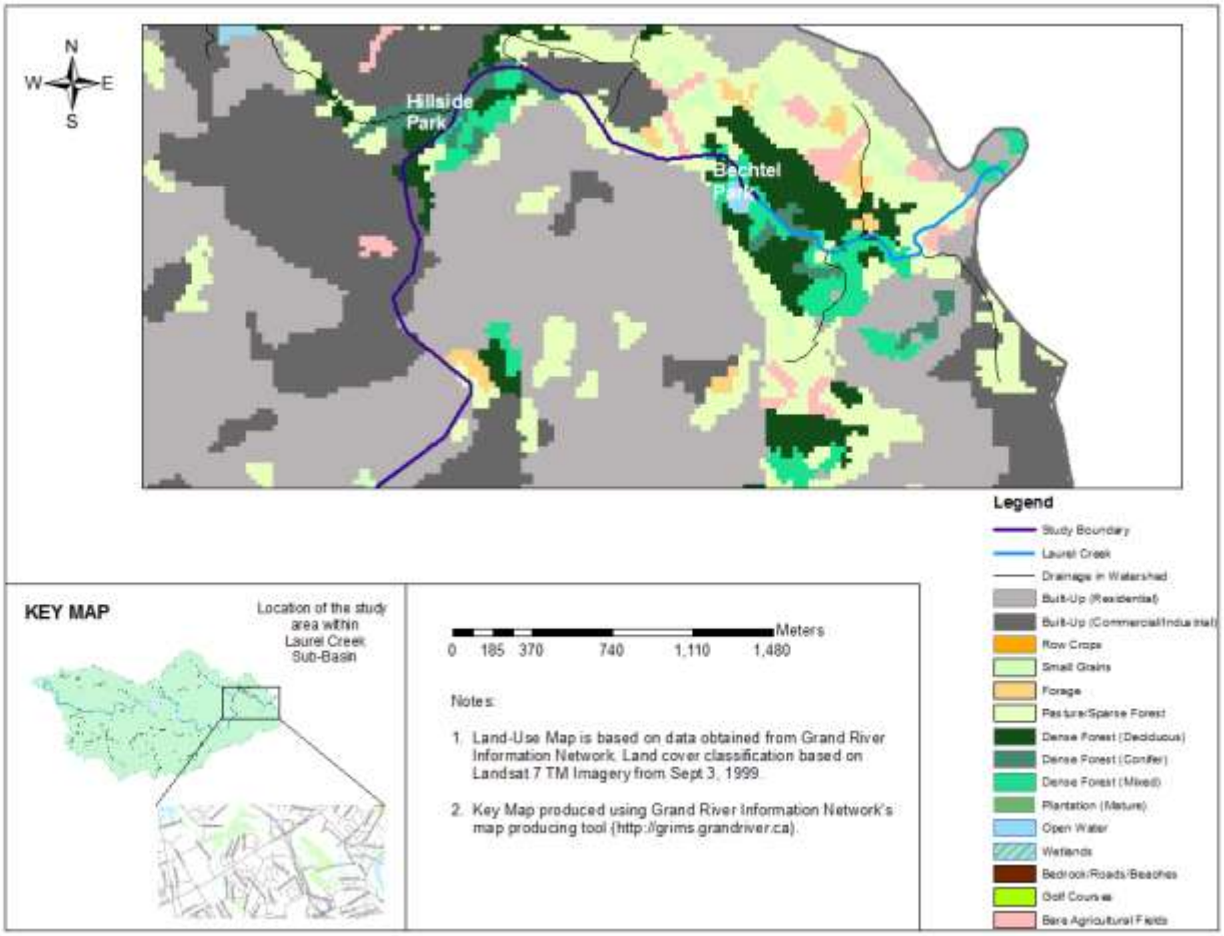

Figure 10: Location of Bechtel Park and Hillside Park

Laurel Creek in Bechtel Park was rehabilitated in two phases between 1993 and 1995. The first phase included erosion control mitigations at a historic landfill site which was threatening the sanitary effluent pipe from the wastewater treatment plant (between Hillside and Bechtel parks). The second phase included channel realignments to increase stream sinuosity, creation of pools and riffles, vortex weirs and bioengineering techniques with live vegetation walls to reduce erosion (Anderson, 2008).

According to a historic geomorphic assessment done by Stantec Consulting Ltd., (2010) using historic air photos from 1930, 1945, 1955, 1978, 2000 and 2006, channel straightening in the study area through Hillside Park occurred between 1945 and 1955. This straightening led to a 29% reduction in channel length. In 2009, Laurel Creek rehabilitation through Hillside Park was proposed as a part of a larger project that involved upgrading of a sewer system to the wastewater treatment plant (WWTP). The rehabilitation proposed included removal of in-stream barriers that cause fish passage issues under low flows, replacement of a pedestrian bridge over the creek, replacement of gabions with bioengineering measures, lowering of an exposed sewer trunk (Forewell Trunk Sewer) located in Laurel Creek downstream of the confluence of Laurel and Forewell Creeks. The project was completed in the fall of 2012. Further restoration projects to remove concrete debris from the abandoned sewer near the WWTP, have also been recommended by Stantec Consulting Ltd. The field component of this project establishes baseline data on Laurel Creek for future studies on the effectiveness of the restoration works.

3.1.2 Preliminary Site Assessments

As a part of the preliminary assessment, the four reaches to be studied were delineated (Figure 11) during a desktop analysis that included a review of aerial photos of the study area. Additionally, geomorphic surveys of the specific sites were performed to morphologically characterize the system. The geomorphic surveys included longitudinal profiles through the reaches and two cross sections that demarcate the upstream (start) and the downstream (end) locations of the seeding site in each reach. Table 2 shows a summary of the geomorphic characteristics of the four study reaches.

Table 2: Geomorphic Characteristics of Study Reaches

Site	1	2	3	4
Location	Immediately north of Bridgeport Rd.	Immediately downstream of University Ave East. through Hillside Park	Immediately downstream of a pedestrian bridge in Hillside Park	Upstream of a pedestrian bridge in Bechtel Park
Land Use	Residential	Residential	Urban Park	Urban Park
Seeding Site Length (m)	18.3	33.3	21.2	19.0
Reach Slope (%)	0.520	0.056	0.286	0.24
Local Slope (%)	1.26	0.29	0.36	1.00
Bankfull Width (m)	9.20	9.86	11.01	10.85
Bankfull Depth (m)	0.41	0.69	0.48	0.5
D_{50} (mm)	36.6	12.6	7.2	27.7
D_{84} (mm)	72	76	56	113
Rosgen Classification	B4	F4	F4	B4

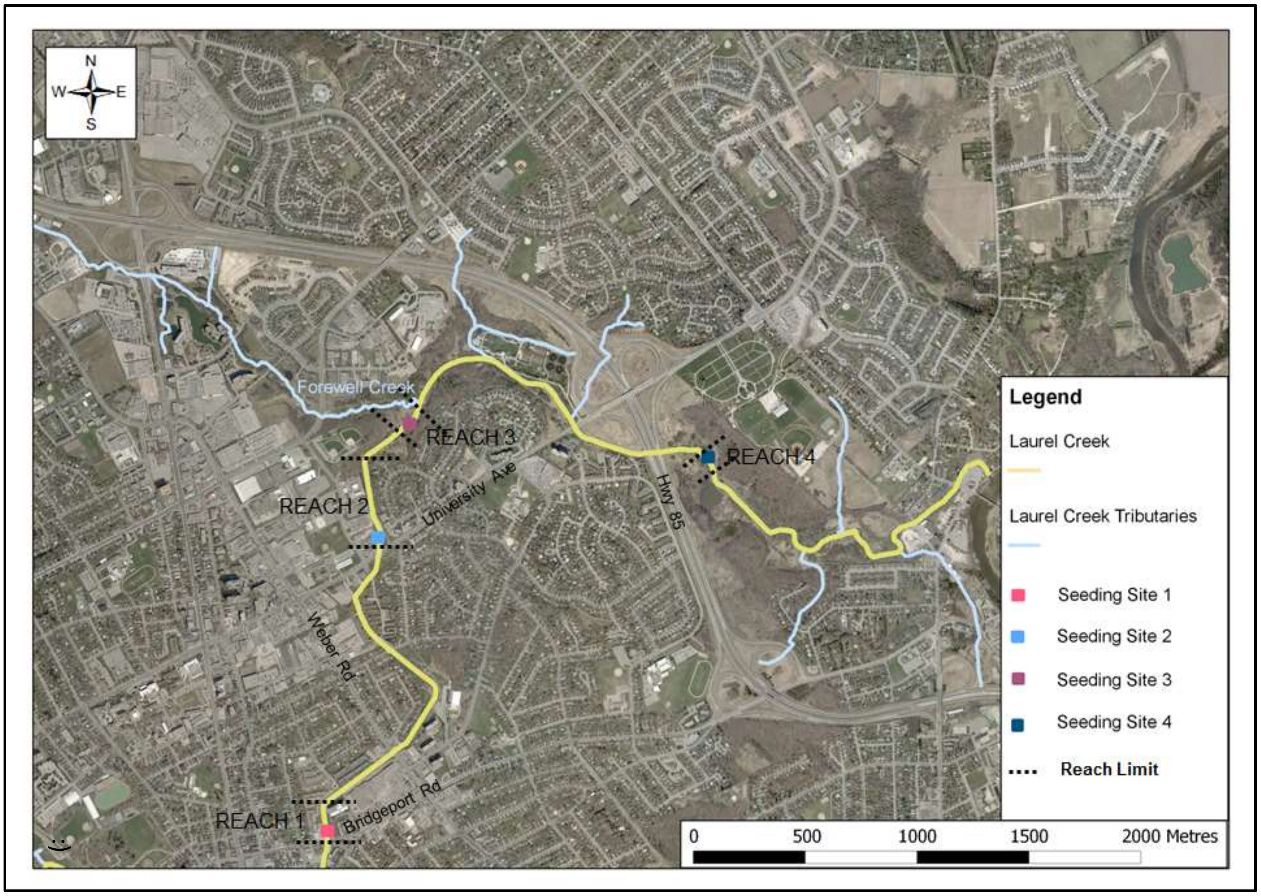

Figure 11: Locations of the Study Reaches

A longitudinal profile of the surveyed portion of creek through Site 1 is shown in Figure 12. The longitudinal profile of the surveyed portion of Laurel Creek through Hillside Park (including Sites 2 and 3) and Bechtel Park (Site 4) is shown in Figure 13 and Figure 14.

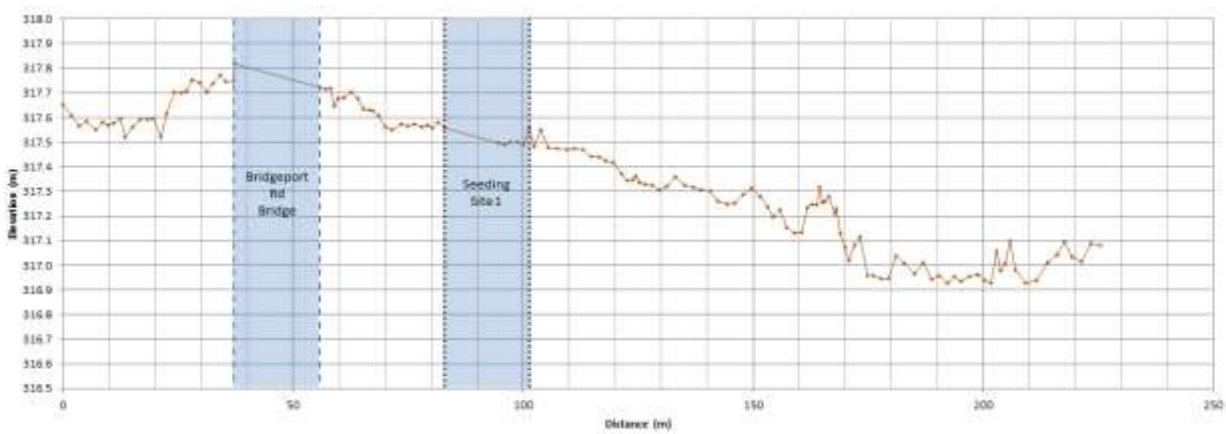

Figure 12: Longitudinal Profile through Site 1

Reach 1 of Laurel Creek is composed of the straight portion of the creek beginning immediately downstream of Bridgeport Road. The seeding site selected within this reach is located on a riffle and is approximately 18 m long. Reach 2 is a straight part of Laurel Creek located at the start of Hillside Park immediately downstream of University Avenue. This reach has the lowest slope of all reaches studied. Reach 3 is located immediately downstream of a pedestrian bridge in Hillside Park and extends to the confluence with Forewell Creek. Reach 4 is located in Bechtel Park approximately 100 m upstream of the pedestrian bridge in the park and extends down to the bridge. The seeding site within this reach is located on a riffle and partially on a run.

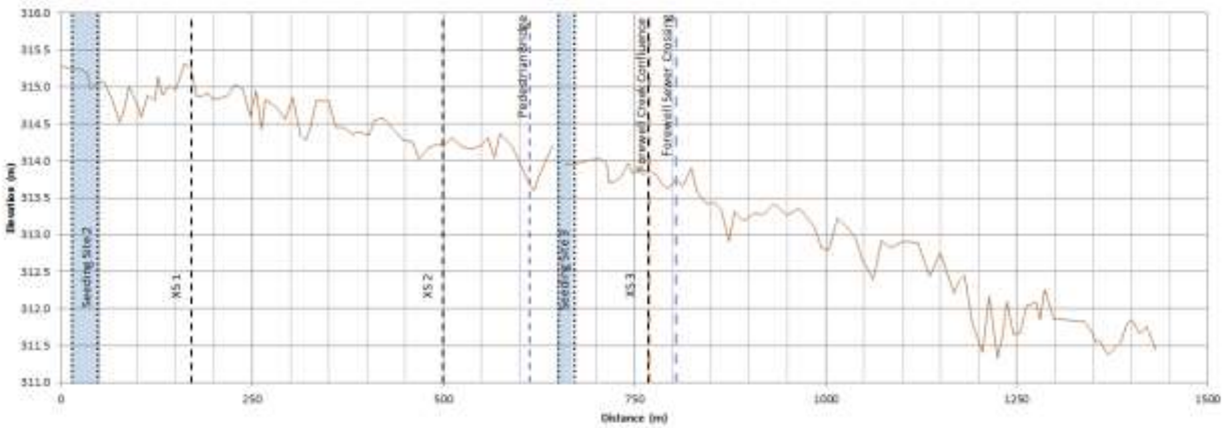

Figure 13: **Longitudinal Profile through Hillside Park**

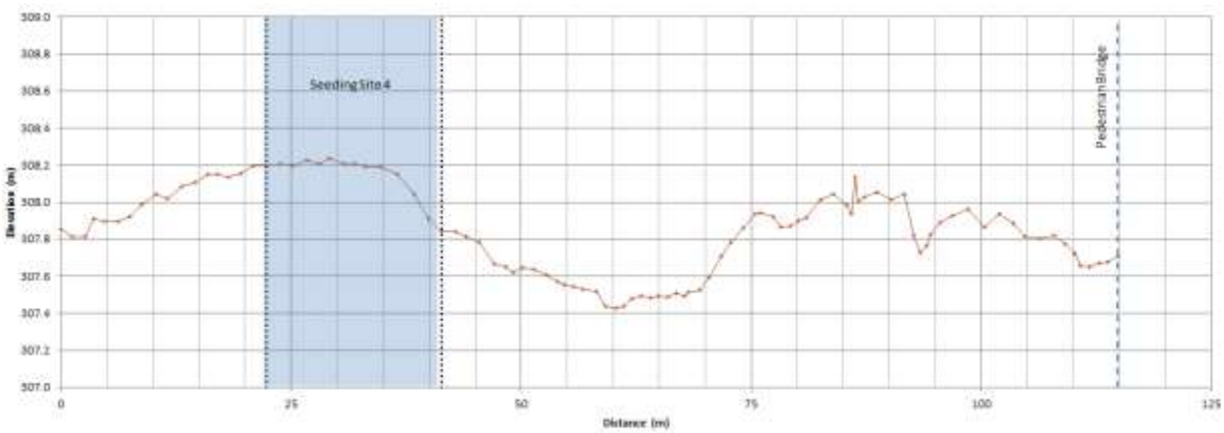

Figure 14: **Longitudinal Profile through Bechtel Park**

3.1.3 Field Work Preparation

Initial site walks and field reconnaissance were conducted to identify site access areas, potential spots for locating benchmarks, identifying potential seeding reaches and to determine the bed material sizes. Benchmarks were then established along the creek to reduce the time taken to survey the locations of tagged rocks following a flood event. Each benchmark was an iron rebar with a piece of flagging marking the benchmark number. Benchmarks were established upstream and downstream of each seeding site on the right and left banks. Additional benchmarks were established approximately 200 m downstream of the seeded reach. The benchmarks were surveyed using a second order differential GPS. A list of benchmark locations and elevations can be found in Appendix A.

Rocks for PIT-tagging were purchased from local landscape supply companies. The rocks were hand selected such that their sizes and lithology (primarily limestone) were similar to those in Laurel Creek. Rocks of sizes ranging from phi classes of -4.5 (22.6 mm) to -7.5 (180 mm) were selected. Table 3 shows the breakdown of the number of rocks in each size category. The lower bound on the range of particle sizes for tagging is limited by the size of the tag, while the upper bound was limited by the largest particle size found at the site during pebble counts and what seemed to be a realistic choice in terms of the size that was expected to be transported.

Table 3: Size Distribution of Rocks

Rock Size					# of Rocks	Tag Size
Bin Size	Lower Bound		Upper Bound			
	mm	Φ	mm	ϕ		
1	22.6	-4.5	32	-5.0	43	Small
2	32	-5.0	45	-5.5	49	Small
3	45	-5.5	64	-6.0	40	Large
4	64	-6.0	90	-6.5	28	Large
5	90	-6.5	128	-7.0	20	Large
6	128	-7.0	180	-7.5	20	Large

Each rock was drilled with either a hammer drill or a drill-press. A drill press was used for the smaller rocks because the smaller limestone rocks were prone to breakage. However, for the larger rocks, a hammer drill was used because it was faster. Masonry drill-bits $\frac{3}{16}$" wide and $2\frac{1}{2}$"

long were used. The rocks were drilled on the face that posed least resistance. Typically, this meant that the rocks were drilled along either a-axis or b-axis. For the smaller rocks, drilling through the a-axis was necessary to accommodate the entire tag. The rocks were then tagged with a PIT-tag and sealed with silicone caulking. Prior to tagging, each tag was programmed with a unique identification code. The mass, volume and size (along a, b, and c axes) of the tagged rocks were then determined. Bin sizes 1 and 2 were tagged with the smaller RFID tags (23 mm); larger tags (32 mm) were used for the remaining bin sizes. Figure 15 shows two drilled rocks and the two different sizes of tags used. The tag number for each rock was written on each rock for quick visual identification during rock placement in the stream.

Figure 15: Drilled rocks and RFID tags

3.1.3.1 Seeding Strategy

Each site was seeded with 200 PIT-tagged rocks in the spring of 2011. Sites 1 and 2 were seeded on April 7, 2011. Sites 3 and 4 were seeded on April 15, 2011 and April 16, 2011, respectively. A total of 800 tagged rocks were used in the field study. The rocks were seeded in 20 cross-sections at each seeding site with 10 rocks in each cross section. Since the creek is of non-uniform width, with the maximum bankfull width of a reach ranging from 8.5 m to 13.5 m in the study sites, the distance between the tagged rocks was often < 0.6 m. The idea behind using large number of tagged rocks in a small section was to ensure that the section of the creek bed chosen for seeding was represented thoroughly.

The representation of the actual bed particles by matching the sizes of introduced tagged rocks to those already present in the bed was important since in-situ material was not used for tagging and seeding. For the purposes of proper representation, data acquired from pebble counts and grain size analysis was put to use. To simplify the process, 200 particles with the same grain size distribution were seeded in each reach. This grain size distribution was matched to that of Site 4. This site was chosen as it contained the coarsest fraction of all sites as shown in Table 4. Though Site 1 has a larger median grain size, the larger D_{84} values in Site 4 indicated that coarser sediment was likely transported through this reach at some point before bed armouring. There seemed to be a possibility for the coarser fraction to move in large flood events. Additionally, the morphology of the creek at Site 4 was more "developed" than Site 1. The presence of point bars, a developed "riffle-pool" sequence, easy access to floodplain and large riparian areas in Site 4 as compared to Site 1 meant that the channel was in the state of continuously evolving through aggradation and erosion without a constrained corridor as was observed in Site 1. In order to determine what material was most likely transported by competent floods, Klingemann surface sampling method was employed to sample substrate from a point bar located immediately upstream of the seeding location at Site 4. Both pavement and sub-pavement samples were collected. The grain size distribution of the collected samples is shown in Figure 16.

Table 4: Summary Size Parameters of Channel Substrate

Category	Site 1	Site 2	Site 3	Site 4
D_{16} (mm)	10.8	2.3	0.6	5.8
D_{35} (mm)	26.4	7.3	4.0	15.2
D_{50} (mm)	36.6	12.6	7.2	27.7
D_{84} (mm)	72	76	56	113
D_{95} (mm)	115	180	90	230
D_{100} (mm)	362	512	512	1024

After the particle size distribution of Site 4 was chosen, a piecewise polynomial function was used to fit the pebble count data. The particle size distribution ranging from 22.6 mm to 1024 mm was truncated to 180 mm and the higher end and was matched to imitate the piecewise polynomial function as close as possible. This distribution is shown in Table 3 and Figure 17. The general shape of the distribution was followed expect at the upper end, i.e., the last two size classes. Size class 5 has fewer particles than size class 6. However, for a reasonable sample size (minimum 10% of total samples), it was necessary that that last two size classes contain a minimum of 20 seeded rocks. Particles, particularly the spherical ones, in the range of 16 to 22.6

mm were not used because they were prone to breakage during the drilling process. Elongated (rod shaped) particles of this range were less prone to breakage. However, they did not bear resemblance to the shape of those in the field. Therefore, this range was ignored.

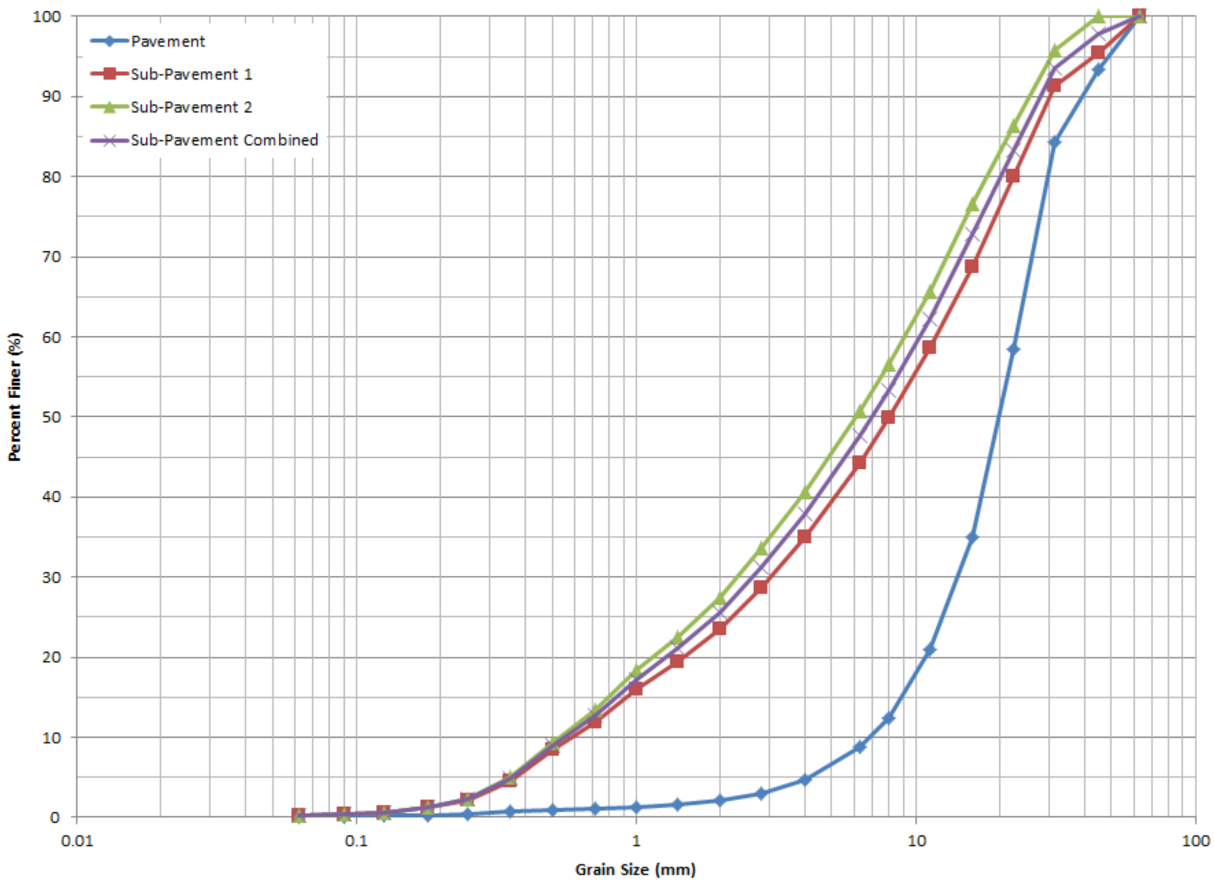

Figure 16: Grain Size Distribution of Bulk Samples from Site 4

At the outset of this study, a single grain size distribution was chosen for the sake of simplicity; however, in hind sight, to represent the bed accurately, it would have been more appropriate to customize the grain size distribution of the seeded particles according to each reach instead of applying the same size distributions to all reaches in the creek. Additionally, the lower sizes classes (11.3 mm to 22.6 mm) could also have been represented with the utilization of smaller RFID tags measuring 12 mm; however, the author was unaware of the availability of these tags at the beginning of the study. The smaller size fractions that the bedload also comprises of are under-represented in this study.

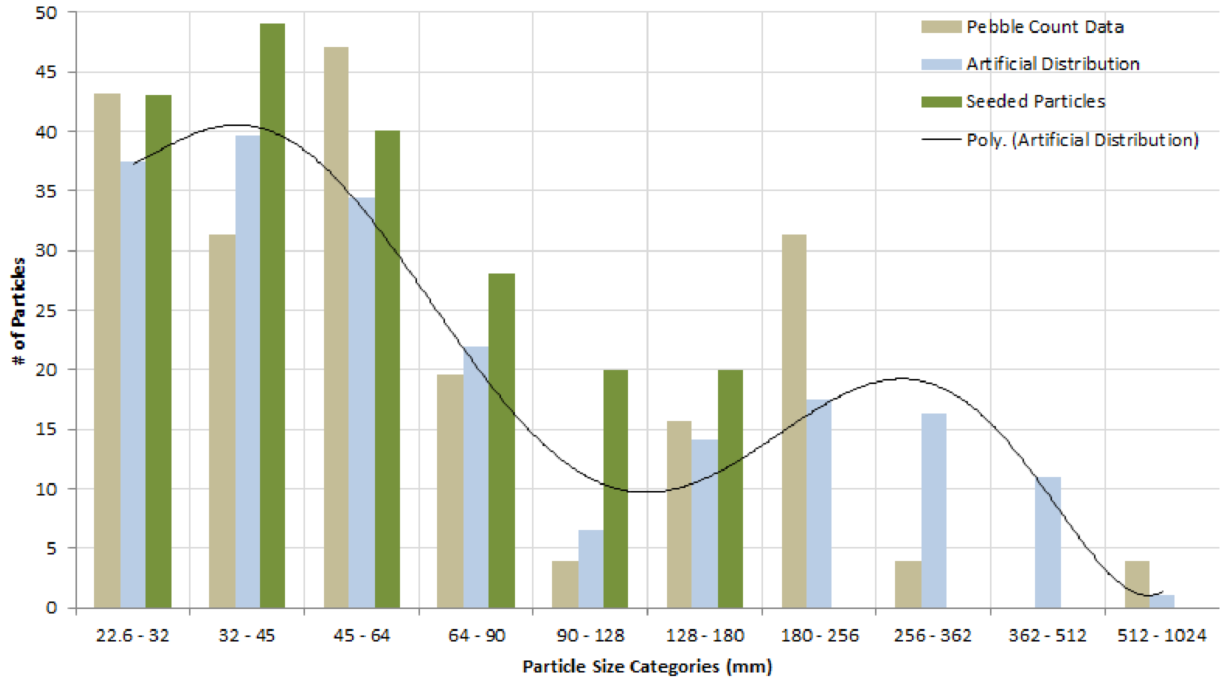

Figure 17: Size Distribution of Particles in Bechtel Park (Site 4)

Once a particle size distribution was determined, the next step was to determine the pattern in which the particles would be seeded. Figure 18 shows the seeded rocks from rows 1 through 20 for Site 3. The rocks are ordered from left bank to right bank going from left to right in the picture. The column of rocks on the left show rocks seeded from rows 1 through 10 and those on the right show rocks from rows 11 to 20. These rocks were used in the third site. The same distribution pattern was used for the other three sites. The size distribution of the rocks was such that each size category was placed along a cross-section. Figure 19 shows a visual distribution of the rocks placed in a seeding reach. Alphabets from ‘a’ to ‘j’ indicate the positions along a cross-section. Numbers from 1 to 20 indicate the cross-sections (rows) of rocks in a seeding reach. The numbers in the coloured boxes indicate the size category or the bin size to which the rocks belong.

Figure 20 shows the four different shapes of rocks used as tracers. The shapes (Disc, Sphere, Blade, and Rod) follow Zingg’s classification system (Zingg, 1935) as found in (García, 2007) is based on the ratios of the long (a axis), intermediate (b axis) and the short axes (c axis) of the rocks. Most of the rocks (42%) used in the study were spherical. 31% of the rocks ware disc-like. Rod like particles and blade like particles composed 19% and 8%, respectively.

Figure 18: Site 3 - Seeded Rocks

	a	b	c	d	e	f	g	h	i	j
1	1	5	2	6	1	1	1	2	4	2
2	2	1	5	2	4	5	2	5	2	1
3	3	2	1	4	2	3	4	3	1	5
4	5	3	3	1	3	2	3	1	6	3
5	1	4	2	3	1	1	1	2	3	2
6	2	1	4	2	5	4	2	4	2	1
7	3	2	1	5	2	3	4	6	1	4
8	4	3	2	1	3	2	5	1	4	3
9	6	5	3	2	1	1	1	2	3	2
10	1	4	6	3	2	4	2	3	2	6
11	2	1	4	4	4	5	3	4	6	1
12	3	2	1	6	6	3	4	5	1	5
13	6	3	2	1	3	2	6	1	5	3
14	4	6	3	2	1	1	1	2	3	2
15	1	4	5	3	2	4	2	3	2	6
16	2	1	4	4	6	2	3	4	4	1
17	3	2	1	5	4	6	6	6	1	3
18	5	3	2	1	3	3	2	1	5	2
19	6	5	3	2	1	1	1	2	3	4
20	2	6	6	3	2	2	3	3	2	5

Bin	# of rocks
1	43
2	49
3	40
4	28
5	20
6	20

Figure 19: Size-distribution of rocks in a seeding reach

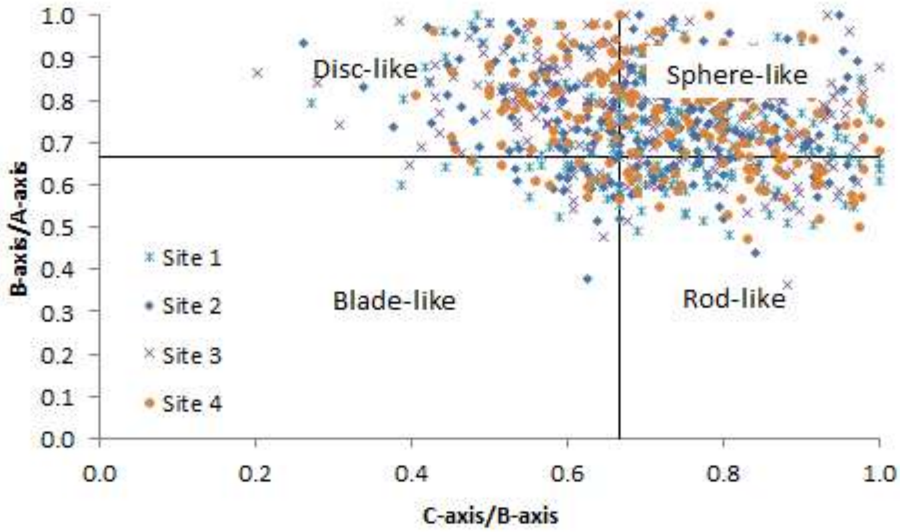

Figure 20: Tracer Shape (Zingg's classification)

3.1.4 Tracking Events

The rocks were tracked on three separate occasions. The dates on which seeding and tracking were undertaken on each site is listed in Table 5. Sites 2 and 3 could not be tracked during the second and the third tracking events because they were inaccessible due to construction. To prevent the loss of tagged rocks during construction through these sites, the rocks were extracted immediately after the first tracking event.

Table 5: Seeding and Tracking Dates

Event	Site 1	Site 2	Site 3	Site 4
Seeding	April 7, 2011	April 7, 2011	April 15, 2011	April 16, 2011
Tracking 1	August 11, 2011	July 25, 2011	July 27, 2011	August 10, 2011
Tracking 2	October 26, 2011	-	-	November 2, 2011
Tracking 3	June 19, 2012	-	-	June 20, 2012

Tracking events generally followed a bankfull flow event during the period of study. Tracking could not be undertaken until the flows from the bankfull events had receded to flows that were safe to wade in. Figure 21 shows the discharge data as obtained from the Water Survey of Canada flow gauge 02GA024 situated at Weber St. Bridge over Laurel Creek (less than 500m upstream of Site 1). The figure also shows the dates of seeding and the tracking events. Tracking was conducted using a Leoni RFID antenna from Aquartis. Once a position of a tagged rock was determined, its position was surveyed using a total station. Due to the large range in the reading distance of the antenna, as discussed on Section 2.2, the surveyed location does not necessarily provide an accurate location of the tag.

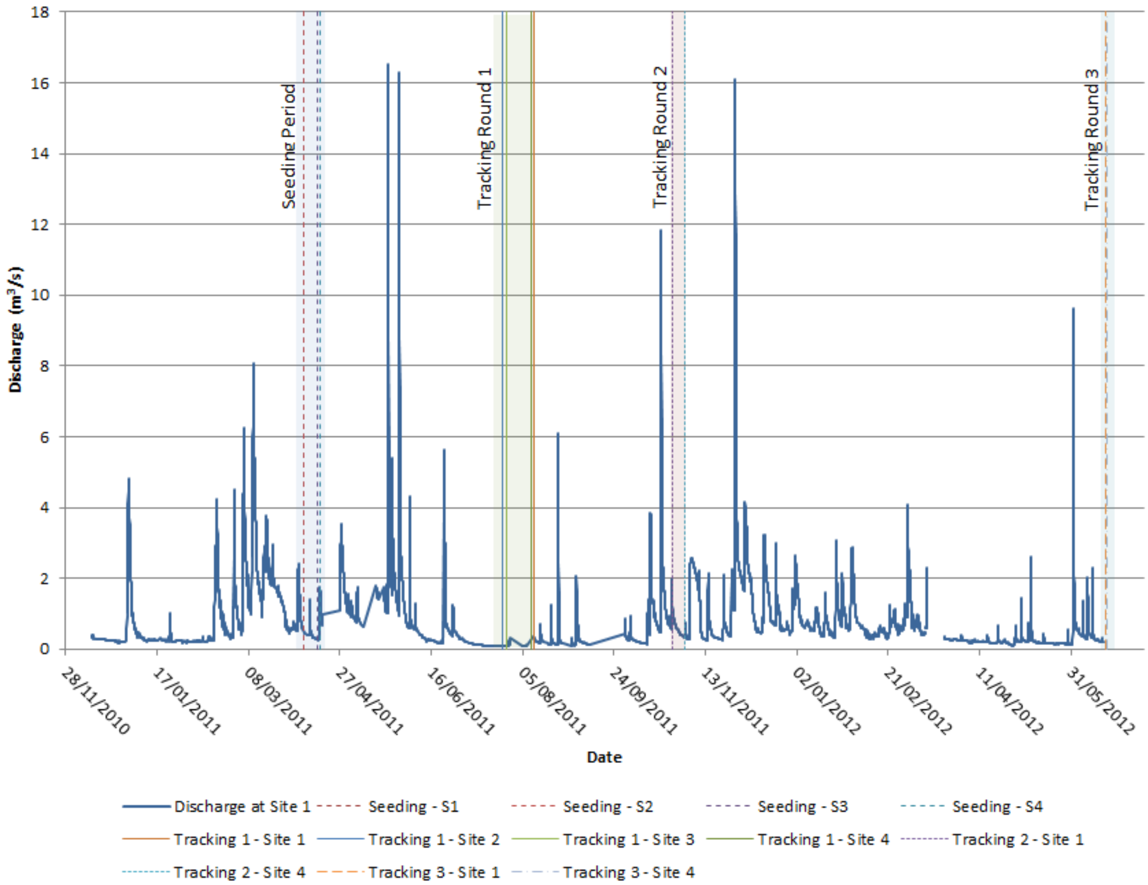

Figure 21: Laurel Creek Discharge at Site 1

3.2 Lab Methods

A box filled with sediment (the "sandbox") was constructed to perform the lab tests designed to help determine the effects of certain factors that confound tracer detection. The sandbox (8' x 8' x 4') was waterproofed before being filled in with ~ 3 cubic yards of granular A material. Since the box had to be strong enough to hold gravel and water, steel banding around the box was used to reinforce the sides. Figure 22 is a collage of the pictures of sandbox under construction. The top left picture (a) shows the bottom frame of the sandbox. The next picture (b) is that of the constructed bottom and 2 sides. The third picture (c) is that of a completely constructed sandbox lined with multiple sheets of polyethylene to render the sandbox waterproof. The picture also shows steel banding along the sides of the box. The bottom left picture (d) shows a 2' long pipe placed in the corner of the box. The pipe was used to house a tube attached to a sump pump that could drain the sandbox after 'wet' experiments. The bottom middle picture (e) shows the box being filled with granular A mix and the last picture (f) is that of the completely constructed sandbox.

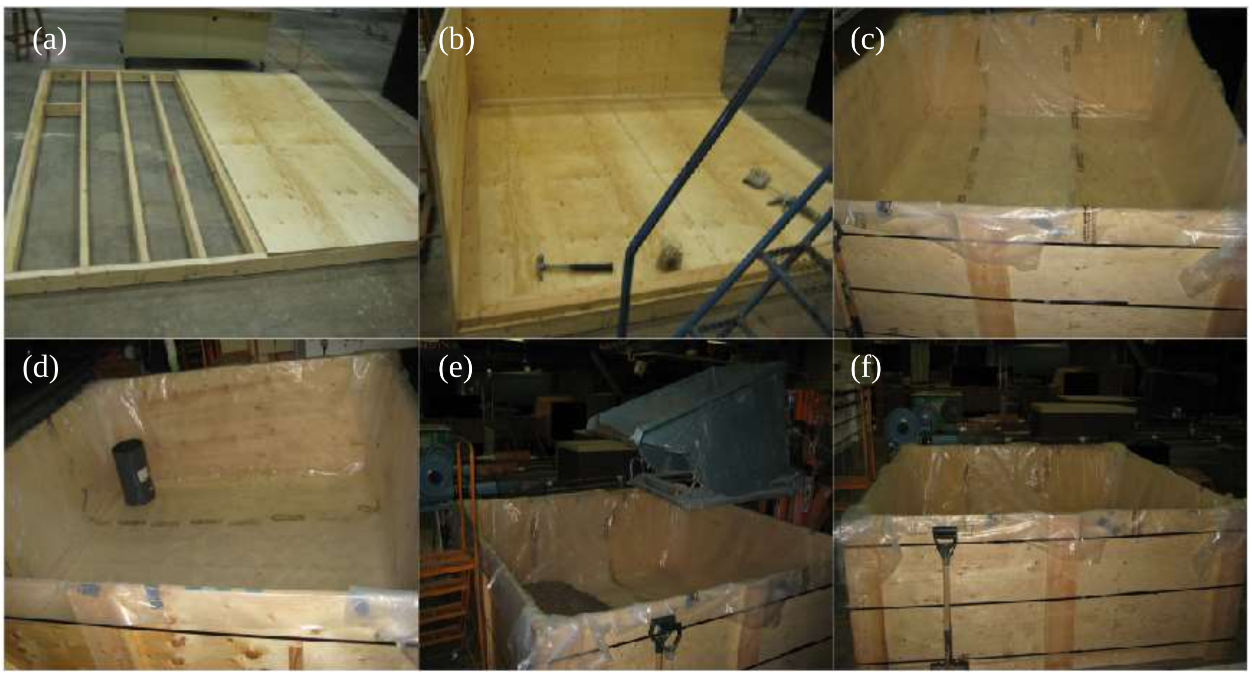

Figure 22: Photos of Sandbox Construction

The RFID system used in the sandbox is the same system as that described in sections 2.2 and 3.1. A total of 36 rocks, 6 rocks for each of the 6 phi class bins (Table 3) were used for laboratory experiments.

3.2.1 Experimental Design

Experiments were designed to study the general range of the antenna, the effect of tagged rock size on the detection distance, the effect of antenna and rock orientations on the detection distances, the effect of the moisture conditions of the substrate (dry, wet – at saturation, wet –

under submerged conditions) and the depth at which the tagged rock is buried on the detection distance. Experiments were also designed to study the detection distances when more than one tag was present in an interrogation zone. Certain zones of no detection were identified in the field sites. These zones of no detection or "skip zones" were also studied in the lab experiments. Lastly, some of the experiments performed in the laboratory were repeated in the field to test the repeatability of the results in a field setting.

3.2.2 Antenna Tests

As noted by Nichols (2004) and as observed in Laurel Creek field tests, the orientation of the antenna affects the signal pick-up and, hence, the maximum detection distance. Antenna tests were designed with different orientations to account for the different detection ranges and to quantify the differences in the orientation. Table 6 shows lists the various characteristics of the antenna tests. The tests can be broadly categorized into two categories: those with the tagged rock in horizontal and vertical orientations. The horizontal orientation of the rock refers to the positioning of the rock such that the tag in the rock is parallel to the plane of the soil substrate that it is placed on or within. Typically, this meant that the rocks were placed such that their a-axes were parallel to the soil substrate. For vertical orientations, the rocks were placed such that their tags were perpendicular to the plane of the soil substrate. Detection ranges for test numbers 1 to 24, as shown in Table 6, were measured along the plane parallel to the plane of the soil substrate. Detection ranges for tests 25 to 31 were measured at an angle and "through the air". These tests were designed to give a "normal" projection of the detection range of the antenna through space. All distance measurements were taken from the "tip" of the antenna. The tip of the antenna is that portion of the antenna that has a black plastic pipe around the aluminum housing. All tests were performed with the antenna held at a distance of 2" above the ground with the antenna held parallel to the surface of the soil.

The general axis of measurement is shown in Figure 23. A total of six antenna tests are shown in the figure. These tests were conducted for all lab experiments whereas tests not shown in the figure were only performed for selected experiments. In each of the picture, the position of the rock is indicated by an orange flag. The yellow ruler shown in the photographs correspond to the x-axis. The naming convention used for the tests describes the orientation of the tag with respect to the soil surface (i.e, horizontal – H, or vertical – V), the angle of measurement (0˚, 45˚ or 90˚

with respect to the y axis) and the orientation of the antenna (a – antenna tip tangential to the tag with the antenna's centroid offset from the centroid of the tag by a distance of the radius of antenna, b – antenna tip farthest from the tag, c – antenna's plane placed perpendicular to the surface of the soil with the antenna tip at the bottom. Tests 25 through 31 listed in Table 6 were given names to reflect the plane and angles along which measurements were taken.

Table 6: Description of Antenna and Rock Orientations for various tests

Tests		Rock Orientation	Antenna Angle			Antenna Orientation	
#	Name	Horiz./Vert.	in x-y Plane	in x-z plane	in y-z plane	with respect to Ground	"tip"
1	H-0	Horizontal	along y	-	-	Parallel	Forward
2	H-45	Horizontal	At 45°	-	-	Parallel	Forward
3	H-90	Horizontal	along x	-	-	Parallel	Forward
4	H-0b	Horizontal	along y	-	-	Parallel	Backward
5	H-45b	Horizontal	At 45°	-	-	Parallel	Backward
6	H-90b	Horizontal	along x	-	-	Parallel	Backward
7	H-0c	Horizontal	along y	-	-	Perpendicular	Bottom
8	H-45c	Horizontal	At 45°	-	-	Perpendicular	Bottom
9	H-90c	Horizontal	along x	-	-	Perpendicular	Bottom
10	H-0a	Horizontal	along y	-	-	Parallel	Tangential
11	H-45a	Horizontal	At 45°	-	-	Parallel	Tangential
12	H-90a	Horizontal	along x	-	-	Parallel	Tangential
13	V-0	Vertical	along y	-	-	Parallel	Forward
14	V-45	Vertical	At 45°	-	-	Parallel	Forward
15	V-90	Vertical	along x	-	-	Parallel	Forward
16	V-0b	Vertical	along y	-	-	Parallel	Backward
17	V-45b	Vertical	At 45°	-	-	Parallel	Backward
18	V-90b	Vertical	along x	-	-	Parallel	Backward
19	V-0c	Vertical	along y	-	-	Perpendicular	Bottom
20	V-45c	Vertical	At 45°	-	-	Perpendicular	Bottom
21	V-90c	Vertical	along x	-	-	Perpendicular	Bottom
22	V-0a	Vertical	along y	-	-	Parallel	Tangential
23	V-45a	Vertical	At 45°	-	-	Parallel	Tangential
24	V-90a	Vertical	along x	-	-	Parallel	Tangential
25	H-z	Horizontal	-	along z	-	Parallel	Forward
26	H-xyz	Horizontal	At 45°	At 45°	At 45°	Parallel	Forward
27	H-yz	Horizontal	along y	-	At 45°	Parallel	Forward
28	H-xz	Horizontal	along x	At 45°	-	Parallel	Forward
29	V-z	Vertical	-	along z	-	Parallel	Forward
30	V-xyz	Vertical	At 45°	At 45°	At 45°	Parallel	Forward
31	V-yz	Vertical	along y	-	At 45°	Parallel	Forward

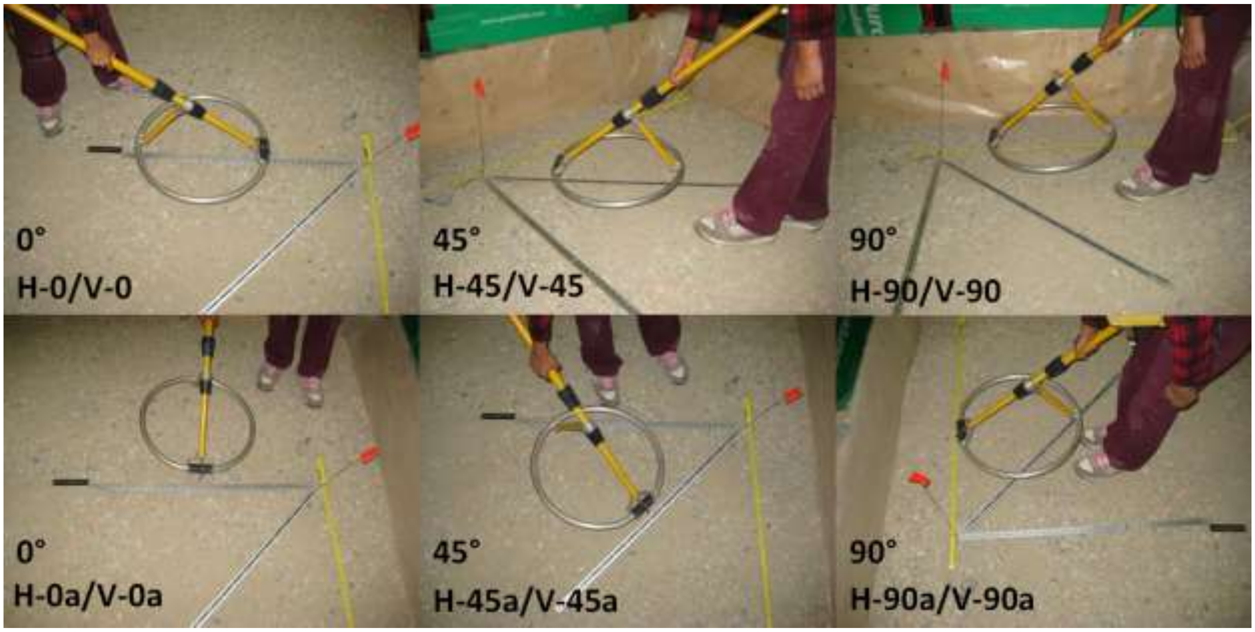

Figure 23: Photographs of Antenna for various tests

3.2.3 Experiments

This section details the experiments performed in the laboratory. All experiments were performed in the sandbox except for the orientation test experiments which were performed on the concrete floor of the laboratory.

3.2.3.1 Antenna Range and Uniformity

To reduce the amount number of laboratory tests conducted, a preliminary test was conducted to examine the uniformity of the antenna's range. If the antenna detection ranges could be found to be more or less equivalent in all four quadrants, testing could be limited to one quadrant and similar results could be expected for other three quadrants. The transponders were placed at the centre of the sandbox. Lateral detection distances were recorded along the horizontal and the vertical axes parallel to the soil surface in all four quadrants. Measurements were also recorded at a 45° angle from both x and y axes in each quadrant. Thus, a total of eight readings were taken for each tag. A total of 25 bare tags each of small and large sizes were tested.

3.2.3.2 Effect of Tag Orientation

To study the effects of tag orientation on detection ranges, 25 bare tags of each size (large and small) were tested. This set of experiments was performed by placing the tags on the concrete floor surface of the laboratory (not in the sandbox) to ensure that the positioning of the bare tags were not affected by the undulations on the surface of sand and gravel mixture in the sandbox. The tags' orientations with respect to the surface were tested, i.e., the tags were placed horizontally (with the long axis of the tag placed parallel to the test surface) and vertically (with the long axis of the tag placed perpendicular to the test surface). For each of these orientations, 0, and 0a tests were performed. In addition to horizontal and vertical orientations, the positioning of the tag with respect to the direction to which the copper turnings within the transponder were pointing was also changed and its effects on the detection distance were studied. The orientation was labeled "north" when the end of the transponder with the copper turnings was faced away from the antenna, and the orientation was named "south" when the end with the copper turnings faced toward the antenna. Tests H-0, H-0a, V-0, and V-0a were performed for both north and south orientations on all 25 small and 25 large tags.

3.2.3.3 Effects of Rock Size

One possible confounding factor in the establishment of definitive detection ranges for RFID tags was identified to be the size of the rock into which the tag was inserted. To study this potential confounding factor, thirty six tagged rocks (six rocks from each of six size categories identified in Table 3) were tested. Rocks from the first two size categories were tagged with small tags and the rest of the rocks were tagged with large tags. All 31 tests listed in Table 6 were performed for the large tags. For the small tags, only tests H-0, H-45, H-90, H-0a, H-45a, H-90a, Hxyz, and their corresponding vertical tests were performed. The rocks were placed in the sandbox such that the tag was at the soil surface. For this configuration, the rocks had to be partially embedded so that the tags in horizontal orientation were aligned to the soil surface, and the tags in vertical orientation were placed so that half of the tag was exposed out of the soil.

3.2.3.4 Effects of Burial depths

To determine if the burial of tags affected detection ranges, tagged rocks were buried at depths of 3", 6", 12" and 18", and a number of tests, (H-0, H-45, H-90, H-0a, H-45a, H-90a, Hxyz, and their corresponding vertical tests) were performed for 24 tagged rocks (12 small tags and 12 large tags). The tagged rocks were buried under thick polythene bags filled to a 3" width with substrate from the sandbox. The bags were placed on a wire mesh attached to ropes for ease in lifting and lowering the bags. The time taken to perform each test was reduced by avoiding having to dig through the sandbox to place the tagged rock at a particular depth, covering the rock with substrate and repeating this process for every rock for each orientation test. Additionally, by placing the tagged rocks at the same location between the bags for each test for a certain burial depth, repeatability of the tests were ensured. Any errors that could have been introduced through having varying degrees of compaction of the substrate above the tagged rock were also eliminated by using bags whose compaction did not vary greatly between tests. However, continued burial tests led to gradual degradation of the box.

3.2.3.5 Effects of Saturation and Submergence

Laboratory experiments to study the dampening effect of water on the detection range were performed by filling the sandbox to the point of saturation, and carrying out H-0, H-45, H-90, H-0a, H-45a, H-90a, Hxyz, and their corresponding vertical tests. These tests were repeated with the level of water in the sandbox being kept constant at 6" above the soil surface. These saturated and submerged tests were performed for 12 tagged rocks (large tags), which were placed at surface level and at a depth of 6". Saturated tests were also performed for tagged rocks placed at a depth of 12". Tagged rocks (12 small tags) were tested at the surface level under conditions of saturation.

For the buried saturated/submergence tests, the same "bag-approach" described in the previous section was used. To ensure that substrate inside the bags was saturated, the polythene bags were pierced to allow for flow of water. To prevent the soil from leaking out of the bags, the polythene bags were put into burlap sacks. Figure 24 is a series of photographs that show the preparation of the sandbox for testing and the conditions within the sandbox during the buried and wet tests. The top left picture (Figure 24 a) shows a dug hole into which a blue recycle box (Figure 24 b) was placed to maintain the shape of the hole. The next figure (Figure 24 c) shows polythene bags filled with substrate placed into the blue box. The rulers were arranged over these bags for the measurement of detection distances. Holes were pierced through the blue box and the bags (Figure 24 d) to allow for seepage in the wet tests. The pierced bags were placed in burlap sacks (Figure 24 e). Figure 24 f shows wire mesh with rope handles that were used to lower the substrate bags into the blue box. Figure 24 g and Figure 24 h show setup for a wet test. In the wet tests, flags were placed to mark positions of the rock and the ends of the blue box. Finally, a completed setup with 6" depth of standing water is shown in Figure 24 i. The rulers for measurement were set in place at a depth that allowed for easy reading using large rocks. This was essential because the visibility through the murky waters was poor.

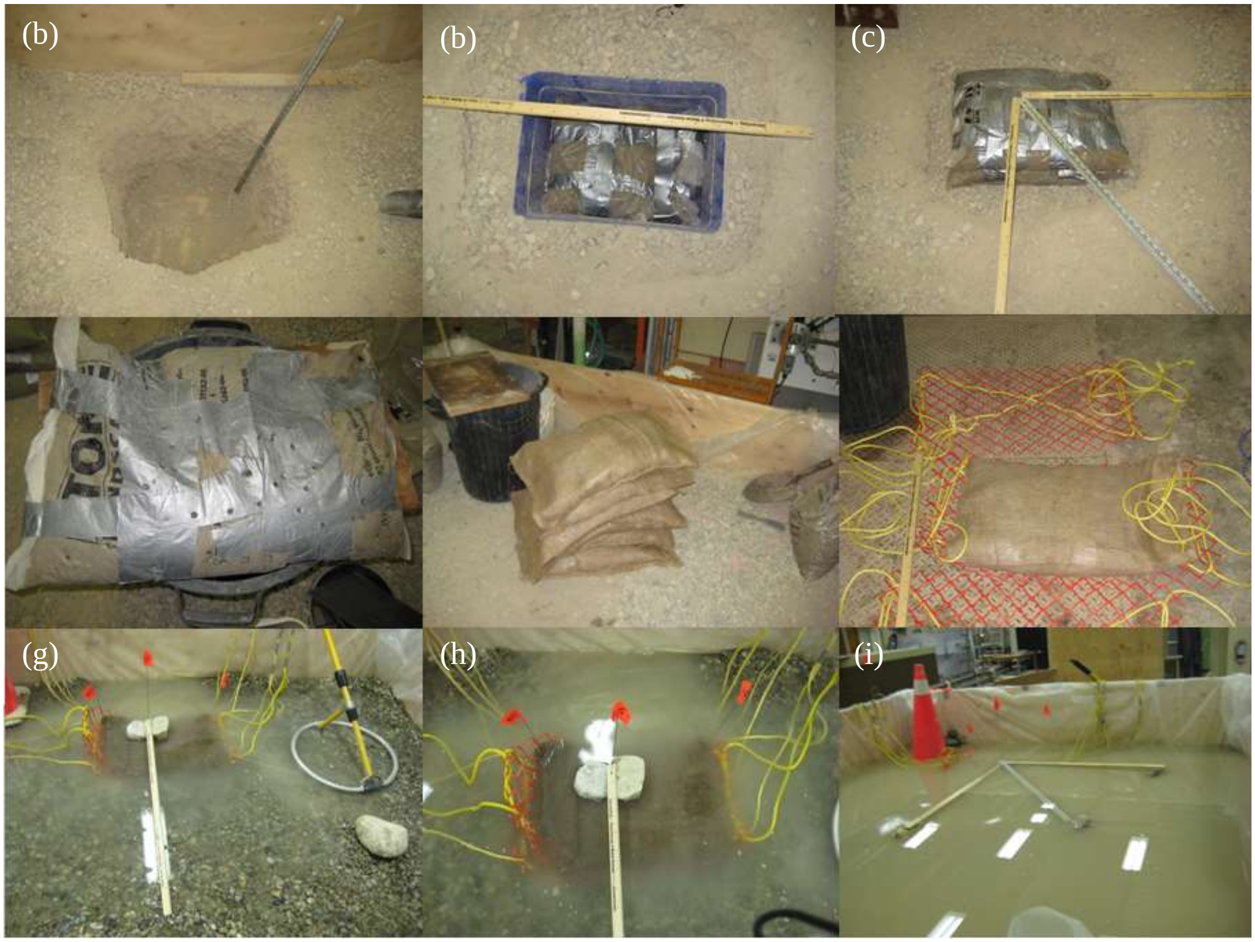

Figure 24: Photographs of Sandbox: Preparation for Burial and Wet Tests

3.2.3.6 Skip Zones

The presence of skip zones was first identified in the field. Lab tests were performed to quantify the skip zones. Tests were performed on a wooden board placed in the sandbox (see Figure 25). Two large tags and two small tags were tested. Each tag was tested in the north and south orientations. Additionally, each test was conducted with the tag placed at 4 rotational positions. The tags were rotated along their long axes by 90° for each test. The test procedure consisted of moving the antenna parallel to the plane of the wooden surface and parallel to the long axis of the tag, offset from the tag by a distance of 2 cm. The offset distance was arbitrarily chosen to keep the antenna from making physical contact with the tag. The distances at which the antenna beeped were recorded.

Figure 25: Skip Zone Testing

3.2.3.7 Effects of Clusters

Another possible confounding factor in the determination of detection distances is the presence of one or more tagged rocks in the interrogation zone of another. Preliminary tests found that the effect of clusters is difficult to fully quantify, even in laboratory conditions. For this reason, the simplest configuration of clusters of two rocks was employed to study how the presence of more than one tag in the interrogation zone could change the detection range. For this purpose, one tagged rock was left stationary, i.e., in the same position throughout the entire experiment. The second rock (movable rock) was placed at different locations and the detection distances were recorded by performing tests H/V-0, H/V-45 and H/V-90. The stationary tagged rock was located at the origin of the axes of measurement whereas the movable tagged rock was placed along the x axis (90°), the y axis (0°) and at a 45° angle between the x and y axes. Along each of these axes, the movable rock was tested at distances ranging 0 to 100 cm from the stationary rock at increments of 5 cm. At each test location, the orientations of the tags were changed. A total of four sets of tests (HH, HV, VH, and VV) were performed by changing between horizontal (H) and vertical (V) orientations. The first and last alphabets in the test names represent the stationary and the movable rocks, respectively, e.g., HV indicates that the stationary rock was in a horizontal orientation while the movable rock was positioned in a vertical orientation.

It is important to note that the detection distances recorded were that of the stationary rock. During the process of carrying out a test, the antenna sometimes did not pick up the signal for the stationary rock till it actually passed over the rock. In these circumstances, the detection distances were recorded as negative numbers.

A total of twelve sets of experiments were performed involving 3 axes of rock positioning with 4 combinations of rock orientations. For each of the twelve sets of experiments, twenty one measurements (i.e., measurement at each of 21 discrete distances between the stationary and the movable rocks) were taken. A test set up showing test VV with the movable rock situated along y axis (0°) 50cm from the stationary rock is presented in Figure 26. The blue arrows show the three axes along which measurements were made for each test.

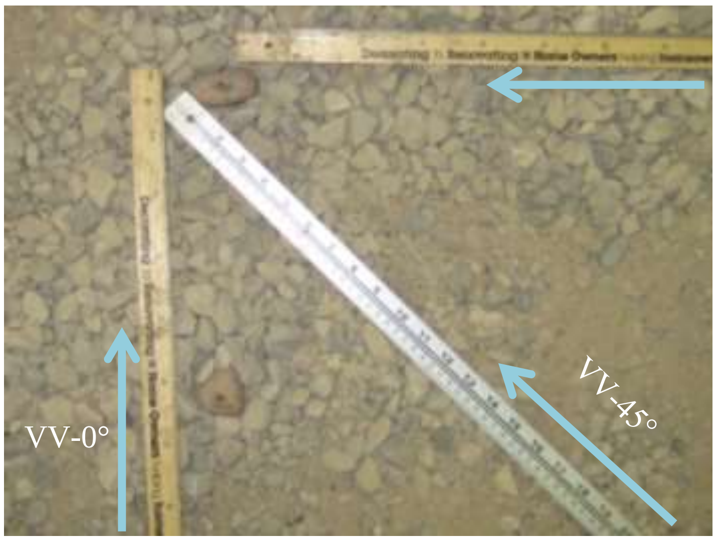

Figure 26: Cluster Test VV Setup with Rock Position at 0°

The measured detection distances from each cluster test were compared to a baseline. The baseline detection distance, L, is the detection distance of the stationary rock of the same tagged rock without another tagged rock in its interrogation zone. The metric $L/_2$, i.e., half the detection distance of the tagged rock (without another in its vicinity) was used to study the results. A sample results figure (see Figure 27) shows the $L/_2$ line for the three axes of measurement. The results for the tests shown (VV-0°, 45°, and 90° for Rock Position at 0°) were normalized by $L/_2$. The movable tagged rock was moved along the 0° axis; both rocks were placed in the vertical position. The measurements for tests VV-0°, 45°, and 90° are plotted in blue, red, and magenta. Each of these lines represents 21 discrete measurements. The abscissa for each of the lines represents the distance between the stationary and the movable rocks. The ordinate for each of the lines represents the normalized distance.

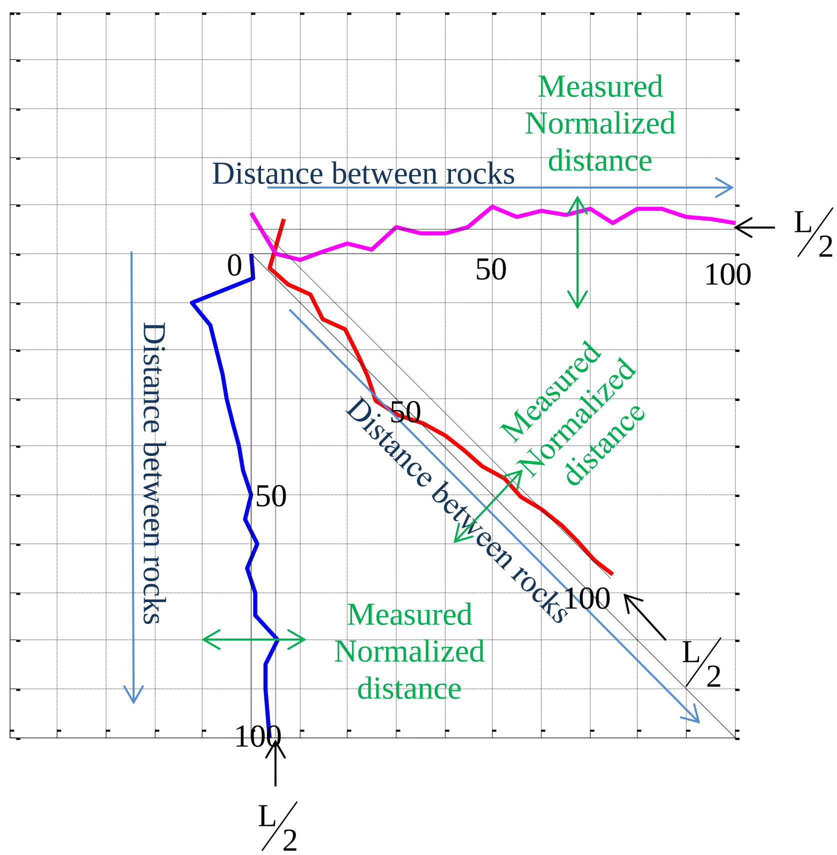

Figure 27: Sample Figure for Cluster Tests VV-0°, 45°, and 90° for Rock Position 0°

3.2.3.8 Field 'Lab' tests

Some field experiments were also performed to confirm the lab results. The experiments were performed in the Bechtel Park site of Laurel Creek on a point bar directly upstream of Site 4 on the right bank. Tests H-0, H-45, H-90, H-0a, H-45a, and H-90a, and the corresponding vertical tests were performed for six rocks tagged with small tags and 12 rocks tagged with large tags. For these tests, the rocks were placed on the surface under dry and saturated conditions. The tests were conducted with the large tagged rocks placed on the surface of the gravel bar. However, the small tagged rocks were tested under both conditions – with the rocks placed on the surface and with the rocks partially embedded in the gravel bar such that the tag in the rock was aligned to the surface of the gravel bar. Surface tests were also performed on rod, disc and wedge shaped tags (Figure 28). In addition to the surface tests, buried tests were also performed for six rocks tagged with small tags. Burial tests were performed at 3”, 6”, and 12”.

Figure 28: Rod, Disc and Wedge Shaped Tags Tested in the Field

4 FIELD RESULTS

The results of the three tracking events discussed in Section 3.1 are presented in this chapter. Relevant survey data are presented in Appendix A. The effects of properties of individual tracers on transport within the four study reaches are presented. Table 7 presents a summary of recovery rates of each tracking event in all sites. Recovery rates reported in Table 7 are the ratio of tracers found to the number of tracers originally seeded, expressed as a percentage. Rates presented for all events are relative to the seeding event. More tagged rocks were found in the third tracking event than the second event. As mentioned previously, Sites 2 and 3 could only be tracked once due to site access limitations.

Table 7: Summary of Recovery Rates

Event	Site 1	Site 2	Site 3	Site 4
Tracking 1	97.0%	93.5%	95.0%	98.0%
Tracking 2	81.5%	-	-	82.5%
Tracking 3	91.5%	-	-	92.0%
Average	*90.0%*	*95.0%*	*95.0%*	*90.8%*

As expected, the average recovery rates of the tagged particles were fairly high, i.e., over 90%. These results are comparable with those obtained by Bradley and Tucker (2012), whose lowest recovery rate is 93% for a total of 893 PIT tagged coarse gravel clasts in a four year period of study.

4.1 Overview of Tracer Movement

In this study, movement (or mobility) is defined as the change in location of a tracer rock by a minimum distance of 1 metre; therefore, if the location of the tracer differed from its original location by less than 1 metre, it was considered not to have moved. This distance was chosen as the minimum required for movement to have taken place, since the Aquartis antenna can detect a tag from up to a distance of 1 meter (Aquartis, 2011). The drawback of this definition of movement is that displacements of less than 1 metre were not included in the determination of path lengths. An improved tracking method would have been required to quantify tracer movement measuring less than 1 metre; investigations leading to the development of such method were the focus of subsequent laboratory experiments, whose results are presented in Section 5. It should also be noted that path lengths is defined in this study as simple two dimensional Euclidean distances (i.e., a straight line between two points in space). In reality, the tracers are likely to have followed more complicated and potentially tortuous trajectories of displacement along the sinuous channel length; however, quantifying such movement is beyond the scope of the study.

During each tracking event, the location of each tracer was surveyed and the distance each tracer had moved from its initial seeding location was calculated. Summary statistics for the movement of all tracers at each site were calculated for each tracking event and are presented in Table 8. Tracking events 1, 2 and 3 are represented by the abbreviations T1, T2, and T3, respectively. The number of tracers that moved in each tracking event is noted in the column entitled "Nm". The largest discharge rate recorded by the WSC gauge 02GA024 preceding the tracking event is also presented in the table. The largest floods occurred between the seeding event and the first Tracking event, and between the second and the third tracking event.

Table 8: Summary Statistics of Tracer Movement

				Path length from initial seeding location (m)	
Site	Event	Flow (m^3/s)*	Nm (%Nm)	Mean ± Standard Error	Minimum-Maximum
1	T1	16.5	89 (44.5 %)	5 ± 0.6	1 - 28.3
	T2	11.8	87 (43.5 %)	4.9 ± 0.6	1 - 28.5
	T3	16.1	127 (63.5 %)	5 ± 0.6	1 - 41.5
2	T1	16.5	34 (17.0 %)	2.7 ± 0.5	1 - 18.8
3	T1	16.5	82 (41.0 %)	10.8 ± 1.3	1 - 50.3
4	T1	16.5	105 (52.5 %)	6.7 ± 1.1	1 - 74.7
	T2	11.8	92 (46.0 %)	4.2 ± 0.3	1 - 15.0
	T3	16.1	104 (52 %)	8.7 ± 1.3	1 - 74.7

* Flow was measured at the WSC gauge station located between Sites 1 and 2.

The largest travel distances were observed in sites 3 and 4. The highest numbers of mobile tracers were observed in sites 1 and 4. Site 2 experienced the least movement with only 34 of the

200 tracers experiencing mobility, possibly on account of this site being a deposition zone. The highest mean tracer path length was observed at Site 3. The maximum distance travelled by a tracer was 74.7 m. This tracer was detected in Site 4 during both the first and the third tracking events, but not in the second tracking event.

A map showing tracer movement in sites 1, 2, 3, and 4 are shown in Figure 29, Figure 30, Figure 31, and Figure 32, respectively. The x and the y axes in the figures refer to the easting and the northing (measured in metres), respectively, of the surveyed points. Aerial photos of all four sites showing the location of the tracers are provided in Appendix B for reference.

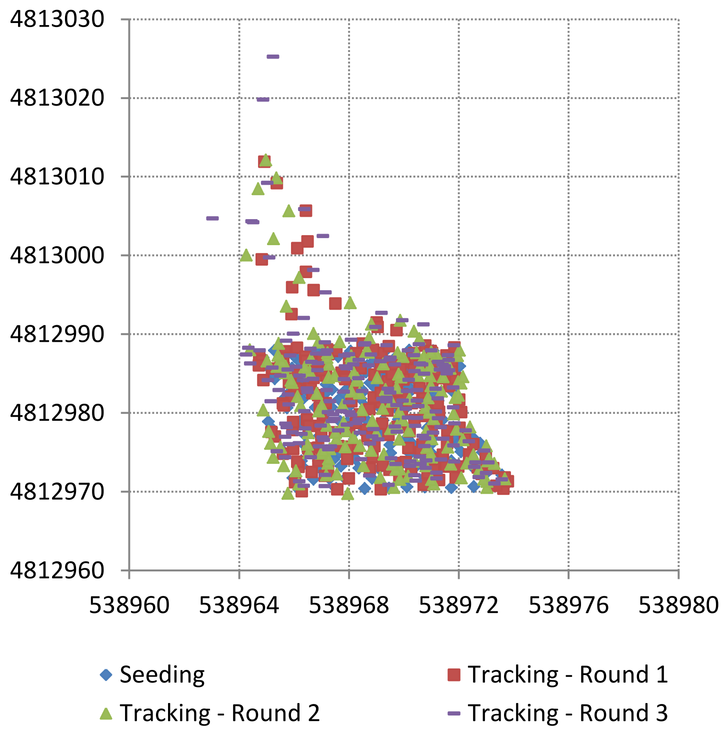

Figure 29: Particle Tracking in Site 1

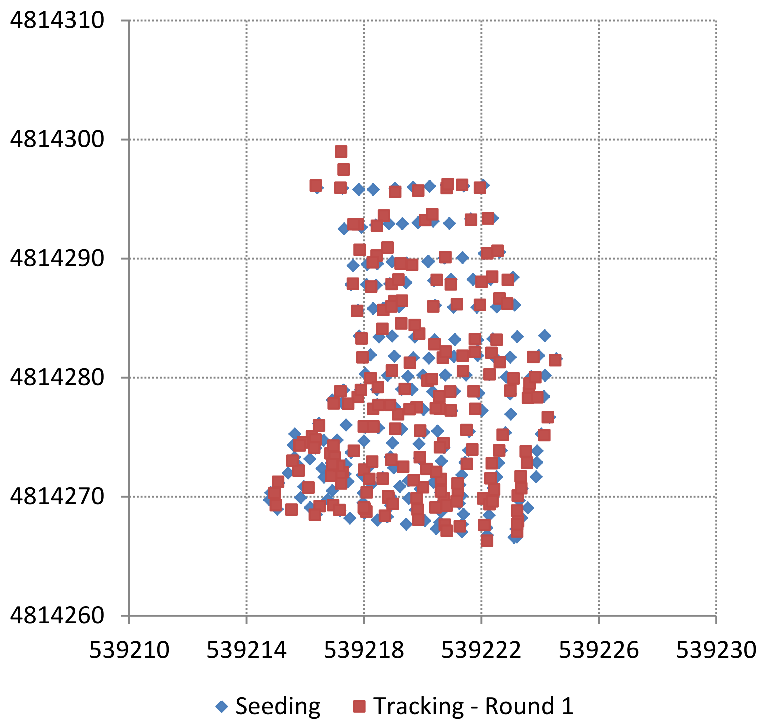

Figure 30: **Particle Tracking in Site 2**

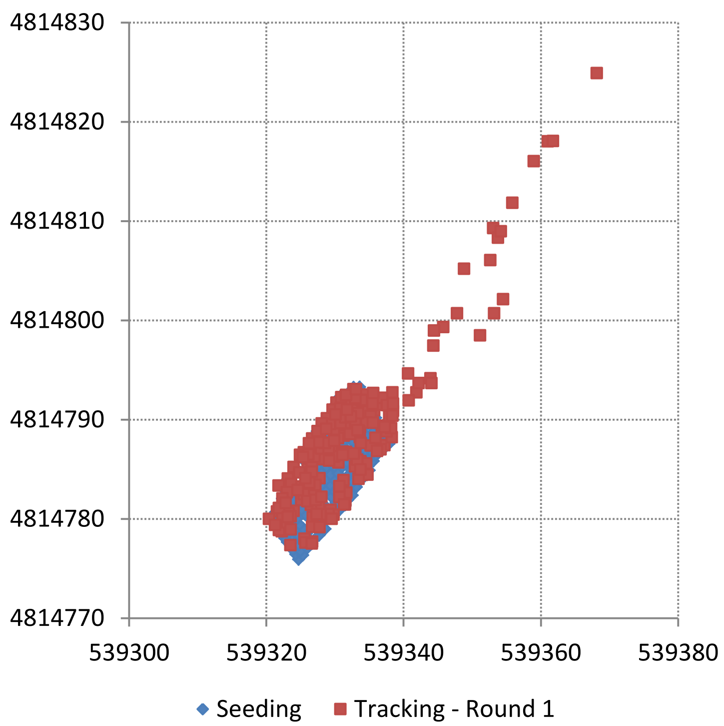

Figure 31: **Particle Tracking in Site 3**

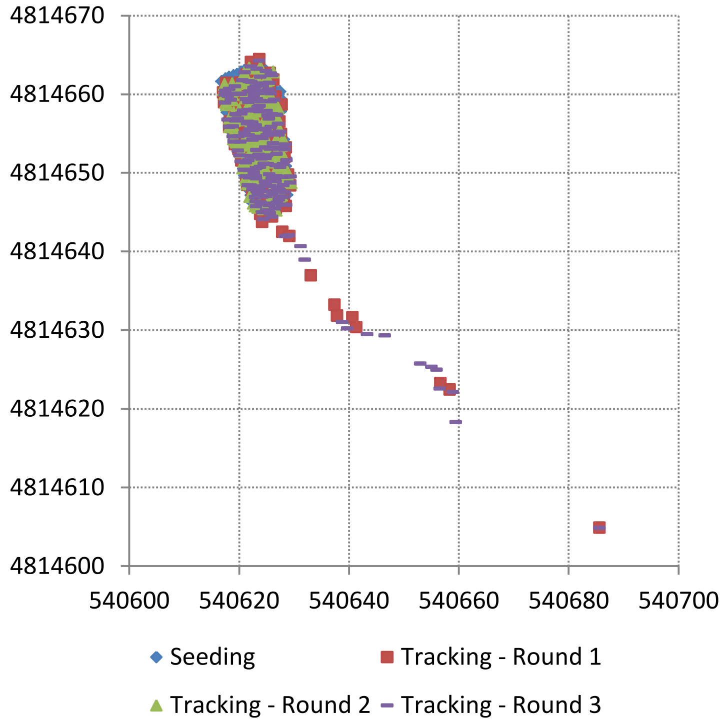

Figure 32: Particle Tracking in Site 4

4.2 Path Length and Size Classes

Particle transport can be very size selective. The results in this section examine the relationship between the various size classes of tracers and their path lengths. Generally, it was expected that the smaller size classes would travel the farthest and larger size classes would travel the least. However, results in this section show that the relationship between size and path length was not linear.

4.2.1 Site 1

Figure 33 shows the normalized path lengths ($L'/L_{D_{50}}{'}$) and percent of mobility (P_m) plotted against normalized grain sizes (D/D_{50}) as per the approach of Church and Hassan (1992) MacVicar and Roy (2011). The path lengths and percent mobility for each tracking event are calculated with respect to the tracer location from the previous tracking event.

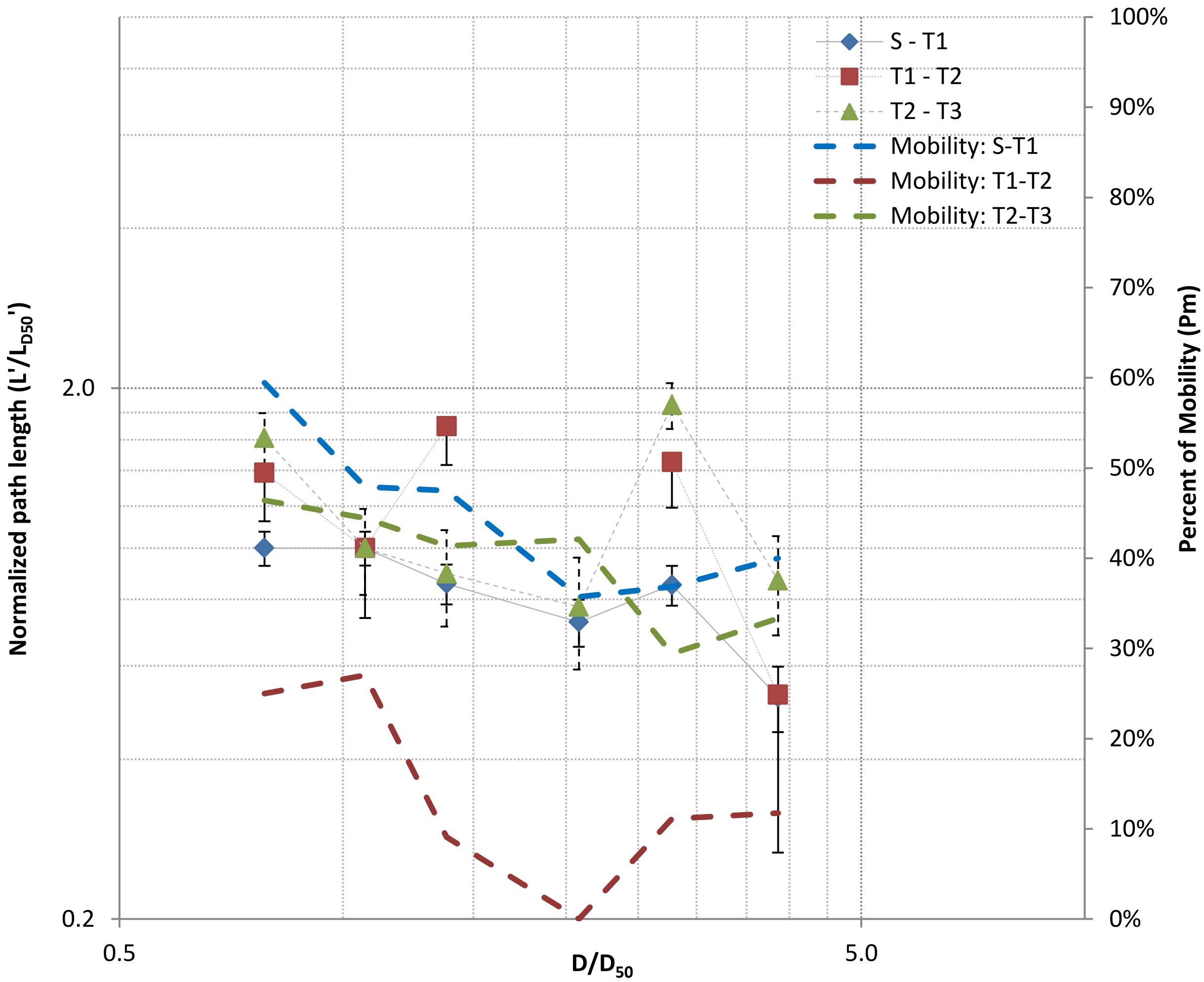

Figure 33: Path length and mobility versus particle size comparisons of various scenarios in chronological order at site 1

The percent of mobility is the percentage of tracers that moved out of all the tracers recovered in a given tracking event. Normalized path length is the geometric mean distance travelled by a certain size class normalized by the geometric mean distance travelled by the median size group of the surface material. The median size group of the surface material was determined using pebble counts (See Appendix A) and the distances travelled by tracers of the same size class as the median size group were used to determine the geometric mean distance travelled by the median size group of the surface material (L_{D50}'). The grain size (D) was normalized using the median b axis diameter of the surface material (D_{50}) since this is the layer of grains that normally gets entrained in the sediment transport process and makes up the bed structure. For this site, the path lengths were normalized to the geometric mean of the path length of the second size class. The second tracking event showed the lowest recovery rates (as shown in Table 7) and also showed the least mobility. During this event, no particle of the fourth size class was observed to have moved. As expected, the percent of mobility (the percentage of tracers that moved at least 1 m) was the highest for the first tracking event. The percent of mobility dropped for subsequent events. It is interesting to note that with an increase in size, the path length dropped, except for the anomalous fifth size class. This supports the hypothesis that smaller rocks are mobilized more easily than larger rocks that need higher shear stresses to be moved.

Figure 34 shows the same metrics as in the previous figure. However, the metrics for tracking events are plotted with respect to the location of the tracers at seeding. The percent mobility was the highest for the third tracking event. This suggests that particles that did not move during previous events moved in the subsequent events. As noted previously, the path lengths generally decreased with increasing particle size. However, the particles in the fifth size class had a greater path length.

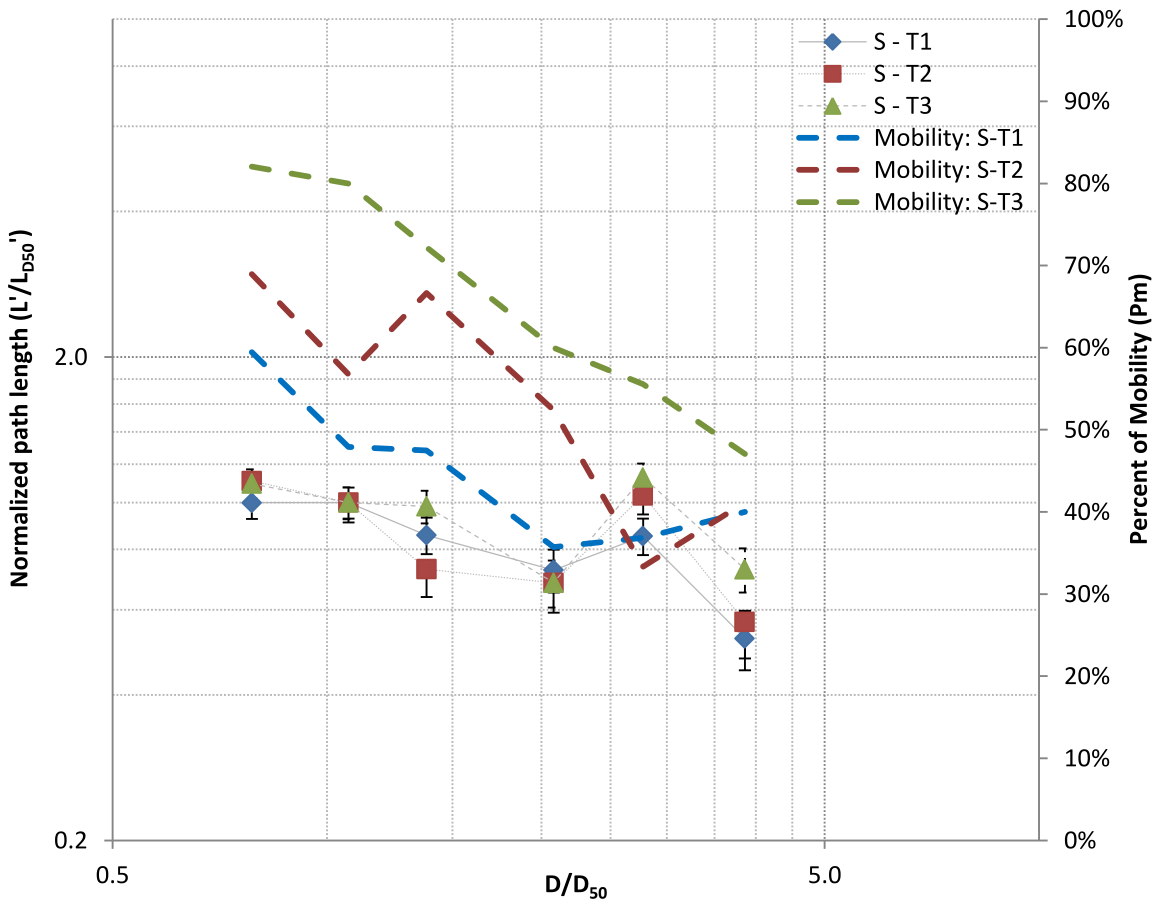

Figure 34: **Path length and mobility versus particle size comparisons between seeding and tracking scenarios at site 1**

4.2.2 Site 2

Figure 35 shows the normalized path lengths and the probability of motion for the various size classes in Site 2. Only the first four size classes showed movement. This site was observed to be a depositional zone. The first and the fourth size classes showed the Figure 37most movement. The sizes classes in between showed the least movement. The percent of mobility declined with the increase in the size of the particles.

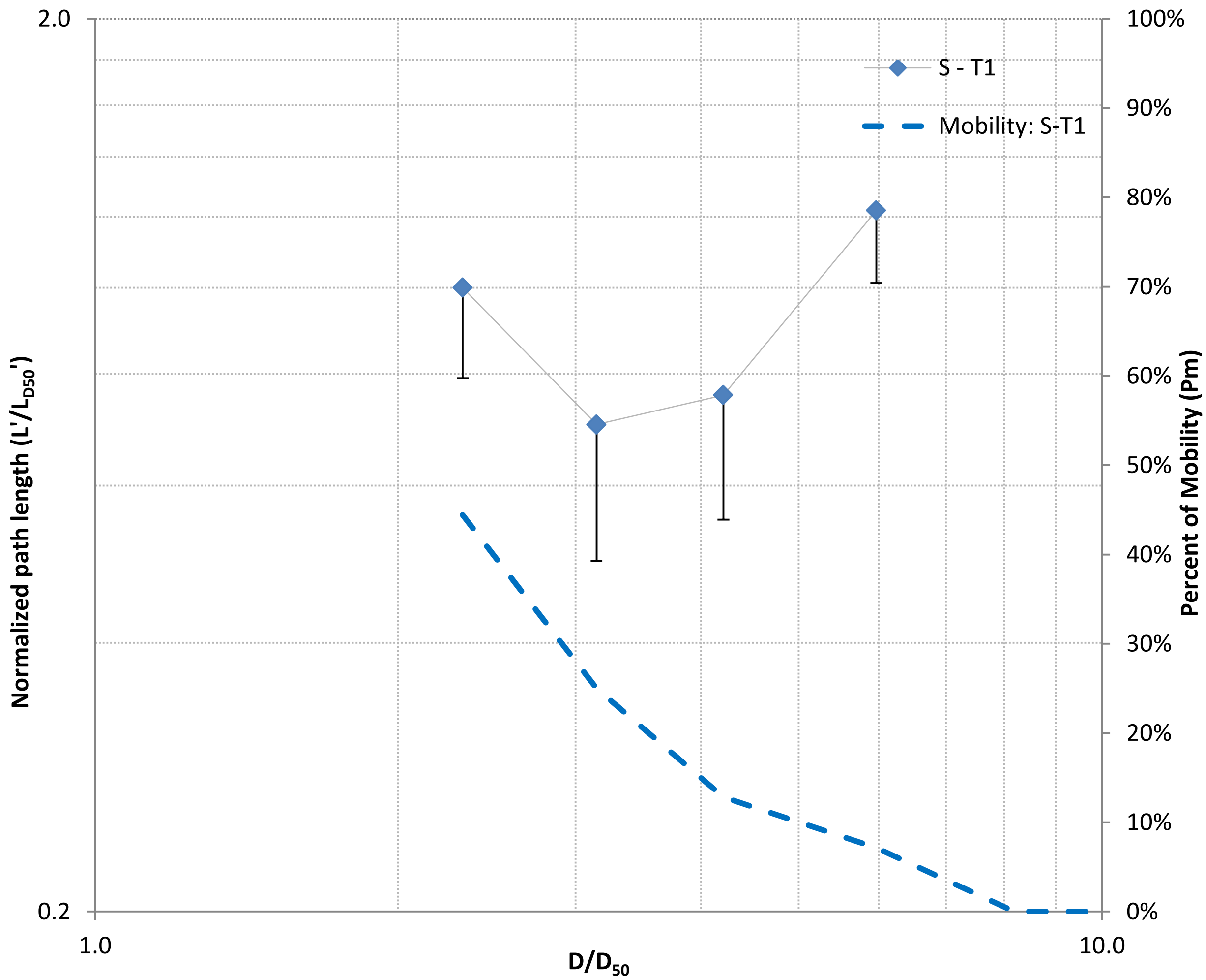

Figure 35: Path length and mobility versus particle size at site 2

4.2.3 Site 3

Figure 36 shows the normalized path lengths and the probability of motion for the various size classes in Site 3. In general, percent mobility and path length declined as the particle size increased.

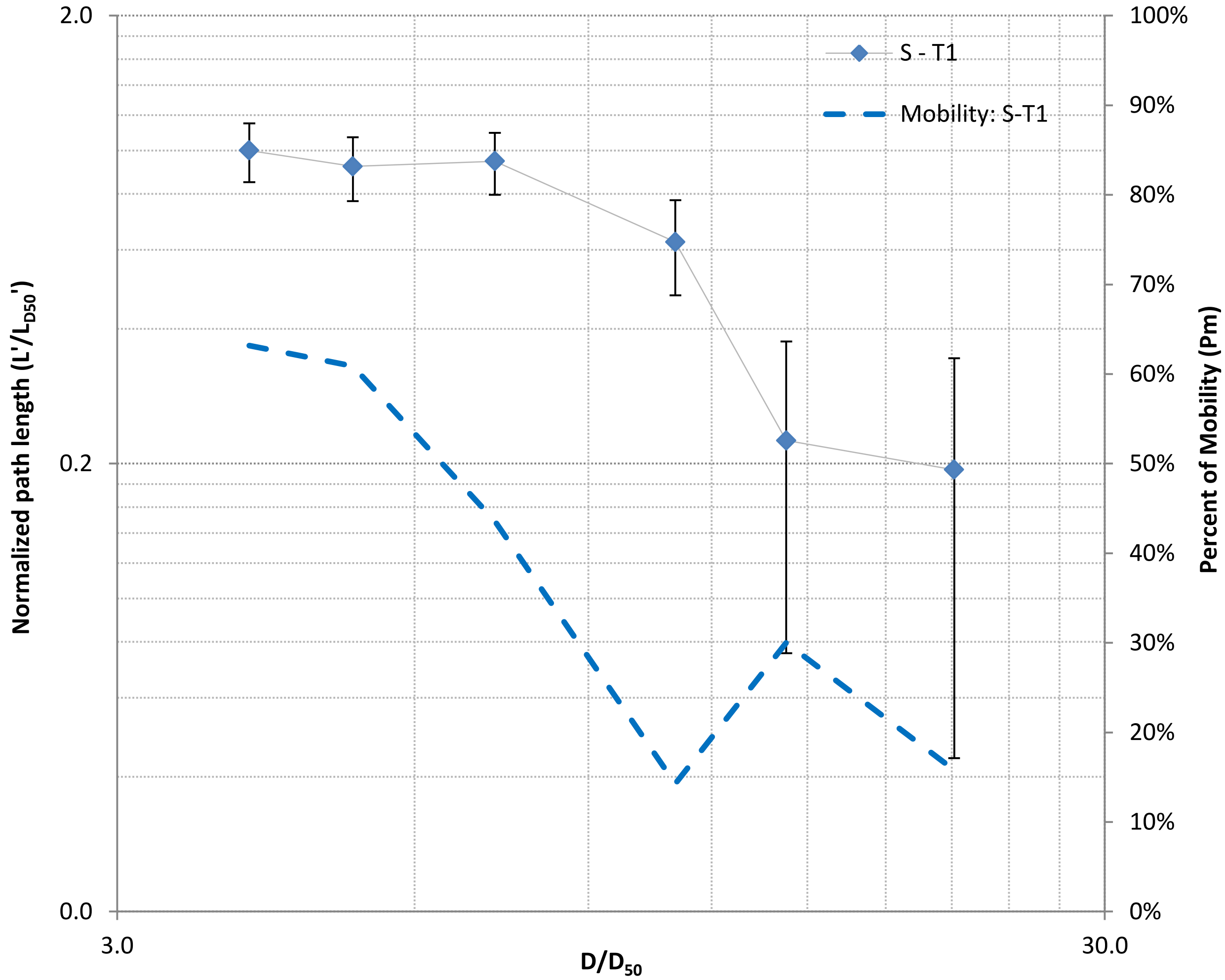

Figure 36: **Path length and mobility versus particle size at site 3**

4.2.4 Site 4

Figure 37 shows normalized path lengths and percent of mobility of particles of various size classes for Site 4. The path lengths and percent mobility plotted in Figure 37, for each tracking event, are calculated with respect to the tracer location from the previous tracking event. The path lengths were normalized to the geometric mean of the first size class for Site 4. Particle recovery was the lowest in the second tracking event. The largest mobility was observed in the first tracking event and the lowest mobility was observed in the second tracking event. It is possible that the low recovery rate affected the percent mobility results since the particles that did move could have remained undetected. The largest path lengths were observed for the first two tracking events and the smallest path lengths were observed for the third tracking event. The first tracking event occurred after the seeding event and after two large flood events. When the tracers were initially seeded, they were placed loosely on the creek bed. Therefore, the path lengths measured reflect the movement of the particles from a “free” state. During the subsequent measurements, the particles would have been incorporated into the native sediment matrix and hence were not in a “free” state. They also would have faced hindrance to motion posed by other neighbouring particles. It is interesting to note that all particles recovered from the sixth size class experienced motion between the seeding event and the first tracking event. The path length for this size class was also the highest as recorded during the first tracking event. For the subsequent tracking events, it is likely that the particles from the higher size classes got trapped by surrounding sediment and were unable to move as far as the smaller size classes.

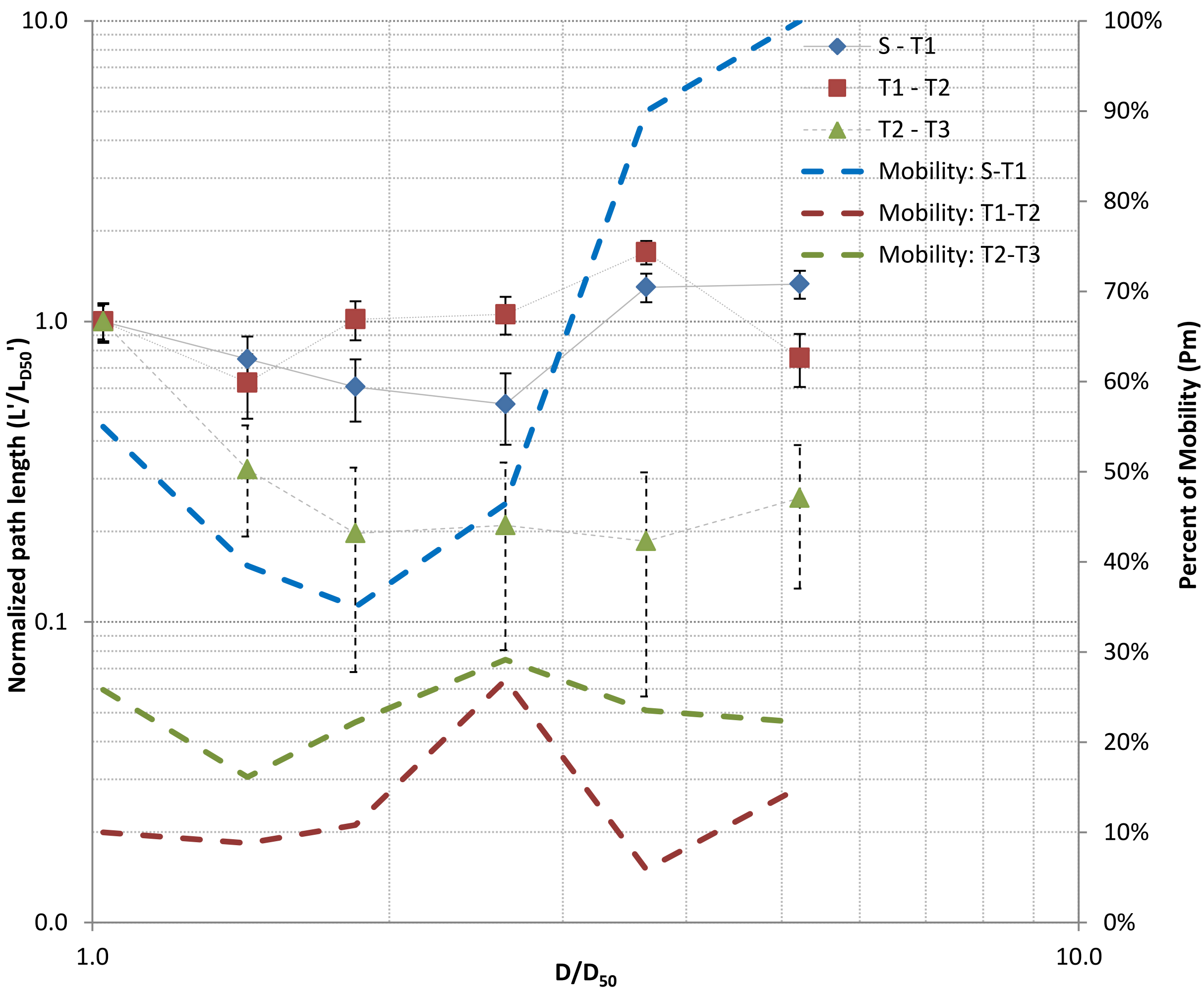

Figure 37: **Path length and mobility versus particle size comparisons of various scenarios in chronological order at site 4**

Figure 38 shows the same metrics as in the previous figure. However, the metrics for tracking events are plotted with respect to the location of the tracers at seeding. Though the recovery rate for the second tracking event was not high, the particles of all size classes except the second size class in Site 4 moved the most between the first and the second tracking events, as can be seen by inspection of normalized path lengths.

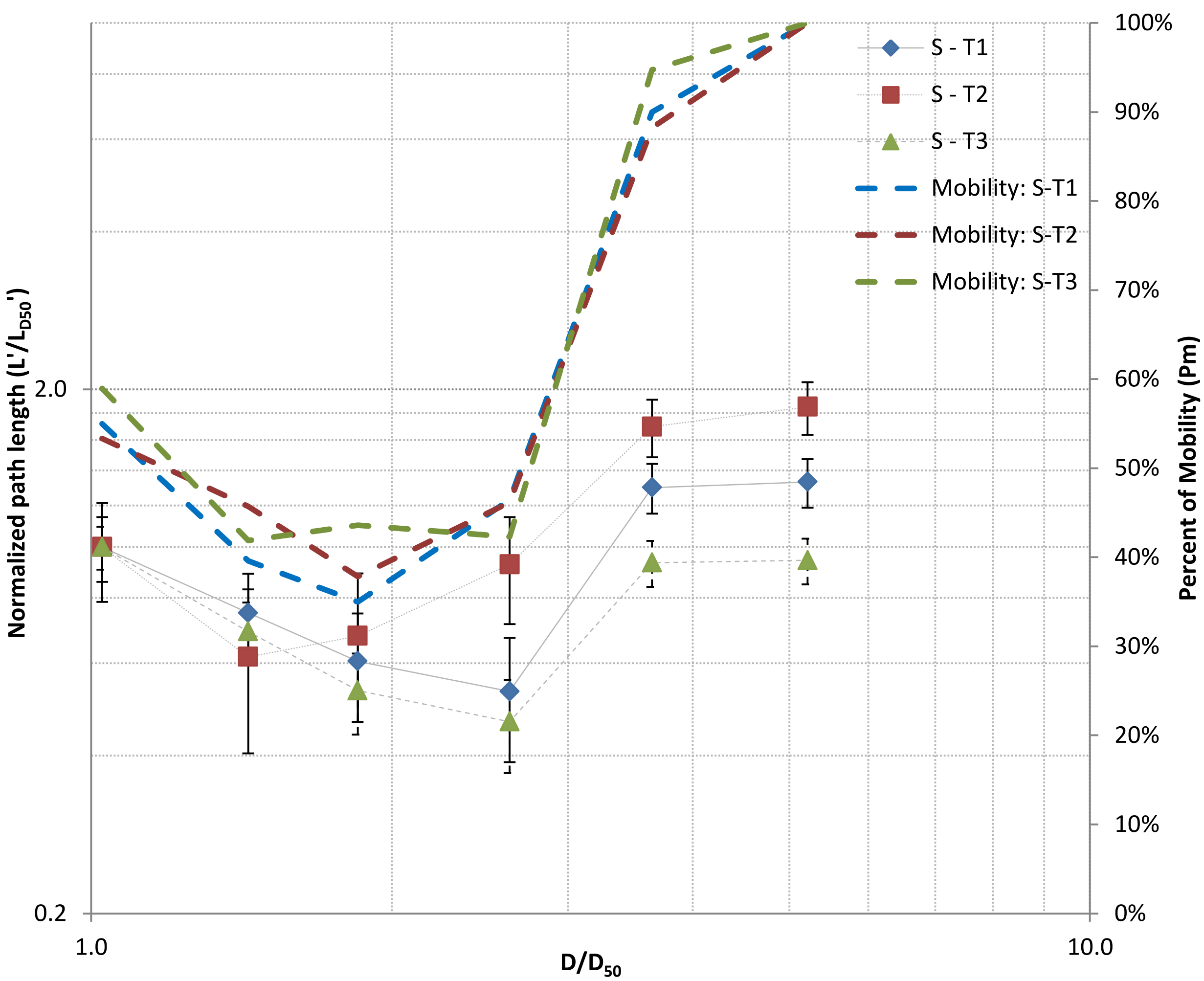

Figure 38: **Path length and mobility versus particle size comparisons between seeding and tracking scenarios at site 4**

5 LAB RESULTS

Raw data from lab tests can be found in Appendix C.

5.1 Tag Orientations

In the tag orientation tests, the tags were oriented either horizontally (i.e., parallel) or vertically (i.e., on its end) with respect to the soil surface. In addition to changing the orientation of the tag with respect to the soil surface, the tag was also oriented according to the copper orientations, i.e., in “south” and “north” directions as mentioned in section 3.2.3.2. Notched box and whisker plots in Figure 39 show the results from the orientation tests. The wide box plots represent the large tags whereas the thin boxplots represent the small tags. Plots are shown for H0, H0a, V0, and V0a tests (see Table 6 in section3.2.2 for descriptions of these tests). Test names are followed by “S” and “N”, which are indicative of the copper orientation.

The large tags had a larger detection range. Tags that were vertically oriented typically showed a larger detection distance for both small and large tags. Tags oriented in the “south” direction also showed a larger detection distance. A comparison of the results for the 0 and 0a tests in the horizontal orientations shows that detection ranges are approximately 5 cm lower for the offset test, where the centroid of the antenna was offset by a distance of the radius of the antenna from the centroid of the tag. Conversely, tests with the tags in vertical orientation showed that the detection ranges obtained for the offset tests were higher for small tags; however, no appreciable differences were observed for large tags.

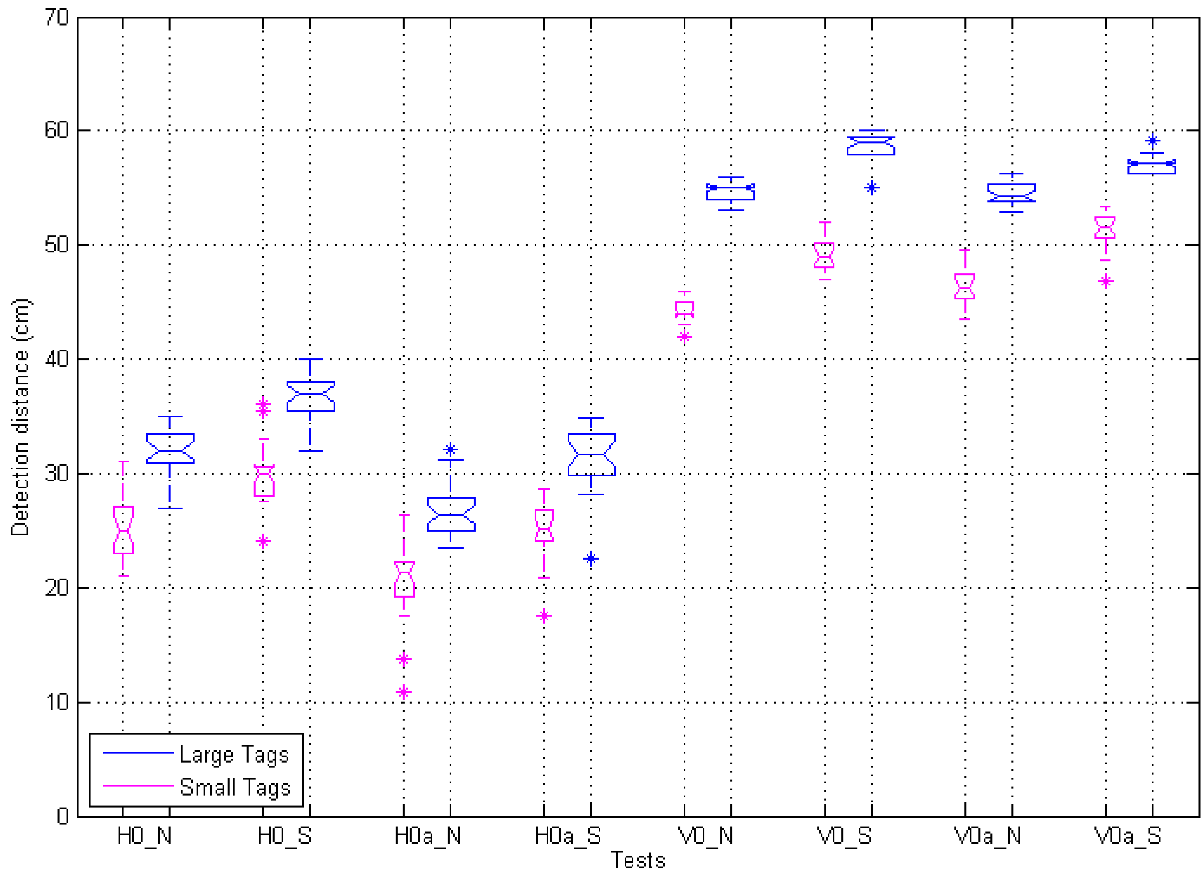

Figure 39: Tag Orientation: Small and Large Tags

5.2 Tracer Size

Results for the rocks tagged with large tags are presented in Table 9. Single factor ANOVA tests were performed to determine whether the 4 different tagged rock size categories, all using the large (32 mm) RFID tag, show statistically different detection ranges. The ANOVA tests were performed for each individual antenna test. The null hypothesis of the test was that the means of the populations of all size groups are the same. The results from the ANOVA tests are provided in Table 9 and tests where the difference was significant at a 5% significance level are highlighted. A comparison of the calculated and the observed F statistic resulted in the failure to reject the null hypothesis for twenty two of the thirty one tests. The null hypothesis was rejected for tests H-90c, V-0, V-0b, V-45a, V-45b, and Vxyz, thereby implying either that the means of the four populations may be the same for most of the tests, or that the tests were not sensitive enough to detect differences in detection range. However, from a practical perspective, rocks sizes can be deemed to be have no significant effect on the detection range of the antenna for most tests.

Table 9: ANOVA test results summary

Tests	Fcrit = 3.098 Fobs	p-value	Variance
H-0	2.971	0.86	45.90
H-45	0.540	0.66	67.13
H-90	1.311	0.30	74.74
H-0b	0.192	0.90	32.61
H-45b	0.687	0.57	50.13
H-90b	0.664	0.58	69.82
H-0c	2.971	0.06	54.60
H-45c	2.798	0.07	389.55
H-90c	4.117	0.02	293.51
H-0a	0.593	0.63	57.64
H-45a	2.039	0.14	33.37
H-90a	1.492	0.25	47.80
V-0	4.486	0.01	5.45
V-45	2.912	0.06	8.85
V-90	2.407	0.10	14.70
V-0b	8.465	0.00	10.29
V-45b	5.949	0.00	14.43
V-90b	2.943	0.06	16.64
V-0c	0.530	0.67	36.22
V-45c	0.245	0.86	31.59
V-90c	1.069	0.38	12.91
V-0a	1.150	0.35	6.76
V-45a	3.482	0.04	8.55
V-90a	2.393	0.10	12.22
H-z	1.249	0.32	57.98
H-xyz	0.459	0.71	47.43
H-yz	2.803	0.07	17.77
H-xz	1.883	0.17	164.68
V-z	0.841	0.49	13.93
V-xyz	3.983	0.02	109.51
V-yz	3.041	0.05	84.97

5.3 Clusters

The results from the cluster experiments are presented in this section.

Figure 40 shows the results from experiments HH with the movable rock moved along the 0° axis. The blue, red and magenta lines show the detection distances measured for tests HH-0°, HH-45°, and HH-90°, respectively. It should be recalled that for tests at the 0° axis, the antenna was moved toward the stationary rock along the 0° axis; similarly, for the 45° axis, the antenna was moved toward the stationary rock along the 45° axis, etc. The axes shown by the three blue arrows are indicative of the distance between the stationary rock and the movable rock, which ranges from 0 to 100 cm. Each grid cell in the figure is equivalent to 10 cm. The axes perpendicular to the previously mentioned axes represent the detection distances (as illustrated by the green double ended arrows). It should be noted that the detection distances are not necessarily always positive; the distance at which the tag was detected was assigned a negative value for every test where the antenna did not detect the presence of the tag before crossing it. As a point of reference, the $L/2$ line is provided. The $L/2$ line indicates 50% of the detection distance for the stationary tracer without interference from a second tracer (i.e., the movable tracer). Figure 41 to Figure 46 present detection distance results in the same manner as presented in Figure 40.

As mentioned previously, L is the distance at which the stationary rock would be detected in the absence of the movable rock for tests HH-0°, HH-45°, and HH-90°. When both rocks are placed in horizontal orientations along the 0° axis, the results show that when the distance between the movable and the stationary rock increase beyond 50 cm, the detection distances steadily increased leading to the magnitude of L.

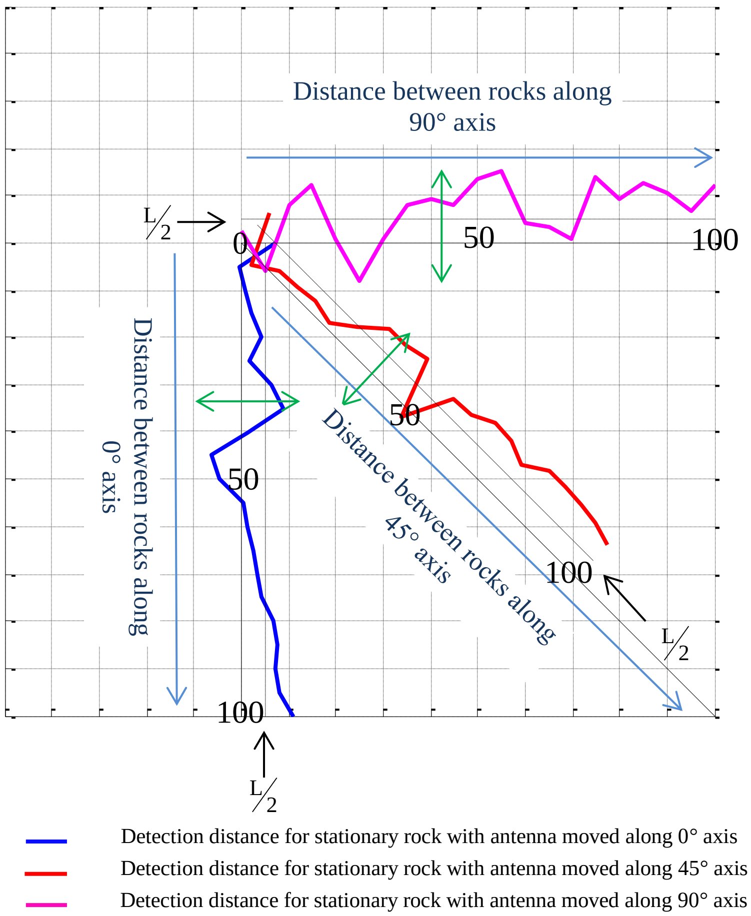

Figure 40: Cluster Test Results: HH-0°, 45°, and 90° for Rock Position 0°

Results shown in Figure 41 are for experiments conducted with the horizontally oriented stationary and vertically oriented movable tagged rocks. Negative readings were obtained when the distances between the two rocks were greater than 50 cm. It is interesting to note that large fluctuations occur within the 50 cm distance, which incidentally is roughly equal to the diameter of the antenna. A possible reason for the fluctuations could be, up to the 50 cm mark, the two rocks are situated within the physical boundary of the antenna and the antenna might intermittently pick up signals from either of the rocks. In general, it was observed that as the distance between the rocks increased, the detection distance tended towards the $L/2$ line.

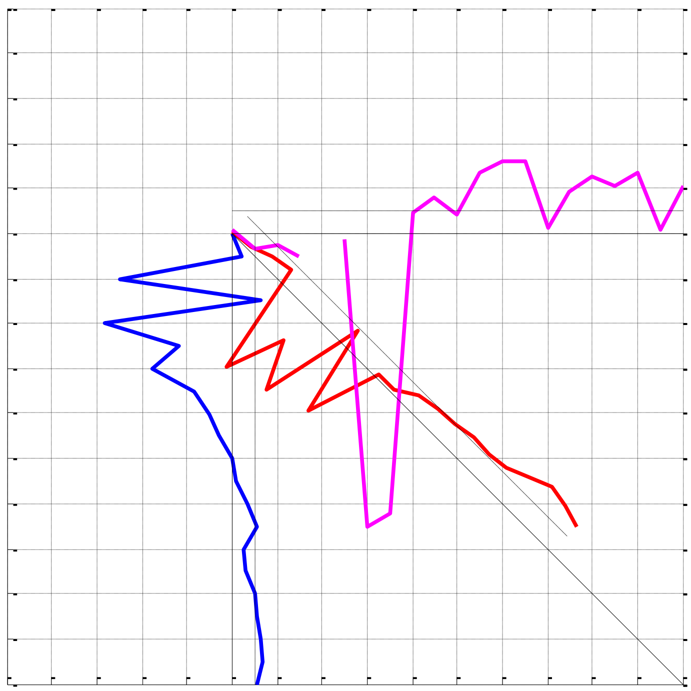

Figure 41: Cluster Test Results: HV-0°, 45°, and 90° for Rock Position 0°

Figure 42 (a) and Figure 42 (b) show the results for VH and VV tests, respectively. Some fluctuations in detection distances were noted for cases where the distances between the two rocks were smaller. For the VH-90° test, the results were very peculiar in that the detection distances did not seem to differ with changing distances between the rocks.

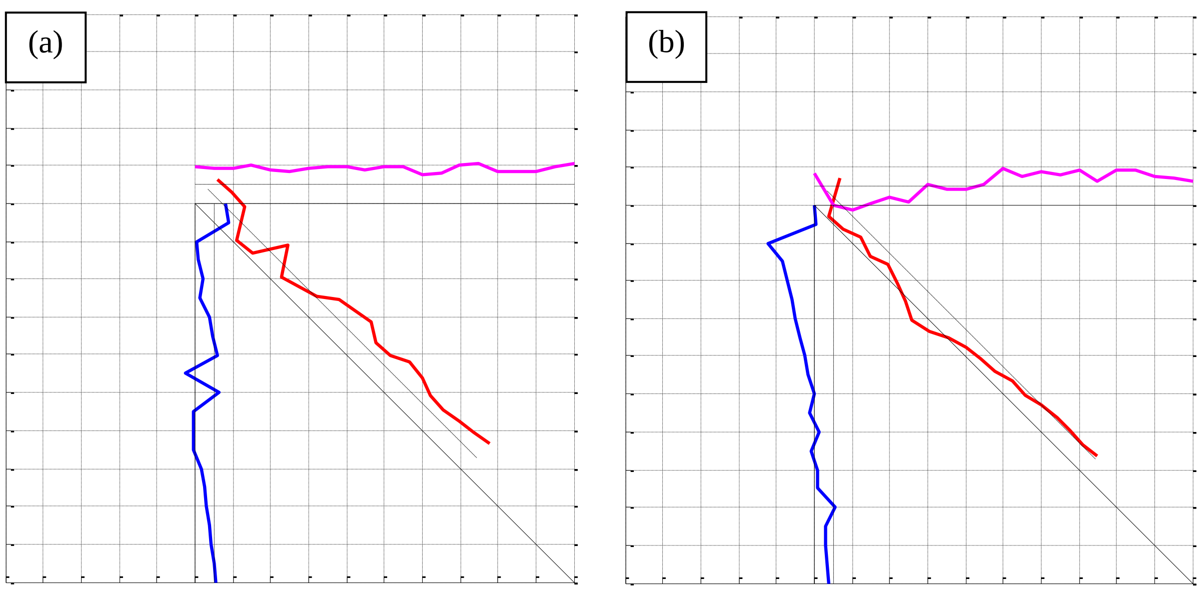

Figure 42: Cluster Test Results for Rock Position 0°: (a): VH-0°, 45°, and 90°; (b) VV-0°, 45°, and 90°

Figure 43 (a) and Figure 43 (b) show results for tests HH and HV, respectively, with the movable rock placed along the 45° axis. The trends followed by the detection distances were similar for both sets of tests. HH-90° and HV-90° had the largest fluctuations in detection distance out of all tests where the distances between the rocks were less than 50cm.

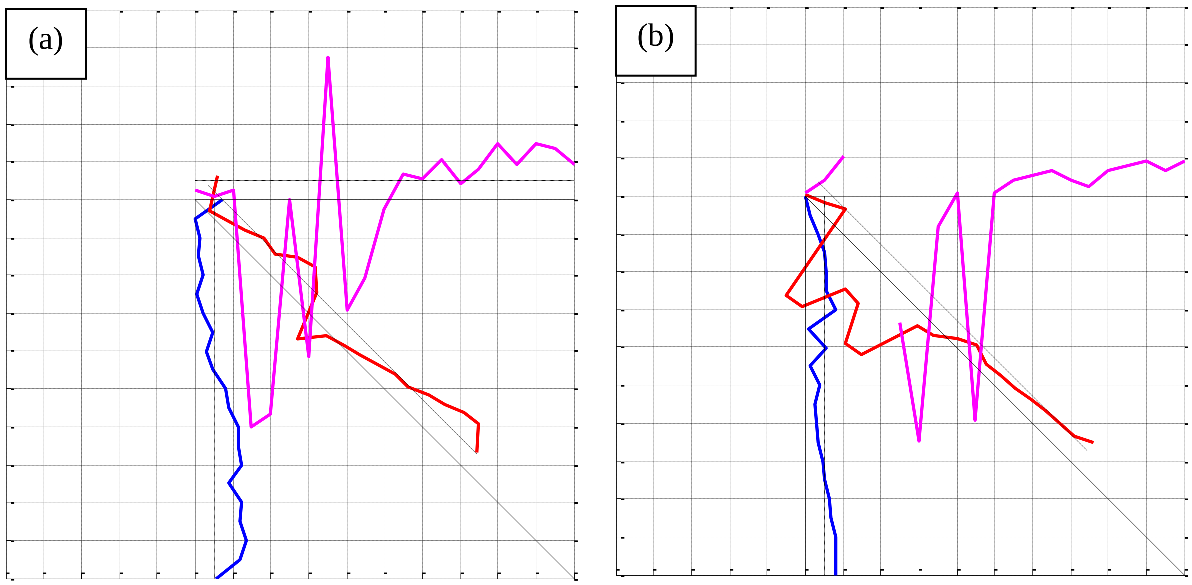

Figure 43: Cluster Test Results for Rock Position 45°: (a): HH-0°, 45°, and 90°; (b) HV-0°, 45°, and 90°

Figure 44 (a) and Figure 44 (b) show results for tests VV and VH, respectively, with the movable rock placed along the 45° axis. The detection distances measured along 0° and 90° axes approached L (twice the distance depicted by the dashed line $L/2$) when the movable rock was placed in a horizontal orientation and moved along the 45° axis, perhaps due to a decrease in interference as the rocks move apart. Similar results were obtained when the movable rock was placed in a vertical orientation. However, in this case, the detection distances only approached the L value when the distance between the rocks was greater than 80 cm. In both VH and VV experiments, it is interesting to note that the tests along the 45° axis yielded detection distances not greater than the $L/2$ value. It is unclear as to whether greater values would have been attained if the distances between the two tagged rocks were to increase beyond the 1m distance used in these experiments.

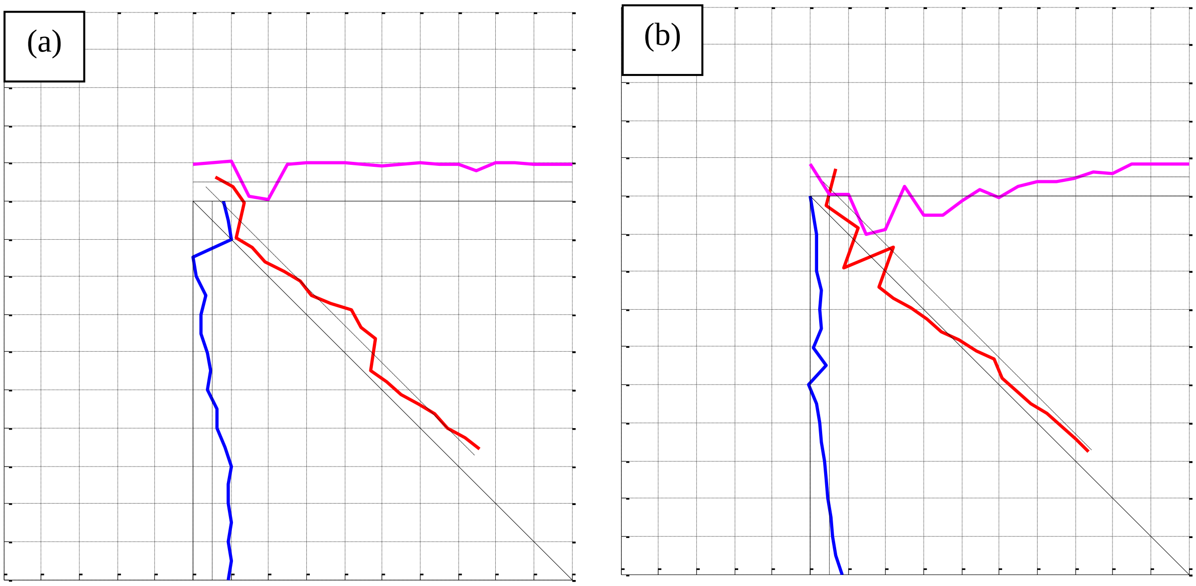

Figure 44: Cluster Test Results for Rock Position 45°: (a): VH-0°, 45°, and 90°; (b) VV-0°, 45°, and 90°

Figure 45 (a) and Figure 45 (b) show results for tests HH and HV, respectively, with the movable rock placed along the 90° axis. The detection distances measured along 0° and 45° axes for both HH and HV tests showed similar trends in that they systematically increased to attain the value of L before dropping to $L/_2$. The 90° tests did not show a clear trend but largely showed a fluctuating trend in the results.

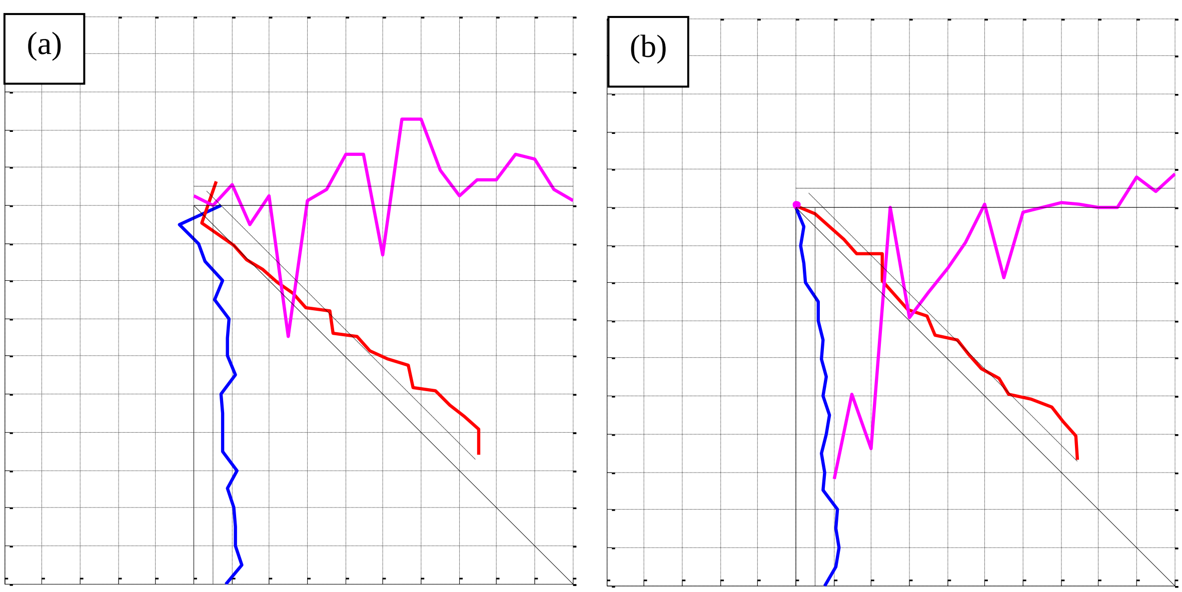

Figure 45: Cluster Test Results for Rock Position 90°: (a): HH-0°, 45°, and 90°; (b) HV-0°, 45°, and 90°

Figure 46 (a) and Figure 46 (b) show results for tests VH and VV, respectively, with the movable rock placed along the 90° axis. Detection distances measured along 0° axis for both tests VH and VV showed a more or less a consistent measurement of distance L. Measurements made along the 90° axis for test VV showed that with the increasing distance between the rocks, the detection distance approached the $L/2$ value.

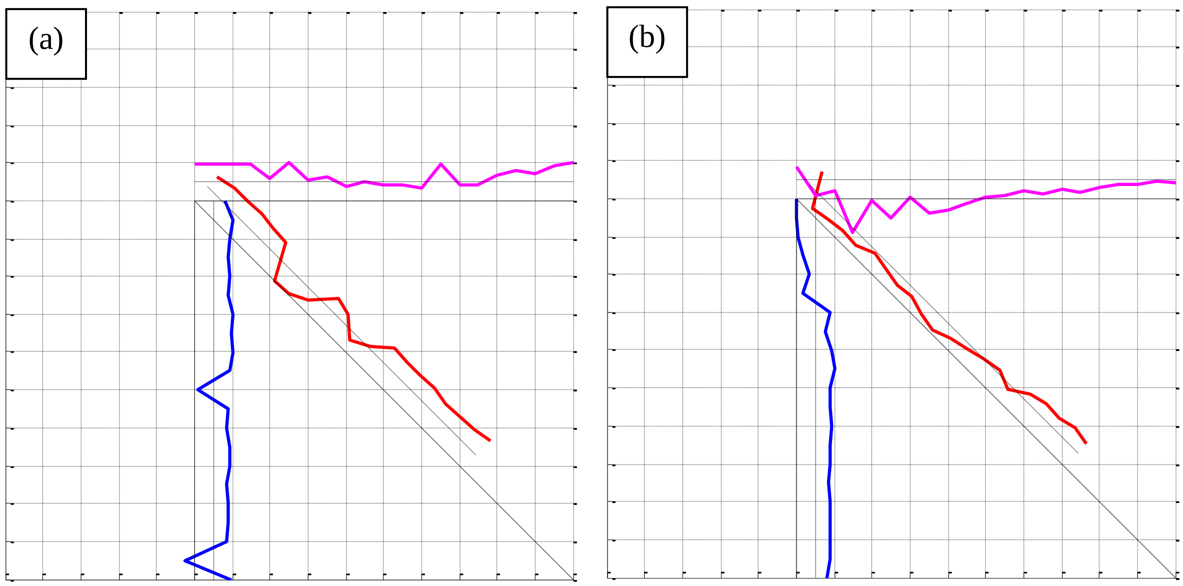

Figure 46: Cluster Test Results for Rock Position 90°: (a): VH-0°, 45°, and 90°; (b) VV-0°, 45°, and 90°

Table 10 shows the summary of the $L/2$ values and the various tests for which the values are valid. Since the $L/2$ value is of the half of the value of the detection distance for the stationary rock without any other rock in its interrogation zone, the values for tests HH are also valid for HV. Similarly, the values for tests VV and VH are the same. The $L/2$ values do not change for different rock axis position.

Table 10: Summary Results from the Cluster Tests

Parameters	Horizontal			Vertical		
	H-0°	H-45°	H-90°	V-0°	V-45°	V-90°
Detection Dist. (cm)	22	21	7.5	45	44	42
$L/2$ Value (cm)	11	10.5	3.75	22.5	22	21
Valid for Tests	HH, HV	HH, HV	HH, HV	VH, VV	VH, VV	VH, VV

5.4 Burial Depths

The results from burial tests under horizontal and vertical orientations for small tags are shown in Figure 47 and Figure 48, respectively, in the form of box and whisker plots. Test results for large tags in horizontal and vertical orientations are shown in Figure 49 and Figure 50, respectively. Tests H and V, shown in the legend, correspond to tests H-xyz and V-xyz, respectively.

A visual observation of the box and whisker plots of small tags placed in horizontal orientation generally shows a decreasing trend, i.e., there was an observable decrease in detection range with an increase in burial depth, particularly at the 18" depth. For test H-90°, an observable decrease in detection range was even seen with the burial depth as small as 3". However, the detection ranges for tags buried in 3" of soil was larger than those when the tags were placed on the surface. Horizontal tests for large tags showed mixed results with an increase in detection ranges as the burial depth increased for some tests, a decrease in detection range for other tests, and an increase followed by a decrease for other tests. For the large tags in vertical orientation, the tests, with the exception of test V, showed a decrease in detection distance with a 3" burial depth followed by an increase in detection distance around the 6" burial depth and a subsequent decrease in detection distance for burial depths beyond 6". For small tags in vertical orientation, similar results were observed.

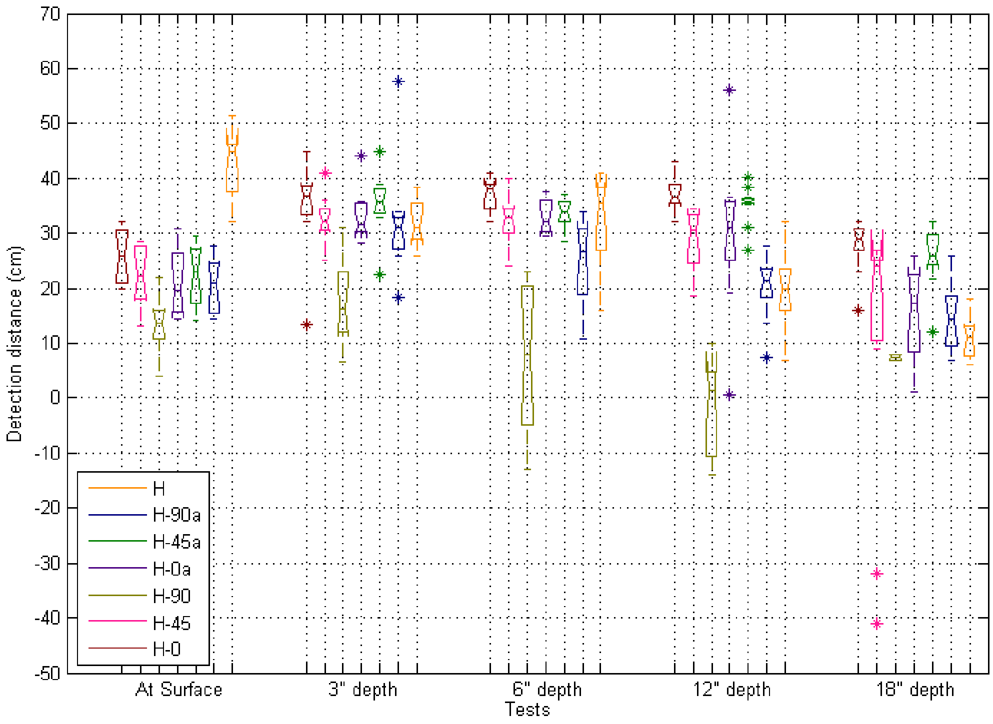

Figure 47: Small Tags - Horizontal Tests

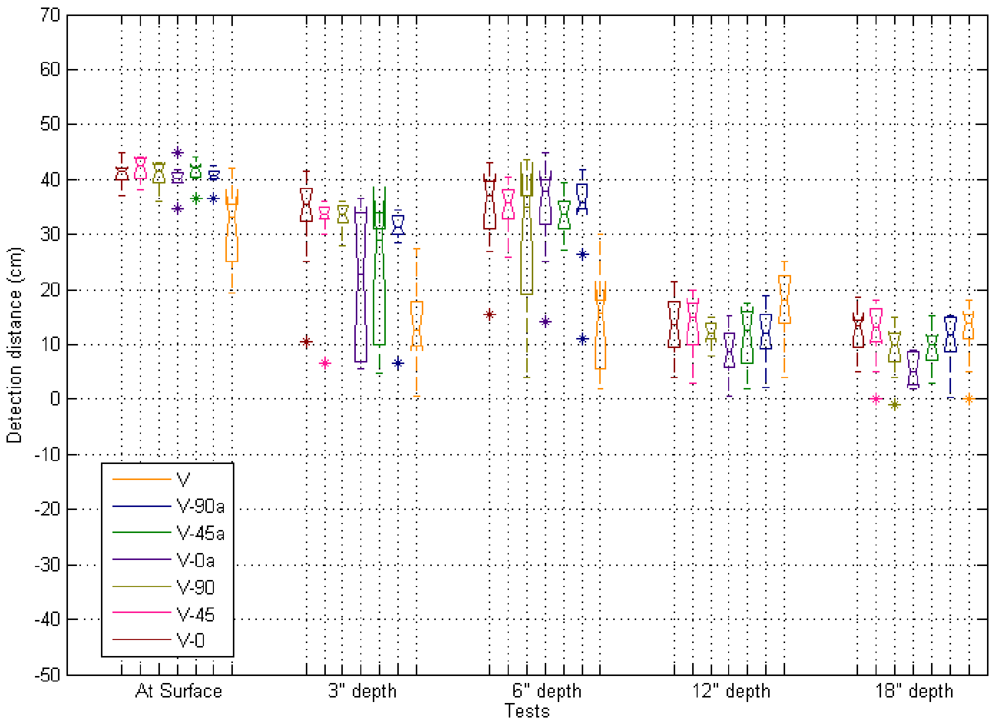

Figure 48: Small Tags - Vertical Tests

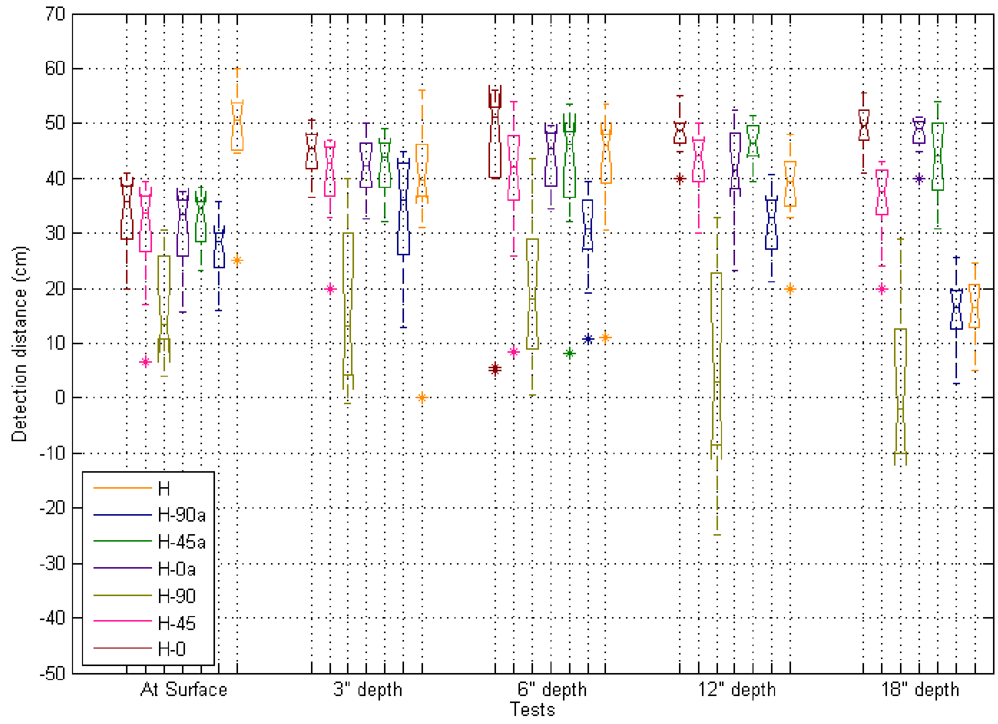

Figure 49: Large Tags - Horizontal Tests

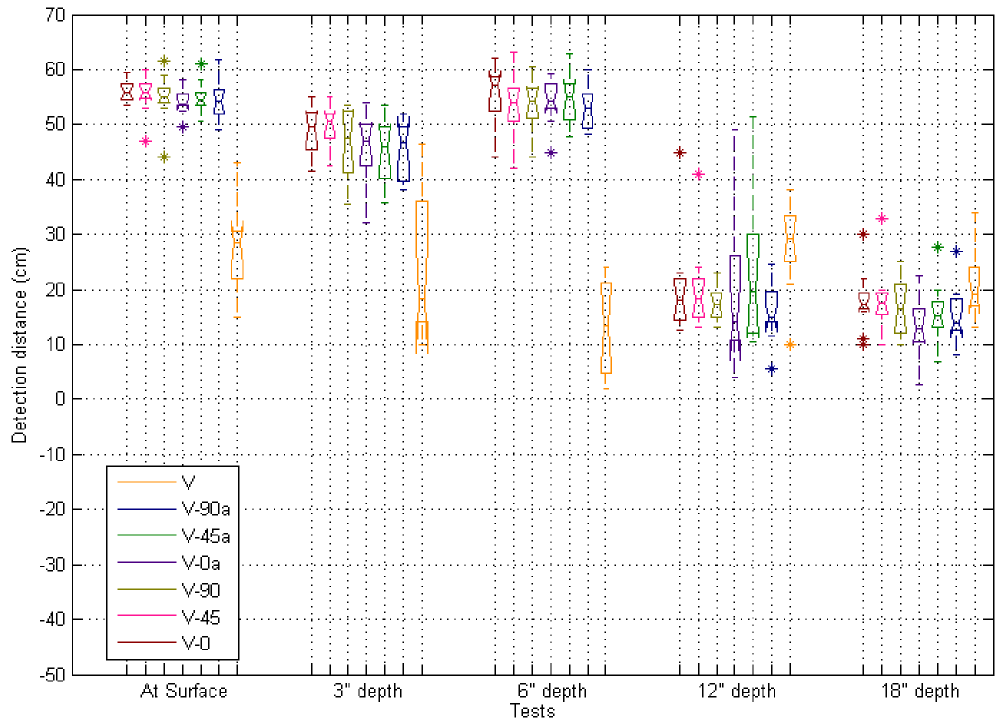

Figure 50: Large Tags - Vertical Tests

5.5 Saturation and Submergence

Results for large tagged rocks buried in 6" of soil under dry, saturated and submerged conditions are shown in Figure 51 for horizontal tests and in Figure 52 for vertical tests. Saturation and submergence did not seem to have an impact on the detection distance for the horizontal tests given the variability within each test. It also was noted that, for the horizontal tests, there was a large amount of variability in the results between different tests within a given saturation condition. However, for the vertical tests, the detection distances were smaller when the tags were submerged, than for the dry conditions for all tests except for test V. Unlike the horizontal tests, there was little variability in the results between different tests at the same saturation condition for all tests expect for test V.

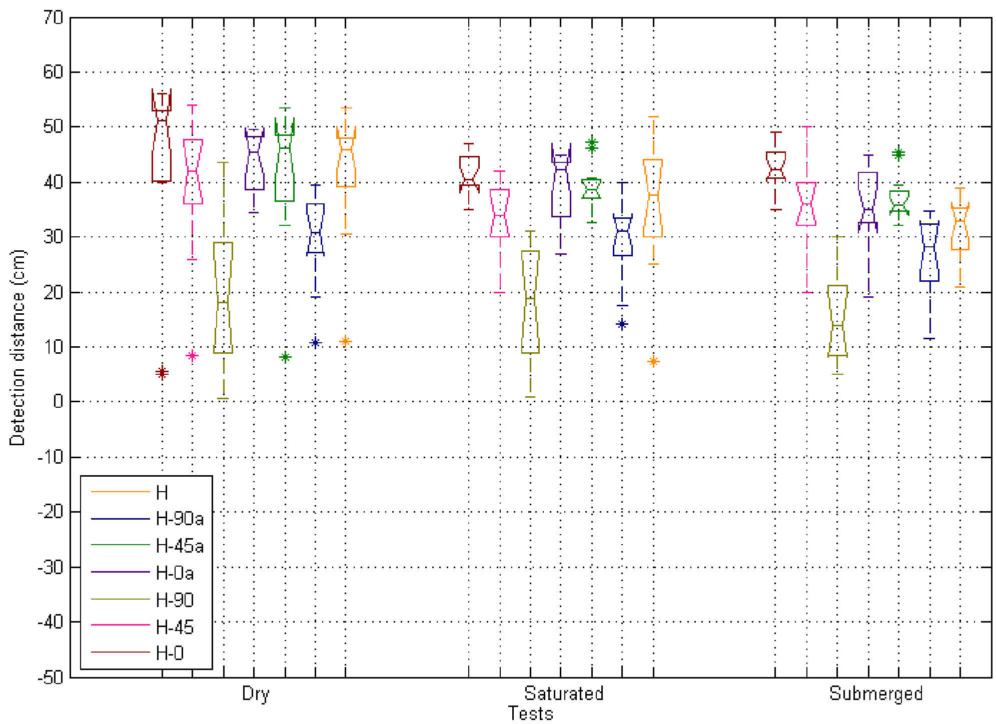

Figure 51: 6" buried results for dry, saturated and submerged tests (horizontal)

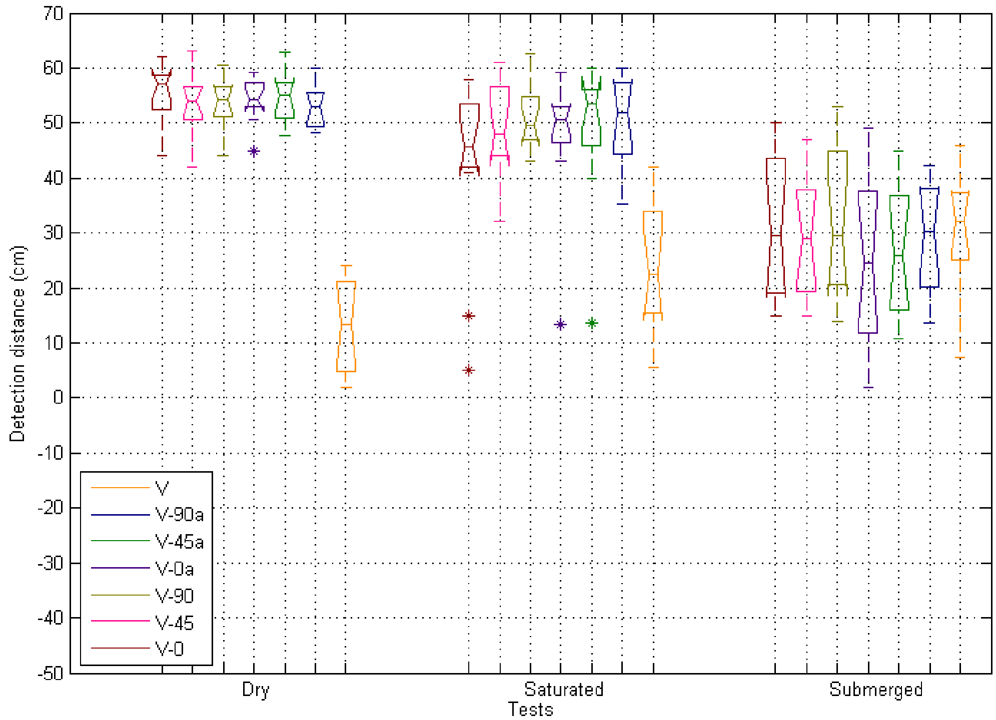

Figure 52: 6" buried results for dry, saturated and submerged tests (vertical)

5.6 Antenna Range – Uniformity

Antenna range uniformity tests were performed on 25 large and 25 small tags by placing them at the centre of the sandbox at a horizontal orientation that was parallel to the ordinate axis of the sandbox. Figure 53 and Figure 54 show a schematic representative of the sandbox with the detection distances plotted. The detection distances were normalized by the largest dimension obtained for a particular test. As is evident in the two figures, for both large and small tags, the distribution of the detection range and hence the field is slightly elongated circle. Further testing is required to confirm the shape of the antenna`s range.

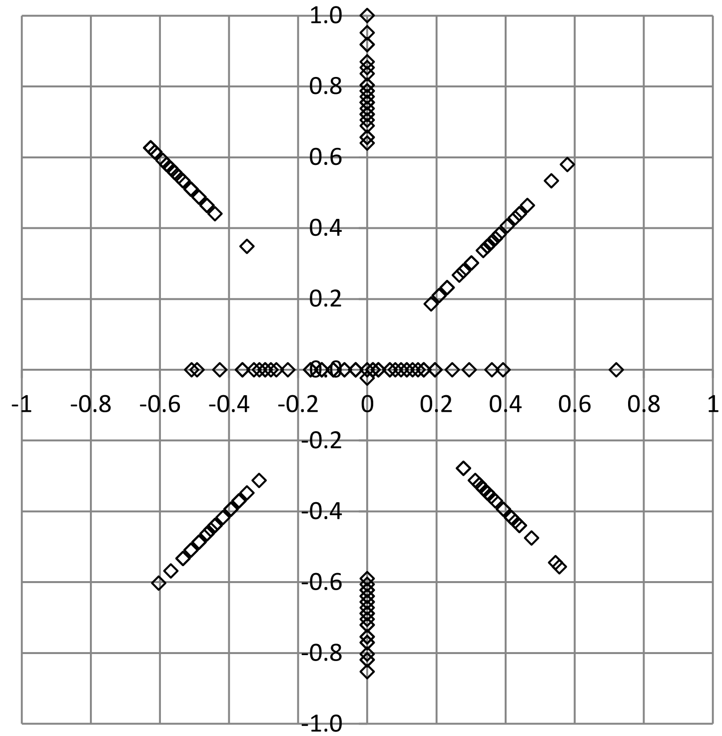

Figure 53: Antenna Range - Large Tags

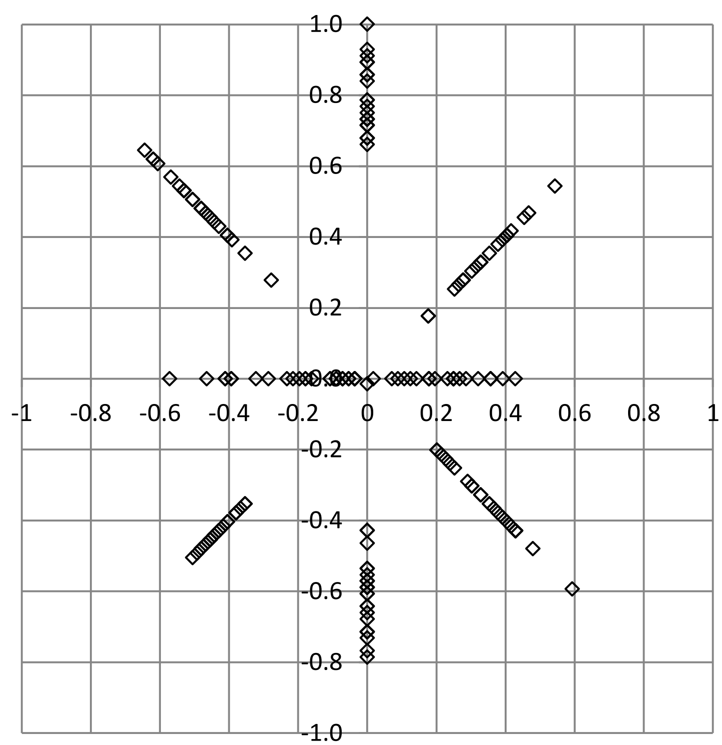

Figure 54: Antenna Range - Small Tags

5.7 Skip Zones

Two skip zones were detected for each tag (four tags were tested: two small and two large tags). These skip zones are shown in black bars in Figure 55 for the north orientation and in Figure 56 for the south orientation of a small tag. The patterns in the results shown for the small tag are typical for the other three tags tested as well. The skip zones for different rotation angles are also shown. However, the positioning of the skip zone did not change by a large amount given the errors expected while measuring the skip zone distances. It is interesting to note that one of the two skips is much smaller than the other and is on the same side as the end of the transponder where the copper turnings are located.

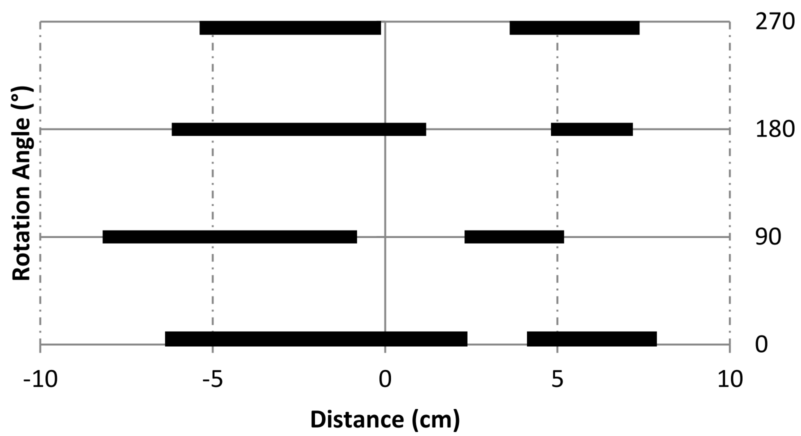

Figure 55: 'North' Orientation Skip Zone Demarcations for a small tag

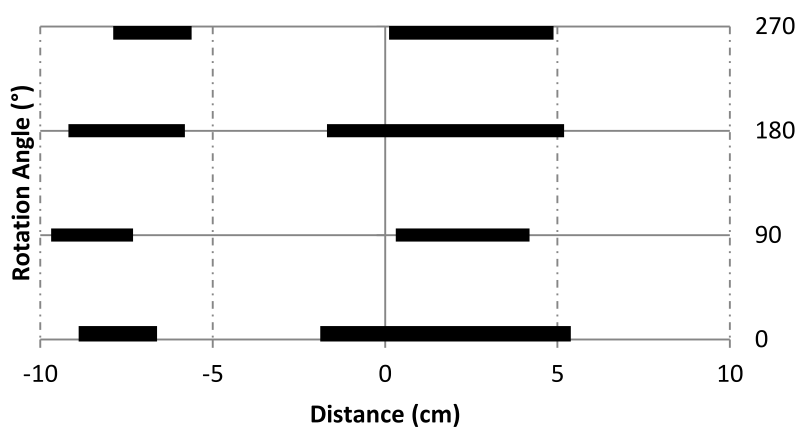

Figure 56: 'South' Orientation Skip Zone Demarcations for a small tag

A range of distances within which skip zones were identified, for each tag, was determined and is shown in Figure 57. Tags 1 and 2 are small tags and tags 3 and 4 are large tags. It is evident that skip zones can be found at least 10 cm on either side of the tag, thus the location of the tag can be narrowed down to 10 cm by using the skip zones to identify the location of the tag.

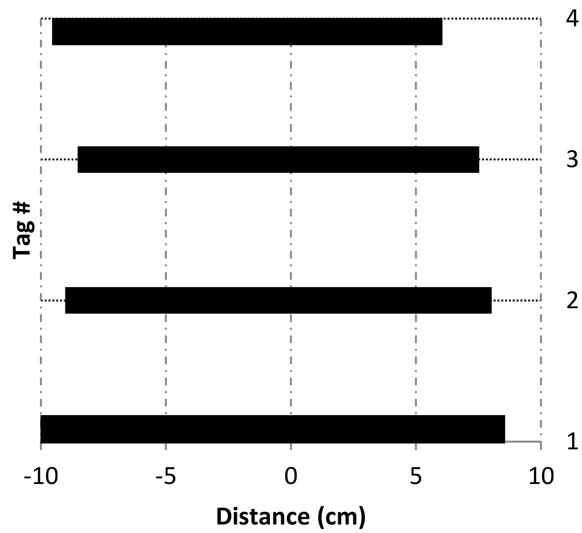

Figure 57: Skip Zone Distances

5.8 Comparison with field tests

Figure 58 shows comparative box and whisker plots of results from field and lab experiments for tests H-0°, H-45°, H-90° and H-xyz. Results for tests H-0a, H-45a, H-90a and H-xyz are shown in Figure 59. Corresponding results for vertical tests are shown in Figure 60 and Figure 61.

A comparison of the field and lab tests with tags placed in horizontal orientation showed that results generally compared well, with the exception of H-90 tests conducted with the tags buried at a depth of 3”. The results obtained from offset tests conducted for tags buried at a depth of 12” also did not compare well. Unfortunately, it cannot be said with certainty whether the lab results yield higher or lower detection distances than the field tests.

A comparison of field and lab test results for tags in vertical orientation yield interesting results. The field results for tags at a depth of 6” consistently produced detection distances that were less that those obtained in the lab for tests V-0, V-45, V-90, V-0a, V-45a and V-90a. The results of tags at 3” depth were not comparable for the offset tests (V-0a, V-45a, and V-90a). Though the results between 3” and 6” are not necessarily comparable, the field and lab results agreed fairly well for surface and 12” depth tests.

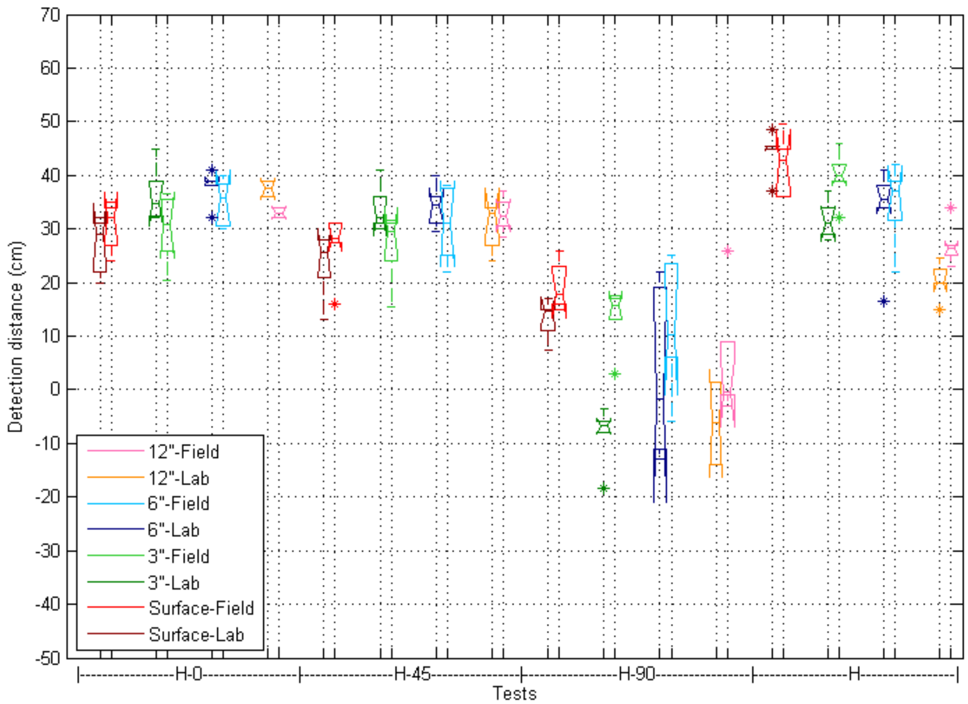

Figure 58: Comparison of Lab and Field Tests - Horizontal Orientation - Set 1

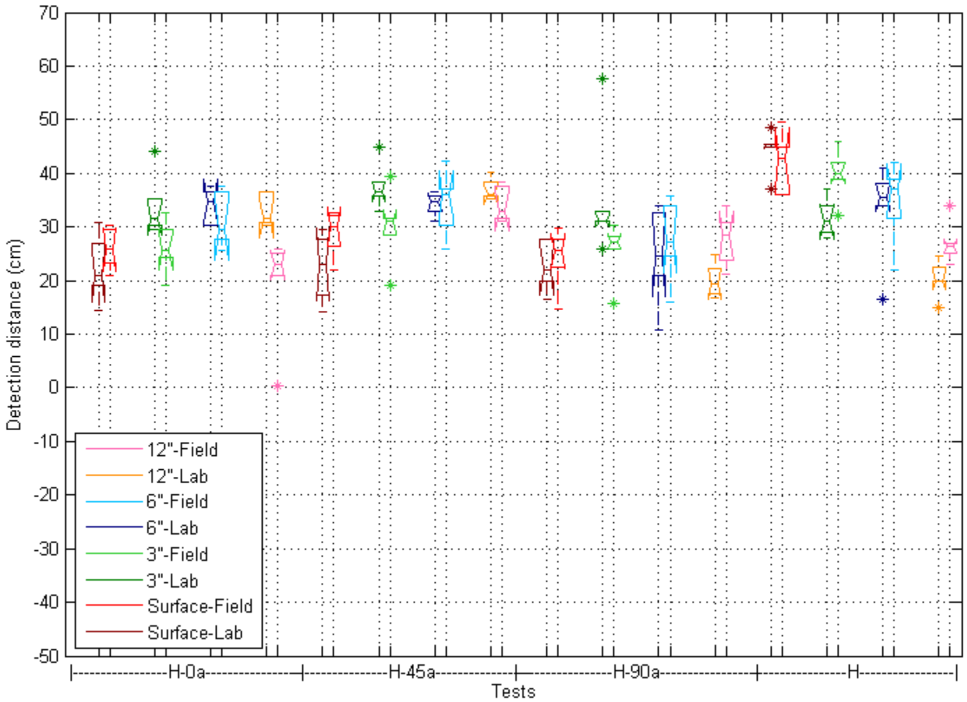

Figure 59: Comparison of Lab and Field Tests - Horizontal Orientation - Set 2

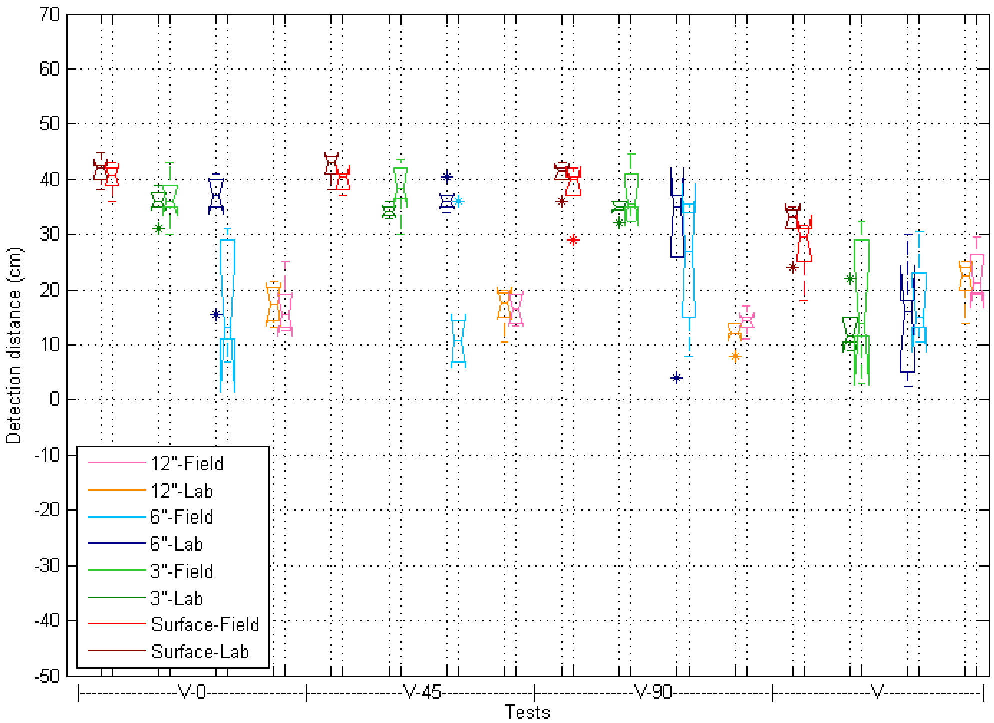

Figure 60: Comparison of Lab and Field Tests - Vertical Orientation - Set 1

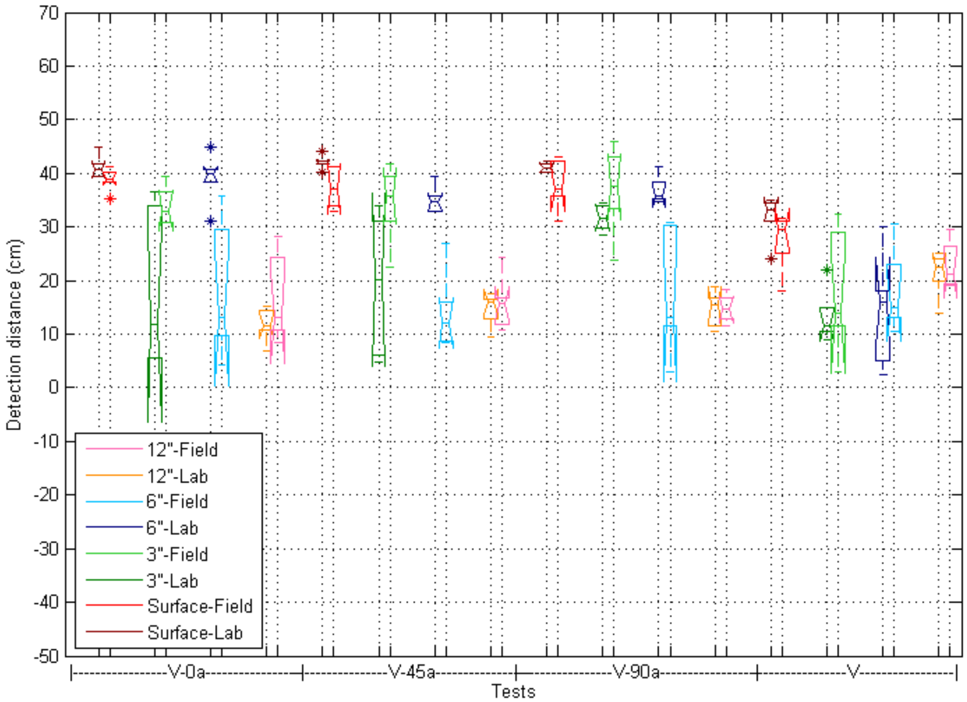

Figure 61: Comparison of Lab and Field Tests - Vertical Orientation - Set 2

6 DISCUSSION

Field and laboratory results are discussed in this chapter in the first two sections. The implications of the results on the procedure of tagging, seeding and tracking RFID tracers to study bedload transport are also discussed.

6.1 Discussion of Field Results

RFID tracers were used to track coarse bedload sediment in Laurel Creek. Results from four study sites and a total of ten tracking events (in all sites combined) over a span of fourteen months (the period between seeding and the final tracking event) show recovery rates between 81.5% and 98%. As previously mentioned in Chapter 4, the recovery rates are comparable to those in other studies involving RFID tracers. Therefore, the idea that RFID tracking is an ideal tracking technique in urban streams is corroborated.

Inspection of Figure 29, Figure 30, Figure 31, Figure 32, and Table 8 shows that tracer movement was larger in some sites than in others. Specifically, the smallest movement was noted in Site 2. Low movement was also seen in Site 1. Sites 3 and 4 showed the largest movements, averaging 10.8 m and 8.7 m, respectively, for the final tracking events for each site.

A visual reconnaissance of Site 1 showed that the bed of this site is fairly armoured. One would expect that in an armoured bed scenario, the loosely placed tracers on top of the bed would move a greater distance during the first flush of a flood event since the tracers would move better over a less mobile bed before they get incorporated into the bed matrix. In subsequent flood events, as the tracers get incorporated into the bed matrix, it would be expected that the tracers would not move much. However, this was not true of Site 1 where a larger mobility for all sizes classes, except the fourth size class, was observed in the third tracking event than the first tracking event. Therefore, the number of floods experienced between the first and the third tracking event may not have been sufficient to incorporate the tracers into the bed matrix; study of the relationship between imbrication and travel of tracers in Laurel Creek and other urban watercourses is an area for potential future study.

A visual reconnaissance of Site 2 showed that it is positioned in a deposition zone. Therefore, there was a high likelihood of tracers being buried over by bed material during the recession of flood events. In fact, during the tracking, it was noted that 83 tracers out of the 187 tracers that were detected could not be physically located and it is hypothesized that they were buried given that almost all other located tracers were physically recovered at the end of the study after much digging. The burial by other sediment likely made it difficult for the tracers to move, particularly the larger tracers which showed the least mobility and path lengths.

Site 3 is located in an urban park, where the watershed in the immediate proximity to the site is largely natural, with a better access to floodplain than the first two sites. A visual reconnaissance during low flows showed evidence of an active channel bed. The largest average path lengths out of all the sites were noted at this site, particularly for the first three size classes. Although the percent mobility of these classes only ranged between 40% and 85%, the path lengths were the same or larger than those of the median surface material at the site. The larger size classes showed the lowest mobility and path lengths. As it stands now, there is insufficient data, given that data for only one tracking event could be collected through this site, to draw conclusions as to how the channel down-cutting had left previously buried Forewell Sewer trunk crossing the creek exposed. The effectiveness of the restoration efforts undertaken by the City of Waterloo can be studied in subsequent RFID tracking studies for which this study provides a baseline.

Site 4 is also located in an urban park, although in a wider floodplain than Site 3. The riffle portion of the seeding site was armoured with large rocks holding the riffle in place. The largest percent mobility was noted in the first tracking event, as expected in the case when tracers are seeded on the surface of a bed. However, even though the largest percent mobility was observed in the first tracking event, it was interesting to note that the largest path lengths were observed during the second tracking event (which showed the lowest percent mobility), where the distance moved by size classes 1, 3 and 4 were the same as those moved by the median grain size.

It must be noted that the field results from Laurel Creek presented are preliminary. Typically, in order to establish bedload transport characteristics of a watercourse, years of bedload monitoring is required. Therefore, the results presented form the baseline data for a continued long-term research. In the future, it would be valuable to obtain tracking data between each individual flood event in order to potentially relate the channel discharge to the tracer movements.

6.2 Discussion of Laboratory Results

The laboratory experiments were geared towards confirming what factors confound an accurate detection of the location of tracers. The results show that tracer orientation, submergence and the presence of other tracers are all factors that affect the detection of the tracers.

6.2.1 Tracer Orientation and Tracer Sizes

The experiments conducted clearly show that the detection distances are largely influenced by the orientation of the tag with respect to the antenna. The results presented in Figure 39 are presented in a summary table (Table 11) showing the average and standard deviation (n=25) of the detection distance of each combination of tracer size and test. On an average when the tags were oriented in a horizontal fashion, the detection range is 68% and 62% smaller than those for tags in a vertical orientation for 23mm and 32mm tags, respectively. Similarly, it can also be noted that the south orientation of the tag (i.e., when the copper turnings within the transponder are located closest to the antenna) shows an average of a 15% increase in detection range than those in the north orientation, for 23 mm tags in the horizontal orientation. The increase in the detection range for 23 mm tags in the vertical orientation is only 7%. Similar results can be noted for the 32 mm tags. The effect of the direction of the copper turnings within the transponder, with respect to the antenna, when the transponder is placed in a vertical orientation is not as pronounced as when the transponder is placed in a horizontal orientation. The most interesting results of these tests here are those that highlight the magnitude of the difference in detection ranges between the horizontal and the vertical tests. These results strongly point to the changing shape of the interrogation zone when the orientation of the tag with respect to the antenna changes.

Table 11: Summary detection distances (cm)

Tests	H0-N	H0-S	H0a-N	H0a-S
23 mm tags	25.1 ± 2.8	29.8 ± 2.5	38.7 ± 4.2	43.8 ± 2.9
32 mm tags	31.7 ± 3.1	36.8 ± 3.3	45.5 ± 4.7	51 ± 4.4
Tests	**V0-N**	**V0-S**	**V0a-N**	**V0a-S**
23 mm tags	44.4 ± 1	49.3 ± 1.4	67.5 ± 1.5	70.2 ± 14
32 mm tags	54.5 ± 2.7	58.8 ± 2.6	76.2 ± 2.5	78.9 ± 15.7

It is hypothesized that the shape of the field, as shown in Figure 6, affects the magnitude of the detection range. The vertical orientation of the tag produces an elongated field which makes for an easier detection. From an in-field usage perspective, easier detection also implies decrease in the accuracy of the tracer location. Therefore, the orientation in which the tag is installed should depend on the on the scale of the study. For example, a study of bedload material travel distances in a small section of a watercourse would require accurate determination of tracer location. For such studies, a horizontal orientation of the tracer with respect to the antenna is desirable. Since it is not possible to predict with a 100% certainty which way the tracer will orient itself, the only possible method of increasing the likelihood of the tracer orienting in the desirable direction is to install the tracer in a suitable manner. Therefore, in a rod or a disc or a blade shaped particle, the tracer can be installed along the a-axis However, if the precision in detection of the exact location is not required to be within 0.5m, it will be more useful if the tracer orientation with respect to the antenna is vertical. This orientation will allow for a quicker detection and hence will require the installation of the transponders along the c axis of the particle.

The tests on orientations were done with bare tags, i.e., simply the transponders. It was necessary to confirm that the insertion of the transponders into stones of various phi classes would not affect the detection distances. To check whether the size of the tracer (a particle containing a transponder) affected the detection distances, various tests were conducted on tracers belonging to six phi classes and results have been reported in Table 9. An examination of these results shows that for the majority of the tests, tracers belonging to all size classes have the same average detection distance. The tests for which this conclusion did not hold true are H-90c, V-0, V0b, V-45b and V-45a. It is possible that for the vertical orientations, the conclusions did not hold true because of the manner in which the detection distances were measured. Though the tracer was buried up to half it's a-axis length (as shown in Figure 62), this method may have affected the measured detection distance by changing the portion of the field above the surface. To ensure comparability, the measurements should have been taken from the centre of the transponder within the tracer so that the detection distances measured would be for fields centred at the same point in space. Therefore, it can be hypothesized that it was not the mass of rock around the transponder that caused a change in detection distance but rather it was the manner in which the measurements were taken, particularly in the vertical orientations due to the nature of the shape of the field. Possibly, the only reason why the mass of the rock around the tracer would affect detection distances would be if the composition of the rock contains a significant portion of a conductive substance that could distort the shape of the electromagnetic field. Given these assumptions and results, further testing for other confounding factors were conducted by amalgamating the various phi classes which resulted in an increased degrees of freedom in all further experiments.

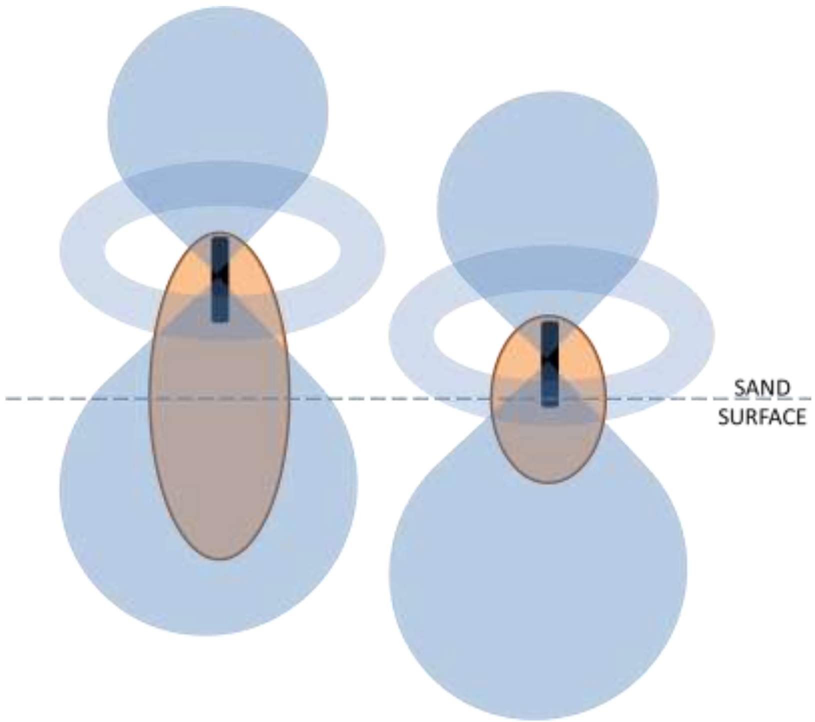

Figure 62: Tracers (shown in brown) of different phi classes showing their detection fields (shown in blue)

6.2.2 Burial, Saturated and Submerged Conditions

Based on results shown in Section 5.4 for both small (23 mm) and large (32 mm) tags, that under the conditions of vertical orientation, the detection distances reduce for tests at the surface to tests at 3” below the surface, thereafter, the distances increase for tests at 6” and then a steady decline in detection distance is observed with the increase of burial depth. A possible reason for this non-linear pattern of detection distance with respect to burial depth could be the shape of the electro-magnetic field. As is illustrated by the conceptual diagram, Figure 63, the ring portion of the field could be picked up by the antenna when the tag is at the surface. However, when the tag is at a depth of 3”, the antenna may pick up the thinner portion of the smaller lobe which causes a drop in the magnitude of the detection distance. As the tracer is buried deeper (at 6”), the antenna picks up the thicker portion of the lobe. Thereafter, with increasing burial depth, the diameter of the lobe that can be detected by the antenna thins out and thus magnitude of the detection distance subsequently reduces.

Similarly, the relationship between detection distances and burial depth for the horizontally positioned tests can be due to the shape of the electro-magnetic field in this orientation. Further testing is required to determine the how the shape of the field influences the detection range in the horizontal tests. While at the same burial depth, in general, the different vertical tests resulted in a similar average detection distances, the horizontal tests registered slightly varying average detection distances. This confirms that the shape of the field under horizontal orientation is more anisotropic than in vertical orientation.

Additionally, it must be noted that though a distinct change in pattern can be observed in the magnitude of detection range with respect to the burial depth, the magnitude of change likely is not affected by the sediment material. The confounding effect of burial is likely due to the sediment physically limiting the portion of the field that is accessible to the antenna.

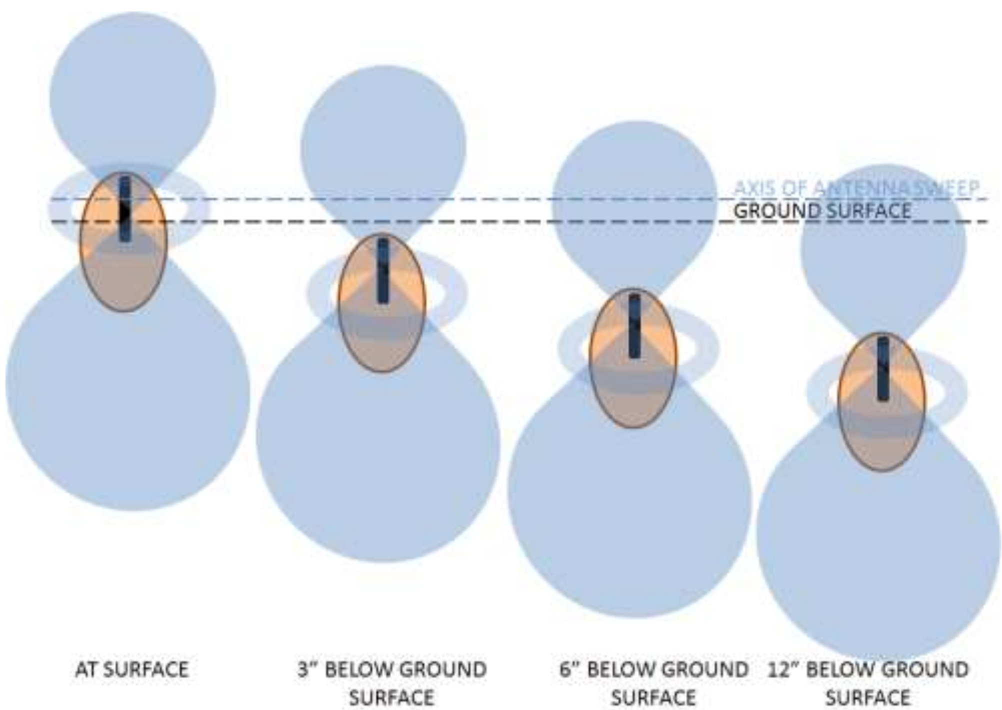

Figure 63: Conceptual diagram (not to scale) of the antenna field under vertical orientation for various burial depths

Tests for large tags buried at a depth of 6" under conditions of saturation and submergence (i.e., standing water at a depth of 12" above the ground surface) showed that the presence of water can reduce detection range for vertically oriented tags. Table 12 shows a summary of test results shown in Figure 51 and Figure 52. For the purposes of summarization, results from tests H-0, H-45, H-90, H-0a, H-45a and H-90a were pooled for the horizontal results and similarly results from tests V-0, V-45, V-90, V-0a, V-45a and V-90a were pooled for the vertical results. For each of these tests, a sample size of 12 tracers was used. Table 12 shows that for the vertical tests, the detection distances reduce with an increase in water content; whereas, for the horizontal tests, submergence and saturation had no significant effect on detection distance given the variability in the data. Figure 64 illustrates the setup of the experiment for vertically oriented tags. The possible retardation of detection distance with the increase of water content could be due to the dispersion of the signal. It is possible that each time the electromagnetic field passes through a different phase/medium, it distorts, thus producing a different zone of detection. In the first case (dry condition), the signal has to travel between two phases, air and a dry soil matrix. In the second case, the signal has to travel through air and a saturated soil matrix. In the third case (submergence), the signal has to travel between water and a saturated soil matrix. It is possible that water distorts the electromagnetic field in such a way that the detection range is reduced; however, it is interesting to note that the difference in the horizontal orientations is almost negligible compared to the vertical orientation. The reason why detection distance is impacted by submergence when tags are in vertical orientation but not in horizontal orientation is unknown and further research is need to investigate this phenomenon. Since dry conditions yield the highest values for detection distance, tracking of tracers would be easier on the exposed portions of the channel bed such point and median bars. Therefore, if the tracking of tracers after flood events is delayed to a point such that more of the channel perimeter is exposed, higher recoveries and a more successful tracking could be achieved. In addition to the potential increase in recovery, the increased visibility through the water after suspended sediment concentrations decrease post storm and water depths lower would also make tracking easier.

Table 12: Summary table showing average and standard deviation (in cm) of detection distances for horizontal and vertical tests for dry, saturated and submerged conditions

Tests	Dry	Saturated	Submerged
Horizontal	36.2 ± 14.7	33.5 ± 10.4	32.4 ± 10.8
Vertical	54.1 ± 4.5	48.3 ± 11.2	28.7 ± 12.7

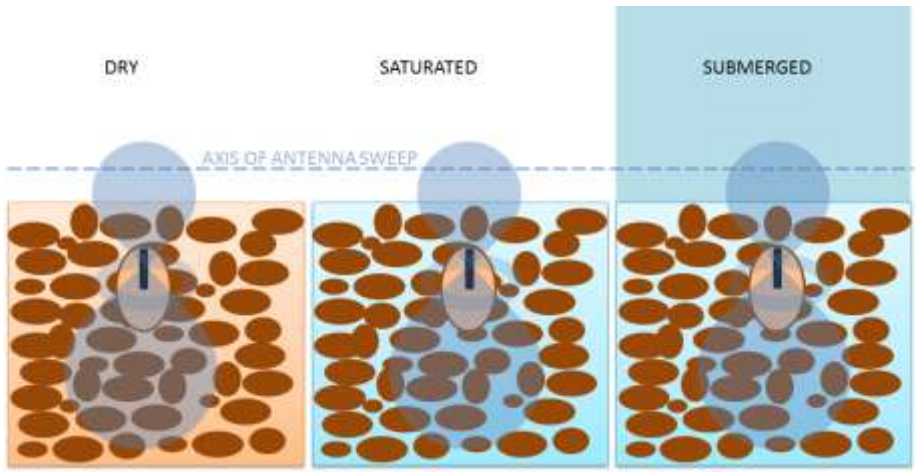

Figure 64: Conceptual diagram showing the three conditions of burial tested (dry, saturated and submerged)

6.2.3 Clustering Effects

Clusters of tracers, in a configuration as simple as two tracers, can impact the measurement of detection distances. In this section the nature of the confounding effect of the clusters on detection distances is briefly discussed for a few of the test results. Figure 65 shows the cases for which the impact of clustering on detection distances are discussed. Three cases (a – c) were taken from the results for HH-0, HH-45, and HH-90 tests with the movable tracer on the 0° axis. Case d is taken from the results for HV-0, HV-45, HV-90 tests with the movable tracer on the 0° axis. These results seem to indicate that the impact of the distance between the tracers on the detection distances is erratic, at least until some minimum separation between the tracers is reached. However, there are a number of factors which might explain variability in the detection distance. Consider Figure 66, which illustrates the results and is based on the approach adopted by Chapuis et al (In Review). The figure shows the zero interference detection zones for the stationary and the mobile tracers in light grey, the antenna loop, and the axes of measurements. The sweep direction is represented by the bold dashed line.

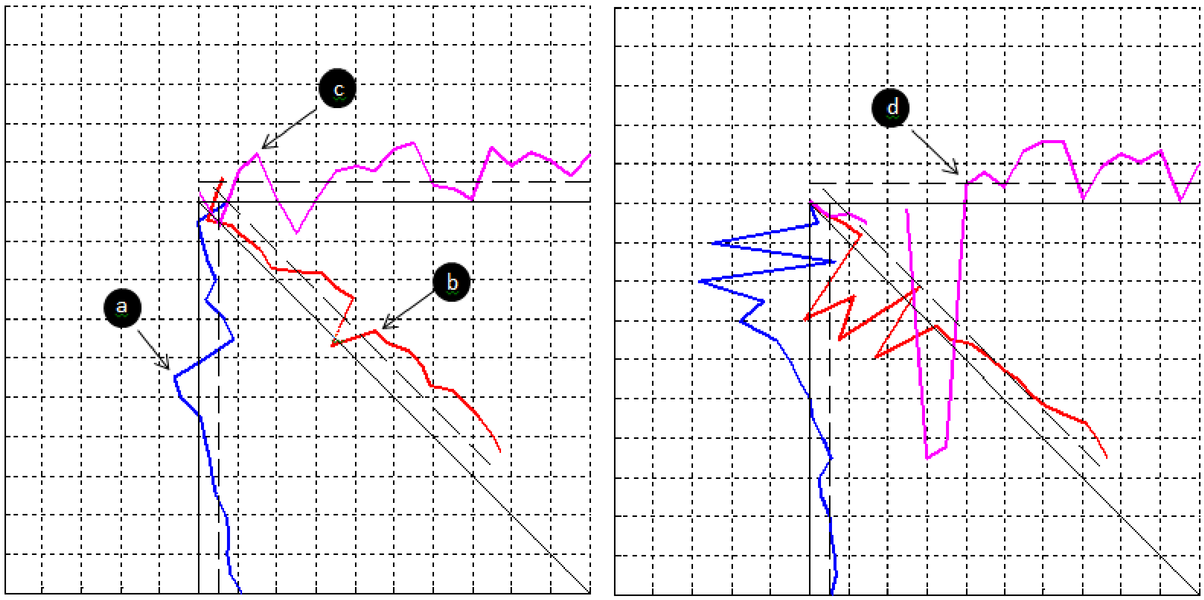

Figure 65: Influence of clustering on detection limits for two sets of experimental results (

Figure 40 on the right and Figure 41 on the left)

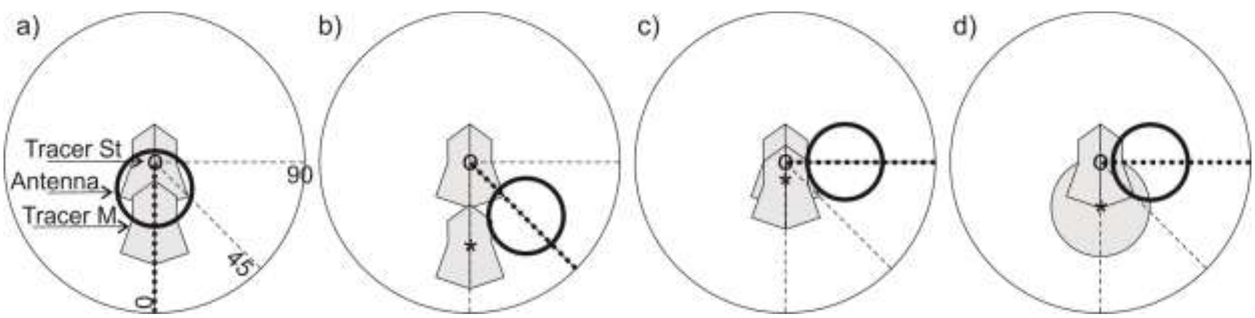

Figure 66: Examples of cluster experiments with cases a – d corresponding with those identified on Figure 65

From Figure 66, it is evident that for the antenna loop to pick up the signal of the stationary tracer, the loop has to be in contact with the field of the stationary tracer. These conceptual illustrations show that factors such as the shape of the electromagnetic fields, the overlapping of the fields of the tracers, and the position of the antenna loop with respect to the tracers all may impact the detection distances as two tracers are moved closer together. A takeaway from these experiments on clusters is that seeding tracers in close proximity is not advisable. The density of seeded particles must be considered carefully during the stages of experimental design to avoid clustering effects that could confound detection of each tracer.

6.2.4 Skip Zones

The existence of skip zones detected during tracking surveys in Laurel Creek was confirmed by laboratory testing. Two distinct skip zones were found in the laboratory tests. However, since the distance between these zones is only a few centimeters, the recognition of two distinct zones in the field might not be possible every time. The two zones together extend to approximately 10 cm on either side of the tag from its either tip. Therefore, by identifying the extent of the skip zones in the field can enable the researcher to identify the location of the tag within an error range 10 cm, which is a vast improvement over the previously used 1m error range used in the tracking surveys for Laurel Creek in this study.

7 CONCLUSIONS AND RECOMMENDATIONS

RFID technology was used to track bedload particles in four sites in Laurel Creek. In the field component of the study, movement of tracers was tracked during up to three tracking events. Three tracking events were conducted for Sites 1 and 4. Only one tracking event was conducted for Sites 2 and 3. For the field component of this study, movement of a tracer was considered to have taken place if the displacement of the tracer from its previous position was greater than one meter. This distance was chosen as it is the maximum distance at which the antenna used could detect a 32 mm RFID transponder. In order to improve the precision of detection, i.e., to consider displacements less than one meter as genuine displacements, the accuracy of the location of the detected tracer had to be improved. Various laboratory experiments were conducted to determine the how various factors affected a precise detection of tracer location, and hence determine the best procedure for tagging, seeding and tracking tracers.

Observations from the field studies are as follows:

- The average recovery rate of the RFID tracers was found to be over 90% even after multiple tracking events. This high recovery rate attests to the success, and the ease of use of RFID technology.
- The tracers were found to have travelled as much as 75 m from the original location.
- Generally, the tracer path length decreased with an increase in tracer size.
- Some interesting trends in tracer mobility and path lengths with respect to size classes were noted. Further field tracking is required to establish definite trends in bedload transport and quantitatively determine the amount of transport.

The conclusions from the laboratory studies are as follows:

- The detection ranges were largest for a vertical orientation of the transponder, i.e., when the longest axis of the transponder was perpendicular to the loop of the antenna. The transponders in a horizontal orientation yielded detection distances as much as 40% lower than those in vertical orientation.

- The size of the tracer was found to have no effect on the detection distance. Similarly, conditions of saturation and submergence (when the tracer was placed in a horizontal orientation) did not show a significant effect on the detection distances. However, a vertical placement of the tracer under conditions of submergence, the detection distances is 47% lower than the detection distance of a vertically oriented tracer in dry conditions.

- Burial depth was found to affect detection distances. When tracers in vertical orientation were buried, the detection distances reduced for tests at the surface to tests at 3" below the surface, thereafter, the distances increase for tests at 6" and then a steady decline in detection distance is observed with the increase of burial depth. Mixed results were seen for tracers in horizontal orientation and further testing is required to determine the how the shape of the field influences the detection range in the horizontal tests. It is hypothesized that the confounding effect of burial is likely due to the sediment physically limiting the portion of the field that is accessible to the antenna.

- Clusters of tracers, in a configuration as simple as two tracers, were found to impact the measurement of detection distances. Factors such as the shape of the electromagnetic fields, the overlapping of the fields of the tracers, and the position of the antenna loop with respect to the tracers may impact the detection distances as two tracers are moved closer together. Further research is required to precisely determine how each factor affects the detection distances.

- Experiments highlighted for the first time the existence of skip zones that have been previously quickly suggested by manufacturers (Aquartis, 2011) but never properly identified nor quantified. Skip zones should theoretically allow a more precise detection (<10 cm error) of the transponder location. In practice, the complex shape of the detection zone might conflicts with this use of the skip zone. Users may also rely on another antenna type rather than solely the skip zone (Carre et al., 2007, Bradley & Tucker, 2012, Chapuis et al., in rev.).

- The shape of the electromagnetic field of a transponder changes depending on the orientation of the transponder with respect to the antenna. The shape of the electromagnetic field of the transponders ("donut shape" of detection zones given by manufacturers (Texas Instruments, 1996; Aquartis, 2011) for a vertical transponder) may help explain some of the results obtained. However, further research is required to establish the how the shape of the field changes when one or more confounding factors are present.

- This research is most significant because it rigourously quantifies the detection distance and confounding factors related to sediment tracking using RFID technology which is now a widely utilized technique. For accurate determination of mobility and accurate quantification of step length, the determination of precise location is required.

The implications and recommendations as a result of the conclusions presented above are as follows.

- Tagging procedure should use a consistent method for tag installation, depending on the purpose of the study. For a quick detection of tracers, the tag should be installed along the c-axis. For a precise detection of it, the tags should rather be drilled along the a-axis.

- The determination of precise locations will enable researches to conduct detailed flume studies and field studies relating bedload movement to micro-topography and clustering patterns. Studies of larger temporal and spatial scales that do not require determination of precise location of tags will also benefit from this work because it helps to reduce uncertainty related to field conditions and inconsistencies in technique.

- The first survey is often considered as not significant because the seeding is not a "natural" process. If it is possible, practitioners might want to pay attention to reproduce the imbrications of natural particles to limit the unnatural placement of tracers. In addition, seeding of tracers might avoid clustering in case of a low-energy river that might not be able to spread tracers as soon as the first flood event occurs. An evenly spaced grid might to be the best way to limit shadowing effects after the first flood.

- During the process of tracking, one must pay attention to the “skip zones”. The detection of such zones when the tracer is favourably oriented can allow for not only a quick detection but also for an accurate determination of tracer location.

- Additional research would be beneficial in quantifying the various confounding factors which may affect detection distances.

BIBLIOGRAPHY

Anderson, K. (2008). *Cemetery Services – Bechtel Park Master Plan.* City of Waterloo, Recreation and Leisure Services. Waterloo: City of Waterloo.

Annable, W. K., Watson, C. C., & Thompson, P. J. (2012). Quasi-equilirium conditions of urban gravel-bed stream channels in southern Ontario, Canada. *River Research and Applications, 28*(3), 302 325.

Aquartis. (2011). *Lenoie System User Guide: Mobile RFID Detection System (HDX 134.2 KHZ).* Aquartis Technology Ltd.

Ashworth, P. J., & Ferguson, R. I. (1989). Size-selective entrainment of bed load in gravel bed streams. *Water Resources Research, 25*(4), 627-634.

Bagnold, R. A. (1956). The flow of cohesionless grains in fluids. *Philosophical Transactions of the Royal Society of London. Series A, Mathematical and Physical Sciences*, 235-297.

Bagnold, R. A. (1966). *An approach to the sediment transport problem from general physics.* U. S. Geological Survey Professional Paper 422-I.

Bagnold, R. A. (1973). The nature and saltation of bed-load transport in water. *Proceedings of the Royal Society of London*, (pp. 473-504).

Benelli, G., & Pozzebon, A. (2013). Radio frequency identification from system to applications. In M. Reaz, *RFID Under Water: Technical Issues and Applications* (pp. 379-396). InTech.

Bennett, S. J., Simon, A., Castro, J. M., Atkinson, J. F., Colleen, E. B., Blersch, S. S., & Rabideau, A. J. (2011). The Evolving Science of Stream Restoration. In A. Simon, S. J. Bennett, & J. M. Castro (Eds.), *Stream Restoration in Dynamic Fluvial Systems* (pp. 1-8). Washington, D.C., USA: American Geophysical Union.

Biedenharn, D. S., Watson, C. C., & Thorne, C. R. (2007). Fundamentals of Fluvial Geomorphology. In M. H. Garcia (Ed.), *Sedimentation Engineering: processes, management, modeling, and practice* (pp. 387-438). Reston, Virgina, USA: ASCE.

Bledsoe, B. P., & Watson, C. C. (2001). Effects of urbanization on channel instability. *Journal of the American Water Resources Association, 37*(2), 255-270.

Booth, D. B. (1990). Stream channel incision following drainage basin urbanization. *Water Resources Bulletin, 26*, 407-417.

Booth, D. B., & Jackson, C. R. (1997). Urbanization of aquatic systems: Degradation thresholds, stormwater detection, and the limits of mitigation. *Journal of the American Water Resources Association, 33*(5), 1077-1090.

Bradley, N. D., & Tucker, G. E. (2012). Measuring gravel transport and dispersion in a mountain river using passive radio tracers. *Earth Surface Processes and Landforms, 37*, 1034-1045.

Brown, C. B. (1950). Sediment Transport. In H. Rouse (Ed.), *Engineering Hydraulics.* John Wiley and Sons Inc.

Carre, D. M., Biron, P. M., & Gaskin, S. J. (2007). Flow dynamics and bedload sediment transport around paired deflectors for fish habitat enhancement: a field study in the Nicolet River. *Canadian Journal of Civil Engineering, 34*(6), 761-769.

Chang, H. H. (1988). *Fluvial processes in river engineering.* New York: John Wiley.

Chapuis, M., Bright, C. J., Hufnagel, J., & MacVicar, B. (In Review). Detection ranges and uncertainty of passive Radio Frequency Identification (RFID) transponders for sediment tracking in rivers and coastal environments. *In Review*.

Chapuis, M., Bright, C. J., Hufnagel, J., & MacVicar, B. (In Review). Detection ranges and uncertainty of passive Radio Frequency Identification (RFID) transponders for sediment tracking in rivers and coastal environments. *In Review*.

Chin, A. (2006). Urban transformation of river landscapes in a global context. *Geomorphology, 79*, 460 - 487.

Church, M., & Hassan, M. A. (1992). Size and distance of travel of unconstrained clasts on a streambed. *Water Resources Research, 28,* 299-303.

Colosimo, M. F., & Wilcock, P. R. (2007). Alluvial sedimentation and erosion in an urbanizing watershed, Gwynns Falls, Maryland. *Journal of American Water Resources Association, 43*(2), 499-521.

Cruise, J. F., Laymon, C. A., & Al-Hamdan, O. Z. (2010). Impact of 20 years of land-cover change on the hydrology of streams in the southeastern United States. *Journal of the American Water Resources Association, 46*(6), 1159-1170.

CWN. (2007). *Comparison of Canadian Watersheds*. (Canadian Water Network) Retrieved August 8, 2012, from Institute for Resources, Environment and Sustainability: http://research.ires.ubc.ca/projects/cwn_on/watersheds/on/characteristics/ON_wschar.htm

Davis, W. M. (1902). Baselevel, Grade and Peneplain. *The Journal of Geology, 10*(1), 77-111.

Dingman, S. L. (2009). *Fluvial Hydraulics.* Oxford: Oxford University Press.

Diplas, P., Dancey, C. L., Celik, A. O., Valyrakis, M., Greer, T., & Akar, T. (2008). The role of impulse on the initiation of particle movement under turbulent flow conditions. *Science, 322*, 717-720.

Diplas, P., Kuhnle, R., Gray, J., Glysson, D., & Edwards, T. (2007). Sediment Transport Measurements. In M. H. Garcia (Ed.), *Sedimentation Engineering: processes, management, modeling, and practice* (pp. 307-353). Reston, Virginia, USA: ASCE.

DuBoys, M. P. (1879). Le Rhône et les Rivières à lit affouillable [The Rhone and rivers with mobile beds]. *Annales des ponts et chaussées, 5*(18), 141-195.

Einstein, H. A. (1937). *Der Geschiebetrieb als Wahrscheinlichkeitsproblem [Bed-load transport as a problem of probablity]*. an der Eidgenossische Technische Hochacule, Mitteilung der Verschsanstalt fur Wasserbau. Zurich: Verlag Rascher & Co.

Einstein, H. A. (1950). *The Bed-Load Function for Sediment Transportation in Open Channel Flows.* Technical Bulletin 1026, United States Department of Agriculture, Soil Conservation Service, Washington, D.C.

Ferencevic, M. V., & Ashmore, P. (2011). Creating and evaluating digital elevation model-based stream-power map as a stream assessment tool. *River Research and Applications, 28*(9), 1394-1416.

Finkenzeller, K. (2003). *RFID Handbook: Fundamentals and Applications in Contactless Smart Cards and Identification.* (R. Waddington, Trans.) West Sussex, UK: John Wiley & Sons Ltd.

Frey, P., & Church, C. (2011). Bedload: a granular phenomenon. *Earth Surface Processes and Landforms, 36*, 58--69.

Galster, J. C., Pazzaglia, F. J., & Germanoski, D. (2008). Measuring the impact of urbanization on channel widths using historic aerial photographs and modern surveys. *Journal of the American Water Resources Association, 44*(4), 948-960.

Galster, J. C., Pazzaglia, F. J., Hargreaves, B. R., Morris, D. P., Peters, S. C., & Weisman, R. N. (2006). Effects of urbanization on watershed hydrology: The scaling of discharge with drainage area. *Geology, 34*(9), 713-716.

Ganti, V., Meerschaert, M. M., Foufoula-Georgiou, E., Viparelli, E., & Parker, .. (2010). Normal and anomalous diffusion of gravel tracer particles in rivers. *Journal of Geophysical Research, 115*, F00A12.

García, M. H. (2007). Sediment transport and morphodynamics. In M. H. García (Ed.), *Sedimentation Engineering: processes, management, modeling, and practice* (pp. 21-164). Reston, Virginia, USA: American Society of Civil Engineers.

Gomez, B. (1991). Bedload transport. *Earth-Science Reviews, 31*, 89-132.

Gray, J. R., Laronne, J. B., & Marr, J. D. (2010). *Bedload-surrogate monitoring technolies.* U. S. Department of the Interior. Reston, Virginia: U. S. Geological Survey.

GRCA. (1993). *Laurel Creek Watershed Study*. Cambridge, Ontario, Canada: Grand River Conservation Authority.

GRCA. (2004). *Laurel Creek Conservation Area Draft Master Plan.* Cambridge, Ontario, Canada: Grand River Conservation Authority.

Gregory, K. J. (1987). River Channels. In K. J. Gregory, & D. E. Walling (Eds.), *Human Activity and Environmental Processes* (pp. 207-235). Chichester, UK: Wiley.

Gregory, K. J., Davis, R. J., & Downs, P. W. (1992). Identification of river channel change to due to urbanization. *Applied Geography, 12*(4), 299-318.

Hammer, T. R. (1972). Stream channel enlargement due to urbanization. *Water Resources Research, 8*, 1530–1540.

Hassan, M. A., & Woodsmith, R. D. (2004). Bed load transport in an obstruction-formed pool in a forest, gravelbed stream. *Geomorphology, 58*, 203 - 221.

Helley, E. J., & Smith, W. (1971). *Development and Calibration of a Pressure-Difference Bedload Sampler.* Open-File, USGS, Water Resources Division, Menlo Park, California.

Hey, R. (1996). Environmentally Sensitive River Engiinnering. In G. E. Petts, & P. Calow (Eds.), *River Restoration* (pp. 80-104). Cambridge, Massachusetts, USA: Blackwell Science Ltd.

Hollis, G. E. (1975). The effects of urbanization on floods of different recurrence interval. *Water Resources Research, 11*, 431-435.

Hubbell, D. W. (1964). *Apparatus and Techniques for Measuring Bedload.* U.S. Geological Survey, United States Department of the Interior. Washington: United States Government Printing Office.

Julien, P. (1995). *Erosion and Sedimentation.* Cambridge: Cambridge University Press.

Lamarre, H., MacVicar, B., & Roy, A. (2005). Using Passive Integrated Transponder (PIT) Tags to Investigate Sediment Transport in Gravel-Bed Rivers. *Journal of Sedimentary Research, 75*, 736-741.

Lane, E. W. (1955). The importance of fluvial morphology in hydraulic engineering. *Proceedings: American Society of Civil Engineers*, *81*.

Langbein, W., & Leopold, L. B. (1964). Quasi-equilibrium states in channel morphology. *American Journal of Science, 262*, 782-794.

Lauth, T. J., & Papanicolaou, A. N. (2009). Application of radio frequency tracers to individual and group particle displacement within a laboratory. *World Environmental and Water Resources Congress* (pp. 2264-2271). Kansas City, Missouri: ASCE.

Lauth, T., J., & Papanicolaou, A. N. (2008). Experimental/feasibility study of radio frequency tracers for monitoring sediment transport and scour around bridges. *World Environmental and Water Resources Congress.* Honolulu, Hawaii: ASCE.

Lehpamer, H. (2012). *RFID Design Principles* (2nd ed.). Norwood, MA: Artech House.

Leopold, L. B. (1968). *Hydrology for urban land planning: A guidebook on the hydrologic effects of urban land use.* U. S. Geological Survey. USGS.

Leopold, L. B., Huppman, R., & Miller, A. (2005). Geomorphic effects of urbanization in forty-one years of observation. *Proceedings of the American Philosophical Society, 149*(3), 349-371.

Leopold, L., & Maddock Jr., T. (1953). *The Hydraulics Geometry of Stream Channels and some Physiographic Implications.* US Department of the Interior. Washington: United States Government Printing Office.

Liébault, F., Bellot, H., Chapuis, M., Klotz, S., & Deschâtres, M. (2011). Bedload tracing in a high-sediment-load mountain stream. *Earth Surface Processes and Landforms, 37*(4), 385–399.

MacArthur, R. C., Neil, C. R., & Hall, B. R. (2007). Overview of Sedimentation Engineering. In M. H. Garcia (Ed.), *Sedimentation Engineering: processes, management, modeling, and practice* (pp. 1-20). American Society of Civil Engineers.

MacVicar, B. J., Piegay, H., Henderson, A., Comiti, F., Oberlin, C., & Pecorari, E. (2009). Quantifying the temporal dynamics of wood in large rivers: field trials of wood surveying, dating, tracking, and monitoring techniques. *Earth Surface Processes and Landforms, 34*(15), 2031-2046.

MacVicar, B. M., & Roy, A. G. (2011). Sediment mobility in a forced riffle-pool. *Geomorphology, 125*(3), 445 - 456.

McGill, R., Tukey, J. W., & Larsen, W. A. (1978). Variations of box plots. *The American Statistician*, *32*(1), 12-16.

Meyer-Peter, E., & Muller, R. (1948). Formulas for bedload transport. *Proceedings of the 2nd Congress* (pp. 36-64). Stockholm: International Association of Hydraulic Structures Research.

Miller, I. M., & Warrick, J. A. (2012, March). Measuring sediment transport and bed disturbance with tracers on a mixed beach. *Marine Geology, 299-302*, 1-17.

Miller, I. M., Warrick, J. A., & Morgan, C. (2011). Observations of coarse sediment movements on the mixed beach of the Elwha Delta, Washington. *Marine Geology, 282*, 201-214.

Nelson, J. M., Shreve, R. L., McLean, S. R., & Drake, T. G. (1995). Role of Near-Bed Turbulence Structure in Bed Load Transport and Bed Form Mechanics. *Water Resources Researach, 31*(8), 2071-2086.

Nichols, M. H. (2004). A Radio Frequency Identification System for Monitoring Coarse Sediment Particle Displacement. *Applied Engineering in Agriculture*, *20*(6), 783-787.

Ninõ, Y., & García, M. (1998). Using Lagrangian particle saltation observations for bedload sediment transport modelling. *Hydrological Processes*, 1197--1218.

Paiement-Paradis, G., Marquis, G., & Roy, A. (2011). Effects of turbulence on teh transport of individual particles as bedload in a gravel-bed river. *Earth Surface Processes and Landforms, 36*, 107-116.

Papanicolaou, A. N., Moustakidis, I. V., & Tsakiris, A. G. (2012). Detection of erosion/deposition depth using a passive RFID technology. In R. M. Muñoz (Ed.), *River Flow 2012* (pp. 1293–1299). Costa Rica: CRC Press.

Parker, G. (2007). Transport of gravel and sediment mixtures. In M. H. Garcia (Ed.), *Sedimentation Engineering: processes, management, modeling, and practice* (pp. 165-252). Reston, VA: ASCE.

Petts, G., & Calow, P. (1996). The Nature of RIvers. In G. Petts, & P. Calow (Eds.), *River Restoration* (pp. 1-6). Cambridge, Massachusetts, USA: Blackwell Science Ltd.

Pizzuto, J. E., Hession, W. E., & McBride, M. (2000). Comparing gravel-bed rivers in paired urban and rural catchments of southeastern Pennsylvania. *Geology, 28*, 79-82.

Pomeroy, C. A., Postel, N. A., O'Neill, P. A., & Roesner, L. A. (2008). Development of Storm-Water Management Design Criteria to Maintain Geomorphic Stability in Kansas City Metropolitan Area Streams. *Journal of Irrigation and Drainage Engineering, 134*, 562-566.

Ranasinghe, D. C., & Cole, P. H. (2008). Networked RFID Systems. In P. H. Cole, & D. C. Ranasinghe (Eds.), *Networked RFID Systems and Lightweight Cryptography* (1 ed., pp. 45-58). Berlin, Germany: Springer-Verlag Berlin/Heidelberg.

Schneider, J., Hegglin, R., Meier, S., Turowski, J. M., Nitsche, M., & Rickenmann, D. (2010). Studying sediment transport in mountain rivers by mobile and stationary RFID antennas. In Dittrich, Koll, Aberle, & Geisenhainer (Ed.), *River Flow* (pp. 1723-1730). Braunschweig, Germany: Bundesanstalt für Wasserbau.

Schumm, S. A. (1969, January). River metamorphosis. *Proceedings of the American Society of Civil Engineers. Journal of the Hydraulic Division, 95*(HY1), 255-273.

Schumm, S. A., Harvey, M. D., & Watson, C. C. (1984). *Incised Channels: Morphology, Dynamics and Control.* Littleton, Colorado, USA: Water Resources Publications.

Shields, A. (1936). *Anwendung der Aehnlichkeitsmechanik und der Turbulenzforschung auf die Geshiebebewegung [Application of similarity principles and turbulence research to bed-*

load movement]. California Institute of Technology, Soil Conservation Service. Berlin: Technischen Hochschule Berlin.

Simon, A. (1989). A model of channel response in disturbed alluvial channels. *Earth Surface Processes and Landforms, 14*, 11-26.

Simon, A., & Rinaldi, M. (2006). Disturbance, stream incision, and channel evolution: The roles of excess transport capacity and boundary materials in controlling channel response. *Geomorphology, 79*, 361 - 383.

Smart, G. M., & Habersack, H. M. (2010). Pressure fluctuations and gravel entrainment in rivers. *Journal of Hydraulic Research, 45*, 661-673.

Sohn, Y. K. (1997). On traction-carpet sedimentation. *Journal of Sedimentary Research, 67*(3), 502-509.

Stantec. (2010). *Class Environmental Assessment and Preliminary Design: Laurel Creek and Sanitary Trunk Sewer Report.* City of Waterloo. Kitchener: Stantec Consulting Ltd.

Sumer, B. M., Chua, L. H., Cheng, N. S., & Fredsøe, J. (2003). Influence of Turbulence on Bed Load Sediment Transport. *Journal of Hydraulic Engineering, 129*, 585-596.

Surian, N., & Rinaldi, M. (2004). Channel adjustments in response to human alteration of sediment fluxes: examples from Italian rivers. In V. Golosov, V. Belyaev, & D. E. Walling (Ed.), *Sediment Transfer through the Fluvial System. 288*, pp. 276-282. Moscow: International Association of Hydrological Sciences.

Texas Instruments. (1996). *Antenna reference guide.* Dallas, TX: Texas Instruments Inc.

TI. (2012, August). *New to RFID?* Retrieved August 2012, from Texas Instruments: http://www.ti.com/rfid/faqs.shtml#Gone

Trimble, S. W. (1997, November 21). Contribution of stream channel erosion to sediment yield from an urbanizing watershed. *Science, 278*, 1442-1444.

Valyrakis, M., Diplas, P., Celik, A. O., & Dancey, C. L. (2010, Spetember 8-10). Incipient rolling of coarse particles in water flows: a dynamical perspective. In Dittrich, Koll, Aberle, & Geisenhainer (Ed.), *River Flow 2010* (pp. 769-776). Braunschweig, Germany: Bundesanstalt für Wasserbau.

Want, R. (2006). *RFID Explained: A Primer on Radio Frequency Identification Technology*. Morgan & Claypool Publishers.

Wilcock, P. R., & McArdell, B. W. (1993). Surface-based fractional transport rates: mobilization thresholds and partial transport of a sand-gravel sediment. *Water Resources Research, 29*(4), 1297-1312.

Wilcock, P. R., & McArdell, B. W. (1997). Partial transport of a sand/gravel sediment. *Water Resources Research, 33*(1), 235-245.

Wilson, K. C. (1987). Analysis of bed-moad motion at high shear stress. *Journal of Hydraulic Engineering, 113*, 97-103.

Wilson, K. C. (1989). Mobile-bed friction at high shear stress. *Journal of Hydraulic Engineering, 115*, 825-830.

Yalin, M. S., & Karahan, E. (1979). Inception of sediment transport. *Journal of the Hydraulics Division, HY11*, 1433–1443.

Zanke, U. (2003). On the influence of turbulence on the initiation of sediment motion. *International Journal of Sediment Research, 18*, 17-31.

Zingg, T. (1935). Beitrag zur Schotteranalyse. *Schweizerische Mineralogische und Petrographische Mitteilungen*, 39-140.

APPENDIX A – FIELD DATA

Table A1: Tracer Characteristics

	Tag #	Seeding site	Grain Size Bin #	Tag Type	Rock# (3 digits)	a	b	c	Mass	Volume
						cm	cm	cm	g	mL
211015	033847	2	1	1	15	4.3	3	1.9	55.65	20.0
211035	03385B	2	1	1	35	4.4	3.1	2.2	58.9	24.0
252161	03D901	2	5	2	161	11.1	11	8.1	1905.4	692.2
221077	035F95	2	2	1	77	5.5	4.3	2	89.74	37.0
262187	04002B	2	6	2	187	19	12.4	8.7	4129.8	2440.8
211037	03385D	2	1	1	37	5	3.1	2.2	70.98	31.0
211034	03385A	2	1	1	34	3.9	3.2	2.6	65.74	28.0
211039	03385F	2	1	1	39	4.9	3	2.9	95.45	34.0
221058	035F82	2	2	1	58	3.8	3.8	3.6	118.99	45.0
242140	03B1DC	2	4	2	140	9.2	6.8	5.3	495.2	192.0
221066	035F8A	2	2	1	66	5.3	3.5	2.3	75.07	32.0
221054	035F7E	2	2	1	54	6.6	4.4	3.5	181.83	66.0
211027	033853	2	1	1	27	4.2	2.5	1.8	37.18	16.0
252164	03D904	2	5	2	164	10.9	9.4	6	867.5	312.7
221056	035F80	2	2	1	56	5.4	4.5	3	129.16	48.0
242148	03B1E4	2	4	2	148	11.3	7	6.4	885.6	322.0
252174	03D90E	2	5	2	174	12	11.6	5.6	1426.5	537.4
221051	035F7B	2	2	1	51	5.3	4	2.7	111.29	40.0
252166	03D906	2	5	2	166	14.3	9.1	5.5	1033.2	376.2
221063	035F87	2	2	1	63	5.3	4.4	3.6	138.63	55.0
232099	038AA3	2	3	2	99	7.2	5.8	4.2	298.29	107.0
221047	035F77	2	2	1	47	5.6	3.5	2.2	84.43	34.0
211021	03384D	2	1	1	21	4.5	3.1	2.8	50.98	20.0
242144	03B1E0	2	4	2	144	9.3	7	4.1	507.4	200.0
221090	035FA2	2	2	1	90	4.3	3.6	3	58.86	30.0
232096	038AA0	2	3	2	96	6.9	5.5	4	234.72	90.0
242134	03B1D6	2	4	2	134	10.7	8	3.4	473.7	188.0
232101	038AA5	2	3	2	101	6.1	5.5	3.3	195.93	73.0
211014	033846	2	1	1	14	4	2.5	2	43.62	17.0
252175	03D90F	2	5	2	175	15	9.8	7.5	2404.6	890.8
252173	03D90D	2	5	2	173	13.2	10.6	8.8	1882.7	684.0
232094	038A9E	2	3	2	94	8.5	5.6	3.7	315.91	119.0
232130	038AC2	2	3	2	130	7.6	4.6	4.3	257.72	40.0

211036	03385C	2	1	1	36	4.2	3	2.5	48.17	21.0
232102	038AA6	2	3	2	102	7.1	6.9	2.9	230.77	88.0
221064	035F88	2	2	1	64	5.8	4.5	4.2	182.65	71.0
232129	038AC1	2	3	2	129	7.2	6.1	3.5	224.21	97.0
211043	033863	2	1	1	43	8.5	3.2	2	149.88	58.0
262191	04002F	2	6	2	191	21.3	14.7	10.8	4815.6	3030.0
232107	038AAB	2	3	2	107	7.5	5.3	4.6	265.63	99.0
211041	033861	2	1	1	41	5.7	2.5	2.1	52.26	21.0
242152	03B1E8	2	4	2	152	11.5	6.6	4.5	618.3	238.0
221055	035F7F	2	2	1	55	4.2	3.3	2.5	63.15	26.0
232122	038ABA	2	3	2	122	7.7	6.4	3.9	238.62	92.0
211013	033845	2	1	1	13	4.9	3.1	2.7	65.89	27.0
211002	03383A	2	1	1	2	4.5	2.9	2	41.09	17.0
211011	033843	2	1	1	11	4	3	2.1	37.23	15.0
221067	035F8B	2	2	1	67	5	3.5	3	105.32	40.0
232131	038AC3	2	3	2	131	5.2	4.6	2.3	99.95	83.0
221048	035F78	2	2	1	48	5.8	3.6	2.6	84.04	35.0
221057	035F81	2	2	1	57	5.7	3.8	3.1	143.33	56.0
211023	03384F	2	1	1	23	4	2.7	1.8	44.89	18.0
242135	03B1D7	2	4	2	135	16.1	8.3	5.3	1201.2	451.0
221089	035FA1	2	2	1	89	5.5	4.5	2.5	134.59	50.0
252167	03D907	2	5	2	167	14.4	10.3	6.9	1759.2	625.4
242155	03B1EB	2	4	2	155	9.5	8	5.4	682.3	270.0
221078	035F96	2	2	1	78	5.9	4.3	3.5	135.03	50.0
242138	03B1DA	2	4	2	138	7.9	6.1	4.8	369.4	155.0
221060	035F84	2	2	1	60	5.5	4.4	2.6	100.24	40.0
211016	033848	2	1	1	16	3.8	2.6	1.8	38.27	15.0
232123	038ABB	2	3	2	123	6.5	5.2	2.7	131.81	49.0
221053	035F7D	2	2	1	53	5.6	4.2	2.7	78.23	31.0
211006	03383E	2	1	1	6	4.7	2.7	1.8	46.39	20.0
252179	03D913	2	5	2	179	14.3	10.4	6.8	1703.6	618.9
221070	035F8E	2	2	1	70	5.8	4.2	2.5	87.64	36.0
232127	038ABF	2	3	2	127	6	5.3	4.1	230.54	88.0
242136	03B1D8	2	4	2	136	11.3	7.8	3.8	646	232.0
262198	040036	2	6	2	198	22	16.5	7.9	4702.6	2216.4
211003	03383B	2	1	1	3	3.3	3.1	2	41.38	17.0
242159	03B1EF	2	4	2	159	11.1	8.2	6.5	882.7	322.0
242142	03B1DE	2	4	2	142	11.1	8.2	3.1	580.9	215.0
232114	038AB2	2	3	2	114	6.6	4.7	4.6	222.64	86.0
221052	035F7C	2	2	1	52	6	4.2	3.8	167.91	64.0
232119	038AB7	2	3	2	119	6.1	5.3	3	168.92	67.0
221072	035F90	2	2	1	72	5	4.4	3	115.24	43.0
252176	03D910	2	5	2	176	16	9.6	7.3	1945.9	684.0

211022	03384E	2	1	1	22	4.4	3.2	2	39.69	16.0
242139	03B1DB	2	4	2	139	9	7	4.6	443.8	175.0
232097	038AA1	2	3	2	97	4.8	4.6	2.1	88.64	35.0
262193	040031	2	6	2	193	15.3	10.4	6.2	2849.5	1739.4
252180	03D914	2	5	2	180	11.4	9.6	6.6	1443.7	527.7
232113	038AB1	2	3	2	113	6.9	6	4.6	286.75	106.0
221049	035F79	2	2	1	49	4.6	3.6	2.5	77.21	31.0
211026	033852	2	1	1	26	4	2.4	1.9	41.61	19.0
211033	033859	2	1	1	33	3.6	2.3	1.7	30.76	13.0
211019	03384B	2	1	1	19	4.2	3.2	2	41.47	16.0
221065	035F89	2	2	1	65	3.9	3.9	2.7	64.37	30.0
221069	035F8D	2	2	1	69	5.5	4.3	3.7	101.18	40.0
211009	033841	2	1	1	9	5	3	2	55.17	23.0
242143	03B1DF	2	4	2	143	13.3	7.6	5	838.1	297.0
262181	040025	2	6	2	181	19.6	15.5	9.7	4908.5	2721.4
232106	038AAA	2	3	2	106	6.4	5	3.6	159.73	66.0
221080	035F98	2	2	1	80	5.8	4.5	3.4	176.32	63.0
242133	03B1D5	2	4	2	133	12.5	7.4	4.3	722.1	270.0
221083	035F9B	2	2	1	83	5.2	4.3	4.1	137.73	57.0
221081	035F99	2	2	1	81	4.5	3.5	2.7	64.87	26.0
262183	040027	2	6	2	183	16.8	14.8	6.6	3545.7	1851.6
221045	035F75	2	2	1	45	6	3.9	3	143.91	56.0
211017	033849	2	1	1	17	4.7	3.1	2.5	56.4	23.0
242137	03B1D9	2	4	2	137	11.7	8	4.3	667.6	255.0
242151	03B1E7	2	4	2	151	11.8	7.5	4	656.1	207.0
242156	03B1EC	2	4	2	156	11	6.8	4	523.6	204.0
252168	03D908	2	5	2	168	11.8	10.6	4.9	752.5	298.0
232098	038AA2	2	3	2	98	5.9	4.6	3.5	150.79	61.0
242150	03B1E6	2	4	2	150	11	7	5.1	651.9	205.0
262186	04002A	2	6	2	186	15.8	14.6	9	3286	2525.0
211020	03384C	2	1	1	20	3.7	2.4	2.3	48.84	22.0
232104	038AA8	2	3	2	104	7	6.1	3.5	204.77	82.0
221088	035FA0	2	2	1	88	6.3	3.7	2.2	94.49	37.0
211025	033851	2	1	1	25	3.8	2.6	2.4	40.28	17.0
262182	040026	2	6	2	182	18.9	18	13	7955	3647.2
262197	040035	2	6	2	197	16.2	15.3	13.5	5308.5	3787.5
232115	038AB3	2	3	2	115	7	4.3	2.8	139.01	53.0
242149	03B1E5	2	4	2	149	10.2	8	5.8	773.6	290.0
211018	03384A	2	1	1	18	3.5	2.9	1.5	32.26	13.0
252162	03D902	2	5	2	162	11.5	10.2	9.3	1710.5	618.9
262195	040033	2	6	2	195	19.6	13.7	6.2	3707.4	1739.4
232117	038AB5	2	3	2	117	6.5	4.7	3.1	162.65	63.0
221086	035F9E	2	2	1	86	4.4	3.9	3.5	91.97	37.0

211038	03385E	2	1	1	38	5.3	2.9	2.3	61.81	24.0
232118	038AB6	2	3	2	118	6.4	4.6	3.5	159.61	62.0
221091	035FA3	2	2	1	91	6.3	4.3	3.4	139.38	58.0
262184	040028	2	6	2	184	18.7	14.2	7.5	3268.1	2104.1
211010	033842	2	1	1	10	5.3	3.2	2.1	61.69	23.0
252171	03D90B	2	5	2	171	9.3	8.5	8.1	1278.6	457.6
232095	038A9F	2	3	2	95	7.5	5.1	3.8	232.69	89.0
242160	03B1F0	2	4	2	160	10	7.5	6	851	317.0
262189	04002D	2	6	2	189	15.7	14	7.1	3311.4	1991.9
232110	038AAE	2	3	2	110	6.3	4.6	3.7	140.55	53.0
211040	033860	2	1	1	40	4.3	3	2.1	55.72	22.0
221068	035F8C	2	2	1	68	5.2	4.1	3.5	118.67	45.0
211007	03383F	2	1	1	7	5.2	3.1	2	64.63	25.0
211024	033850	2	1	1	24	4	3.1	2.7	65.68	26.0
221074	035F92	2	2	1	74	5.2	4.3	3.6	129.89	51.0
232112	038AB0	2	3	2	112	5.3	4.5	3.2	148.77	55.0
221076	035F94	2	2	1	76	6	4.4	2.7	120.63	45.0
211028	033854	2	1	1	28	4	3	2.3	45.49	22.0
242146	03B1E2	2	4	2	146	11	7.9	6.5	903.8	335.0
252172	03D90C	2	5	2	172	14.3	10.5	7.8	1793.9	651.4
232103	038AA7	2	3	2	103	7.3	6	3.1	213.12	84.0
221082	035F9A	2	2	1	82	5.5	4.4	2.9	110.74	41.0
242153	03B1E9	2	4	2	153	8.5	8	6.2	841.4	310.0
221062	035F86	2	2	1	62	4.6	3.6	2.9	61.93	25.0
232109	038AAD	2	3	2	109	7.1	5.1	4.7	295.92	117.0
221073	035F91	2	2	1	73	4.3	3.6	2.1	47.75	19.0
262194	040032	2	6	2	194	19.8	14.1	10.8	3981.9	3030.0
221079	035F97	2	2	1	79	6.5	3.7	3.4	136.55	52.0
211042	033862	2	1	1	42	3.7	3.1	2.3	52.56	21.0
242145	03B1E1	2	4	2	145	10.2	7.5	6.5	776.7	290.0
242158	03B1EE	2	4	2	158	13	8	4.8	974.2	377.0
262192	040030	2	6	2	192	16.7	16	12.9	5437.8	3619.1
221059	035F83	2	2	1	59	5.4	4.2	2.4	93.51	36.0
232124	038ABC	2	3	2	124	6	5.5	3.3	174.89	69.0
242147	03B1E3	2	4	2	147	12.9	7.6	4.8	874.6	331.0
211029	033855	2	1	1	29	3.9	2.7	1.8	43.26	20.0
232108	038AAC	2	3	2	108	8.2	5.3	3.9	326.24	120.0
221084	035F9C	2	2	1	84	5	3.8	2.7	87.09	34.0
211001	033839	2	1	1	1	5.1	3.1	2.2	67.58	27.0
252169	03D909	2	5	2	169	12.5	9.2	8.7	1774.8	659.6
242141	03B1DD	2	4	2	141	8	7	5.7	503.9	205.0
262199	040037	2	6	2	199	19.4	13.2	10.1	4221.3	2833.6
262190	04002E	2	6	2	190	15.8	10.1	6.3	2604.6	1767.5

262200	040038	2	6	2	200	17.1	14.1	8.5	4033.6	2384.7
211012	033844	2	1	1	12	3.7	2.9	2.3	43.51	16.0
232111	038AAF	2	3	2	111	7	6.5	3.4	226.24	87.0
252163	03D903	2	5	2	163	13.6	11.4	7.5	1923.7	710.1
232126	038ABE	2	3	2	126	6.2	5.3	3.7	183.74	71.0
221075	035F93	2	2	1	75	5.3	3.9	2.9	114.14	43.0
211030	033856	2	1	1	30	4.9	3	2.5	64.11	25.0
232100	038AA4	2	3	2	100	5.6	5.5	2.9	197.39	73.0
232116	038AB4	2	3	2	116	5.4	4.7	2.5	98.4	38.0
221050	035F7A	2	2	1	50	5.5	4.1	3	106.98	41.0
211005	03383D	2	1	1	5	5.8	3	2.4	79.48	31.0
252170	03D90A	2	5	2	170	11	9.4	9	1662.4	587.9
221061	035F85	2	2	1	61	3.7	3.3	3.2	79.27	32.0
262185	040029	2	6	2	185	16.7	15.6	4.1	2683.1	1150.3
252177	03D911	2	5	2	177	14	9	8.3	1556.6	570.0
232105	038AA9	2	3	2	105	6.9	5.6	2.5	158.61	66.0
221092	035FA4	2	2	1	92	4	3.3	2.2	42.83	20.0
211031	033857	2	1	1	31	4	3.2	1.9	45.29	18.0
211032	033858	2	1	1	32	4.6	2.8	1.5	43.26	18.0
211004	03383C	2	1	1	4	3.3	2.6	2.1	33.68	14.0
221071	035F8F	2	2	1	71	4.6	3.3	2.1	45.91	21.0
232132	038AC4	2	3	2	132	7.4	5.1	3	210.48	69.0
242157	03B1ED	2	4	2	157	10.5	7.4	5.4	806	297.0
221044	035F74	2	2	1	44	4.1	3.7	3.3	103.05	40.0
262196	040034	2	6	2	196	18.8	15.6	5.3	2849.5	1486.9
262188	04002C	2	6	2	188	21	14.3	7.5	4388.2	2104.1
232120	038AB8	2	3	2	120	5.5	4.9	2.6	106	41.0
221085	035F9D	2	2	1	85	4.4	4	3.1	84.29	35.0
221087	035F9F	2	2	1	87	5.4	4.1	3.6	133.75	49.0
232093	038A9D	2	3	2	93	8.7	4.5	3	217.76	85.0
252178	03D912	2	5	2	178	13	12.5	6.7	1675.3	631.9
211008	033840	2	1	1	8	4.3	3.2	2.5	52.45	22.0
221046	035F76	2	2	1	46	4.7	3.3	3	71.67	30.0
232121	038AB9	2	3	2	121	7.4	5.2	3.1	196.06	76.0
232125	038ABD	2	3	2	125	6.2	6	4.1	210.45	78.0
232128	038AC0	2	3	2	128	6.7	5.5	4	188	87.0
242154	03B1EA	2	4	2	154	10	7.9	5.1	580.6	230.0
252165	03D905	2	5	2	165	13.2	9.3	6.4	1119.1	395.8

Table A2: Survey Benchmarks

Point #	Northing	Easting	Elevation	Description
18	4814569	540710.8	308.8055	21_L
19	4814565	540698.2	308.4875	22_R
20	4814616	540658.2	308.9642	20_R
21	4814625	540641.8	309.0297	18_R
22	4814632	540645.9	308.8241	17_L
23	4814628	540661.9	308.6329	19_L
24	4814268	539210.7	316.4372	7_L
25	4814266	539225	316.7059	8_R*
26	4814298	539224.6	316.7079	10_R
27	4814295	539213.3	316.0471	9_L*
28	4814761	539314.4	314.8995	12_R
29	4814772	539304.2	315.3323	11_L
30	4814788	539321.2	315.1519	13_L
31	4814778	539333.3	314.858	14_R
32	4814902	539401.6	315.0201	16_R
33	4814908	539389.4	314.9985	15_L
34	4814240	539210	317.6242	X_CUT_DS_UNI
35	4812986	538959.5	319.9675	25_L
36	4812970	538962.1	320.1278	23_L
37	4812969	538981.6	319.5438	24_R
38	4812990	538981.5	319.4737	26_R
39	4812943	538971.8	320.6753	BRIDGE
40	4813203	539087	320.148	1_L*
41	4813216	539105.1	319.3967	3_L
42	4813320	539249.3	320.0753	5_L
43	4813306	539259.9	319.8305	6_R
44	4813203	539114.6	319.2691	4_R
45	4813190	539098.4	320.3379	2_R*
647	4814616	540690.5	309.7657	PED_BRIDGE
P336	4814632	540646	308.745	17L_resection
P337	4814616	540658.2	308.966	20R_resection
P338	4814624	540641.8	309.001	18R_resection
P339	4814659	540606.5	309.345	4U_R_resection
P340	4814672	540624.2	308.91	4U_L_resection
P341	4814650	540637.2	309.354	4D_L_resection
P342	4814642	540620.3	309.189	4D_R_resection
P369	4814616	540690.4	309.735	PED__BRIDGE_resection
P370	4814614	540688.5	309.727	on_PED__BRIDGE_STN_SETUP
STN_RESECTION	4814583	540695.3	308.59	RESECTION
P372	4812990	538981.5	319.446	26l resect
P538	4812990	538981.5	319.445	1C_26R_Recheck
P539	4812986	538959.5	319.971	1C_25L_Recheck
P676	4812979	538971.6	317.772	1C_REBAR-IN-CHANNEL
P687	4813075	538951.3	317.494	41_L

P688	4813107	538964.7	317.546	42_R
1455	4814789	539353	314.846	30_R
1443	4814803	539338.8	314.74	29_l
1254	4814774	539335.9	314.834	28_R
964	4814791	539310.1	315.763	13L_JUNE
965	4814807	539327.4	315.356	29L_JUNE
1063	4814296	539214.1	316.801	9l_ts
943	4814759	539290.1	314.041	PED_BRIDGE
849	4814783	539359.5	315.163	MANHOLE

Table A3a: Laurel Creek Survey Profile – Site 1

Point #	Northing	Easting	Elevation	Description
P447	4812890	538966.8	317.652	1C_THAL
P446	4812892	538966.8	317.607	1C_THAL
P445	4812893	538966.9	317.566	1C_THAL
P444	4812895	538967.2	317.583	1C_THAL
P443	4812897	538967.7	317.549	1C_THAL
P442	4812898	538967.8	317.579	1C_THAL
P441	4812900	538967.8	317.568	1C_THAL
P440	4812901	538968.2	317.576	1C_THAL
P439	4812902	538968.7	317.596	1C_THAL
P438	4812903	538969	317.521	1C_THAL
P437	4812905	538968.9	317.56	1C_THAL
P436	4812906	538969.2	317.591	1C_THAL
P435	4812908	538969.2	317.594	1C_THAL
P434	4812909	538969.1	317.595	1C_THAL
P433	4812911	538969.8	317.521	1C_THAL
P432	4812912	538969.8	317.615	1C_THAL
P431	4812914	538970	317.703	1C_THAL
P430	4812915	538970.5	317.7	1C_THAL
P429	4812916	538970.6	317.707	1C_THAL
P428	4812917	538971.1	317.751	1C_THAL
P427	4812919	538971.3	317.741	1C_THAL
P426	4812921	538971.5	317.704	1C_THAL
P425	4812922	538971	317.737	1C_THAL
P424	4812923	538970.1	317.772	1C_THAL
P423	4812924	538969.5	317.746	1C_THAL
P422	4812926	538969	317.748	1C_THAL
P421	4812926	538969	317.817	1C_THAL_C_U
P420	4812944	538970.7	317.722	1C_THAL_C_D

P419	4812945	538971.7	317.714	1C_THAL
P418	4812946	538972.6	317.717	1C_THAL
P417	4812946	538973.1	317.646	1C_THAL
P416	4812947	538973.2	317.675	1C_THAL
P415	4812948	538973.1	317.681	1C_THAL
P414	4812950	538973.2	317.702	1C_THAL
P413	4812951	538973.3	317.675	1C_THAL
P412	4812953	538973.2	317.636	1C_THAL
P411	4812954	538973.2	317.631	1C_THAL
P410	4812955	538973.2	317.627	1C_THAL
P409	4812956	538972.4	317.608	1C_THAL
P408	4812957	538972	317.561	1C_THAL
P407	4812958	538971.4	317.552	1C_THAL
P406	4812960	538971.4	317.575	1C_THAL
P405	4812962	538971.1	317.565	1C_THAL
P404	4812963	538970.8	317.572	1C_THAL
P403	4812965	538970.7	317.561	1C_THAL
P402	4812966	538970.6	317.569	1C_THAL
P401	4812967	538970.5	317.558	1C_THAL
P400	4812968	538970.4	317.581	1C_THAL
P399	4812970	538970.2	317.557	1C_THAL
P448	4812981	538968.7	317.496	1C_THAL
P449	4812983	538968.3	317.488	1C_THAL
P450	4812984	538968.1	317.499	1C_THAL
P451	4812985	538967.8	317.501	1C_THAL
P452	4812987	538967.9	317.489	1C_THAL
P453	4812988	538967.5	317.556	1C_THAL
P454	4812989	538967.3	317.483	1C_THAL
P455	4812990	538967.2	317.551	1C_THAL
P456	4812992	538967.2	317.476	1C_THAL
P457	4812994	538966.5	317.474	1C_THAL
P458	4812996	538966.3	317.471	1C_THAL
P459	4812998	538966.4	317.475	1C_THAL
P460	4812999	538966.6	317.469	1C_THAL
P461	4813001	538966.7	317.44	1C_THAL
P462	4813003	538967	317.441	1C_THAL
P463	4813004	538967	317.423	1C_THAL
P464	4813006	538966.7	317.415	1C_THAL
P465	4813008	538966.5	317.369	1C_THAL
P466	4813009	538966.7	317.343	1C_THAL
P467	4813010	538966.4	317.346	1C_THAL
P468	4813011	538966.3	317.363	1C_THAL
P469	4813012	538966.4	317.336	1C_THAL

P470	4813013	538966.5	317.33	1C_THAL
P471	4813014	538966.2	317.324	1C_THAL
P472	4813016	538965.9	317.306	1C_THAL
P473	4813017	538965.5	317.321	1C_THAL
P474	4813019	538964.7	317.36	1C_THAL
P475	4813021	538964.1	317.323	1C_THAL
P476	4813023	538963.8	317.317	1C_THAL
P477	4813025	538963.2	317.304	1C_THAL
P478	4813026	538962.7	317.302	1C_THAL
P479	4813028	538962.1	317.259	1C_THAL
P480	4813030	538961.6	317.248	1C_THAL
P481	4813032	538961.2	317.252	1C_THAL
P482	4813033	538961.1	317.286	1C_THAL
P483	4813035	538960.9	317.312	1C_THAL
P484	4813037	538960.7	317.28	1C_THAL
P485	4813039	538960.5	317.236	1C_THAL
P486	4813040	538960.4	317.196	1C_THAL
P487	4813041	538960.2	317.227	1C_THAL
P488	4813043	538959.7	317.154	1C_THAL
P489	4813044	538959.2	317.13	1C_THAL
P490	4813046	538958.9	317.135	1C_THAL
P491	4813047	538959.1	317.232	1C_THAL
P492	4813048	538959.2	317.249	1C_THAL
P493	4813049	538958.8	317.243	1C_THAL
P494	4813050	538958.6	317.318	1C_THAL
P495	4813050	538958.2	317.257	1C_THAL
P496	4813051	538958	317.261	1C_THAL
P497	4813051	538958.2	317.278	1C_THAL
P498	4813052	538958.5	317.209	1C_THAL
P499	4813053	538958.3	317.228	1C_THAL
P500	4813054	538958.3	317.128	1C_THAL
P501	4813055	538958	317.074	1C_THAL
P502	4813056	538957.7	317.019	1C_THAL
P503	4813057	538957.5	317.08	1C_THAL
P504	4813058	538957.1	317.115	1C_THAL
P505	4813059	538956.9	316.959	1C_THAL
P506	4813061	538956.6	316.958	1C_THAL
P507	4813062	538956.2	316.948	1C_THAL
P508	4813064	538955.9	316.948	1C_THAL
P509	4813065	538955.5	317.038	1C_THAL
P510	4813067	538955	317.007	1C_THAL
P511	4813069	538954.3	316.965	1C_THAL
P512	4813071	538954	317.011	1C_THAL

P513	4813073	538954	316.942	1C_THAL
P514	4813075	538954.2	316.959	1C_THAL
P515	4813077	538954.2	316.926	1C_THAL
P516	4813078	538953.9	316.954	1C_THAL
P517	4813079	538953.7	316.936	1C_THAL
P518	4813081	538953.7	316.955	1C_THAL
P519	4813083	538953.6	316.96	1C_THAL
P520	4813083	538953.6	316.961	1C_THAL
P521	4813084	538953.7	316.938	1C_THAL
P522	4813086	538953.5	316.927	1C_THAL
P523	4813087	538953.5	317.056	1C_THAL
P524	4813088	538953.8	316.978	1C_THAL
P525	4813089	538953.9	317.008	1C_THAL
P526	4813090	538954.1	317.099	1C_THAL
P689	4813090	538955.2	316.981	1C_THAL
P690	4813092	538955.6	316.928	1C_THAL
P691	4813094	538956.5	316.937	1C_THAL
P692	4813096	538958.1	317.01	1C_THAL
P693	4813097	538959.3	317.041	1C_THAL
P694	4813099	538960.4	317.094	1C_THAL
P695	4813100	538961.9	317.033	1C_THAL
P696	4813101	538962.7	317.017	1C_THAL
P697	4813103	538964.2	317.086	1C_THAL
P698	4813104	538965.5	317.082	1C_THAL

Table A3b: Laurel Creek Survey Profile – Site 2 and Site 3

Point #	Northing	Easting	Elevation	Description
864	539218.8	4814249	315.2961	THAL
865	539221	4814264	315.2415	THAL
866	539221	4814274	315.2388	THAL
867	539222.1	4814283	315.1899	THAL
868	539223.3	4814287	314.9736	THAL
869	539219.2	4814296	315.067	THAL
870	539218.2	4814305	315.069	RC
871	539215.4	4814315	314.8126	THAL
872	539211.7	4814322	314.5208	THAL
873	539209	4814327	314.6472	THAL
874	539204.7	4814332	314.9214	THAL
875	539204.1	4814333	315.0073	THAL
876	539197.7	4814345	314.7036	THAL

877	539203.9	4814330	315.5003	TP1
878	539197.4	4814347	314.5905	THAL
879	539193.6	4814354	314.8802	THAL
880	539189	4814364	314.8239	THAL
881	539188	4814367	315.1343	RC
882	539185.3	4814372	314.8817	THAL
883	539183.3	4814378	314.9745	THAL
884	539180.5	4814382	315.0101	THAL
885	539178.1	4814389	314.9651	THAL
886	539174.1	4814399	315.3147	RC
887	539170.7	4814407	315.2615	RC
888	539174.1	4814396	315.6642	TP2
889	539177.6	4814406	316.3541	XS
890	539176.9	4814405	316.1612	XS
891	539176	4814405	315.2322	XS
892	539173.3	4814405	315.0411	XS
893	539170.5	4814405	315.0416	XS
894	539168.2	4814403	315.2364	XS
895	539168	4814403	316.094	XS
896	539154.5	4814506	315.2486	TP3
897	539165.2	4814402	316.742	XS
898	539153.9	4814503	314.8378	THAL
899	539172.5	4814407	315.2515	RC
900	539154.8	4814498	314.4224	THAL
901	539171.4	4814415	314.871	THAL
902	539156.4	4814491	314.9448	RC
903	539169.6	4814423	314.8858	THAL
904	539158.1	4814484	314.6013	THAL
905	539168.5	4814430	314.9211	THAL
906	539160.1	4814474	314.9665	THAL
907	539167.1	4814436	314.8269	THAL
908	539161.2	4814463	315.0354	THAL
909	539165	4814443	314.8441	THAL
910	539162.7	4814454	314.8857	THAL
911	539151.2	4814518	314.7181	THAL
912	539150.1	4814528	314.5626	THAL
913	539149.2	4814539	314.8549	RC
914	539146.3	4814548	314.3514	THAL
915	539145.2	4814555	314.2862	THAL
916	539143.9	4814561	314.4508	THAL
917	539142.2	4814568	314.8231	THAL
918	539140	4814584	314.8097	RC
919	539137.5	4814593	314.4458	THAL

920	539135.3	4814604	314.4524	THAL
921	539133.2	4814615	314.3498	THAL
922	539127.5	4814642	316.0952	TP4
923	539133.2	4814619	314.4047	THAL
924	539132.7	4814636	314.3464	THAL
925	539135.9	4814643	314.5567	THAL
926	539141.3	4814652	314.577	RC
927	539152.8	4814659	314.427	THAL
928	539165.3	4814664	314.2872	THAL
929	539176.3	4814669	314.2596	THAL
930	539183.2	4814674	314.0356	THAL
931	539194.1	4814681	314.1803	THAL
932	539201.9	4814687	314.2143	THAL
933	539204.9	4814688	314.8134	TP5
934	539207	4814694	314.2041	THAL
935	539215.1	4814701	314.3105	THAL
936	539225.9	4814708	314.1922	THAL
937	539235.9	4814716	314.1527	THAL
938	539246.3	4814723	314.2097	THAL
939	539253.3	4814729	314.3106	THAL
940	539260.2	4814734	314.0483	THAL
941	539265.5	4814739	314.3724	RC
942	539278.8	4814749	314.1888	THAL
943	539290.1	4814759	314.0412	PED_BRIDGE
944	539295.6	4814763	313.6896	THAL
945	539199.1	4814700	315.8452	XS
946	539201	4814697	315.6172	XS
947	539201.7	4814696	315.2509	XS
948	539202	4814696	314.6033	XS
949	539203.7	4814694	314.1822	XS
950	539206.6	4814691	314.1423	XS
951	539208	4814689	314.3013	XS
952	539208.3	4814688	315.5232	XS
953	539208.9	4814687	315.5934	XS
954	539301.4	4814767	314.631	TP6
955	539296.7	4814770	313.5913	THAL
956	539303.5	4814775	313.8555	THAL
957	539314.3	4814786	314.2057	THAL
958	539326.3	4814795	313.9534	THAL
959	539335.4	4814804	313.9493	THAL
960	539345.6	4814818	313.9977	THAL
961	539355.7	4814830	314.0308	THAL
962	539361.2	4814837	313.962	THAL

963	539359.9	4814835	314.4198	TP7
964	539310.1	4814791	315.763	13L_JUNE
965	539327.4	4814807	315.3556	29L_JUNE
966	539362.1	4814841	313.7002	THAL
967	539364.5	4814850	313.7187	THAL
968	539365.5	4814857	313.7949	THAL
969	539366.5	4814865	313.9619	THAL
970	539368.3	4814871	313.8195	THAL
971	539370.3	4814877	313.862	THAL
972	539371.9	4814884	313.8161	THAL
973	539374.2	4814893	313.856	THAL
974	539375.7	4814898	313.8165	THAL
975	539373.2	4814898	314.4187	TP8
976	539367	4814895	316.2106	XS
977	539368.6	4814895	315.9296	XS
978	539369.2	4814894	315.5534	XS
979	539369.8	4814893	314.1336	XS
980	539370	4814892	314.0427	XS
981	539371.4	4814891	313.989	XS
982	539372	4814891	313.8244	XS
983	539373.4	4814890	313.848	XS
984	539375	4814889	313.7455	XS
985	539376.6	4814888	313.9039	XS
986	539377.5	4814888	313.9746	XS
987	539377.6	4814888	314.6894	XS
988	539377.8	4814887	314.7126	XS
989	539378	4814888	315.4609	XS
990	539379	4814887	315.3965	XS
991	539371.9	4814891	313.8785	CONFL_FORWELL
992	539367.2	4814890	313.9714	FORWELL
993	539376.7	4814895	313.8235	THAL
994	539380.2	4814903	313.7012	THAL
995	539383	4814912	313.6251	THAL
996	539386.3	4814921	314.1251	SEWER
997	539412.6	4814975	313.8285	TP9
998	539386.4	4814922	313.7628	THAL
999	539388.6	4814930	313.6604	THAL
1000	539411.1	4814976	313.3277	THAL
1001	539392.5	4814940	313.8987	RC
1002	539396	4814947	313.58	THAL
1003	539401.2	4814958	313.4207	THAL
1004	539406.9	4814968	313.4245	THAL
1005	539416.1	4814983	312.9086	THAL

1006	539420.4	4814990	313.3125	THAL
1007	539428.8	4814997	313.1833	THAL
1008	539439	4815007	313.2924	THAL
1009	539447.8	4815017	313.2764	THAL
1010	539457	4815027	313.4188	RC
1011	539467.3	4815039	313.2599	THAL
1012	539479.4	4815050	313.3528	THAL
1013	539488.2	4815060	313.5387	TP10
1014	539496.7	4815061	313.0938	THAL
1015	539503.9	4815065	312.8172	THAL
1016	539513.2	4815069	312.7895	THAL
1017	539523.6	4815073	313.2327	RC
1018	539536.5	4815078	313.0808	THAL
1019	539544.9	4815082	312.964	THAL
1020	539553.1	4815084	312.6804	THAL
1021	539567.2	4815088	312.3978	THAL
1022	539577.9	4815092	312.9156	THAL
1023	539587.6	4815096	312.8187	THAL
1024	539598	4815100	313.1776	TP11
1025	539604.9	4815098	312.9143	THAL
1026	539623.5	4815099	312.8938	RC
1027	539639.8	4815099	312.4337	THAL
1028	539652.7	4815099	312.751	RC
1029	539670.4	4815098	312.7182	SEWER
1030	539671.5	4815098	312.2045	THAL
1031	539690.1	4815095	312.6806	TP12
1032	539678.2	4815097	312.3751	THAL
1033	539685.2	4815095	312.4557	RC
1034	539693.8	4815091	311.811	THAL
1035	539706.3	4815085	311.401	THAL
1036	539713.3	4815079	312.1727	THAL
1037	539721.6	4815074	311.3262	THAL
1038	539726.8	4815070	311.6083	THAL
1039	539732.4	4815066	312.0985	THAL
1040	539738.7	4815061	311.653	THAL
1041	539745.5	4815055	311.6741	THAL
1042	539751.3	4815049	312.0464	THAL
1043	539760.9	4815042	312.0753	THAL
1044	539765.4	4815039	311.854	THAL
1045	539770.8	4815035	312.2637	THAL
1046	539780.6	4815028	311.8549	THAL
1047	539790.8	4815023	311.845	THAL
1048	539804	4815013	312.2494	TP13

1049	539814.5	4815009	311.8292	THAL
1050	539823.1	4815004	311.6817	THAL
1051	539827.5	4815001	311.5454	THAL
1052	539832.3	4814999	311.571	THAL
1053	539841.8	4814993	311.3847	THAL
1054	539847.9	4814991	311.4429	THAL
1055	539857.1	4814987	311.5494	THAL
1056	539864.6	4814984	311.788	THAL
1057	539870.8	4814984	311.8546	RC
1058	539867.9	4814980	312.5741	TP14
1059	539880.8	4814985	311.6621	THAL
1060	539890.2	4814987	311.7664	RC
1061	539901.6	4814990	311.4386	THAL
1062	539908.5	4814994	312.9365	TP15

Table A3c: Laurel Creek Survey Profile – Site 4

Point #	Northing	Easting	Elevation	Description
P699	4814680	540606.3	307.857	4C_THAL
P700	4814679	540607.2	307.816	4C_THAL
P701	4814678	540608.2	307.813	4C_THAL
P702	4814678	540609	307.912	4C_THAL
P703	4814677	540609.9	307.895	4C_THAL
P704	4814676	540610.8	307.897	4C_THAL
P705	4814675	540611.8	307.92	4C_THAL
P706	4814674	540612.4	307.988	4C_THAL
P707	4814673	540613.2	308.043	4C_THAL
P708	4814672	540614.1	308.019	4C_THAL
P709	4814670	540614.6	308.082	4C_THAL
P710	4814669	540615.7	308.105	4C_THAL
P711	4814668	540616.6	308.15	4C_THAL
P712	4814667	540617.2	308.153	4C_THAL
P713	4814667	540618.1	308.133	4C_THAL
P714	4814666	540619.1	308.154	4C_THAL
P715	4814665	540619.9	308.194	4C_THAL
P716	4814664	540620.9	308.196	4C_THAL
P717	4814662	540621.6	308.206	4C_THAL
P718	4814661	540622.1	308.197	4C_THAL
P719	4814660	540622.6	308.228	4C_THAL
P720	4814658	540623	308.207	4C_THAL
P721	4814657	540623.3	308.239	4C_THAL

P722	4814656	540623.2	308.205	4C_THAL
P723	4814654	540623.4	308.205	4C_THAL
P724	4814653	540623.6	308.19	4C_THAL
P725	4814652	540623.7	308.191	4C_THAL
P726	4814650	540623.6	308.153	4C_THAL
P727	4814648	540624.1	308.045	4C_THAL
P728	4814647	540624.8	307.91	4C_THAL
P729	4814645	540625.4	307.845	4C_THAL
P730	4814644	540626.2	307.84	4C_THAL
P731	4814643	540626.9	307.814	4C_THAL
P732	4814642	540627.8	307.782	4C_THAL
P733	4814641	540628.8	307.667	4C_THAL
P734	4814640	540629.8	307.651	4C_THAL
P735	4814639	540630.2	307.623	4C_THAL
P736	4814639	540630.9	307.645	4C_THAL
P737	4814637	540631.5	307.636	4C_THAL
P738	4814636	540632.2	307.606	4C_THAL
P739	4814635	540633	307.571	4C_THAL
P740	4814635	540633.5	307.554	4C_THAL
P741	4814634	540634.4	307.543	4C_THAL
P742	4814634	540635.1	307.527	4C_THAL
P743	4814633	540636.1	307.521	4C_THAL
P744	4814632	540637	307.439	4C_THAL
P745	4814631	540637.8	307.429	4C_THAL
P746	4814631	540638.5	307.439	4C_THAL
P747	4814631	540639.4	307.478	4C_THAL
P748	4814630	540640.2	307.493	4C_THAL
P749	4814630	540641.3	307.484	4C_THAL
P750	4814630	540642	307.491	4C_THAL
P751	4814629	540643	307.487	4C_THAL
P752	4814629	540643.7	307.51	4C_THAL
P753	4814629	540644.6	307.493	4C_THAL
P754	4814629	540645	307.513	4C_THAL
P755	4814628	540646.1	307.525	4C_THAL
P756	4814628	540647	307.596	4C_THAL
P757	4814627	540648.3	307.705	4C_THAL
P758	4814627	540649.2	307.785	4C_THAL
P759	4814626	540650.4	307.859	4C_THAL
P760	4814625	540651.6	307.939	4C_THAL
P761	4814625	540652.2	307.943	4C_THAL
P762	4814624	540653.1	307.922	4C_THAL
P763	4814624	540653.1	307.866	4C_THAL
P764	4814623	540653.5	307.871	4C_THAL

P765	4814622	540654.2	307.902	4C_THAL
P766	4814622	540655	307.916	4C_THAL
P767	4814622	540656.5	308.012	4C_THAL
P768	4814621	540657.9	308.043	4C_THAL
P769	4814621	540659.4	307.983	4C_THAL
P770	4814621	540659.8	307.936	4C_THAL
P771	4814621	540660.2	308.135	4C_THAL
P772	4814621	540660.5	308.003	4C_THAL
P773	4814621	540661.2	308.03	4C_THAL
P774	4814621	540662.5	308.055	4C_THAL
P775	4814620	540663.9	308.012	4C_THAL
P776	4814620	540665.4	308.042	4C_THAL
P777	4814620	540666.4	307.821	4C_THAL
P778	4814620	540667.1	307.726	4C_THAL
P779	4814620	540667.8	307.762	4C_THAL
P780	4814620	540668.2	307.823	4C_THAL
P781	4814619	540669	307.893	4C_THAL
P782	4814619	540670.4	307.924	4C_THAL
P783	4814619	540672.1	307.961	4C_THAL
P784	4814618	540673.8	307.864	4C_THAL
P785	4814618	540675.4	307.939	4C_THAL
P786	4814617	540676.8	307.888	4C_THAL
P787	4814617	540677.8	307.815	4C_THAL
P788	4814617	540679.5	307.804	4C_THAL
P789	4814617	540681.1	307.818	4C_THAL
P790	4814617	540682.2	307.776	4C_THAL
P791	4814617	540683.2	307.721	4C_THAL
P792	4814617	540683.2	307.721	4C_THAL
P793	4814617	540683.8	307.656	4C_THAL
P794	4814617	540684.6	307.65	4C_THAL
P795	4814616	540685.4	307.67	4C_THAL
P796	4814615	540685.9	307.677	4C_THAL
P797	4814614	540686.4	307.709	4C_THAL

Table A4a: Sediment Substrate Data: Pebble count Site 1

Pebble Count			
d/s of Bridgeport Road			
Site 1			
	Pebble Count		
		mm	04-Nov-10
S/C	Silt/Clay	<.062	1
SAND	Very Fine	0.062-0.125	
	Fine	0.125-0.25	2
	Medium	0.25-0.50	
	Coarse	0.50-1.0	1
	Very Coar	1.0-2	3
GRAVEL	Very Fine	2-4	2
	Fine	4-5.7	1
	Fine	5.7-8	1
	Medium	8-11.3	6
	Medium	11.3-16	
	Coarse	16-22.6	12
	Coarse	22.6-32	15
	Very Coar	32-45	17
	Very Coar	45-64	19
COBBLES	Small	64-90	13
	Small	90-128	3
	Large	128-180	2
	Large	180-256	1
BOULDER	Small	256-362	1
	Small	362-512	
	Medium	512-1024	
	Large	1024-2048	
	Large-Ver	1024-2048	
BDRK			

Table A4b: Sediment Substrate Data: Pebble count Site 2

Pebble Count				
University and Marsland - Highland Park				
Site 2				
	Pebble Count			
		mm	15-Oct-10	03-Nov-10
S/C	Silt/Clay	<.062		
SAND	Very Fine	0.062-0.125		
	Fine	0.125-0.25		
	Medium	0.25-0.50	1	2
	Coarse	0.50-1.0	3	3
	Very Coar	1.0-2	4	2
GRAVEL	Very Fine	2-4	4	3
	Fine	4-5.7	3	4
	Fine	5.7-8	4	5
	Medium	8-11.3	5	4
	Medium	11.3-16	6	7
	Coarse	16-22.6	2	3
	Coarse	22.6-32	4	2
	Very Coar	32-45	5	2
	Very Coar	45-64	3	2
COBBLES	Small	64-90	2	2
	Small	90-128	3	1
	Large	128-180		5
	Large	180-256	1	
BOULDER	Small	256-362		2
	Small	362-512	1	1
	Medium	512-1024		
	Large	1024-2048		
	Large-Ver	1024-2048		
BDRK				

Table A4c: Sediment Substrate Data: Pebble count Site 3

Pebble Count				
Highland Park - d/s of ped bridge				
Site 3				
	Pebble Count			
		mm	15-Oct-10	03-Nov-10
S/C	Silt/Clay	<.062		
SAND	Very Fine	0.062-0.125		
	Fine	0.125-0.25		1
	Medium	0.25-0.50	5	8
	Coarse	0.50-1.0	6	7
	Very Coar	1.0-2	2	4
GRAVEL	Very Fine	2-4		2
	Fine	4-5.7	7	6
	Fine	5.7-8	1	2
	Medium	8-11.3	2	2
	Medium	11.3-16	5	
	Coarse	16-22.6	2	3
	Coarse	22.6-32	2	4
	Very Coar	32-45	4	1
	Very Coar	45-64	10	4
COBBLES	Small	64-90	2	3
	Small	90-128		
	Large	128-180	1	2
	Large	180-256	1	
BOULDER	Small	256-362		
	Small	362-512		1
	Medium	512-1024		
	Large	1024-2048		
	Large-Ver	1024-2048		
BDRK				

Table A4d: Sediment Substrate Data: Pebble count Site 4

Pebble Count			
Bechtel Park			
Site 4			
	Pebble Count		
		mm	04-Nov-10
S/C	Silt/Clay	<.062	3
SAND	Very Fine	0.062-0.125	
	Fine	0.125-0.25	1
	Medium	0.25-0.50	1
	Coarse	0.50-1.0	2
	Very Coar	1.0-2	4
GRAVEL	Very Fine	2-4	2
	Fine	4-5.7	1
	Fine	5.7-8	8
	Medium	8-11.3	7
	Medium	11.3-16	3
	Coarse	16-22.6	7
	Coarse	22.6-32	11
	Very Coar	32-45	8
	Very Coar	45-64	12
COBBLES	Small	64-90	5
	Small	90-128	1
	Large	128-180	4
	Large	180-256	8
BOULDER	Small	256-362	1
	Small	362-512	
	Medium	512-1024	1
	Large	1024-2048	
	Large-Ver	1024-2048	
BDRK			

Table A4d: Sediment Substrate Data: Sieve Analysis

Sieve Analysis				
Sample taken at Laurel Creek Site 4 on the upstream point bar				
Same location where field - "lab" tests were performed				
Wet Mass (kg):	12.295	13.285	5.49	masses include bag weight
Dry Mass (kg):	5.505	11.49	12.505	dry mass: mass lost to water and transferring loss (includes glass pieces, debris, and so)

Mass sieved (g):		2632	2814.5	2938.8	2646.6	3105.7	2892.3
ϕ	Size (mm)	Sample Retained (g)					
		Pavement		Sub-Pavement 1		Sub-Pavement 2	
		Sample 1	Sample 2	Sample 1	Sample 2	Sample 1	Sample 2
-6.0	63	0	0	0	0	0	0
-5.5	45	270.6	88.2	252.4	0	0	0
-5.0	31.5	207	283.3	92.3	139.5	139.7	117.6
-4.5	22.4	687.1	719	348.8	281.9	332	230.9
-4.0	16	509.7	771.8	338.8	286.9	325.4	253.4
-3.5	11.2	366	393.1	269.9	292.5	376.1	281.6
-3.0	8	244.3	215.6	247.3	239.1	281.6	264.3
-2.7	6.3	100.3	98.8	159.3	158.7	174.6	167.4
-2.0	4	109.5	113.1	265.4	249.6	298	308.6
-1.5	2.8	45.3	47.4	176.1	178.2	205	222.4
-1.0	2	24	24	142.4	145.8	170.8	191.3
-0.5	1.4	14.2	13.9	109.6	115.3	140.8	155.3
0.0	1	8.3	7.9	96.8	100.6	120.7	132.6
0.5	0.71	6	5.8	111	115.2	141.3	147.7
1.0	0.5	4.6	4.5	94.3	98.5	119.1	126.6
1.5	0.355	6	6	104.7	107.5	131.6	133
2.0	0.25	6.6	7.9	65.3	68.5	77.3	82.5
2.5	0.180	4.4	4.5	28	28.9	31.6	34.9
3.0	0.125	3	3.3	14.5	15.1	16.2	17.6
3.5	0.090	1.5	1.5	6.3	6.2	6.2	7
4.0	0.0625	1.2	1.1	4.7	4.6	4.6	5.4
4.5	<0.063	1.4	1.3	6.8	7	6.4	7

Table A5a: Seeding Survey – Site 1

point #	east	north	elev	desc	Tag #
83	538968.2	4812974	317.5519	section_d	111001
197	538970.7	4812985	317.4775	section_p	111002
182	538968.8	4812984	317.516	section_n	111003
79	538971.7	4812974	317.5232	section_d	111004
86	538966.3	4812974	317.5782	section_d	111005
173	538967.9	4812983	317.4694	section_m	111006
181	538969	4812984	317.476	section_n	111007
51	538970.1	4812971	317.5498	section_a	111008
205	538972	4812986	317.5266	section_q	111009
114	538966.9	4812977	317.5254	section_g	111010
158	538970.7	4812983	317.5024	section_l	11011
230	538968.3	4812987	317.4628	section_s	111012
119	538970.1	4812978	317.4747	section_h	111013
214	538965.1	4812986	317.426	section_q	111014
123	538967.1	4812978	317.5478	section_h	111015
90	538970.2	4812975	317.4966	section_e	111016
130	538969.2	4812979	317.4863	section_i	111017
169	538970.2	4812983	317.4657	section_m	11018
136	538965.1	4812979	317.5729	section_i	111019
68	538971.1	4812973	317.4941	section_c	111020
155	538965.6	4812982	317.497	section_k	111021
132	538968	4812979	317.4731	section_i	111022
105	538966.8	4812976	317.5577	section_f	111023
231	538967.6	4812987	317.4825	section_s	111024
164	538966.6	4812982	317.4583	section_l	111025
52	538969.5	4812970	317.5248	section_a	111026
180	538969.5	4812984	317.4652	section_n	111027
208	538970	4812986	317.5137	section_q	111028
74	538967.7	4812973	317.5728	section_c	111029
131	538968.7	4812979	317.489	section_i	111036
232	538966.7	4812987	317.4793	section_s	111031
108	538971.8	4812977	317.5015	section_g	111032
50	538970.8	4812971	317.5324	section_a	111033
91	538969.5	4812975	317.5361	section_e	111034
65	538966	4812972	317.6219	section_b	111035
219	538968.9	4812987	317.4723	section_r	111030
147	538971.9	4812982	317.453	section_k	111037
57	538973	4812972	317.5163	section_b	111038
92	538968.8	4812975	317.5106	section_e	111039
186	538971.3	4812985	317.4694	section_o	111040

223	538965.6	4812986	317.4404	section_r	111041
97	538972.8	4812976	317.5783	section_f	111042
46	538973.7	4812971	317.5464	section_a	111043
104	538967.5	4812976	317.5247	section_f	121044
171	538969	4812983	317.4842	section_m	121045
48	538972.6	4812971	317.5472	section_a	121046
62	538967.9	4812972	317.5558	section_b	121047
99	538971	4812976	317.5317	section_f	121048
55	538966.2	4812970	317.6651	section_a	121049
81	538970.1	4812974	317.5164	section_d	121050
140	538969.7	4812981	317.4533	section_j	121051
56	538973.6	4812972	317.5266	section_b	121052
95	538966.5	4812975	317.5897	section_e	121053
135	538966.2	4812979	317.5438	section_i	121054
240	538968.1	4812988	317.4495	section_t	121055
107	538972.5	4812977	317.5292	section_g	121056
118	538970.9	4812978	317.5028	section_h	121057
121	538968.6	4812978	317.4768	section_h	121058
179	538970	4812984	317.4699	section_n	121059
102	538968.9	4812976	317.5101	section_f	121060
192	538966.5	4812984	317.4422	section_o	121061
236	538971.1	4812988	317.4327	section_t	121062
168	538970.6	4812983	317.4751	section_m	121063
218	538969.6	4812986	317.4993	section_r	121064
157	538971.1	4812983	317.4711	section_l	121065
183	538968	4812984	317.4864	section_n	121066
241	538967.5	4812988	317.4535	section_t	121067
207	538970.8	4812986	317.4617	section_q	121068
96	538965.6	4812975	317.5798	section_e	121069
67	538972.5	4812973	317.5296	section_c	121070
201	538967.9	4812985	317.4617	section_p	121071
144	538967.4	4812981	317.5034	section_j	121072
129	538969.8	4812979	317.4422	section_i	121073
244	538965.3	4812988	317.4415	section_t	121074
233	538966	4812987	317.4673	section_s	121075
93	538967.6	4812975	317.5455	section_e	121076
133	538967.7	4812979	317.5031	section_i	121077
222	538966.2	4812986	317.4441	section_r	121078
190	538968.3	4812985	317.4819	section_o	121079
185	538966.2	4812984	317.4196	section_n	121080
53	538968.6	4812970	317.6092	section_a	121081
196	538971.4	4812985	317.4645	section_p	121082
146	538965.7	4812981	317.5171	section_j	121083

70	538970.4	4812973	317.4782	section_c	121084
194	538965.3	4812984	317.4171	section_o	121085
110	538970.1	4812977	317.4916	section_g	121086
88	538972.1	4812975	317.5092	section_e	121087
229	538969.1	4812987	317.4866	section_s	121088
64	538966.7	4812972	317.6253	section_b	121089
225	538971.9	4812987	317.5108	section_s	121090
59	538970.8	4812972	317.5051	section_b	121091
142	538968.6	4812981	317.522	section_j	121092
220	538968	4812987	317.4504	section_r	132093
243	538966.1	4812988	317.4701	section_t	132094
239	538968.8	4812988	317.4442	section_t	132095
89	538971	4812975	317.501	section_e	132096
111	538969.1	4812977	317.4779	section_g	132097
178	538970.4	4812984	317.4981	section_n	132098
167	538971	4812983	317.4877	section_m	132099
202	538967.1	4812985	317.4459	section_p	132100
139	538970.1	4812981	317.4787	section_j	132101
143	538968	4812981	317.4894	section_j	132102
134	538967.1	4812979	317.5236	section_i	132103
189	538969.1	4812985	317.4564	section_o	132104
117	538971.8	4812978	317.4858	section_h	132105
94	538967.3	4812975	317.5346	section_e	132106
120	538969.3	4812978	317.4967	section_h	132107
217	538970.4	4812987	317.4663	section_r	132108
80	538971	4812974	317.491	section_d	132109
156	538971.8	4812983	317.4918	section_l	132110
184	538967.2	4812984	317.4745	section_n	132111
128	538970.4	4812979	317.4485	section_i	132112
73	538968.4	4812973	317.571	section_c	132113
206	538971.4	4812986	317.482	section_q	132114
78	538972.4	4812974	317.52	section_d	132115
85	538966.9	4812974	317.5586	section_d	132116
82	538969.3	4812974	317.573	section_d	132117
152	538968.4	4812982	317.4882	section_k	132118
221	538967.1	4812987	317.4589	section_r	132119
125	538966	4812978	317.549	section_h	132120
228	538969.7	4812987	317.456	section_s	132121
242	538966.8	4812988	317.4625	section_t	132122
161	538968.5	4812982	317.5012	section_l	132123
170	538969.6	4812983	317.48	section_m	132124
193	538966	4812984	317.4363	section_o	132125
215	538971.8	4812987	317.5122	section_r	132126

234	538964.9	4812987	317.4233	section_s	132127
77	538972.9	4812974	317.5277	section_d	132128
71	538969.6	4812973	317.536	section_c	132129
106	538966.4	4812976	317.5337	section_f	132130
175	538966.4	4812983	317.4354	section_m	132131
66	538973.2	4812973	317.5188	section_c	132132
203	538966.1	4812985	317.4457	section_p	142133
87	538972.9	4812975	317.5481	section_e	142134
204	538965.2	4812985	317.438	section_p	142135
210	538968.7	4812986	317.4968	section_q	142136
149	538970.6	4812981	317.4985	section_k	142137
148	538971.3	4812982	317.4555	section_k	142138
198	538970	4812985	317.477	section_p	142139
72	538969.1	4812973	317.5834	section_c	142140
116	538965.3	4812977	317.6293	section_g	142141
191	538967.7	4812985	317.4616	section_o	142142
60	538970	4812972	317.5092	section_b	142143
162	538967.8	4812983	317.4819	section_l	142144
124	538966.5	4812978	317.5503	section_h	142145
112	538968.1	4812977	317.5554	section_g	142146
199	538969.4	4812985	317.4751	section_p	142147
141	538969.1	4812981	317.4868	section_j	142148
176	538971.9	4812984	317.4917	section_n	142149
115	538966.4	4812977	317.5643	section_g	142150
103	538968.2	4812976	317.5316	section_f	142151
150	538969.9	4812982	317.4876	section_k	142152
187	538970.6	4812985	317.4951	section_o	142153
235	538971.9	4812988	317.5128	section_t	142154
153	538967.6	4812982	317.4912	section_k	142155
69	538970.4	4812973	317.4944	section_c	142156
98	538971.9	4812976	317.5681	section_f	142157
137	538972.1	4812980	317.474	section_j	142158
101	538969.5	4812976	317.5161	section_f	142159
54	538967.5	4812970	317.583	section_a	142160
63	538967.3	4812972	317.5786	section_b	152161
165	538965.8	4812983	317.4489	section_l	153162
216	538971.1	4812987	317.4628	section_r	153163
127	538971.4	4812979	317.4352	section_i	152164
224	538964.9	4812986	317.4452	section_r	152165
61	538968.8	4812972	317.5411	section_b	152166
58	538971.9	4812972	317.5266	section_b	152167
47	538973.1	4812971	317.5545	section_a	152168
109	538971	4812977	317.4833	section_g	152169

	538965.7	4812988	316.8516	1_170	
76	538966.3	4812973	317.6078	section_c	152171
209	538969.3	4812986	317.5242	section_q	152172
122	538967.9	4812978	317.5064	section_h	152173
151	538969.2	4812982	317.4785	section_k	152174
227	538970.3	4812987	317.4396	section_s	152175
188	538969.8	4812985	317.4772	section_o	152176
163	538967.1	4812982	317.4695	section_l	152177
100	538970.3	4812976	317.4973	section_f	152178
75	538966.9	4812973	317.5553	section_c	152179
174	538967.4	4812983	317.4703	section_m	152180
213	538965.9	4812986	317.4428	section_q	162181
159	538970.1	4812982	317.479	section_l	162182
195	538971.8	4812986	317.4775	section_p	162183
226	538971.2	4812987	317.4448	section_s	162184
212	538966.9	4812986	317.4474	section_q	162185
211	538968	4812986	317.5404	section_q	162186
49	538971.7	4812971	317.5305	section_a	162187
237	538970.2	4812988	317.4235	section_t	162188
160	538969.4	4812982	317.5059	section_l	162189
154	538966.3	4812982	317.5003	section_k	162190
138	538971.1	4812981	317.4801	section_j	162191
238	538969.4	4812988	317.4591	section_t	162192
84	538967.5	4812974	317.5487	section_d	162193
166	538971.8	4812983	317.5575	section_m	162194
200	538968.6	4812985	317.4577	section_p	162195
145	538966.8	4812981	317.4743	section_j	162196
126	538965.2	4812978	317.5688	section_h	162197
172	538968.4	4812983	317.4489	section_m	162198
113	538967.6	4812977	317.5149	section_g	162199
177	538971.1	4812984	317.4898	section_n	162200

Table A5b: Seeding Survey – Site 2

point #	east	north	elev	desc	Tag #
408	539221.72	4814288.22	315.0427	section_uq	211001
290	539219.22	4814270.84	315.2512	section_ue	211002
313	539216.16	4814273.16	315.2308	section_ug	211003
433	539218.85	4814292.91	315.1833	section_us	211004
424	539218.46	4814289.55	315.2148	section_ur	211005
307	539221.34	4814271.80	315.2307	section_ug	211006
381	539221.07	4814281.76	315.1704	section_un	211007
335	539224.05	4814275.25	315.2841	section_uj	211008
318	539220.64	4814272.95	315.2505	section_uh	211009
373	539219.50	4814280.08	315.2047	section_um	211010
291	539218.27	4814271.03	315.2218	section_ue	211011
414	539218.09	4814287.79	315.3098	section_uq	211012
289	539219.92	4814270.62	315.2287	section_ue	211013
273	539215.85	4814269.90	315.2366	section_uc	211014
264	539214.79	4814269.70	315.3455	section_ub	211015
304	539215.75	4814272.68	315.2141	section_uf	211016
346	539223.01	4814276.91	315.2312	section_uk	211017
364	539217.90	4814278.96	315.2593	section_ul	211018
331	539218.01	4814274.65	315.2147	section_ui	211019
354	539216.92	4814278.09	315.2202	section_uk	211020
267	539221.39	4814268.49	315.2458	section_uc	211021
322	539216.93	4814273.88	315.199	section_uh	211022
296	539222.41	4814270.71	315.3262	section_uf	211023
382	539220.22	4814281.60	315.1821	section_un	211024
357	539222.99	4814278.60	315.2388	section_ul	211025
329	539219.88	4814274.41	315.24	section_ui	211026
256	539222.19	4814267.38	315.3119	section_ub	211027
386	539224.17	4814283.48	315.1705	section_uo	211028
405	539217.80	4814285.63	315.2295	section_up	211029
419	539220.76	4814290.02	315.1268	section_ur	211030
431	539219.85	4814292.98	315.1438	section_us	211031
432	539219.31	4814292.90	315.1514	section_us	211032
330	539218.97	4814274.49	315.1852	section_ui	211033
250	539219.44	4814267.66	315.2669	section_ua	211034
245	539223.22	4814266.59	315.3454	section_ua	211035
278	539220.68	4814269.56	315.2473	section_ud	211036
249	539220.47	4814267.28	315.2577	section_ua	211037
369	539222.27	4814280.25	315.2214	section_um	211038
251	539218.46	4814268.02	315.2672	section_ua	211039
379	539222.44	4814281.73	315.1934	section_un	211040

285	539223.30	4814269.64	315.3718	section_ue	211041
397	539222.53	4814285.91	315.0124	section_up	211042
282	539216.93	4814270.50	315.2272	section_ud	211043
437	539222.07	4814296.13	315.3091	section_ut	221044
345	539224.33	4814276.64	315.2928	section_uk	221045
403	539218.67	4814285.80	315.259	section_up	221046
266	539222.27	4814268.43	315.3269	section_uc	221047
294	539215.43	4814271.98	315.2827	section_ue	221048
328	539220.73	4814274.09	315.2583	section_ui	221049
423	539218.96	4814289.70	315.1707	section_ur	221050
261	539218.02	4814268.58	315.2389	section_ub	221051
317	539221.45	4814272.84	315.2804	section_uh	221052
306	539222.53	4814271.64	315.2917	section_ug	221053
255	539223.19	4814267.26	315.3789	section_ub	221054
287	539221.33	4814270.06	315.2474	section_ue	221055
258	539220.59	4814267.81	315.2458	section_ub	221056
295	539223.39	4814270.65	315.4003	section_uf	221057
252	539217.53	4814268.18	315.2842	section_ua	221058
401	539219.28	4814286.37	315.2485	section_up	221059
303	539216.58	4814272.35	315.2193	section_uf	221060
426	539217.63	4814289.38	315.3347	section_ur	221061
392	539219.74	4814283.40	315.1836	section_uo	221062
263	539216.17	4814269.07	315.1972	section_ub	221063
280	539218.92	4814269.98	315.2097	section_ud	221064
332	539217.09	4814274.74	315.1716	section_ui	221065
254	539215.05	4814268.93	315.2707	section_ua	221066
292	539217.46	4814271.25	315.2327	section_ue	221067
380	539221.88	4814281.82	315.1843	section_un	221068
334	539215.65	4814275.25	315.1982	section_ui	221069
309	539219.02	4814272.39	315.2106	section_ug	221070
434	539218.41	4814292.79	315.2093	section_us	221071
320	539218.91	4814273.30	315.2192	section_uh	221072
394	539218.51	4814283.40	315.1893	section_uo	221073
383	539219.69	4814281.65	315.1798	section_un	221074
418	539221.36	4814290.06	315.0961	section_ur	221075
385	539218.23	4814281.89	315.2186	section_un	221076
247	539222.21	4814266.75	315.2866	section_ua	221077
301	539217.95	4814271.77	315.2239	section_uf	221078
396	539223.14	4814286.09	314.9061	section_up	221079
339	539220.05	4814275.38	315.2226	section_uj	221080
343	539217.40	4814275.99	315.1449	section_uj	221081
390	539221.10	4814283.19	315.2347	section_uo	221082
341	539218.49	4814275.75	315.1497	section_uj	221083

407	539222.32	4814288.23	315.1185	section_uq	221084
441	539219.68	4814295.98	315.1711	section_ut	221085
368	539222.85	4814280.04	315.2299	section_um	221086
442	539219.06	4814295.88	315.2004	section_ut	221087
356	539223.61	4814278.42	315.2159	section_ul	221088
298	539220.37	4814271.18	315.2251	section_uf	221089
269	539219.76	4814268.86	315.257	section_uc	221090
371	539220.78	4814280.19	315.1825	section_um	221091
430	539220.36	4814293.11	315.1064	section_us	221092
443	539218.33	4814295.78	315.2387	section_ut	232093
276	539222.31	4814269.36	315.3284	section_ud	232094
375	539218.05	4814280.31	315.2565	section_um	232095
270	539218.92	4814269.25	315.2599	section_uc	232096
324	539215.60	4814274.29	315.161	section_uh	232097
351	539219.05	4814277.54	315.2282	section_uk	232098
265	539223.38	4814268.19	315.4113	section_uc	232099
420	539220.21	4814289.73	315.1968	section_ur	232100
272	539216.77	4814269.73	315.2216	section_uc	232101
279	539219.53	4814269.85	315.2354	section_ud	232102
389	539221.87	4814283.14	315.1832	section_uo	232103
355	539224.13	4814278.38	315.2375	section_ul	232104
429	539220.92	4814292.93	315.1464	section_us	232105
338	539220.51	4814275.49	315.2262	section_uj	232106
284	539215.11	4814271.12	315.3091	section_ud	232107
406	539223.09	4814288.42	315.2049	section_uq	232108
393	539218.97	4814283.46	315.1481	section_uo	232109
378	539222.99	4814281.70	315.1976	section_un	232110
415	539217.57	4814287.80	315.4339	section_uq	232111
384	539219.04	4814281.76	315.2186	section_un	232112
327	539221.57	4814273.88	315.2458	section_ui	232113
316	539222.59	4814272.82	315.3209	section_uh	232114
360	539220.36	4814278.78	315.1963	section_ul	232115
422	539219.45	4814289.61	315.1774	section_ur	232116
367	539223.70	4814280.06	315.1957	section_um	232117
370	539221.49	4814280.18	315.2066	section_um	232118
319	539219.90	4814273.21	315.2452	section_uh	232119
440	539220.24	4814296.04	315.1548	section_ut	232120
333	539216.64	4814274.70	315.1815	section_ui	232121
288	539220.63	4814270.31	315.2354	section_ue	232122
305	539223.87	4814271.65	315.3847	section_ug	232123
402	539219.20	4814285.95	315.3137	section_up	232124
417	539222.10	4814290.40	315.1512	section_ur	232125
342	539218.05	4814275.80	315.1829	section_uj	232126

310	539218.18	4814272.49	315.2295	section_ug	232127
444	539217.83	4814295.77	315.2349	section_ut	232128
281	539217.98	4814270.30	315.242	section_ud	232129
277	539221.25	4814269.42	315.2317	section_ud	232130
293	539216.65	4814271.63	315.2358	section_ue	232131
435	539217.92	4814292.60	315.2706	section_us	232132
340	539219.29	4814275.64	315.1673	section_uj	242133
271	539217.97	4814269.48	315.2374	section_uc	242134
297	539221.28	4814270.96	315.2553	section_uf	242135
311	539217.40	4814272.66	315.1704	section_ug	242136
347	539222.03	4814277.22	315.217	section_uk	242137
302	539217.36	4814271.89	315.1734	section_uf	242138
323	539216.36	4814274.05	315.1983	section_uh	242139
253	539216.38	4814268.48	315.2695	section_ua	242140
410	539220.38	4814288.11	315.1532	section_uq	242141
315	539223.90	4814272.86	315.3864	section_uh	242142
336	539222.82	4814275.34	315.3152	section_uj	242143
268	539220.63	4814268.69	315.2411	section_uc	242144
398	539221.86	4814285.88	314.9992	section_up	242145
403	539218.67	4814285.80	315.259	section_up	242146
404	539218.32	4814285.77	315.2404	section_up	242147
259	539220.08	4814267.96	315.2799	section_ub	242148
362	539219.29	4814279.01	315.214	section_ul	242149
352	539218.46	4814277.72	315.2328	section_uk	242150
348	539220.99	4814277.22	315.2384	section_uk	242151
286	539222.28	4814269.69	315.3109	section_ue	242152
391	539220.42	4814283.14	315.1613	section_uo	242153
445	539217.28	4814295.88	315.238	section_ut	242154
300	539218.65	4814271.55	315.2651	section_uf	242155
349	539220.03	4814277.30	315.2084	section_uk	242156
436	539217.33	4814292.48	315.322	section_us	242157
399	539221.06	4814285.88	315.0876	section_up	242158
314	539215.64	4814273.27	315.2324	section_ug	242159
376	539224.56	4814281.56	315.2519	section_un	242160
246	539223.12	4814266.56	315.3625	section_ua	252161
365	539217.30	4814278.92	315.2782	section_ul	252162
416	539222.63	4814290.52	315.1701	section_ur	252163
257	539221.35	4814267.65	315.257	section_ub	252164
363	539218.45	4814278.99	315.2779	section_ul	252165
262	539217.18	4814268.79	315.2653	section_ub	252166
299	539219.52	4814271.33	315.2247	section_uf	252167
350	539219.60	4814277.37	315.2675	section_uk	252168
409	539220.98	4814288.23	315.1293	section_uq	252169

425	539218.11	4814289.49	315.3164	section_ur	252170
374	539218.81	4814280.17	315.2143	section_um	252171
388	539222.40	4814283.24	315.2212	section_uo	252172
275	539223.59	4814269.04	315.4042	section_ud	252173
260	539218.81	4814268.28	315.2649	section_ub	252174
274	539214.83	4814270.30	315.3225	section_uc	252175
321	539217.57	4814273.69	315.1926	section_uh	252176
428	539221.65	4814293.31	315.1589	section_us	252177
446	539216.42	4814295.92	315.2968	section_ut	252178
308	539220.33	4814272.14	315.211	section_ug	252179
326	539222.69	4814273.86	315.3083	section_ui	252180
337	539221.60	4814275.46	315.2273	section_uj	262181
358	539221.92	4814278.67	315.2039	section_ul	262182
344	539216.47	4814276.12	315.1704	section_uj	262183
372	539220.01	4814280.18	315.1591	section_um	262184
427	539222.39	4814293.37	315.3499	section_us	262185
353	539217.27	4814277.89	315.1774	section_uk	262186
248	539221.34	4814267.01	315.2543	section_ua	262187
439	539220.82	4814296.17	315.2091	section_ut	262188
377	539223.95	4814281.82	315.1806	section_un	262189
412	539218.89	4814287.85	315.2498	section_uq	262190
283	539215.95	4814270.82	315.2589	section_ud	262191
400	539220.44	4814286.05	315.1832	section_up	262192
325	539223.90	4814273.83	315.3965	section_ui	262193
395	539217.84	4814283.47	315.2252	section_uo	262194
366	539224.17	4814280.16	315.2644	section_um	262195
438	539221.41	4814296.07	315.2177	section_ut	262196
359	539221.10	4814278.83	315.1909	section_ul	262197
312	539216.90	4814272.80	315.2102	section_ug	262198
411	539219.43	4814287.97	315.2162	section_uq	262199
413	539218.42	4814287.74	315.3242	section_uq	262200

Table A5c: Seeding Survey – Site 3

surveyed point #	corrected point #	east	north	elev	desc	Tag #
648	648	539324.7	4814776	313.2935	SECTION_HILL_A	311001
699	699	539328.1	4814779	313.4184	SECTION_HILL_F	311002
810	810	539334.9	4814787	313.5168	SECTION_HILL_Q	311003
833	832	539334.9	4814790	313.5178	SECTION_HILL_S	311004
659	659	539325	4814777	313.3524	SECTION_HILL_B	311005
788	788	539335	4814785	313.378	SECTION_HILL_O	311006
771	771	539331.8	4814786	313.5509	SECTION_HILL_M	311007
681	681	539325.4	4814779	313.4811	SECTION_HILL_D	311008
816	816	539331.2	4814792	313.4262	SECTION_HILL_Q	311009
822	821	539334.6	4814788	313.5576	SECTION_HILL_R	311010
826	825	539332.5	4814791	313.3993	SECTION_HILL_R	311011
782	782	539331.8	4814787	313.5952	SECTION_HILL_N	311012
834	833	539334.1	4814790	313.4007	SECTION_HILL_S	311013
685	685	539323.6	4814781	313.5144	SECTION_HILL_D	311014
652	652	539323.1	4814778	313.327	SECTION_HILL_A	311015
799	799	539335.2	4814786	313.4189	SECTION_HILL_P	311016
760	760	539331.9	4814784	313.4885	SECTION_HILL_L	311017
783	783	539331.1	4814788	313.5763	SECTION_HILL_N	311018
670	670	539325.3	4814778	313.4371	SECTION_HILL_C	311019
732	732	539328.8	4814784	313.5291	SECTION_HILL_I	311020
707	707	539323.1	4814784	313.4721	SECTION_HILL_F	311021
688	688	539327.7	4814778	313.364	SECTION_HILL_E	311022
749	749	539332.1	4814783	313.3433	SECTION_HILL_K	311023
807	807	539330.2	4814792	313.4841	SECTION_HILL_P	311024
692	692	539325.7	4814780	313.5637	SECTION_HILL_E	311025
775	775	539329.3	4814788	313.4492	SECTION_HILL_M	311026
766	766	539327.9	4814788	313.4123	SECTION_HILL_L	311027
733	733	539328.1	4814785	313.5697	SECTION_HILL_I	311028
710	710	539328.7	4814781	313.4354	SECTION_HILL_G	311029
653	653	539322.7	4814778	313.3832	SECTION_HILL_A	311030
734	734	539327.4	4814785	313.5487	SECTION_HILL_I	311031
693	693	539325.2	4814781	313.593	SECTION_HILL_E	311032
725	725	539326.1	4814785	313.5063	SECTION_HILL_H	311033
738	738	539331.9	4814782	313.3528	SECTION_HILL_J	311034
721	721	539328.7	4814783	313.5058	SECTION_HILL_H	311035
757	757	539326.9	4814788	313.4912	SECTION_HILL_K	311036
716	716	539324.9	4814785	313.4746	SECTION_HILL_G	311037
676	676	539322.4	4814781	313.5214	SECTION_HILL_C	311038
667	667	539321.4	4814781	313.4821	SECTION_HILL_B	311039

694	694	539324.5	4814781	313.564	SECTION_HILL_E	311040
784	784	539330.4	4814788	313.4806	SECTION_HILL_N	311041
654	654	539322.2	4814779	313.4012	SECTION_HILL_A	311042
835	834	539333.9	4814791	313.3763	SECTION_HILL_S	311043
742	742	539329.4	4814784	313.5387	SECTION_HILL_J	321044
698	698	539328.6	4814779	313.3875	SECTION_HILL_F	321045
839	838	539337.9	4814788	313.4788	SECTION_HILL_T	321046
709	709	539329.3	4814781	313.4188	SECTION_HILL_G	321047
781	781	539332.3	4814786	313.5542	SECTION_HILL_N	321048
650	650	539323.9	4814777	313.3532	SECTION_HILL_A	321049
843	842	539335.9	4814790	313.4662	SECTION_HILL_T	321050
701	701	539326.8	4814781	313.4844	SECTION_HILL_F	321051
690	690	539326.9	4814780	313.4241	SECTION_HILL_E	321052
785	785	539329.8	4814789	313.4494	SECTION_HILL_N	321053
669	669	539325.7	4814777	313.38	SECTION_HILL_C	321054
731	731	539329.3	4814783	313.5058	SECTION_HILL_I	321055
809	809	539335.5	4814787	313.4431	SECTION_HILL_Q	321056
792	792	539332.5	4814788	313.5618	SECTION_HILL_O	321057
821	820	539335.4	4814788	313.5309	SECTION_HILL_R	321058
794	794	539331.3	4814789	313.467	SECTION_HILL_O	321059
695	695	539323.9	4814782	313.5643	SECTION_HILL_E	321060
770	770	539332.3	4814785	313.4928	SECTION_HILL_M	321061
658	658	539325.3	4814776	313.2912	SECTION_HILL_B	321062
748	748	539332.5	4814782	313.3127	SECTION_HILL_K	321063
704	704	539325.1	4814782	313.5737	SECTION_HILL_F	321064
661	661	539324.1	4814778	313.3762	SECTION_HILL_B	321065
744	744	539328	4814786	313.5395	SECTION_HILL_J	321066
798	798	539335.6	4814786	313.4524	SECTION_HILL_P	321067
720	720	539329.5	4814782	313.4678	SECTION_HILL_H	321068
735	735	539326.9	4814786	313.4555	SECTION_HILL_I	321069
825	824	539333.1	4814790	313.4004	SECTION_HILL_R	321070
796	796	539330.2	4814790	313.4431	SECTION_HILL_O	321071
844	843	539335.5	4814791	313.4212	SECTION_HILL_T	321072
655	655	539321.7	4814779	313.4284	SECTION_HILL_A	321073
657	657	539320.5	4814780	313.4499	SECTION_HILL_A	321074
672	672	539324.2	4814779	313.4505	SECTION_HILL_C	321075
697	697	539322.4	4814783	313.4745	SECTION_HILL_E	321076
827	826	539332.1	4814792	313.4312	SECTION_HILL_R	321077
723	723	539327.5	4814784	313.5671	SECTION_HILL_H	321078
832	831	539335.6	4814789	313.5416	SECTION_HILL_S	321079
847	846	539334.2	4814792	313.3486	SECTION_HILL_T	321080
773	773	539330.5	4814787	313.5673	SECTION_HILL_M	321081
759	759	539332.6	4814784	313.3657	SECTION_HILL_L	321082

737	737	539325.7	4814787	313.4638	SECTION_HILL_I	321083
664	664	539322.9	4814779	313.4838	SECTION_HILL_B	321084
803	803	539332.6	4814789	313.5492	SECTION_HILL_P	321085
683	683	539324.4	4814780	313.5264	SECTION_HILL_D	321086
706	706	539323.6	4814783	313.4751	SECTION_HILL_F	321087
836	835	539333.5	4814792	313.3833	SECTION_HILL_S	321088
746	746	539326.8	4814787	313.476	SECTION_HILL_J	321089
666	666	539322.1	4814780	313.4758	SECTION_HILL_B	321090
712	712	539327.4	4814783	313.5327	SECTION_HILL_G	321091
787	787	539328.9	4814790	313.4802	SECTION_HILL_N	321092
780	780	539333	4814786	313.5469	SECTION_HILL_N	332093
804	804	539332	4814790	313.4308	SECTION_HILL_P	332094
758	758	539333.1	4814783	313.3156	SECTION_HILL_L	332095
791	791	539333.2	4814787	313.5619	SECTION_HILL_O	332096
741	741	539329.9	4814784	313.5057	SECTION_HILL_J	332097
745	745	539327.5	4814786	313.4575	SECTION_HILL_J	332098
719	719	539330.2	4814782	313.3912	SECTION_HILL_H	332099
763	763	539329.8	4814787	313.549	SECTION_HILL_L	332100
722	722	539328.1	4814783	313.5339	SECTION_HILL_H	332101
842	841	539336.5	4814789	313.5179	SECTION_HILL_T	332102
769	769	539333.1	4814784	313.4096	SECTION_HILL_M	332103
820	819	539335.9	4814787	313.5079	SECTION_HILL_R	332104
831	830	539336.1	4814788	313.5578	SECTION_HILL_S	332105
837	836	539333.2	4814792	313.4042	SECTION_HILL_S	332106
786	786	539329.3	4814789	313.4471	SECTION_HILL_N	332107
823	822	539334.1	4814789	313.5481	SECTION_HILL_R	332108
772	772	539331.1	4814786	313.5628	SECTION_HILL_M	332109
808	808	539336	4814786	313.4921	SECTION_HILL_Q	332110
795	795	539330.8	4814790	313.4337	SECTION_HILL_O	332111
675	675	539322.9	4814780	313.4823	SECTION_HILL_C	332112
777	777	539328.1	4814790	313.4536	SECTION_HILL_M	332113
727	727	539325.1	4814786	313.486	SECTION_HILL_H	332114
708	708	539329.8	4814780	313.3692	SECTION_HILL_G	332115
845	844	539335.1	4814791	313.4159	SECTION_HILL_T	332116

Table A5d: Seeding Survey – Site 4

surveyed	east	north	elev	desc	Rock#
447	540616.9	4814662	308.2679	SECTION_BECH_a	1
531	540622.9	4814656	308.1856	SECTION_BECH_I	2
498	540619.1	4814657	308.28	SECTION_BECH_F	3
587	540621.4	4814649	308.1624	SECTION_BECH_O	4
598	540622.5	4814648	308.1544	SECTION_BECH_P	5
451	540619.7	4814663	308.2444	SECTION_BECH_a	6
487	540617.8	4814658	308.2797	SECTION_BECH_E	7
469	540619.8	4814660	308.2626	SECTION_BECH_C	8
480	540621.5	4814660	308.2521	SECTION_BECH_D	9
452	540620.4	4814663	308.2568	SECTION_BECH_a	10
620	540624.6	4814647	307.9634	SECTION_BECH_R	11
570	540623.5	4814652	308.1368	SECTION_BECH_M	12
581	540624.5	4814651	308.1651	SECTION_BECH_N	13
559	540622.1	4814653	308.2182	SECTION_BECH_L	14
458	540618	4814661	308.2584	SECTION_BECH_B	15
624	540626.9	4814648	308.0983	SECTION_BECH_R	16
537	540619.4	4814653	308.2897	SECTION_BECH_J	17
631	540625.3	4814647	307.9976	SECTION_BECH_S	18
565	540626.8	4814654	308.3462	SECTION_BECH_L	19
632	540625.9	4814647	308.1135	SECTION_BECH_S	20
475	540625.3	4814662	308.3536	SECTION_BECH_C	21
453	540621	4814663	308.225	SECTION_BECH_a	22
466	540624.5	4814663	308.3164	SECTION_BECH_B	23
491	540621.7	4814659	308.2571	SECTION_BECH_E	24
484	540624.6	4814661	308.3365	SECTION_BECH_D	25
492	540622.3	4814660	308.2231	SECTION_BECH_E	26
509	540620.6	4814657	308.279	SECTION_BECH_G	27
520	540621.6	4814657	308.249	SECTION_BECH_H	28
532	540623.6	4814656	308.2056	SECTION_BECH_I	29
582	540625.1	4814652	308.1901	SECTION_BECH_N	30
583	540625.5	4814652	308.1571	SECTION_BECH_N	31
606	540628.5	4814651	308.3048	SECTION_BECH_P	32
533	540624.2	4814657	308.1997	SECTION_BECH_I	33
609	540623.7	4814648	308.0093	SECTION_BECH_Q	34
493	540623.5	4814660	308.2295	SECTION_BECH_E	35
548	540620.8	4814653	308.2464	SECTION_BECH_K	36
506	540627.5	4814660	308.2848	SECTION_BECH_F	37
615	540627.7	4814650	308.254	SECTION_BECH_Q	38
574	540626.7	4814654	308.3272	SECTION_BECH_M	39
633	540626.4	4814647	308.0662	SECTION_BECH_S	40

556	540627.5	4814655	308.3335	SECTION_BECH_K	41
524	540625	4814658	308.2663	SECTION_BECH_H	42
515	540626.3	4814659	308.2841	SECTION_BECH_G	43
530	540622.1	4814656	308.2074	SECTION_BECH_I	44
508	540619.5	4814657	308.316	SECTION_BECH_G	45
457	540617.2	4814661	308.2809	SECTION_BECH_B	46
569	540622.6	4814652	308.1301	SECTION_BECH_M	47
468	540618.6	4814660	308.2692	SECTION_BECH_C	48
497	540618	4814657	308.2548	SECTION_BECH_F	49
500	540621.3	4814658	308.2769	SECTION_BECH_F	50
511	540622.6	4814658	308.2121	SECTION_BECH_G	51
608	540622.9	4814648	308.1098	SECTION_BECH_Q	52
489	540619.9	4814659	308.3425	SECTION_BECH_E	53
547	540619.9	4814653	308.201	SECTION_BECH_K	54
494	540624.3	4814660	308.2779	SECTION_BECH_E	55
519	540620.6	4814656	308.2661	SECTION_BECH_H	56
449	540618.2	4814662	308.2735	SECTION_BECH_a	57
637	540623.9	4814645	308.0614	SECTION_BECH_T	58
641	540626.3	4814646	307.9158	SECTION_BECH_T	59
522	540623.3	4814657	308.2018	SECTION_BECH_H	60
580	540623.6	4814651	308.0933	SECTION_BECH_N	61
534	540625.1	4814657	308.3035	SECTION_BECH_I	62
591	540624.6	4814650	308.1234	SECTION_BECH_O	63
558	540621.3	4814652	308.1816	SECTION_BECH_L	64
471	540622	4814661	308.1757	SECTION_BECH_C	65
482	540622.9	4814661	308.2126	SECTION_BECH_D	66
630	540624.7	4814647	307.9544	SECTION_BECH_S	67
597	540621.8	4814648	308.1826	SECTION_BECH_P	68
454	540621.7	4814663	308.2351	SECTION_BECH_a	69
619	540624	4814647	308.0061	SECTION_BECH_R	70
460	540619.7	4814661	308.3016	SECTION_BECH_B	71
463	540622.2	4814662	308.2018	SECTION_BECH_B	72
503	540624.2	4814659	308.2371	SECTION_BECH_F	73
593	540625.9	4814651	308.1635	SECTION_BECH_O	74
496	540626.5	4814661	308.3017	SECTION_BECH_E	75
634	540627	4814648	308.1028	SECTION_BECH_S	76
541	540623.3	4814655	308.1832	SECTION_BECH_J	77
572	540624.9	4814653	308.1352	SECTION_BECH_M	78
456	540623.5	4814664	308.2532	SECTION_BECH_a	79
465	540623.9	4814663	308.318	SECTION_BECH_B	80
623	540626.3	4814648	308.0805	SECTION_BECH_R	81
602	540625.6	4814650	308.169	SECTION_BECH_P	82
505	540626.5	4814660	308.2907	SECTION_BECH_F	83

626	540628.7	4814649	308.2893	SECTION_BECH_R	84
584	540626	4814652	308.1757	SECTION_BECH_N	85
642	540626.9	4814646	308.0215	SECTION_BECH_T	86
543	540624.7	4814656	308.2503	SECTION_BECH_J	87
645	540628	4814647	308.1609	SECTION_BECH_T	88
536	540627.6	4814658	308.3179	SECTION_BECH_I	89
586	540628.3	4814653	308.2595	SECTION_BECH_N	90
545	540626.3	4814656	308.3266	SECTION_BECH_J	91
595	540627.7	4814652	308.3253	SECTION_BECH_O	92
507	540618.3	4814656	308.2536	SECTION_BECH_G	93
540	540622.5	4814655	308.1577	SECTION_BECH_J	94
518	540619.7	4814656	308.2994	SECTION_BECH_H	95
568	540621.7	4814651	308.137	SECTION_BECH_M	96
640	540625.5	4814646	307.8291	SECTION_BECH_T	97
467	540617.4	4814660	308.2618	SECTION_BECH_C	98
557	540620.5	4814652	308.2024	SECTION_BECH_L	99
478	540619.9	4814660	308.3016	SECTION_BECH_D	100
512	540623.3	4814658	308.1879	SECTION_BECH_G	101
553	540624.9	4814655	308.1937	SECTION_BECH_K	102
607	540622.2	4814647	308.1636	SECTION_BECH_Q	103
643	540627.3	4814647	308.084	SECTION_BECH_T	104
490	540620.8	4814659	308.3027	SECTION_BECH_E	105
529	540621.2	4814655	308.2755	SECTION_BECH_I	106
618	540623.3	4814647	308.1207	SECTION_BECH_R	107
479	540620.9	4814660	308.2725	SECTION_BECH_D	108
579	540622.9	4814651	308.1315	SECTION_BECH_N	109
621	540625.2	4814648	308.0404	SECTION_BECH_R	110
544	540625.3	4814656	308.2265	SECTION_BECH_J	111
481	540622.3	4814661	308.2046	SECTION_BECH_D	112
472	540622.8	4814661	308.2014	SECTION_BECH_C	113
474	540624.4	4814662	308.3547	SECTION_BECH_C	114
483	540623.8	4814661	308.3014	SECTION_BECH_D	115
571	540624.3	4814653	308.1864	SECTION_BECH_M	116
585	540627.1	4814653	308.3729	SECTION_BECH_N	117
590	540623.7	4814650	308.0927	SECTION_BECH_O	118
535	540626.3	4814657	308.2854	SECTION_BECH_I	119
616	540628.6	4814650	308.291	SECTION_BECH_Q	120
622	540625.7	4814648	308.0655	SECTION_BECH_R	121
521	540622.6	4814657	308.1731	SECTION_BECH_H	122
486	540626.1	4814662	308.3361	SECTION_BECH_D	123
594	540626.4	4814651	308.1993	SECTION_BECH_O	124
576	540628.2	4814654	308.2388	SECTION_BECH_M	125
562	540624.5	4814654	308.1669	SECTION_BECH_L	126

629	540624.1	4814646	307.9883	SECTION_BECH_S	127
526	540627.2	4814658	308.3294	SECTION_BECH_H	128
635	540627.5	4814648	308.1013	SECTION_BECH_S	129
644	540627.7	4814647	308.1321	SECTION_BECH_T	130
495	540625.4	4814660	308.2972	SECTION_BECH_E	131
603	540626.2	4814650	308.179	SECTION_BECH_P	132
549	540621.8	4814653	308.2387	SECTION_BECH_K	133
599	540623.2	4814649	308.0575	SECTION_BECH_P	134
538	540620.5	4814654	308.277	SECTION_BECH_J	135
542	540623.8	4814655	308.1884	SECTION_BECH_J	136
517	540618.6	4814655	308.2692	SECTION_BECH_H	137
550	540622.8	4814654	308.1678	SECTION_BECH_K	138
600	540623.8	4814649	308.0614	SECTION_BECH_P	139
551	540623.6	4814654	308.1947	SECTION_BECH_K	140
588	540622.1	4814649	308.0888	SECTION_BECH_O	141
525	540625.9	4814658	308.3456	SECTION_BECH_H	142
488	540619	4814658	308.2917	SECTION_BECH_E	143
461	540620.3	4814662	308.2364	SECTION_BECH_B	144
611	540625.1	4814649	308.0913	SECTION_BECH_Q	145
470	540620.9	4814661	308.2849	SECTION_BECH_C	146
513	540623.9	4814659	308.2289	SECTION_BECH_G	147
563	540625.1	4814654	308.1971	SECTION_BECH_L	148
604	540627.1	4814650	308.3436	SECTION_BECH_P	149
473	540623.5	4814662	308.2762	SECTION_BECH_C	150
554	540625.7	4814655	308.2116	SECTION_BECH_K	151
499	540620.2	4814658	308.2974	SECTION_BECH_F	152
592	540625.2	4814651	308.1608	SECTION_BECH_O	153
455	540622.5	4814663	308.2039	SECTION_BECH_a	154
502	540623.3	4814659	308.2346	SECTION_BECH_F	155
636	540629.2	4814649	308.2995	SECTION_BECH_S	156
504	540625.5	4814660	308.2738	SECTION_BECH_F	157
577	540621.1	4814650	308.1996	SECTION_BECH_N	158
516	540627.7	4814659	308.319	SECTION_BECH_G	159
605	540627.9	4814651	308.3224	SECTION_BECH_P	160
564	540625.6	4814654	308.1785	SECTION_BECH_L	161
448	540617.5	4814662	308.2967	SECTION_BECH_a	162
617	540622.5	4814646	308.1729	SECTION_BECH_R	163
477	540618.6	4814659	308.2514	SECTION_BECH_D	164
628	540623.6	4814646	308.0774	SECTION_BECH_S	165
510	540621.5	4814658	308.2856	SECTION_BECH_G	166
523	540623.9	4814657	308.2342	SECTION_BECH_H	167
610	540624.3	4814648	308.0236	SECTION_BECH_Q	168
459	540618.7	4814661	308.294	SECTION_BECH_B	169

589	540623.2	4814650	308.0689	SECTION_BECH_O	170
625	540627.4	4814648	308.0803	SECTION_BECH_R	171
552	540624.3	4814655	308.1828	SECTION_BECH_K	172
646	540628.8	4814647	308.2755	SECTION_BECH_T	173
575	540627.4	4814654	308.3831	SECTION_BECH_M	174
528	540620.1	4814655	308.2993	SECTION_BECH_I	175
596	540628.6	4814652	308.3696	SECTION_BECH_O	175
566	540627.6	4814655	308.2749	SECTION_BECH_L	176
501	540622.4	4814659	308.2005	SECTION_BECH_F	177
476	540617.4	4814659	308.2703	SECTION_BECH_D	178
462	540621.6	4814662	308.2184	SECTION_BECH_B	179
464	540623	4814663	308.2515	SECTION_BECH_B	180
578	540622	4814650	308.1621	SECTION_BECH_N	181
560	540623.1	4814653	308.147	SECTION_BECH_L	182
601	540625	4814649	308.1318	SECTION_BECH_P	183
450	540619	4814662	308.2778	SECTION_BECH_a	184
627	540623.3	4814645	308.0897	SECTION_BECH_S	185
638	540624.2	4814645	308.0356	SECTION_BECH_T	186
539	540621.5	4814654	308.2395	SECTION_BECH_J	187
567	540620.8	4814651	308.1875	SECTION_BECH_M	188
527	540619.1	4814654	308.2141	SECTION_BECH_I	189
555	540626.6	4814655	308.3507	SECTION_BECH_K	190
573	540625.5	4814653	308.1813	SECTION_BECH_M	191
485	540625.2	4814662	308.4343	SECTION_BECH_D	192
612	540625.7	4814649	308.1202	SECTION_BECH_Q	193
613	540626.3	4814649	308.1023	SECTION_BECH_Q	194

Table A6a: Tracking Survey 1 – Site 1

point #	east	north	elev	desc	Rock #
1717	538966.9	4812976	317.5746	1_001	1
1825	538967.9	4812984	317.4441	1_003	3
1702	538971	4812974	317.4965	1_004	4
1705	538973	4812975	317.5981	1_005	5
1753	538964.9	4813012	317.3564	1_007	7
1674	538969.2	4812970	317.5347	1_008	8
1850	538965.2	4812986	317.3862	1_009	9
1729	538966.5	4812978	317.5617	1_010	10
1773	538970.7	4812982	317.4595	1_011	11
1763	538969	4812991	317.4433	1_012	12
1755	538966.4	4813006	317.3985	1_013	13
1851	538965.6	4812986	317.4505	1_014	14
1727	538966.5	4812979	317.5386	1_015	15
1750	538969.2	4812979	317.492	1_016	16
1840	538967.3	4812987	317.4605	1_017	17
1807	538970	4812984	317.4491	1_018	18
1744	538972.1	4812980	317.5046	1_019	19
1688	538971.1	4812973	317.4753	1_020	20
1856	538966.1	4812983	317.4263	1_021	21
1760	538965.9	4812996	317.4565	1_022	22
1721	538966	4812975	317.548	1_023	23
1818	538968.9	4812988	317.4196	1_024	24
1830	538966.7	4812982	317.4743	1_025	25
1690	538969.5	4812973	317.5253	1_026	26
1806	538970.4	4812985	317.4594	1_027	27
1694	538966.7	4812972	317.5908	1_029	29
1766	538965.9	4812993	317.4705	1_031	31
1683	538973.3	4812973	317.5268	1_032	32
1673	538970.7	4812971	317.5277	1_033	33
1699	538968.9	4812974	317.5416	1_034	34
1677	538966.1	4812971	317.6277	1_035	35
1765	538969.7	4812990	317.4317	1_036	36
1770	538971.3	4812981	317.4476	1_037	37
1670	538972.8	4812972	317.5565	1_038	38
1733	538968	4812978	317.5188	1_039	39

1708	538971.6	4812976	317.4735	1_042	42
1668	538973.8	4812971	317.5802	1_043	43
1718	538966.5	4812976	317.5461	1_044	44
1767	538968.5	4812989	317.4503	1_045	45
1667	538973.4	4812971	317.5437	1_046	46
1698	538967.9	4812974	317.5364	1_047	47
1711	538970.2	4812976	317.4772	1_048	48
1676	538966.3	4812970	317.645	1_049	49
1692	538969.2	4812973	317.518	1_050	50
1808	538969.8	4812984	317.4789	1_051	51
1669	538973.7	4812972	317.5639	1_052	52
1722	538965.6	4812975	317.5854	1_053	53
1776	538970.3	4812981	317.4499	1_054	54
1764	538969.1	4812991	317.4513	1_055	55
1707	538972.2	4812977	317.4965	1_056	56
1738	538969.8	4812978	317.4539	1_057	57
1828	538967.2	4812981	317.4978	1_058	58
1778	538969.2	4812981	317.4722	1_059	59
1842	538967.2	4812988	317.4664	1_060	60
1761	538966.7	4812996	317.4359	1_061	61
1796	538971.9	4812988	317.5091	1_062	62
1775	538970.6	4812983	317.466	1_063	63
1802	538970	4812986	317.4405	1_064	64
1774	538970.7	4812983	317.4653	1_065	65
1762	538967.5	4812994	317.4326	1_066	66
1756	538966.5	4813002	317.3722	1_067	67
1790	538971.1	4812985	317.4534	1_068	68
1706	538972.5	4812976	317.5406	1_069	69
1684	538972.8	4812973	317.5091	1_070	70
1834	538967.2	4812985	317.4237	1_071	71
1827	538966.9	4812981	317.5031	1_072	72
1749	538969.4	4812980	317.4743	1_073	73
1824	538967.8	4812985	317.4503	1_074	74
1843	538966.4	4812987	317.4418	1_075	75
1720	538967	4812975	317.566	1_076	76
1728	538967.1	4812979	317.529	1_077	77
1844	538966.5	4812987	317.4679	1_078	78
1815	538969.3	4812986	317.4327	1_079	79
1855	538966	4812983	317.4175	1_080	80
1714	538968.3	4812975	317.5238	1_081	81
1791	538971.7	4812985	317.4857	1_082	82
1771	538972	4812982	317.5082	1_083	83

1700	538969.8	4812974	317.5099	1_084	84
1854	538965.8	4812984	317.4168	1_085	85
1737	538969.5	4812977	317.4794	1_086	86
1703	538971.4	4812975	317.4749	1_087	87
1693	538967.3	4812973	317.5669	1_089	89
1849	538964.7	4812986	317.4104	1_090	90
1672	538971.3	4812971	317.5027	1_091	91
1841	538967.6	4812988	317.4641	1_092	92
1819	538968.3	4812988	317.4195	1_093	93
1758	538964.8	4812999	317.4546	1_094	94
1816	538969.2	4812988	317.4412	1_095	95
1712	538970.6	4812975	317.4853	1_096	96
1736	538968.7	4812977	317.4922	1_097	97
1804	538970.4	4812985	317.4725	1_098	98
1787	538971.4	4812984	317.4666	1_099	99
1823	538967.7	4812985	317.4479	1_100	100
1780	538968.9	4812982	317.4673	1_101	101
1837	538967	4812986	317.4523	1_102	102
1726	538966	4812979	317.5479	1_103	103
1811	538969.6	4812985	317.4924	1_104	104
1740	538971	4812978	317.4649	1_105	105
1719	538966.6	4812975	317.5591	1_106	106
1779	538968.1	4812981	317.4534	1_107	107
1793	538971.2	4812986	317.5137	1_108	108
1701	538970.1	4812974	317.4968	1_109	109
1785	538971.8	4812984	317.5069	1_110	110
1838	538966.9	4812987	317.4812	1_111	111
1747	538970.4	4812979	317.4508	1_112	112
1716	538967.6	4812976	317.5683	1_113	113
1792	538971.8	4812986	317.5174	1_114	114
1687	538971.5	4812973	317.4882	1_115	115
1696	538966.1	4812974	317.5752	1_116	116
1752	538968.4	4812980	317.4943	1_117	117
1832	538966.6	4812984	317.4423	1_118	118
1754	538965.4	4813009	317.3447	1_119	119
1724	538965.2	4812978	317.5825	1_120	120
1801	538970.3	4812987	317.4414	1_121	121
1759	538966.5	4812998	317.4267	1_122	122
1822	538968.4	4812986	317.4613	1_123	123
1809	538969.4	4812984	317.4778	1_124	124
1833	538966.7	4812984	317.4314	1_125	125
1846	538964.7	4812987	317.4158	1_126	126

1845	538965.6	4812987	317.4347	1_127	127
1686	538972	4812973	317.5106	1_128	128
1691	538968.8	4812973	317.5196	1_129	129
1742	538972	4812978	317.494	1_130	130
1831	538966.6	4812983	317.4384	1_131	131
1682	538972.7	4812973	317.5309	1_132	132
1812	538968.9	4812985	317.4273	1_133	133
1704	538972.4	4812975	317.5044	1_134	134
1852	538966.1	4812985	317.4193	1_135	135
1817	538969.5	4812988	317.4441	1_136	136
1777	538969.8	4812981	317.4946	1_137	137
1772	538970.8	4812981	317.457	1_138	138
1803	538970.6	4812986	317.4745	1_139	139
1734	538968.3	4812979	317.5088	1_140	140
1741	538971.6	4812978	317.4914	1_141	141
1810	538969.4	4812984	317.4766	1_142	142
1680	538969.8	4812972	317.5238	1_143	143
1839	538967	4812987	317.4456	1_144	144
1725	538966	4812978	317.5829	1_145	145
1732	538967.5	4812978	317.5293	1_146	146
1805	538969.9	4812986	317.4513	1_147	147
1751	538968.8	4812980	317.461	1_148	148
1788	538971.9	4812984	317.4984	1_149	149
1723	538965.3	4812977	317.5607	1_150	150
1715	538968	4812976	317.5417	1_151	151
1783	538969.8	4812983	317.4676	1_152	152
1789	538971.4	4812985	317.4629	1_153	153
1847	538964.8	4812987	317.4192	1_154	154
1829	538966.9	4812982	317.4936	1_155	155
1689	538970.3	4812973	317.4879	1_156	156
1710	538970.7	4812976	317.5046	1_157	157
1745	538971.3	4812980	317.5102	1_158	158
1713	538968.9	4812976	317.4962	1_159	159
1675	538967.6	4812970	317.55	1_160	160
1678	538967.1	4812972	317.563	1_161	161
1857	538965.9	4812982	317.4275	1_162	162
1794	538971.7	4812987	317.4898	1_163	163
1746	538970.8	4812980	317.4586	1_164	164
1848	538965.5	4812986	317.4191	1_165	165
1679	538968	4812972	317.4903	1_166	166
1671	538971.9	4812972	317.5173	1_167	167
1666	538973.6	4812970	317.5774	1_168	168
1739	538970.2	4812978	317.4954	1_169	169

1769	538965.7	4812988	316.8516	1_170	170
1685	538973	4812974	317.5039	1_171	171
1814	538969.6	4812986	317.4653	1_172	172
1730	538967	4812978	317.5374	1_173	173
1799	538971	4812988	317.4539	1_175	175
1797	538970.8	4812989	317.4208	1_176	176
1757	538966.1	4813001	317.4208	1_177	177
1735	538968.6	4812978	317.488	1_178	178
1695	538966.2	4812973	317.5662	1_179	179
1835	538967	4812985	317.4531	1_180	180
1836	538966.8	4812986	317.4338	1_181	181
1782	538970	4812982	317.4938	1_182	182
1853	538964.9	4812984	317.3844	1_183	183
1795	538971.6	4812987	317.4669	1_184	184
1820	538968	4812987	317.4484	1_185	185
1821	538968.1	4812986	317.4734	1_186	186
1681	538970.9	4812972	317.4876	1_187	187
1798	538971	4812988	317.4369	1_188	188
1781	538969.2	4812983	317.4823	1_189	189
1859	538965.6	4812981	317.4974	1_190	190
1748	538969.9	4812980	317.4548	1_191	191
1800	538970.4	4812988	317.4414	1_192	192
1697	538966.9	4812974	317.5765	1_193	193
1784	538971.7	4812983	317.4823	1_194	194
1813	538969.1	4812986	317.4632	1_195	195
1858	538965.6	4812981	317.5006	1_196	196
1743	538971.2	4812979	317.4706	1_197	197
1826	538968.2	4812983	317.4534	1_198	198
1731	538967	4812977	317.5687	1_199	199
1786	538971.1	4812984	317.4876	1_200	200

Table A6b: Tracking Survey 1 – Site 2

point #	east	north	elev	desc	Rock #	In stream (*)
1237	539222.0	4814288.0	315.083	2_001*	1	*
1215	539220.6	4814277.4	315.2325	2_002*	2	*
1098	539216.2	4814275.0	315.1693	2_003	3	
1247	539218.7	4814293.6	315.1183	2_004*	4	*
1243	539218.4	4814290.2	315.2124	2_005*	5	*
1131	539221.4	4814281.8	315.173	2_007	7	
1209	539224.2	4814275.1	315.3472	2_008*	8	*
1101	539220.7	4814274.5	315.2399	2_009	9	
1122	539219.6	4814281.2	315.207	2_010	10	
1107	539218.0	4814272.2	315.1795	2_011	11	
1189	539220.0	4814270.8	315.2581	2_013*	13	*
1198	539217.3	4814272.0	315.2213	2_014*	14	*
1173	539215.0	4814269.3	315.2903	2_015*	15	*
1221	539223.6	4814278.7	315.2524	2_017*	17	*
1217	539217.8	4814278.3	315.2529	2_018*	18	*
1211	539218.3	4814277.3	315.2032	2_019*	19	*
1212	539217.0	4814277.8	315.2598	2_020*	20	*
1188	539221.2	4814270.5	315.2448	2_021*	21	*
1201	539216.9	4814273.6	315.2114	2_022*	22	*
1193	539222.4	4814270.6	315.1302	2_023*	23	*
1132	539220.7	4814281.6	315.2025	2_024	24	
1218	539223.0	4814278.9	315.2252	2_025*	25	*
1185	539220.7	4814269.8	315.2713	2_026*	26	*
1236	539219.0	4814286.4	315.2762	2_029*	29	*
1241	539220.8	4814290.1	315.1538	2_030*	30	*
1246	539220.1	4814293.2	315.1115	2_031*	31	*
1205	539217.0	4814274.3	315.2131	2_032*	32	*
1214	539219.8	4814277.5	315.2631	2_033*	33	*
1162	539218.8	4814269.9	315.2213	2_034	34	
1180	539220.8	4814267.6	315.2833	2_037*	37	*
1130	539222.3	4814280.2	315.0131	2_038	38	
1183	539219.8	4814268.9	315.2336	2_039*	39	*
1229	539222.4	4814282.0	315.2354	2_040*	40	*

1187	539223.3	4814270.0	315.3744	2_041*	41	*
1235	539222.6	4814286.6	314.9892	2_042*	42	*
1106	539217.2	4814271.7	315.2227	2_043	43	
1251	539222.0	4814295.9	315.2542	2_044*	44	*
1216	539224.3	4814276.6	315.2728	2_045*	45	*
1179	539223.3	4814267.9	315.3287	2_047*	47	*
1197	539215.8	4814272.2	315.2298	2_048*	48	*
1208	539220.6	4814274.1	315.2379	2_049	49	
1244	539218.8	4814290.9	315.1819	2_050*	50	*
1176	539218.1	4814268.7	315.228	2_051*	51	*
1203	539221.5	4814272.7	315.3136	2_052*	52	*
1171	539222.3	4814271.5	315.3022	2_053*	53	*
1077	539223.2	4814267.0	315.277	2_054	54	
1186	539222.1	4814269.8	315.2532	2_055*	55	*
1182	539220.8	4814269.2	315.2504	2_056*	56	*
1192	539223.4	4814270.7	315.3337	2_057*	57	*
1068	539218.0	4814269.0	315.2608	2_058	58	
1149	539220.4	4814285.9	315.1481	2_059	59	
1200	539217.0	4814273.3	315.2488	2_060*	60	*
1151	539217.9	4814290.7	315.2766	2_061	61	
1231	539219.9	4814283.7	315.284	2_062*	62	*
1174	539216.5	4814269.2	315.2246	2_063*	63	*
1191	539218.8	4814270.0	315.257	2_064*	64	*
1222	539217.9	4814278.9	315.2826	2_065*	65	*
1172	539215.5	4814268.9	315.2724	2_066*	66	*
1105	539217.2	4814271.1	315.2491	2_067	67	
1125	539221.8	4814282.1	315.2232	2_068	68	
1206	539215.9	4814274.5	315.2164	2_069*	69	*
1103	539219.4	4814272.5	315.1758	2_070	70	
1245	539218.5	4814292.7	315.248	2_071*	71	*
1202	539218.9	4814273.1	315.2401	2_072*	72	*
1232	539218.6	4814284.1	315.2047	2_073*	73	*
1233	539219.7	4814284.4	315.1507	2_074*	74	*
1177	539222.1	4814267.6	315.2078	2_077*	77	*
1195	539218.2	4814271.4	315.2479	2_078*	78	*
1234	539222.9	4814286.2	315.0135	2_079*	79	*
1100	539219.9	4814275.5	315.207	2_080	80	
1210	539219.2	4814276.9	315.1952	2_083*	83	*

1238	539222.4	4814288.4	315.1255	2_084*	84	*
1249	539219.9	4814295.7	315.1975	2_085*	85	*
1225	539223.1	4814279.9	315.2391	2_086*	86	*
1248	539219.1	4814295.6	315.2162	2_087*	87	*
1219	539223.6	4814278.3	315.2308	2_088*	88	*
1194	539220.6	4814271.4	315.2727	2_089*	89	*
1199	539220.1	4814272.3	315.2294	2_090*	90	*
1126	539220.8	4814282.2	315.2072	2_091	91	
1253	539220.3	4814293.7	315.1248	2_092*	92	*
1169	539217.2	4814299.0	315.2557	2_093	93	
1078	539222.3	4814269.3	315.3024	2_094	94	
1223	539218.2	4814279.9	315.2746	2_095*	95	*
1181	539219.0	4814269.4	315.2558	2_096*	96	*
1089	539215.8	4814274.3	315.152	2_097	97	
1213	539218.9	4814277.7	315.2373	2_098*	98	*
1178	539223.2	4814267.6	315.4327	2_099*	99	*
1239	539219.7	4814289.4	315.1884	2_100*	100	*
1175	539217.0	4814269.2	315.2592	2_101*	101	*
1069	539219.8	4814269.8	315.2307	2_102	102	
1134	539221.8	4814283.2	315.2005	2_103	103	
1220	539223.9	4814278.3	315.2721	2_104*	104	*
1118	539220.6	4814278.4	315.2124	2_106	106	
1190	539215.1	4814271.2	315.3616	2_107*	107	*
1147	539222.9	4814288.2	315.0967	2_108	108	
1137	539219.3	4814284.5	315.1618	2_109	109	
1227	539222.6	4814281.3	315.2228	2_110*	110	*
1148	539217.6	4814287.9	315.3884	2_111	111	
1226	539218.0	4814281.7	315.2276	2_112*	112	*
1102	539221.7	4814273.9	315.2893	2_113	113	
1093	539222.4	4814272.8	315.2912	2_114	114	
1128	539220.2	4814279.7	315.1845	2_115	115	
1240	539219.3	4814289.5	315.1878	2_116*	116	*
1224	539223.6	4814279.5	315.1614	2_117*	117	*
1121	539221.4	4814280.5	315.2181	2_118	118	
1092	539219.9	4814273.3	315.2167	2_119	119	
1250	539220.8	4814295.9	315.2802	2_120*	120	*
1207	539216.4	4814274.7	315.2108	2_121*	121	*
1080	539220.6	4814270.4	315.275	2_122	122	
1170	539223.4	4814271.7	315.3243	2_123*	123	*
1139	539219.3	4814286.4	315.2862	2_124	124	
1242	539222.2	4814290.4	315.1291	2_125*	125	*
1099	539218.0	4814275.9	315.1662	2_126	126	

1083	539218.3	4814272.9	315.2493	2_127	127	
1252	539217.3	4814297.4	315.2754	2_128*	128	*
1104	539218.1	4814270.3	315.2194	2_129	129	
1079	539221.2	4814269.6	315.2918	2_130	130	
1196	539216.9	4814271.7	315.2444	2_131*	131	*
1152	539217.8	4814292.8	315.2463	2_132	132	
1096	539219.1	4814275.7	315.2168	2_133	133	
1184	539218.0	4814269.1	315.2715	2_134*	134	*
1086	539221.2	4814271.1	315.2262	2_135	135	
1084	539217.2	4814272.6	315.2427	2_136	136	
1163	539221.8	4814277.3	315.2071	2_137	137	
1091	539218.3	4814275.9	315.14	2_138	138	
1087	539216.3	4814274.1	315.1855	2_139	139	
1067	539216.3	4814268.5	315.2618	2_140	140	
1146	539220.5	4814288.2	315.1346	2_141	141	
1204	539223.6	4814272.8	315.4517	2_142*	142	*
1112	539222.7	4814275.2	315.324	2_143	143	
1161	539220.5	4814269.1	315.2119	2_144	144	
1141	539222.0	4814286.1	315.0405	2_145	145	
1140	539217.8	4814285.6	315.2485	2_146	146	
1136	539218.7	4814285.6	315.2778	2_147	147	
1159	539219.9	4814268.0	315.2069	2_148	148	
1108	539219.4	4814279.0	315.2115	2_149	149	
1115	539218.5	4814277.7	315.208	2_150	150	
1119	539221.0	4814277.2	315.2331	2_151	151	
1160	539222.4	4814269.6	315.2998	2_152	152	
1230	539220.4	4814282.8	315.3255	2_153*	153	*
1157	539217.2	4814295.9	315.2264	2_154	154	
1070	539218.6	4814271.5	315.2339	2_155	155	
1109	539220.5	4814277.4	315.2213	2_156	156	
1153	539217.7	4814292.9	315.2553	2_157	157	
1135	539218.9	4814285.9	315.2997	2_158	158	
1085	539215.6	4814273.0	315.1987	2_159	159	
1165	539224.5	4814281.4	315.2853	2_160	160	
1066	539222.2	4814266.3	315.3587	2_161	161	
1164	539217.2	4814278.8	315.2675	2_162	162	
1166	539222.6	4814290.6	315.183	2_163	163	
1076	539221.3	4814267.5	315.2446	2_164	164	
1116	539218.5	4814279.2	315.2812	2_165	165	
1064	539217.2	4814268.9	315.2309	2_166	166	
1074	539219.7	4814271.4	315.1825	2_167	167	
1113	539219.6	4814277.3	315.2257	2_168	168	
1145	539221.0	4814287.8	315.0969	2_169	169	

1150	539218.3	4814289.7	315.2528	2_170	170	
1124	539219.0	4814280.6	315.2299	2_171	171	
1127	539222.5	4814283.1	315.2416	2_172	172	
1081	539223.2	4814268.8	315.3671	2_173	173	
1065	539218.7	4814268.4	315.2688	2_174	174	
1158	539215.0	4814270.3	315.3225	2_175	175	
1088	539217.7	4814273.8	315.1987	2_176	176	
1167	539221.7	4814293.2	315.1277	2_177	177	
1168	539216.4	4814296.1	315.3363	2_178	178	
1071	539220.5	4814272.0	315.2141	2_179	179	
1095	539222.6	4814273.8	315.3179	2_180	180	
1111	539221.5	4814275.6	315.2495	2_181	181	
1120	539221.7	4814278.8	315.2054	2_182	182	
1097	539216.5	4814276.0	315.1571	2_183	183	
1117	539220.3	4814279.8	315.2175	2_184	184	
1154	539222.2	4814293.3	315.2254	2_185	185	
1114	539217.5	4814277.8	315.1734	2_186	186	
1082	539220.8	4814267.1	315.2166	2_187	187	
1156	539220.9	4814296.2	315.2319	2_188	188	
1228	539223.8	4814281.7	315.2375	2_189*	189	*
1143	539219.0	4814287.8	315.262	2_190	190	
1075	539216.1	4814270.7	315.2312	2_191	191	
1138	539221.2	4814286.1	315.077	2_192	192	
1094	539223.5	4814273.8	315.4158	2_193	193	
1133	539217.9	4814283.3	315.2266	2_194	194	
1129	539223.8	4814280.0	315.2396	2_195	195	
1155	539221.4	4814296.2	315.2575	2_196	196	
1110	539221.0	4814278.8	315.2138	2_197	197	
1073	539216.9	4814272.7	315.2481	2_198	198	
1144	539219.2	4814288.2	315.2401	2_199	199	
1142	539218.3	4814287.6	315.2997	2_200	200	

Table A6c: Tracking Survey 1 – Site 3

point #	east	north	elev	desc	Rock #	In stream (*)
1367	539329.4	4814781	313.4033	3_001*	1	*
1364	539328.7	4814780	313.3895	3_002*	2	*
1453	539355.9	4814812	313.3251	3_003*	3	*
1410	539335.8	4814791	313.3952	3_004*	4	*
1425	539341.9	4814793	313.3162	3_006*	6	*
1363	539327.7	4814781	313.4872	3_008*	8	*
1350	539331.6	4814792	313.4043	3_009	9	
1449	539353.1	4814809	313.3275	3_010*	10	*
1398	539332.6	4814791	313.3944	3_011*	11	*
1394	539333.7	4814788	313.5918	3_012*	12	*
1356	539324	4814781	313.4937	3_014*	14	*
1361	539326.5	4814781	313.5292	3_015*	15	*
1436	539353.2	4814801	313.1234	3_016*	16	*
1437	539354.6	4814802	313.2819	3_017*	17	*
1388	539331.3	4814788	313.4959	3_018*	18	*
1343	539331.7	4814787	313.5731	3_020	20	
1255	539323.2	4814784	313.4393	3_021	21	
1377	539331.5	4814782	313.2986	3_022*	22	*
1427	539342.3	4814794	313.3505	3_023*	23	*
1390	539330.3	4814792	313.4613	3_024*	24	*
1444	539348.9	4814805	313.2872	3_025*	25	*
1391	539331.2	4814790	313.4001	3_026*	26	*
1381	539327.9	4814788	313.4201	3_027*	27	*
1401	539333.8	4814790	313.4199	3_028*	28	*
1409	539336.9	4814789	313.5288	3_029*	29	*
1376	539328	4814786	313.5183	3_031*	31	*
1382	539331.2	4814787	313.586	3_032*	32	*
1369	539326.1	4814785	313.5158	3_033*	33	*
1405	539336.9	4814787	313.5069	3_034*	34	*
1451	539361.1	4814818	313.3464	3_035*	35	*
1375	539326.7	4814788	313.461	3_036*	36	*
1359	539324	4814785	313.449	3_037*	37	*
1322	539324.4	4814783	313.4958	3_038	38	
1355	539321.6	4814781	313.4681	3_039*	39	*
1360	539326.2	4814783	313.5718	3_040*	40	*

1387	539330.5	4814788	313.4681	3_041*	41	*
1258	539322.3	4814779	313.424	3_042	42	
1415	539335.1	4814792	313.3722	3_043*	43	*
1450	539359	4814816	313.3825	3_044*	44	*
1368	539329.9	4814780	313.3507	3_045*	45	*
1442	539344	4814794	313.381	3_046*	46	*
1365	539329.1	4814780	313.4327	3_047*	47	*
1423	539338.4	4814793	313.2582	3_048*	48	*
1431	539347.8	4814801	313.2853	3_050*	50	*
1429	539344.4	4814797	313.273	3_051*	51	*
1386	539333.8	4814786	313.4673	3_052*	52	*
1338	539329.9	4814789	313.419	3_053	53	
1419	539338.5	4814791	313.3963	3_054*	54	*
1417	539336.3	4814791	313.3519	3_055*	55	*
1454	539368.2	4814825	313.3104	3_056*	56	*
1393	539332.9	4814789	313.5432	3_057*	57	*
1316	539338	4814790	313.4304	3_058	58	
1392	539332.1	4814790	313.4782	3_059*	59	*
1324	539325.1	4814783	313.5523	3_060	60	
1406	539337.3	4814787	313.5129	3_062*	62	*
1407	539338.3	4814788	313.4735	3_063*	63	*
1328	539325.1	4814782	313.5383	3_064	64	
1430	539345.8	4814799	313.2827	3_065*	65	*
1380	539328.8	4814788	313.4422	3_066*	66	*
1408	539337.7	4814789	313.5353	3_068*	68	*
1372	539326.7	4814786	313.491	3_069*	69	*
1402	539334.1	4814791	313.374	3_070*	70	*
1389	539329.7	4814791	313.4397	3_071*	71	*
1421	539336.9	4814792	313.3346	3_072*	72	*
1354	539321.9	4814779	313.4268	3_073*	73	*
1260	539320.4	4814780	313.4499	3_074	74	
1420	539337.6	4814791	313.3729	3_075*	75	*
1357	539321.8	4814783	313.515	3_076*	76	*
1397	539332.4	4814792	313.4402	3_077*	77	*
1333	539329.8	4814786	313.5436	3_078	78	
1418	539338.4	4814790	313.3968	3_079*	79	*
1413	539334.3	4814792	313.3554	3_080*	80	*
1345	539333.1	4814790	313.4571	3_081	81	
1432	539351.2	4814798	313.2126	3_082*	82	*
1371	539325.5	4814787	313.5039	3_083*	83	*

1320	539323.1	4814780	313.4202	3_084	84	
1399	539333.7	4814789	313.5326	3_085*	85	*
1411	539335.2	4814790	313.471	3_086*	86	*
1256	539323.6	4814783	313.4596	3_087	87	
1412	539334	4814792	313.3774	3_088*	88	*
1374	539326.8	4814787	313.4181	3_089*	89	*
1319	539322.4	4814780	313.4146	3_090	90	
1362	539327.2	4814782	313.5461	3_091*	91	*
1336	539328.9	4814790	313.4732	3_092	92	
1452	539361.8	4814818	313.3452	3_093*	93	*
1347	539332.3	4814790	313.4341	3_094	94	
1384	539334	4814784	313.3091	3_095*	95	*
1447	539353.8	4814808	313.2866	3_096*	96	*
1301	539333	4814787	313.5711	3_097	97	
1373	539327	4814786	313.4342	3_098*	98	*
1379	539329.6	4814787	313.5076	3_100*	100	*
1339	539344.5	4814799	313.2155	3_101	101	
1448	539354.2	4814809	313.2862	3_102*	102	*
1428	539344.1	4814794	313.3373	3_103*	103	*
1424	539340.8	4814792	313.2692	3_104*	104	*
1445	539352.7	4814806	313.2869	3_105*	105	*
1403	539333	4814792	313.3968	3_106*	106	*
1337	539329.3	4814790	313.4049	3_107	107	
1346	539334.7	4814790	313.4935	3_108	108	
1342	539331.2	4814787	313.5448	3_109	109	
1400	539336.7	4814787	313.479	3_110*	110	*
1351	539330.9	4814790	313.3821	3_111	111	
1321	539323.3	4814781	313.4484	3_112	112	
1335	539328.1	4814790	313.4337	3_113	113	
1370	539325	4814786	313.483	3_114*	114	*
1366	539329.6	4814780	313.3525	3_115*	115	*
1414	539335.6	4814792	313.347	3_116*	116	*
1383	539333	4814785	313.4551	3_118*	118	*
1327	539326.8	4814780	313.397	3_119	119	
1395	539333	4814790	313.4272	3_120*	120	*
1378	539328.7	4814787	313.4791	3_121*	121	*
1340	539326.6	4814783	313.5673	3_122	122	
1422	539338.5	4814792	313.326	3_123*	123	*
1341	539327.8	4814784	313.5568	3_124	124	
1358	539323	4814783	313.4379	3_125*	125	*
1267	539326.7	4814779	313.3812	3_126	126	

1266	539326.7	4814778	313.3274	3_127	127	
1325	539327.2	4814783	313.5333	3_128	128	
1323	539325.5	4814782	313.5654	3_129	129	
1330	539326.2	4814786	313.381	3_130	130	
1416	539335.6	4814793	313.3872	3_131*	131	*
1329	539322.4	4814782	313.425	3_132	132	
1396	539331	4814792	313.4747	3_133*	133	*
1273	539327.9	4814780	313.3867	3_133	133	
1314	539332.7	4814793	313.4758	3_134	134	
1274	539326	4814782	313.5715	3_135	135	
1307	539335.2	4814787	313.4979	3_136	136	
1385	539334.8	4814784	313.3792	3_137*	137	*
1275	539324.6	4814783	313.56	3_138	138	
1304	539334.6	4814786	313.4323	3_139	139	
1331	539328	4814787	313.3924	3_140	140	
1297	539333.6	4814789	313.5571	3_141	141	
1294	539332.2	4814789	313.5499	3_142	142	
1284	539331.3	4814784	313.4937	3_143	143	
1259	539321.3	4814779	313.4634	3_144	144	
1278	539326.3	4814784	313.5682	3_145	145	
1334	539331.5	4814781	313.2083	3_146	146	
1310	539333.3	4814786	313.4942	3_147	147	
1344	539333.8	4814788	313.5414	3_148	148	
1426	539340.7	4814795	313.2738	3_149*	149	*
1276	539324.8	4814785	313.4588	3_150	150	
1352	539331.5	4814790	313.3416	3_151	151	
1268	539327.8	4814779	313.3682	3_152	152	
1285	539331.7	4814783	313.3059	3_153	153	
1348	539330.8	4814791	313.3981	3_154	154	
1280	539325.4	4814786	313.4568	3_155	155	
1290	539330.5	4814786	313.5573	3_156	156	
1289	539329.9	4814786	313.5559	3_157	157	
1332	539329.1	4814787	313.4626	3_158	158	
1272	539327.4	4814780	313.4733	3_159	159	
1269	539323.6	4814780	313.4764	3_160	160	
1263	539325.6	4814778	313.3439	3_161	161	
1279	539326.7	4814785	313.5553	3_162	162	
1281	539330.7	4814782	313.3937	3_163	163	
1261	539321.9	4814781	313.4844	3_164	164	
1288	539328.6	4814788	313.4231	3_165	165	
1262	539323.6	4814779	313.3588	3_166	166	
1264	539325.7	4814778	313.3362	3_167	167	
1326	539327.3	4814782	313.467	3_168	168	

1271	539323.2	4814780	313.4789	3_169	169	
1318	539328.1	4814782	313.4855	3_170	170	
1308	539335.6	4814790	313.531	3_171	171	
1265	539326.7	4814777	313.338	3_172	172	
1293	539327.5	4814789	313.4252	3_173	173	
1309	539336	4814788	313.4967	3_174	174	
1295	539328.8	4814789	313.4494	3_175	175	
1298	539329.2	4814786	313.5524	3_176	176	
1306	539336.2	4814787	313.4791	3_177	177	
1349	539331.7	4814792	313.4716	3_178	178	
1404	539333.1	4814793	313.4544	3_179*	179	*
1317	539337.6	4814789	313.5103	3_180	180	
1299	539333.5	4814784	313.2645	3_181	181	
1283	539330.7	4814783	313.4231	3_182	182	
1303	539333.4	4814791	313.3879	3_183	183	
1302	539332.8	4814787	313.5639	3_184	184	
1270	539322.9	4814782	313.5016	3_186	186	
1313	539338.2	4814789	313.4699	3_187	187	
1296	539333.3	4814789	313.5284	3_188	188	
1282	539331.4	4814781	313.2764	3_189	189	
1291	539331.1	4814786	313.5486	3_190	190	
1300	539333.7	4814785	313.3618	3_191	191	
1292	539329.9	4814788	313.476	3_192	192	
1257	539323.6	4814777	313.3124	3_193	193	
1287	539327.6	4814788	313.3871	3_194	194	
1311	539337.3	4814789	313.507	3_195	195	
1312	539330.1	4814790	313.4164	3_196	196	
1277	539325.7	4814784	313.5545	3_197	197	
1315	539332.4	4814790	313.3842	3_198	198	
1286	539326.3	4814788	313.491	3_199	199	
1305	539331.8	4814791	313.3857	3_200	200	

Table A6d: Tracking Survey 1 – Site 4

point #	east	north	elev	desc	Rock #
1537	540618	4814660	308.2415	4_001	1
1473	540623.2	4814656	308.1601	4_002	2
1480	540619.5	4814657	308.3056	4_003	3
1635	540621.5	4814648	308.161	4_004	4
1521	540627.9	4814642	307.7864	4_005	5
1529	540658.4	4814622	308.0344	4_006	6
1482	540618.9	4814656	308.2643	4_007	7
1626	540623	4814651	308.1455	4_008	8
1544	540621.4	4814659	308.2655	4_009	9
1560	540621.7	4814659	308.2644	4_010	10
1522	540629.2	4814642	307.6989	4_012	12
1501	540624.8	4814650	308.1105	4_013	13
1493	540622.6	4814651	308.1361	4_014	14
1536	540618.4	4814660	308.269	4_015	15
1510	540626.9	4814649	308.1284	4_016	16
1623	540620	4814653	308.2232	4_017	17
1609	540627.2	4814653	308.4102	4_019	19
1513	540626.1	4814647	308.0059	4_020	20
1464	540623.8	4814662	308.2965	4_021	21
1533	540621.4	4814662	308.2419	4_022	22
1550	540625.6	4814663	308.3336	4_023	23
1561	540621.9	4814658	308.2395	4_024	24
1557	540624.5	4814661	308.3028	4_025	25
1559	540622.6	4814659	308.2236	4_026	26
1528	540656.7	4814623	308.0673	4_027	27
1524	540637.4	4814633	307.585	4_028	28
1578	540623.6	4814655	308.1784	4_029	29
1498	540625.3	4814651	308.1409	4_030	30
1628	540625.5	4814651	308.204	4_031	31
1617	540629	4814649	308.316	4_032	32
1576	540624.1	4814656	308.1962	4_033	33
1577	540623.9	4814656	308.1988	4_035	35
1527	540641.4	4814630	307.5237	4_036	36
1470	540625.8	4814659	308.2835	4_037	37
1616	540628.1	4814649	308.2866	4_038	38
1607	540627	4814653	308.3276	4_039	39
1661	540626.5	4814646	307.9243	4_040	40

1602	540627.7	4814655	308.2786	4_041	41
1587	540624.6	4814655	308.2062	4_042	42
1598	540625.8	4814657	308.3067	4_043	43
1486	540622.2	4814655	308.2183	4_044	44
1569	540619.9	4814656	308.2832	4_045	45
1542	540617.1	4814660	308.2574	4_046	46
1518	540626.3	4814645	307.7474	4_047	47
1479	540619.2	4814658	308.2937	4_048	48
1564	540618.4	4814657	308.2721	4_049	49
1566	540621.4	4814658	308.2915	4_050	50
1572	540622.8	4814657	308.1768	4_051	51
1643	540623	4814648	308.1022	4_052	52
1565	540620.3	4814657	308.2865	4_053	53
1490	540620.3	4814653	308.2116	4_054	54
1467	540624.3	4814660	308.3046	4_055	55
1485	540621	4814655	308.3143	4_056	56
1456	540618.4	4814661	308.2871	4_057	57
1662	540624.3	4814644	308.0992	4_058	58
1523	540633.1	4814637	307.7241	4_059	59
1472	540623.6	4814656	308.1978	4_060	60
1627	540623.4	4814651	308.142	4_061	61
1584	540624.8	4814656	308.2369	4_062	62
1502	540624.5	4814650	308.0961	4_063	63
1642	540623.4	4814648	308.0232	4_064	64
1555	540623.3	4814660	308.283	4_066	66
1516	540626.1	4814644	307.7812	4_067	67
1659	540625	4814645	307.8751	4_068	68
1532	540622.2	4814664	308.1793	4_069	69
1665	540685.6	4814605	307.9664	4_070	70
1487	540622.1	4814656	308.26	4_071	71
1460	540622.3	4814662	308.1892	4_072	72
1567	540624.2	4814659	308.1887	4_073	73
1649	540626.1	4814648	308.0849	4_074	74
1574	540626.1	4814659	308.2655	4_075	75
1511	540627.3	4814647	308.1195	4_076	76
1582	540623.2	4814655	308.1644	4_077	77
1500	540625.4	4814652	308.1655	4_078	78
1530	540623.7	4814664	308.1821	4_079	79
1548	540624.1	4814663	308.3188	4_080	80
1654	540626.3	4814646	307.9526	4_081	81
1506	540626.1	4814649	308.1261	4_082	82
1471	540626.6	4814660	308.2896	4_083	83

1618	540628.6	4814649	308.3034	4_084	84
1630	540626.3	4814651	308.2347	4_085	85
1515	540626.7	4814645	307.8602	4_086	86
1583	540624.8	4814655	308.2109	4_087	87
1656	540628	4814646	308.0756	4_088	88
1601	540627.4	4814656	308.3118	4_089	89
1606	540628.3	4814652	308.2911	4_090	90
1608	540626.7	4814652	308.3572	4_091	91
1613	540629	4814650	308.3114	4_092	92
1568	540618.3	4814656	308.2893	4_093	93
1594	540622.8	4814654	308.1787	4_094	94
1645	540623.2	4814647	308.1023	4_095	95
1492	540621.8	4814651	308.1352	4_096	96
1519	540628.6	4814646	308.0427	4_097	97
1538	540618	4814659	308.2781	4_098	98
1625	540620.5	4814652	308.2106	4_099	99
1552	540619	4814659	308.2841	4_100	100
1570	540623.3	4814657	308.1956	4_101	101
1586	540625.2	4814655	308.1983	4_102	102
1644	540622.5	4814647	308.1362	4_103	103
1655	540626.8	4814646	307.9953	4_104	104
1477	540620.9	4814657	308.3028	4_105	105
1622	540621.7	4814654	308.2248	4_106	106
1646	540624	4814646	308.023	4_107	107
1562	540621	4814659	308.3282	4_108	108
1631	540623.1	4814650	308.0989	4_109	109
1514	540625.6	4814646	307.8904	4_110	110
1585	540625.3	4814656	308.2007	4_111	111
1546	540622.1	4814661	308.1767	4_112	112
1545	540622.4	4814661	308.1761	4_113	113
1465	540624.1	4814661	308.3024	4_114	114
1466	540623.7	4814661	308.25	4_115	115
1497	540623.6	4814652	308.1362	4_116	116
1629	540626.5	4814652	308.2515	4_117	117
1526	540640.7	4814632	307.6681	4_118	118
1599	540626.5	4814657	308.3171	4_119	119
1615	540628.6	4814649	308.3204	4_120	120
1512	540626.5	4814648	308.1227	4_121	121
1474	540622.6	4814656	308.2374	4_122	122
1551	540626.3	4814662	308.3528	4_123	123
1505	540626.3	4814650	308.1467	4_124	124
1605	540628.6	4814653	308.2874	4_125	125
1496	540624.3	4814652	308.128	4_126	126

1525	540637.9	4814632	307.4843	4_127	127
1600	540626.5	4814658	308.3515	4_128	128
1620	540628.2	4814647	308.2241	4_129	129
1653	540627.2	4814647	308.0668	4_130	130
1468	540625.2	4814660	308.3029	4_131	131
1640	540626.3	4814649	308.1084	4_132	132
1494	540622.7	4814652	308.1539	4_133	133
1641	540623.9	4814648	307.9629	4_134	134
1489	540620.8	4814653	308.247	4_135	135
1592	540623.7	4814654	308.1702	4_136	136
1579	540619.3	4814655	308.2054	4_137	137
1647	540624.5	4814648	307.9089	4_138	138
1657	540625.5	4814645	307.8477	4_139	139
1495	540623.4	4814652	308.1677	4_140	140
1637	540622.3	4814649	308.16	4_141	141
1539	540625.9	4814657	308.3861	4_142	142
1636	540621.9	4814649	308.1354	4_143	143
1458	540620.2	4814661	308.2787	4_144	144
1648	540625.1	4814648	308.0523	4_145	145
1488	540621.6	4814656	308.256	4_146	146
1571	540623.7	4814657	308.2099	4_147	147
1589	540625.4	4814654	308.1587	4_148	148
1621	540627.3	4814650	308.2436	4_149	149
1463	540623.2	4814662	308.2836	4_150	150
1588	540625.4	4814655	308.1579	4_151	151
1478	540620.4	4814658	308.3303	4_152	152
1504	540625.5	4814649	308.0942	4_153	153
1462	540623.5	4814661	308.2867	4_154	154
1558	540623.4	4814659	308.2035	4_155	155
1619	540629.4	4814648	308.2725	4_156	156
1469	540625	4814659	308.2938	4_157	157
1634	540621.4	4814649	308.1423	4_158	158
1575	540627.8	4814659	308.3017	4_159	159
1611	540628	4814650	308.2802	4_160	160
1632	540622.4	4814650	308.085	4_161	161
1595	540623.6	4814653	308.1384	4_162	162
1503	540624.9	4814649	308.1046	4_163	163
1535	540619.5	4814661	308.3035	4_164	164
1658	540623.9	4814645	308.0465	4_165	165
1660	540624.4	4814645	308.0412	4_166	166
1624	540621.9	4814654	308.2074	4_167	167
1491	540621.1	4814651	308.157	4_168	168
1580	540619.3	4814654	308.2497	4_169	169

1603	540627	4814654	308.3203	4_170	170
1499	540625.6	4814653	308.1735	4_171	171
1556	540625.6	4814661	308.3885	4_172	172
1507	540625.6	4814649	308.067	4_173	173
1508	540626.5	4814649	308.1159	4_174	174
1610	540628.3	4814652	308.264	4_175	175
1596	540624.2	4814653	308.174	4_176	176
1517	540625.4	4814645	307.8284	4_177	177
1639	540627.1	4814649	308.1599	4_178	178
1663	540621.9	4814661	308.2105	4_179	179
1573	540625.4	4814658	308.3608	4_180	180
1590	540625.6	4814653	308.203	4_181	181
1457	540617.7	4814661	308.2752	4_182	182
1650	540623.2	4814646	308.0684	4_183	183
1554	540617.3	4814659	308.2623	4_184	184
1651	540624.5	4814646	307.8605	4_185	185
1476	540621.7	4814657	308.2668	4_186	186
1593	540623.5	4814654	308.1698	4_187	187
1652	540625.1	4814646	307.8665	4_188	188
1543	540619.6	4814660	308.3466	4_189	189
1638	540623.5	4814649	308.0615	4_190	190
1509	540627.6	4814648	308.1155	4_191	191
1520	540628.1	4814646	308.0583	4_192	192
1591	540624.4	4814654	308.1979	4_193	193
1612	540628.4	4814650	308.3139	4_194	194
1581	540620.2	4814654	308.2619	4_195	195
1604	540627.6	4814654	308.2719	4_196	196
1475	540622.2	4814657	308.2311	4_197	197
1549	540625	4814662	308.326	4_198	198
1459	540621.6	4814662	308.1827	4_199	199
1461	540623	4814662	308.2675	4_200	200

Table A7a: Tracking Survey 2 – Site 1

point #	easting	northing	elev	desc	Rock #
P120	538968.3	4812984	317.453	4A_003	3
P35	538970.7	4812974	317.483	4A_004	4
P34	538973.1	4812974	317.572	4A_005	5
P141	538968.1	4812987	317.471	4A_006	6
P169	538965	4813012	317.318	4A_007	7
P9	538969.6	4812971	317.504	4A_008	8
P128	538965.4	4812986	317.421	4A_009	9
P85	538966.9	4812980	317.546	4A_010	10
P92	538970.9	4812982	317.462	4A_011	11
P160	538969.9	4812992	317.447	4A_012	12
P166	538965.8	4813006	317.345	4A_013	13
P129	538966.4	4812986	317.444	4A_014	14
P83	538969.2	4812981	317.491	4A_016	16
P154	538967.7	4812989	317.482	4A_017	17
P109	538970.5	4812985	317.488	4A_018	18
P79	538971.8	4812980	317.47	4A_019	19
P55	538965.5	4812976	317.594	4A_022	22
P28	538969.7	4812973	317.524	4A_026	26
P107	538971	4812985	317.541	4A_027	27
P54	538966.5	4812975	317.587	4A_029	29
P162	538965.7	4812994	317.469	4A_031	31
P58	538971	4812977	317.495	4A_032	32
P8	538971.1	4812971	317.53	4A_033	33
P42	538969.3	4812975	317.534	4A_034	34
P20	538966.2	4812971	317.623	4A_035	35
P157	538970.4	4812990	317.453	4A_036	36
P15	538972.9	4812972	317.678	4A_038	38
P71	538967.9	4812978	317.517	4A_039	39
P106	538972.2	4812985	317.565	4A_040	40

P48	538971.6	4812976	317.514	4A_042	42
P53	538967.1	4812975	317.556	4A_044	44
P155	538968.7	4812990	317.457	4A_045	45
P7	538973	4812971	317.57	4A_046	46
P63	538967.5	4812978	317.538	4A_047	47
P57	538969.8	4812977	317.489	4A_048	48
P11	538965.8	4812970	317.655	4A_049	49
P50	538968.4	4812976	317.573	4A_050	50
P16	538973.7	4812972	317.574	4A_052	52
P44	538965.3	4812974	317.65	4A_053	53
P159	538968.8	4812991	317.439	4A_055	55
P59	538972.2	4812977	317.521	4A_056	56
P89	538967.8	4812981	317.511	4A_058	58
P90	538969.6	4812981	317.5	4A_059	59
P147	538967.2	4812988	317.484	4A_060	60
P150	538972	4812988	317.546	4A_062	62
P95	538971.4	4812983	317.528	4A_065	65
P161	538968.1	4812994	317.423	4A_066	66
P165	538965.3	4813002	317.385	4A_067	67
P49	538973	4812976	317.576	4A_069	69
P33	538973.1	4812974	317.638	4A_070	70
P117	538966.6	4812985	317.459	4A_071	71
P88	538967	4812981	317.564	4A_072	72
P152	538965.5	4812989	317.472	4A_074	74
P143	538966.6	4812987	317.47	4A_075	75
P45	538967	4812975	317.558	4A_076	76
P153	538966.9	4812989	317.497	4A_078	78
P132	538969.3	4812986	317.446	4A_079	79
P114	538965.9	4812984	317.434	4A_080	80
P75	538967.8	4812979	317.508	4A_081	81
P93	538971.9	4812982	317.5	4A_083	83

P36	538969.6	4812974	317.513	4A_084	84
P116	538965.7	4812985	317.516	4A_085	85
P70	538969.5	4812978	317.493	4A_086	86
P39	538971	4812974	317.52	4A_087	87
P43	538967.3	4812974	317.57	4A_089	89
P13	538971	4812972	317.527	4A_091	91
P140	538968.6	4812988	317.464	4A_092	92
P148	538968.7	4812988	317.439	4A_093	93
P164	538964.3	4813000	317.434	4A_094	94
P139	538969.8	4812988	317.461	4A_095	95
P41	538971	4812975	317.487	4A_096	96
P60	538968.2	4812977	317.583	4A_097	97
P108	538970.7	4812985	317.464	4A_098	98
P119	538968.2	4812985	317.469	4A_100	100
P158	538966.7	4812990	317.47	4A_102	102
P121	538969.8	4812985	317.48	4A_104	104
P65	538970.2	4812978	317.482	4A_105	105
P56	538966.5	4812976	317.558	4A_106	106
P125	538971.4	4812986	317.461	4A_108	108
P32	538970.4	4812974	317.488	4A_109	109
P105	538972.1	4812984	317.519	4A_110	110
P77	538970	4812979	317.474	4A_112	112
P52	538967.3	4812975	317.54	4A_113	113
P124	538971.7	4812986	317.492	4A_114	114
P26	538971.7	4812973	317.501	4A_115	115
P37	538965.6	4812973	317.626	4A_116	116
P113	538967.3	4812985	317.451	4A_118	118
P168	538965.4	4813010	317.382	4A_119	119
P73	538965.1	4812978	317.597	4A_120	120
P134	538970.7	4812987	317.46	4A_121	121
P163	538966.2	4812997	317.45	4A_122	122
P133	538970	4812987	317.452	4A_123	123
P101	538969.8	4812983	317.477	4A_124	124
P151	538964.4	4812988	317.516	4A_126	126

P144	538965.6	4812987	317.447	4A_127	127
P25	538972.3	4812974	317.502	4A_128	128
P31	538968.5	4812973	317.521	4A_129	129
P68	538972.4	4812978	317.565	4A_130	130
P126	538970.6	4812986	317.407	4A_131	131
P23	538972.7	4812973	317.513	4A_132	132
P111	538969	4812984	317.456	4A_133	133
P40	538972.5	4812975	317.547	4A_134	134
P123	538971	4812986	317.446	4A_139	139
P76	538968.9	4812979	317.506	4A_140	140
P67	538971.9	4812978	317.509	4A_141	141
P110	538969.9	4812985	317.474	4A_142	142
P12	538969.9	4812972	317.527	4A_0143	143
P142	538967.2	4812987	317.494	4A_144	144
P72	538966.5	4812977	317.577	4A_145	145
P84	538968.5	4812980	317.503	4A_148	148
P103	538972	4812984	317.522	4A_149	149
P51	538967.9	4812976	317.516	4A_151	151
P96	538969.3	4812983	317.479	4A_152	152
P122	538971.4	4812985	317.446	4A_153	153
P145	538965	4812987	317.441	4A_154	154
P99	538966.8	4812982	317.463	4A_155	155
P27	538970.8	4812973	317.501	4A_156	156
P47	538970.8	4812976	317.491	4A_157	157
P82	538970.8	4812981	317.493	4A_158	158
P46	538968.8	4812975	317.538	4A_159	159
P10	538968	4812970	317.566	4A_160	160
P21	538967.2	4812972	317.561	4A_161	161
P100	538966.1	4812982	317.516	4A_162	162
P135	538971.5	4812987	317.491	4A_163	163
P80	538970.9	4812980	317.485	4A_164	164
P127	538965.7	4812986	317.467	4A_165	165
P19	538969.2	4812972	317.527	4A_166	166
P14	538972.1	4812972	317.523	4A_167	167
P6	538973	4812971	317.561	4A_168	168
P66	538970.8	4812978	317.502	4A_169	169

P146	538965.4	4812987	317.465	4A_170	170
P24	538973.3	4812974	317.576	4A_171	171
P74	538967.2	4812978	317.589	4A_173	173
P112	538968.3	4812984	317.476	4A_174	174
P137	538971.2	4812987	317.459	4A_175	175
P156	538970.6	4812989	317.451	4A_176	176
P167	538964.7	4813008	317.336	4A_177	177
P64	538969	4812977	317.516	4A_178	178
P30	538966.1	4812973	317.611	4A_179	179
P118	538967.5	4812985	317.458	4A_180	180
P130	538967.3	4812986	317.466	4A_181	181
P91	538970.2	4812982	317.485	4A_182	182
P115	538965.9	4812984	317.411	4A_183	183
P136	538972	4812987	317.53	4A_184	184
P131	538968	4812986	317.493	4A_186	186
P149	538971	4812988	317.434	4A_188	188
P97	538968.4	4812983	317.518	4A_189	189
P86	538964.9	4812980	317.584	4A_190	190
P81	538969.8	4812980	317.48	4A_191	191
P138	538970.5	4812988	317.442	4A_192	192
P38	538967.2	4812974	317.557	4A_93	193
P94	538972	4812982	317.518	4A_194	194
P87	538966.3	4812981	317.471	4A_196	196
P78	538971.1	4812979	317.461	4A_197	197
P98	538968.1	4812983	317.477	4A_198	198
P61	538967.6	4812977	317.551	4A_199	199
P102	538971	4812983	317.477	4A_200	200

Table A7b: Tracking Survey 2 – Site 4

point #	northing	easting	elev	desc	Rock #
P175	4814660	540617.4	308.295	4B_001	1
P241	4814655	540623	308.194	4B_002	2
P220	4814657	540619.1	308.308	4B_003	3
P308	4814649	540621.5	308.119	4B_004	4
P223	4814656	540618.8	308.264	4B_007	7
P288	4814650	540622.6	308.146	4B_008	8
P191	4814660	540621.5	308.299	4B_009	9
P207	4814659	540621.9	308.287	4B_010	10
P302	4814651	540624.6	308.119	4B_013	13
P287	4814652	540621.9	308.174	4B_014	14
P176	4814660	540617.7	308.278	4B_015	15
P327	4814648	540626.8	308.095	4B_016	16
P273	4814653	540620.4	308.199	4B_017	17
P256	4814654	540627	308.335	4B_019	19
P326	4814647	540625.9	308.097	4B_020	20
P196	4814662	540624.9	308.344	4B_021	21
P173	4814663	540621	308.209	4B_022	22
P216	4814658	540622.1	308.307	4B_024	24
P200	4814661	540624.5	308.376	4B_025	25
P203	4814660	540621.2	308.309	4B_026	26
P239	4814655	540623.8	308.188	4B_029	29
P295	4814652	540626	308.152	4B_031	31
P238	4814656	540624.4	308.239	4B_033	33
P242	4814654	540622.4	308.219	4B_035	35
P228	4814659	540626	308.295	4B_037	37
P265	4814649	540627.8	308.268	4B_038	38
P260	4814653	540627	308.348	4B_039	39

P252	4814655	540627.4	308.31	4B_041	41
P277	4814655	540624.6	308.187	4B_042	42
P235	4814657	540625	308.256	4B_043	43
P240	4814655	540622.4	308.242	4B_044	44
P222	4814655	540619.3	308.287	4B_045	45
P174	4814661	540617.2	308.29	4B_046	46
P205	4814658	540619.1	308.313	4B_048	48
P204	4814657	540618.3	308.274	4B_049	49
P230	4814657	540622.6	308.232	4B_051	51
P317	4814648	540622.7	308.138	4B_052	52
P219	4814657	540620	308.297	4B_053	53
P209	4814659	540624.7	308.281	4B_055	55
P247	4814655	540621.2	308.24	4B_056	56
P171	4814661	540618.8	308.307	4B_057	57
P229	4814657	540623.2	308.232	4B_060	60
P301	4814651	540623.8	308.133	4B_061	61
P271	4814655	540625	308.194	4B_062	62
P304	4814650	540624.3	308.111	4B_063	63
P316	4814648	540623.1	308.11	4B_064	64
P190	4814660	540621	308.313	4B_065	65
P202	4814660	540622.7	308.181	4B_066	66
P172	4814663	540621.9	308.223	4B_069	69
P232	4814656	540622.3	308.253	4B_071	71
P185	4814661	540621.6	308.227	4B_072	72
P213	4814659	540624.3	308.235	4B_073	73
P227	4814658	540625.5	308.324	4B_075	75
P276	4814654	540623.3	308.178	4B_077	77
P292	4814653	540624.8	308.175	4B_078	78
P181	4814663	540623.9	308.313	4B_079	79
P182	4814663	540624.1	308.344	4B_080	80
P212	4814659	540625.9	308.272	4B_083	83

P269	4814649	540629.1	308.368	4B_084	84
P303	4814651	540625.7	308.115	4B_085	85
P248	4814656	540624.6	308.197	4B_087	87
P251	4814657	540627	308.348	4B_089	89
P258	4814652	540627.9	308.285	4B_090	90
P261	4814652	540626.6	308.367	4B_091	91
P267	4814650	540628.9	308.35	4B_092	92
P221	4814656	540618.3	308.264	4B_093	93
P275	4814654	540623	308.2	4B_094	94
P319	4814646	540622.6	308.142	4B_095	95
P286	4814651	540621.4	308.127	4B_096	96
P188	4814659	540617.7	308.315	4B_098	98
P284	4814651	540620.9	308.188	4B_099	99
P187	4814659	540618.8	308.327	4B_100	100
P236	4814656	540623.2	308.196	4B_101	101
P278	4814654	540624.9	308.195	4B_102	102
P318	4814647	540622	308.227	4B_103	103
P334	4814646	540627	308.052	4B_104	104
P218	4814657	540620.8	308.325	4B_105	105
P274	4814653	540622.4	308.229	4B_106	106
P321	4814646	540623.7	308.07	4B_107	107
P224	4814657	540621.3	308.321	4B_108	108
P299	4814650	540622.9	308.116	4B_109	109
P332	4814646	540625.7	307.848	4B_110	110
P249	4814656	540625.3	308.284	4B_111	111
P193	4814661	540622.5	308.219	4B_112	112
P192	4814660	540622.1	308.237	4B_113	113
P195	4814661	540623.8	308.264	4B_114	114
P201	4814661	540623.7	308.306	4B_115	115
P291	4814652	540624.2	308.174	4B_116	116
P262	4814652	540626.7	308.334	4B_117	117
P234	4814658	540626.1	308.346	4B_119	119
P268	4814650	540628.8	308.306	4B_120	120
P333	4814645	540626.7	307.865	4B_121	121
P225	4814657	540622.6	308.254	4B_122	122
P198	4814663	540626.3	308.386	4B_123	123
P328	4814649	540626.6	308.096	4B_124	124
P257	4814653	540627.8	308.262	4B_125	125
P290	4814652	540623.9	308.169	4B_126	126

P233	4814658	540627.1	308.338	4B_128	128
P324	4814647	540627.7	308.129	4B_129	129
P335	4814646	540627	308.052	4B_130	130
P210	4814660	540625.1	308.3	4B_131	131
P310	4814650	540626.4	308.254	4B_132	132
P283	4814652	540622.1	308.165	4B_133	133
P315	4814648	540623.8	308.026	4B_134	134
P245	4814654	540620.8	308.244	4B_135	135
P289	4814651	540623.3	308.186	4B_136	136
P243	4814654	540619.4	308.21	4B_137	137
P314	4814648	540624.1	308.014	4B_138	138
P296	4814651	540622.9	308.143	4B_140	140
P307	4814649	540621.3	308.171	4B_141	141
P237	4814656	540625.7	308.385	4B_142	142
P306	4814649	540621.9	308.142	4B_143	143
P179	4814662	540620.2	308.292	4B_144	144
P322	4814648	540625.8	308.054	4B_145	145
P231	4814656	540621.9	308.274	4B_146	146
P214	4814658	540623.4	308.207	4B_147	147
P279	4814654	540625.1	308.163	4B_148	148
P266	4814650	540626.6	308.231	4B_149	149
P194	4814661	540623	308.248	4B_150	150
P255	4814654	540626.6	308.382	4B_151	151
P206	4814658	540620.1	308.329	4B_152	152
P186	4814661	540619.8	308.346	4B_154	154
P208	4814660	540624.1	308.234	4B_155	155
P270	4814649	540629.5	308.283	4B_156	156
P211	4814660	540625.7	308.276	4B_157	157
P297	4814649	540621.3	308.197	4B_158	158
P250	4814657	540626.7	308.315	4B_159	159
P263	4814650	540627.6	308.338	4B_160	160
P298	4814649	540622.1	308.136	4B_161	161
P300	4814650	540623.5	308.12	4B_162	162
P309	4814649	540624.6	308.141	4B_163	163
P178	4814660	540618.9	308.321	4B_164	164
P329	4814646	540623.4	308.093	4B_165	165
P272	4814653	540621.5	308.257	4B_167	167
P285	4814651	540620.7	308.215	4B_168	168
P244	4814654	540619	308.216	4B_169	169

P254	4814654	540627	308.34	4B_170	170
P294	4814652	540625.4	308.155	4B_171	171
P199	4814662	540625.3	308.359	4B_172	172
P313	4814649	540625.2	308.137	4B_173	173
P312	4814649	540626.2	308.131	4B_174	174
P259	4814651	540627.9	308.375	4B_175	175
P281	4814653	540624.6	308.144	4B_176	176
P311	4814649	540626.7	308.224	4B_178	178
P226	4814658	540625.3	308.366	4B_180	180
P293	4814653	540624.9	308.129	4B_181	181
P170	4814661	540617.4	308.282	4B_182	182
P320	4814646	540623	308.118	4B_183	183
P189	4814659	540617.6	308.289	4B_184	184
P330	4814645	540624.5	307.964	4B_185	185
P217	4814658	540621.5	308.314	4B_186	186
P282	4814653	540624	308.166	4B_187	187
P331	4814646	540625	307.903	4B_188	188
P177	4814660	540618.8	308.332	4B_189	189
P305	4814649	540623.5	308.102	4B_190	190
P323	4814647	540626.7	308.071	4B_191	191
P325	4814647	540627.5	308.171	4B_192	192
P280	4814653	540624.2	308.154	4B_193	193
P264	4814650	540628.3	308.313	4B_194	194
P246	4814654	540619.5	308.209	4B_195	195
P253	4814654	540628	308.328	4B_196	196
P215	4814658	540622.9	308.2	4B_197	197
P197	4814662	540625.1	308.356	4B_198	198
P184	4814661	540622.4	308.21	4B_199	199
P183	4814662	540623.2	308.309	4B_200	200

Table A8a: Tracking Survey 3 – Site 1

point #	easting	northing	elev	desc	Rock #
P577	538967.3	4812975	317.561	1C_001	1
P675	538970.6	4812989	317.45	1C_002	2
P630	538968.2	4812986	317.492	1C_003	3
P556	538970.6	4812974	317.503	1C_004	4
P562	538972.9	4812975	317.587	1C_005	5
P648	538968	4812987	317.474	1C_006	6
P686	538965.2	4813025	317.257	1C_007	7
P529	538969.5	4812971	317.536	1C_008	8
P624	538965.2	4812986	317.446	1C_009	9
P603	538967.4	4812980	317.528	1C_010	10
P612	538970.2	4812984	317.495	1C_011	11
P672	538969.2	4812993	317.473	1C_012	12
P682	538966.4	4813006	317.409	1C_013	13
P626	538966.1	4812986	317.466	1C_014	14
P606	538967.3	4812980	317.541	1C_015	15
P390	538970	4812982	317.496	1C_016	16
P664	538967.1	4812989	317.488	1C_017	17
P617	538970.4	4812985	317.498	1C_018	18
P395	538971.8	4812981	317.479	1C_019	19
P557	538970.8	4812974	317.513	1C_020	20
P608	538965.5	4812983	317.437	1C_021	21
P684	538963	4813005	317.449	1C_022	22
P583	538965.8	4812976	317.581	1C_023	23
P667	538968.6	4812989	317.493	1C_024	24
P553	538969.7	4812974	317.538	1C_026	26
P646	538970.2	4812988	317.462	1C_028	28
P582	538966.2	4812976	317.6	1C_029	29
P681	538964.5	4813004	317.449	1C_031	31
P567	538971.1	4812978	317.514	1C_032	32
P540	538970.4	4812971	317.546	1C_033	33
P594	538968.9	4812977	317.543	1C_034	34
P532	538966.2	4812971	317.632	1C_035	35
P670	538970	4812992	317.461	1C_036	36
P394	538971.2	4812982	317.478	1C_037	37
P546	538972.6	4812973	317.544	1C_038	38
P598	538967.9	4812979	317.541	1C_039	39

P652	538966.6	4812987	317.481	1C_041	41
P564	538971.4	4812977	317.569	1C_042	42
P528	538973.6	4812972	317.571	1C_043	43
P590	538966.4	4812978	317.594	1C_044	44
P665	538968.1	4812989	317.5	1C_045	45
P544	538972.7	4812972	317.588	1C_046	46
P605	538967.7	4812980	317.533	1C_047	47
P574	538969.8	4812978	317.515	1C_048	48
P531	538966.4	4812971	317.619	1C_049	49
P575	538969.1	4812977	317.558	1C_050	50
P545	538973	4812972	317.558	1C_052	52
P584	538965.4	4812975	317.602	1C_053	53
P610	538969.4	4812982	317.493	1C_054	54
P669	538969	4812991	317.455	1C_055	55
P568	538972.3	4812978	317.55	1C_056	56
P596	538969.7	4812978	317.482	1C_057	57
P386	538967.3	4812982	317.538	1C_058	58
P377	538969.5	4812983	317.506	1C_059	59
P660	538967.2	4812988	317.51	1C_060	60
P680	538964.5	4813004	317.46	1C_061	61
P644	538971.8	4812989	317.527	1C_062	62
P639	538969.5	4812987	317.484	1C_064	64
P375	538970.5	4812983	317.528	1C_065	65
P674	538967.2	4812995	317.449	1C_066	66
P679	538967.1	4813002	317.416	1C_067	67
P634	538971.5	4812986	317.484	1C_068	68
P563	538972.4	4812976	317.549	1C_069	69
P627	538966.9	4812985	317.48	1C_071	71
P380	538967.2	4812983	317.492	1C_072	72
P388	538969.2	4812982	317.503	1C_073	73
P662	538965.7	4812989	317.498	1C_074	74
P658	538966.8	4812988	317.474	1C_075	75
P580	538967.1	4812977	317.568	1C_076	76
P599	538967.4	4812979	317.561	1C_077	77
P663	538966	4812990	317.492	1C_078	78
P641	538969.5	4812987	317.476	1C_079	79
P621	538966.3	4812984	317.462	1C_080	80
P604	538968	4812980	317.521	1C_081	81
P376	538970.1	4812983	317.562	1C_082	82
P374	538971.2	4812983	317.524	1C_083	83

P559	538969.5	4812974	317.524	1C_084	84
P625	538965.8	4812986	317.463	1C_085	85
P597	538968.3	4812979	317.504	1C_086	86
P558	538970.6	4812974	317.524	1C_087	87
P587	538965.9	4812978	317.601	1C_089	89
P653	538964.4	4812986	317.51	1C_090	90
P542	538971.2	4812972	317.548	1C_091	91
P649	538967.9	4812987	317.496	1C_092	92
P666	538968.6	4812989	317.487	1C_093	93
P678	538965.1	4813000	317.483	1C_094	94
P560	538970.8	4812976	317.53	1C_096	96
P593	538968.4	4812978	317.537	1C_097	97
P633	538970.7	4812986	317.506	1C_098	98
P616	538971.3	4812986	317.504	1C_099	99
P628	538967.9	4812986	317.499	1C_100	100
P611	538969.4	4812983	317.509	1C_101	101
P673	538966.4	4812992	317.485	1C_102	102
P607	538966.4	4812980	317.559	1C_103	103
P640	538969.2	4812987	317.488	1C_104	104
P572	538970.5	4812979	317.469	1C_105	105
P586	538966.3	4812977	317.572	1C_106	106
P379	538967.8	4812983	317.51	1C_107	107
P636	538971.3	4812987	317.465	1C_108	108
P554	538970.2	4812974	317.53	1C_109	109
P659	538967.1	4812988	317.482	1C_111	111
P398	538970.2	4812979	317.475	1C_112	112
P578	538967.4	4812976	317.578	1C_113	113
P549	538971.8	4812974	317.546	1C_115	115
P537	538965.7	4812974	317.606	1C_116	116
P602	538968.1	4812980	317.533	1C_117	117
P620	538966.7	4812984	317.456	1C_118	118
P683	538965	4813009	317.384	1C_119	119
P589	538965.7	4812979	317.613	1C_120	120
P642	538970.4	4812987	317.489	1C_121	121
P677	538966.7	4812998	317.428	1C_122	122
P647	538968.8	4812987	317.488	1C_0123	123
P622	538966.2	4812985	317.464	1C_125	125
P656	538964.3	4812988	317.508	1C_126	126

P657	538965.9	4812987	317.48	1C_127	127
P550	538971.4	4812974	317.493	1C_128	128
P535	538968.5	4812974	317.561	1C_129	129
P570	538971.9	4812979	317.517	1C_130	130
P381	538966.5	4812983	317.465	1C_131	131
P548	538973.1	4812974	317.568	1C_132	132
P618	538968.4	4812984	317.463	1C_133	133
P561	538971.8	4812976	317.526	1C_134	134
P623	538965.5	4812985	317.449	1C_135	135
P668	538969.4	4812989	317.461	1C_136	136
P389	538969.4	4812982	317.495	1C_137	137
P391	538970.5	4812982	317.488	1C_138	138
P638	538970.6	4812986	317.498	1C_139	139
P601	538968.4	4812979	317.54	1C_140	140
P569	538971.4	4812978	317.536	1C_141	141
P541	538970.4	4812972	317.538	1C_143	143
P661	538966.6	4812988	317.495	1C_144	144
P588	538965.8	4812978	317.587	1C_145	145
P592	538967.6	4812978	317.557	1C_146	146
P387	538968	4812981	317.517	1C_148	148
P614	538971.6	4812985	317.501	1C_149	149
P585	538965.7	4812977	317.6	1C_150	150
P579	538966.9	4812976	317.569	1C_151	151
P615	538971.7	4812985	317.51	1C_153	153
P654	538964.3	4812987	317.54	1C_154	154
P382	538966.5	4812983	317.495	1C_155	155
P552	538970.2	4812973	317.517	1C_156	156
P566	538970.7	4812977	317.501	1C_157	157
P396	538970.5	4812981	317.493	1C_158	158
P576	538968.8	4812976	317.527	1C_159	159
P530	538967.1	4812971	317.593	1C_160	160
P533	538967.1	4812972	317.581	1C_161	161
P383	538965.8	4812982	317.507	1C_162	162
P635	538971.4	4812986	317.515	1C_163	163
P392	538969.7	4812981	317.481	1C_164	164
P534	538968.8	4812972	317.558	1C_166	166
P543	538971.2	4812972	317.525	1C_167	167
P527	538973.3	4812971	317.562	1C_168	168
P573	538970.4	4812978	317.496	1C_169	169

P655	538964.8	4812988	317.484	1C_170	170
P547	538972.6	4812974	317.539	1C_171	171
P632	538969.7	4812986	317.509	1C_172	172
P591	538967	4812978	317.579	1C_173	173
P619	538967.8	4812984	317.467	1C_174	174
P643	538971.6	4812987	317.507	1C_175	175
P671	538970.7	4812991	317.472	1C_176	176
P685	538964.9	4813020	317.303	1C_177	177
P595	538968.9	4812978	317.541	1C_178	178
P600	538967.5	4812979	317.538	1C_179	179
P651	538966.9	4812986	317.466	1C_181	181
P609	538965.1	4812984	317.452	1C_183	183
P637	538971.6	4812987	317.497	1C_184	184
P650	538968.4	4812987	317.516	1C_185	185
P629	538967.9	4812986	317.458	1C_186	186
P551	538970.8	4812973	317.496	1C_187	187
P645	538971	4812988	317.466	1C_188	188
P378	538968.5	4812983	317.525	1C_189	189
P385	538965.8	4812981	317.516	1C_190	190
P393	538970.1	4812981	317.472	1C_191	191
P631	538968.7	4812986	317.485	1C_192	192
P536	538966.6	4812974	317.564	1C_193	193
P373	538971.8	4812983	317.517	1C_194	194
P384	538965.2	4812981	317.508	1C_196	196
P397	538971.2	4812980	317.463	1C_197	197
P581	538967	4812977	317.611	1C_199	199
P613	538970.7	4812985	317.518	1C_200	200

Table A8b: Tracking Survey 3 – Site 4

point #	northing	easting	elev	desc	Rock #
P809	4814660	540617.4	308.319	4C_001	1
P880	4814655	540622.6	308.233	4C_002	2
P824	4814657	540619.3	308.3	4C_003	3
P926	4814648	540621.6	308.225	4C_004	4
P971	4814639	540632	307.795	4C_005	5
P980	4814622	540659	308.051	4C_006	6
P822	4814656	540618.9	308.276	4C_007	7
P921	4814651	540623.1	308.19	4C_008	8
P830	4814659	540621.3	308.315	4C_009	9
P831	4814659	540621.7	308.293	4C_010	10
P977	4814625	540656	308.126	4C_011	11
P970	4814641	540631.3	307.833	4C_012	12
P917	4814651	540625.3	308.186	4C_013	13
P905	4814652	540621.8	308.21	4C_014	14
P810	4814660	540617.7	308.314	4C_015	15
P954	4814648	540627	308.13	4C_016	16
P901	4814653	540619.8	308.207	4C_017	17
P833	4814653	540627.1	308.422	4C_019	19
P953	4814647	540626.1	308.059	4C_020	20
P839	4814661	540623.9	308.305	4C_021	21
P805	4814663	540621	308.225	4C_022	22
P800	4814663	540625.8	308.445	4C_023	23
P829	4814658	540621.6	308.34	4C_024	24
P840	4814661	540624.4	308.338	4C_025	25
P849	4814659	540623	308.13	4C_026	26
P979	4814623	540656.6	308.04	4C_027	27
P978	4814625	540655.1	308.108	4C_028	28
P872	4814656	540623.1	308.205	4C_029	29
P915	4814651	540624.5	308.152	4C_030	30
P889	4814650	540629.3	308.456	4C_032	32
P873	4814656	540623.8	308.229	4C_033	33
P973	4814630	540639.8	307.46	4C_034	34
P981	4814618	540659.5	308.161	4C_035	35
P976	4814626	540653	307.99	4C_036	36
P853	4814650	540626.9	308.282	4C_038	38
P876	4814652	540626.8	308.388	4C_039	39

P834	4814655	540627.2	308.352	4C_041	41
P895	4814654	540624.3	308.184	4C_042	42
P857	4814657	540625.2	308.3	4C_043	43
P881	4814656	540621.9	308.278	4C_044	44
P916	4814650	540621.9	308.162	4C_045	45
P807	4814660	540617.5	308.28	4C_046	46
P969	4814642	540629.2	307.703	4C_047	47
P825	4814657	540619.4	308.305	4C_048	48
P820	4814657	540618	308.281	4C_049	49
P828	4814658	540620.8	308.337	4C_050	50
P870	4814658	540623	308.213	4C_051	51
P947	4814648	540623.2	308.111	4C_052	52
P826	4814657	540619.8	308.326	4C_053	53
P902	4814652	540620.1	308.208	4C_054	54
P842	4814660	540624.5	308.317	4C_055	55
P877	4814655	540621.8	308.265	4C_056	56
P963	4814644	540624.5	308.058	4C_058	58
P975	4814629	540646.6	307.752	4C_059	59
P869	4814658	540623.7	308.222	4C_060	60
P920	4814651	540623.9	308.142	4C_061	61
P931	4814649	540624.9	308.127	4C_063	63
P946	4814647	540623.5	308.101	4C_064	64
P816	4814660	540620.4	308.339	4C_065	65
P837	4814661	540622.7	308.218	4C_066	66
P964	4814644	540626.1	307.816	4C_067	67
P957	4814645	540625	307.889	4C_068	68
P804	4814664	540622.2	308.241	4C_069	69
	4814605	540685.6			70
P884	4814656	540622.1	308.279	4C_071	71
P818	4814662	540621.8	308.208	4C_072	72
P846	4814659	540624	308.224	4C_073	73
P845	4814659	540625.8	308.283	4C_075	75
P966	4814646	540627.9	308.076	4C_076	76
P943	4814647	540625.1	307.967	4C_077	77
P912	4814652	540624.9	308.189	4C_078	78
P798	4814664	540623.7	308.265	4C_079	79
P803	4814663	540623.3	308.27	4C_080	80
P933	4814649	540626	308.189	4C_082	82
P844	4814659	540626.4	308.297	4C_083	83

P892	4814648	540628.1	308.268	4C_084	84
P965	4814645	540626.6	307.881	4C_086	86
P874	4814656	540624.9	308.233	4C_087	87
P960	4814647	540627.4	308.105	4C_088	88
P859	4814657	540626.9	308.383	4C_089	89
P864	4814653	540628.4	308.275	4C_090	90
P890	4814650	540629.5	308.448	4C_092	92
P821	4814656	540618.3	308.312	4C_093	93
P896	4814655	540623.2	308.197	4C_094	94
P949	4814646	540623.1	308.132	4C_095	95
P904	4814651	540621.3	308.192	4C_096	96
P967	4814646	540628.6	308.109	4C_097	97
P811	4814660	540618	308.29	4C_098	98
P903	4814651	540620.4	308.232	4C_099	99
P812	4814659	540618.6	308.272	4C_100	100
P879	4814656	540622.6	308.253	4C_101	101
P875	4814655	540625.5	308.238	4C_102	102
P948	4814647	540623	308.167	4C_103	103
P961	4814646	540626.9	308.085	4C_104	104
P882	4814657	540621.7	308.292	4C_105	105
P930	4814648	540623.7	308.057	4C_106	106
P951	4814646	540623.9	308.047	4C_107	107
P885	4814655	540621.1	308.299	4C_108	108
P922	4814650	540622.7	308.15	4C_109	109
P955	4814646	540625.5	307.869	4C_0110	110
P868	4814656	540625.8	308.462	4C_111	111
P848	4814660	540622.8	308.195	4C_112	112
P832	4814660	540622	308.219	4C_113	113
P838	4814661	540623.1	308.237	4C_114	114
P841	4814660	540623.6	308.292	4C_115	115
P914	4814652	540624.2	308.152	4C_116	116
P854	4814651	540626.7	308.296	4C_117	117
P974	4814630	540643.4	307.53	4C_118	118
P852	4814657	540626	308.344	4C_119	119
P888	4814650	540628.2	308.333	4C_120	120
P878	4814656	540622.5	308.258	4C_122	122
P801	4814662	540626	308.385	4C_123	123
P935	4814649	540626.2	308.13	4C_124	124
P862	4814654	540628.5	308.323	4C_125	125
P913	4814652	540624.2	308.217	4C_126	126

P972	4814631	540638.8	307.413	4C_127	127
P860	4814656	540627.2	308.201	4C_128	128
P893	4814648	540628.4	308.301	4C_129	129
P939	4814647	540627.3	308.069	4C_130	130
P835	4814661	540625.4	308.357	4C_131	131
P940	4814649	540626.7	308.137	4C_132	132
P906	4814652	540622.1	308.226	4C_133	133
P945	4814648	540623.8	308.013	4C_134	134
P900	4814654	540620.3	308.289	4C_135	135
P823	4814655	540618.9	308.274	4C_137	137
P944	4814647	540624.3	307.964	4C_138	138
P962	4814645	540625.6	307.824	4C_139	139
P928	4814649	540623.1	308.118	4C_140	140
P924	4814648	540622.2	308.154	4C_141	141
P858	4814657	540625.5	308.387	4C_142	142
P923	4814649	540621.9	308.213	4C_143	143
P806	4814662	540620.6	308.259	4C_144	144
P942	4814648	540625.5	308.077	4C_145	145
P883	4814656	540621.5	308.302	4C_146	146
P850	4814659	540623.8	308.24	4C_147	147
P909	4814653	540624.8	308.179	4C_148	148
P936	4814649	540626.6	308.214	4C_149	149
P855	4814655	540625.1	308.195	4C_151	151
P827	4814658	540620.4	308.318	4C_152	152
P934	4814650	540625.5	308.143	4C_153	153
P836	4814662	540623.9	308.343	4C_154	154
P856	4814658	540623.4	308.177	4C_155	155
P891	4814649	540629.4	308.329	4C_156	156
P843	4814660	540625.8	308.29	4C_157	157
P919	4814650	540621.3	308.195	4C_158	158
P861	4814655	540627.5	308.386	4C_159	159
P887	4814651	540627.5	308.344	4C_160	160
P925	4814648	540622.5	308.159	4C_161	161
P929	4814648	540623.8	308.09	4C_162	162
P932	4814649	540624.8	308.154	4C_163	163
P817	4814661	540619.3	308.329	4C_164	164
P959	4814645	540624.2	308.015	4C_165	165
P958	4814645	540624.7	307.961	4C_166	166
P897	4814654	540622.5	308.235	4C_167	167
P918	4814650	540620.9	308.211	4C_168	168
P899	4814654	540619.1	308.281	4C_169	169

P866	4814654	540626.2	308.454	4C_170	170
P911	4814652	540625.1	308.201	4C_171	171
P802	4814661	540625.6	308.375	4C_172	172
P941	4814648	540625.8	308.134	4C_173	173
P865	4814652	540628.7	308.344	4C_175	175
P908	4814652	540623.6	308.16	4C_176	176
P956	4814645	540625.4	307.853	4C_177	177
P937	4814649	540626.6	308.135	4C_178	178
P867	4814653	540626.4	308.438	4C_179	179
P851	4814658	540625.1	308.299	4C_180	180
P910	4814653	540625.7	308.203	4C_181	181
P808	4814661	540618.2	308.307	4C_182	182
P950	4814646	540623.1	308.087	4C_183	183
P813	4814659	540617.5	308.331	4C_184	184
P968	4814642	540628.4	307.724	4C_185	185
P907	4814653	540623.2	308.174	4C_187	187
P952	4814646	540624.8	307.913	4C_188	188
P815	4814660	540619.7	308.338	4C_189	189
P927	4814650	540623.1	308.131	4C_190	190
P938	4814648	540627.5	308.137	4C_191	191
P894	4814647	540628.2	308.223	4C_192	192
P886	4814651	540628	308.377	4C_194	194
P898	4814655	540619.9	308.285	4C_195	195
P863	4814653	540628	308.266	4C_196	196
P871	4814658	540622.8	308.229	4C_197	197
P799	4814663	540625	308.345	4C_198	198
P819	4814662	540622.3	308.238	4C_199	199
P847	4814659	540623.3	308.234	4C_200	200

APPENDIX B – TRACER MAPS

This appendix contains tracer maps.

Site 1: Seeding

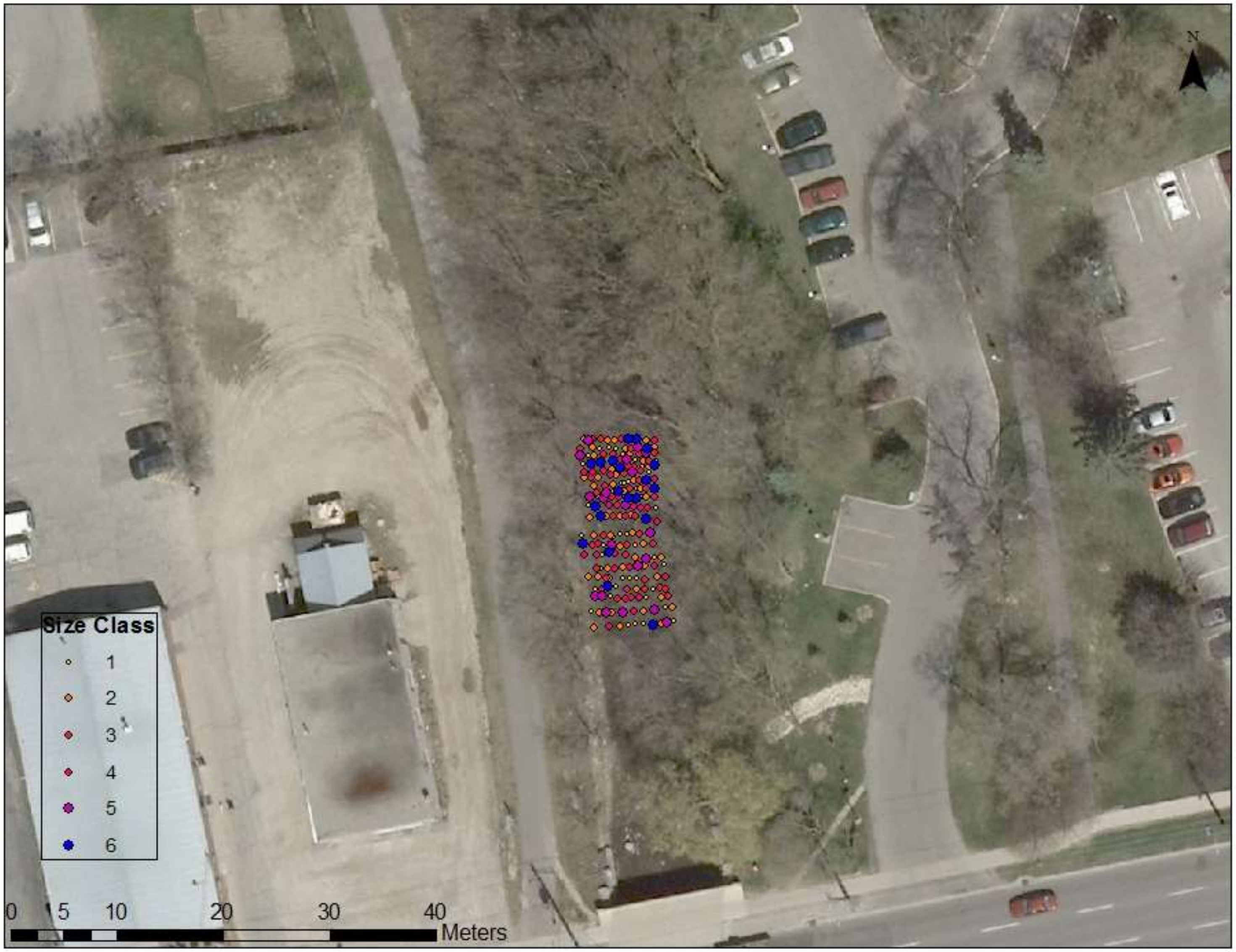

Site 1: Tracking Round 1

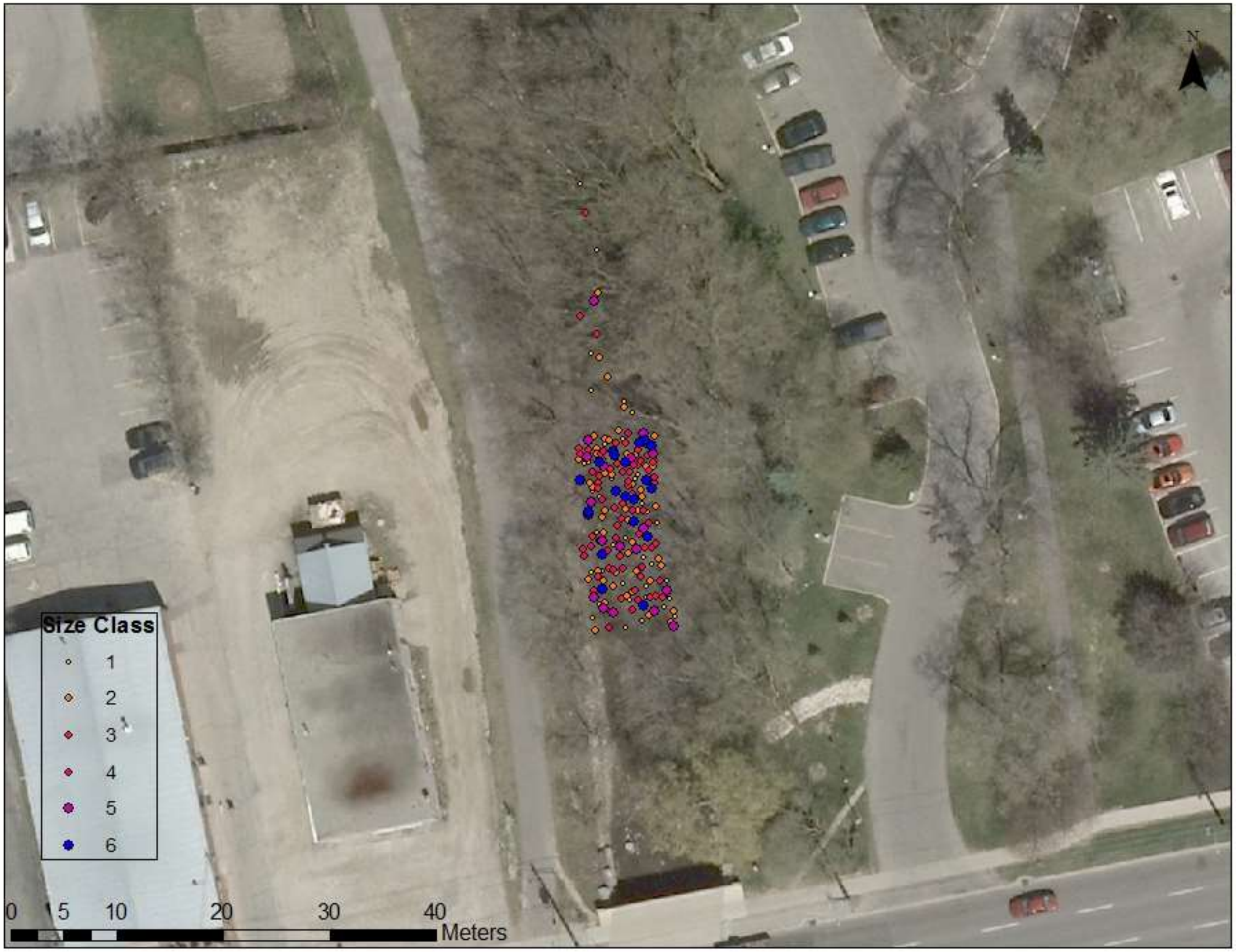

Site 1: Tracking Round 2

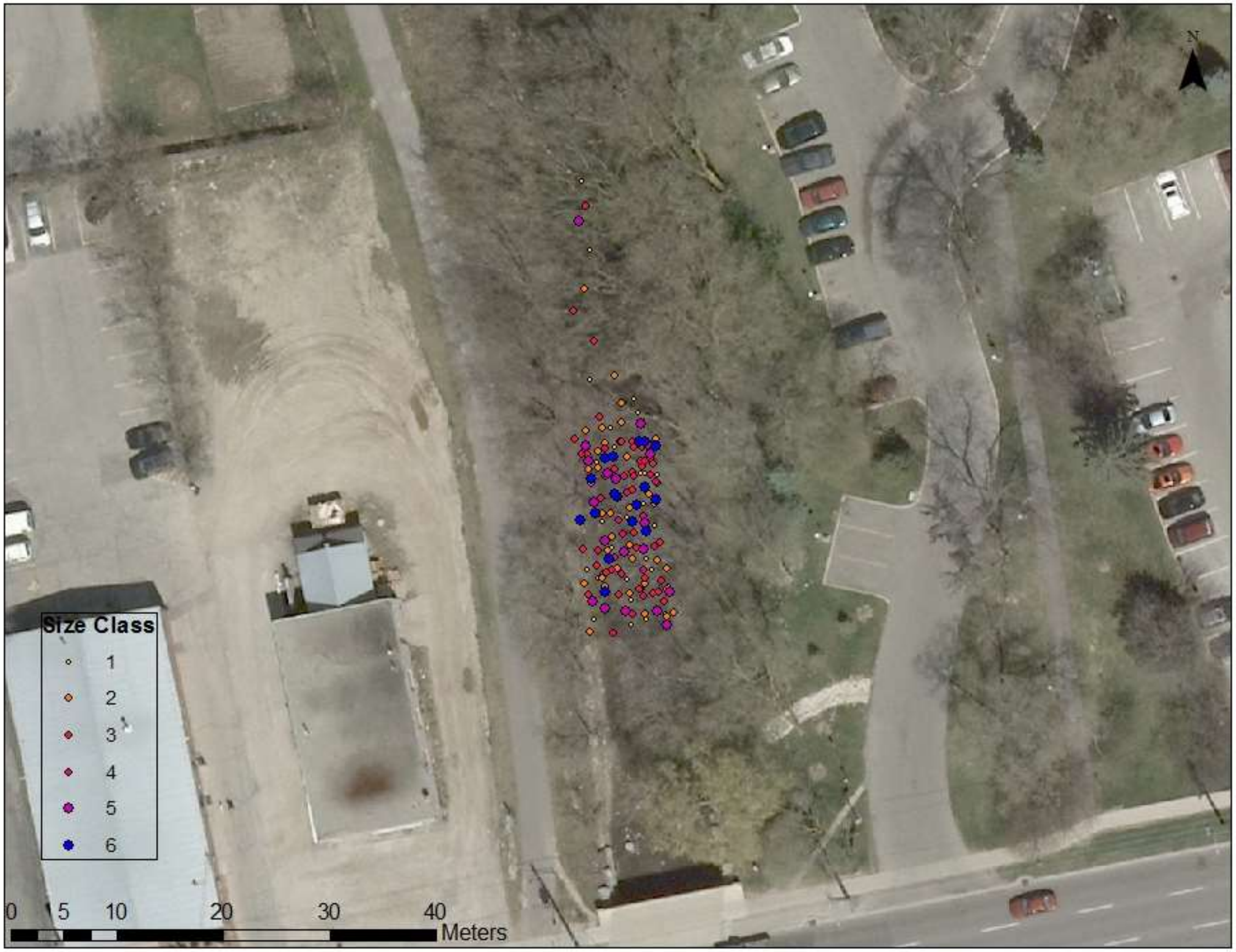

Site 1: Tracking Round 3

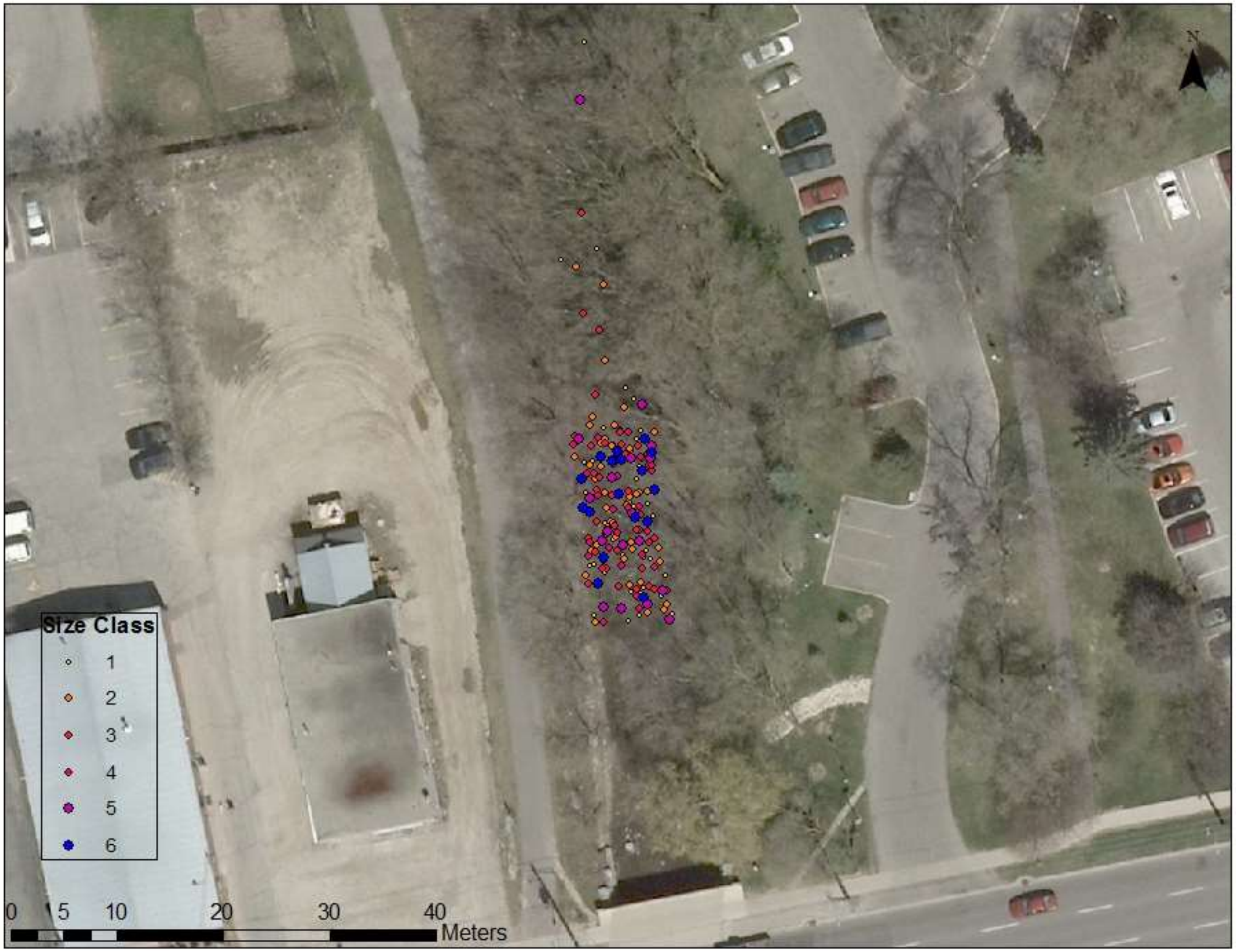

Site 2: Seeding

Site 2: Tracking Round 1

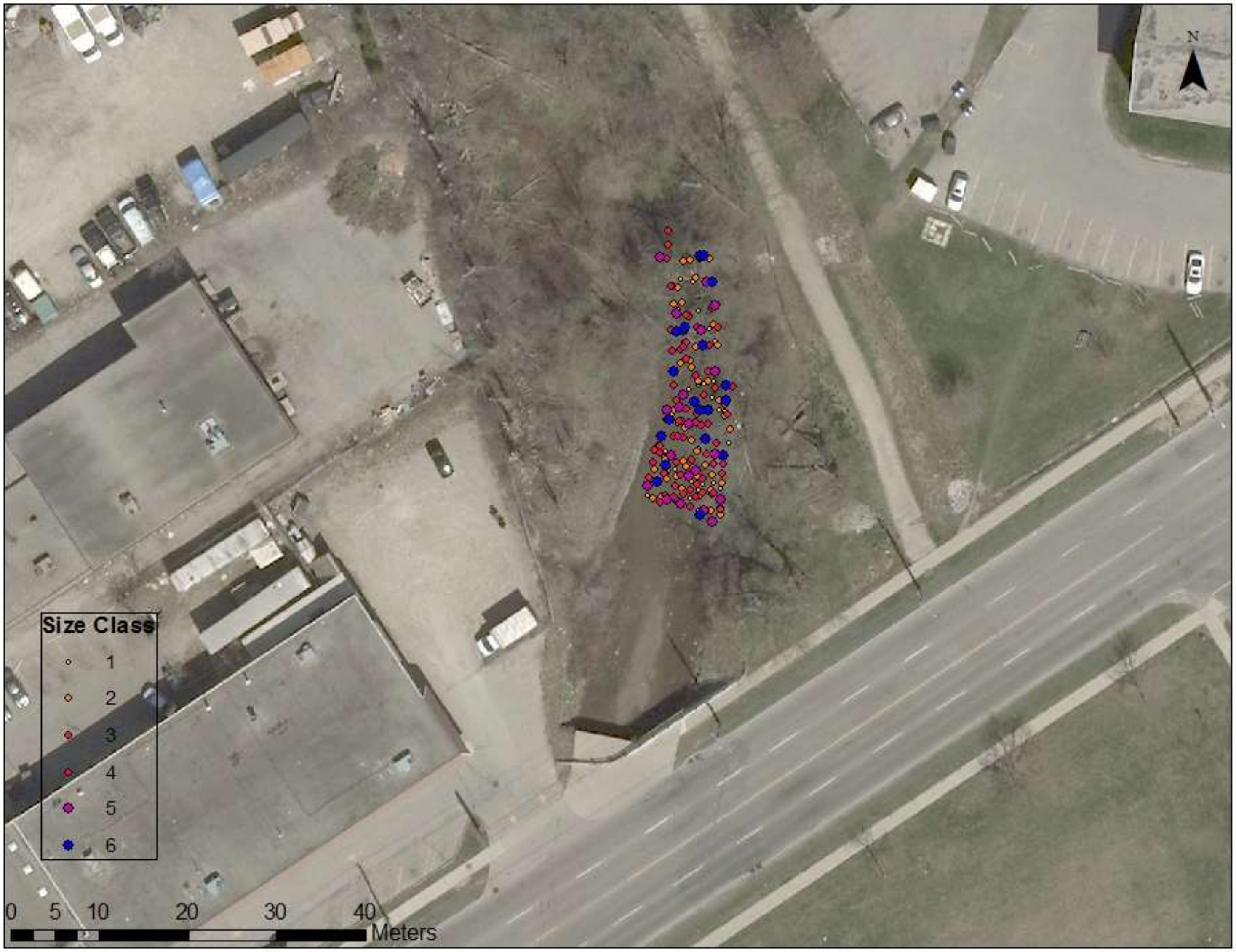

Site 3: Seeding

Site 3: Tracking Round 1

Site 4: Seeding

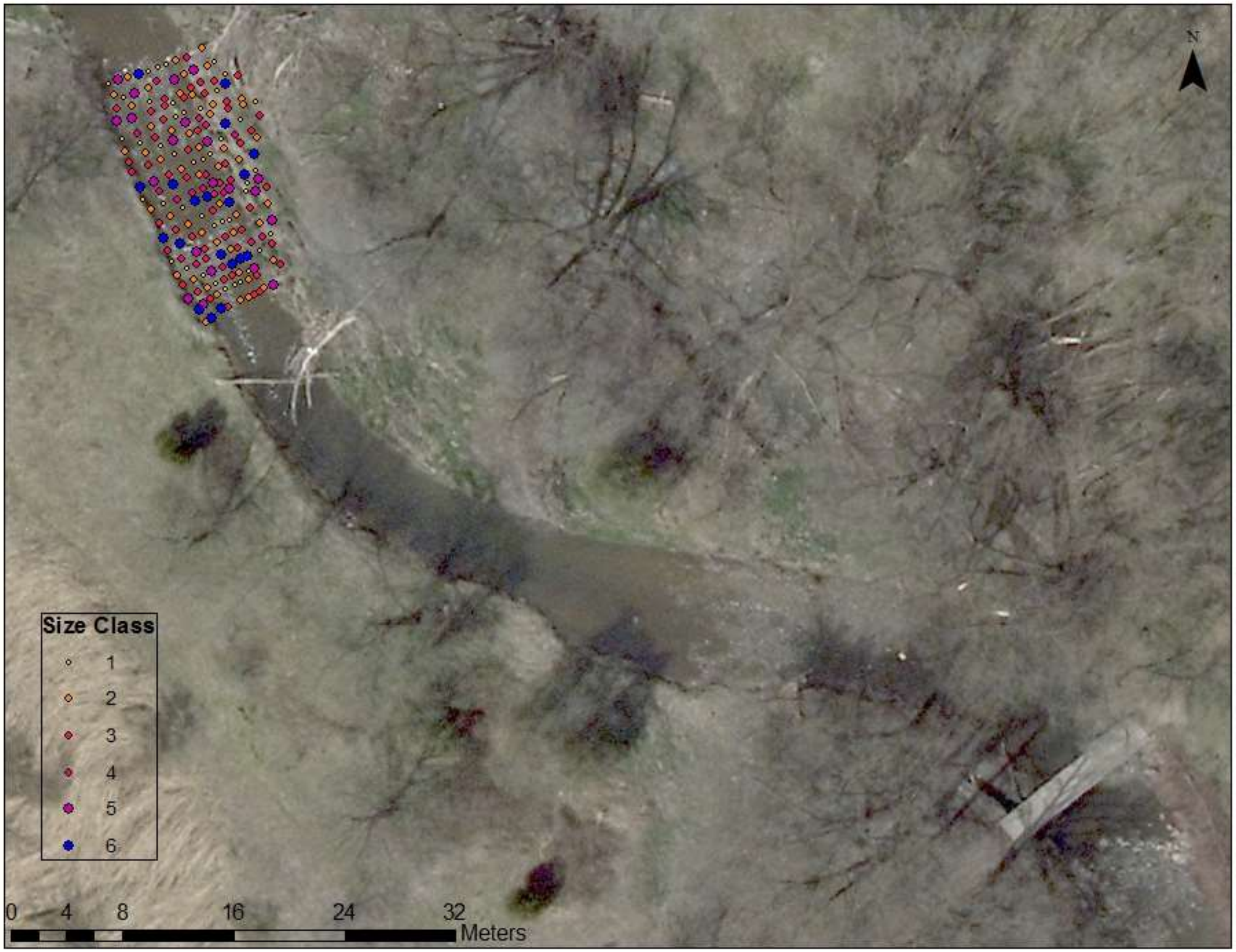

Site 4: Tracking Round 1

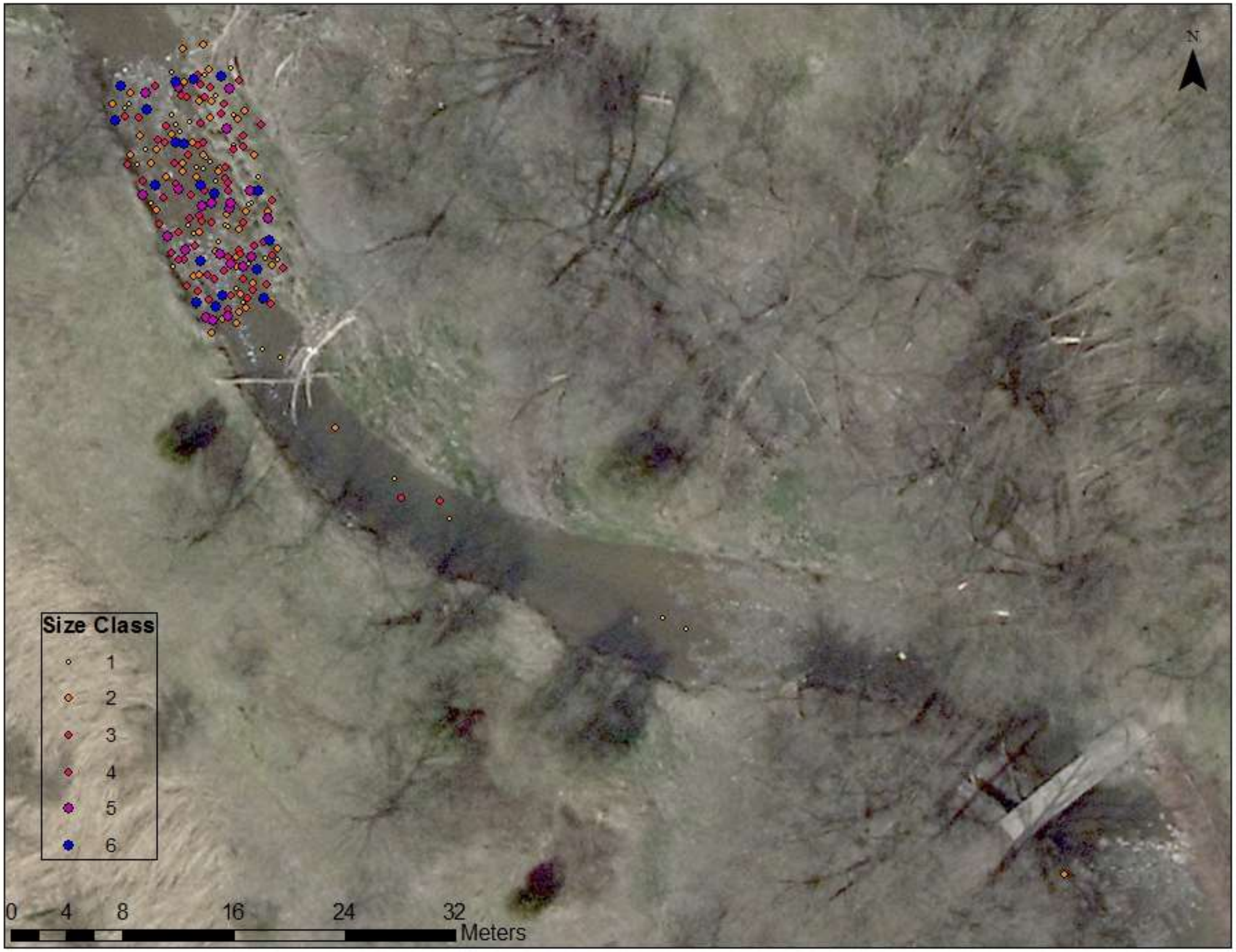

Site 4: Tracking Round 2

Site 4: Tracking Round 3

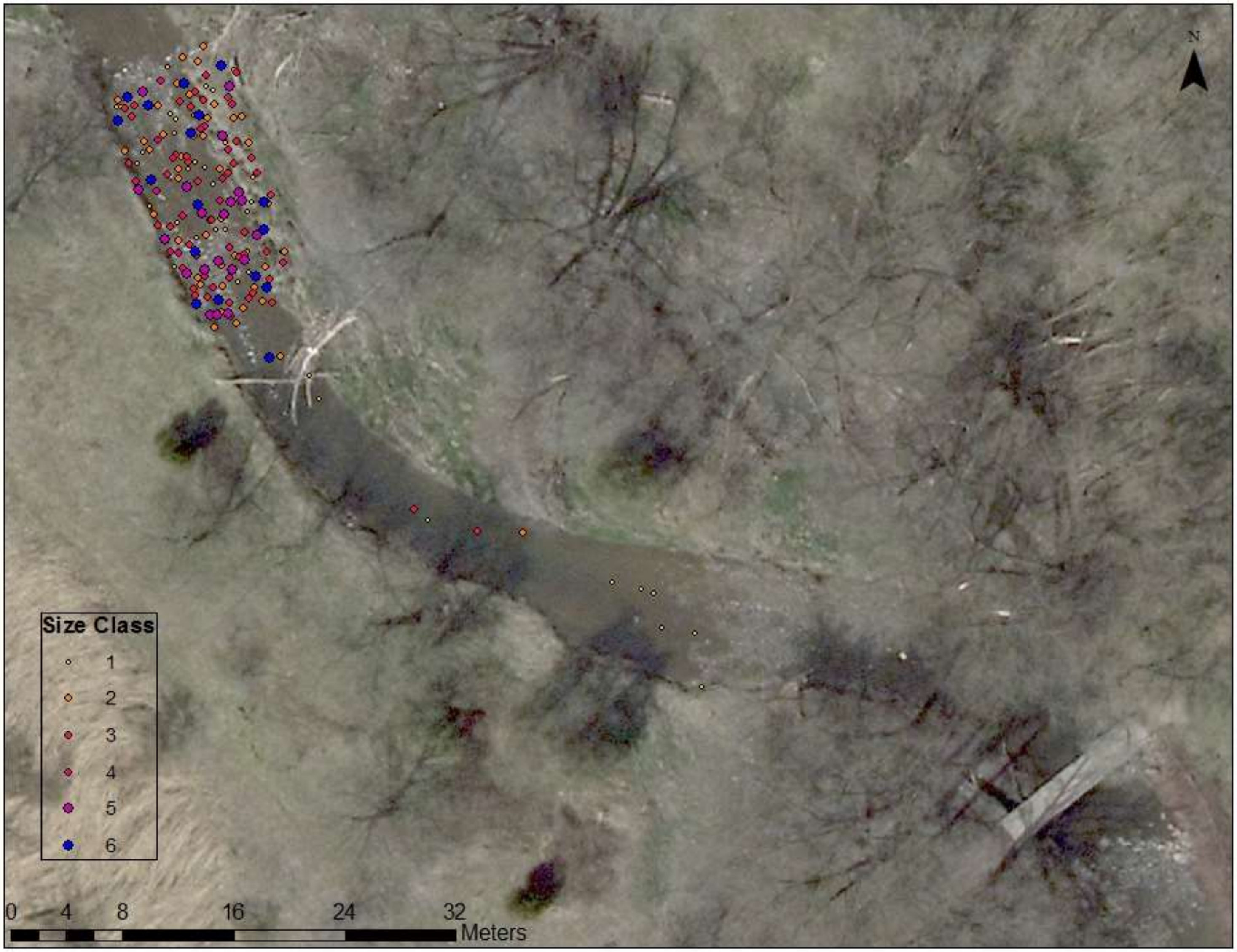

APPENDIX C – LAB DATA

Table C1 23 mm Tag Orientation Tests

Tag#	H0-N	H0-S	H0a-N	H0a-S	V0-N	V0-S	V0a-N	V0a-S
800001	28	30	39.5	41	46	49	68	75
800002	28	30.5	36	39	45	48	69	68
800003	27	29	40	44	44	51.5	68	75
800004	21	35.5	26	45	43	51	71	74
800005	26	31	41	43	44	48	69	3.5
800006	31	36	30	44	45	48	68.5	71
800007	24	30	37	42	44	49	66.5	74
800008	25	32	36.5	43	45	48	68	75
800009	21.5	30	35	44	43.5	50	65	75
800010	28	33	42	41	45	52	67	73.5
800011	27.5	30.5	37	44.5	44	49.5	66.5	72
800012	25.5	31	40.5	45	46	49	67	73
800013	31	29	38	41	45	50	69	71.5
800014	23	29	45	44	44	51	70	72.5
800015	27	30	45.5	35	45	51	67.5	75
800016	25	24	45	43	44.5	51	65.5	73.5
800017	25	28	38	47	44	50	64.5	73
800018	23	29	39.5	47	46	50	69	73
800019	22	28	39.5	44.5	44	48.5	66.5	74.5
800020	23	30	39	48	42	48	67	72
800021	25	27.5	39.5	46	44	49	68	74
800022	22.5	28	41.5	45	45	48	68	73
800023	23	28	38	46	44	49	67	72.5
800024	24	28.5	38.5	46	43	47	66	71
800025	22	28	40	48	44	47	66	70

Table C2 32 mm Tag Orientation Tests

Tag#	H0-N	H0-S	H0a-N	H0a-S	V0-N	V0-S	V0a-N	V0a-S
900001	34	35	51	54	55	55	77	78
900002	33.5	37	52	55	55	58	76	79
900003	28	36.5	44.5	55	55	58	78	78
900004	34	37	50	53.5	53	58	75.5	78
900005	32	35	47	53	55	58.5	75.5	79
900006	30	38	46.5	53.5	54.5	59	77	78
900007	28	37	47	51.5	55	58	76	78
900008	35	35.5	50.5	55	54	59	77	79
900009	32.5	37.5	45.5	54.5	55	58	76	78
900010	30.5	40	47.5	53	55	59	76.5	79
900011	32	38	45.5	50.5	55	59.5	76	78
900012	31	36	44	50	55	58	77	79
900013	33.5	39	45.5	49	55	59.5	76.5	79
900014	35	39	42	51.5	56	60	77	79
900015	34.5	34	45.5	51	54.5	58	75.5	78.5
900016	27	38	46	51.5	54	59	75.5	79
900017	32	32	45	51	53	59	75	79.5
900018	33	37.5	44.5	52	55	60	77.5	79
900019	31	36	43.5	47.5	54	58	76.5	80
900020	33	39	43	49	55	58	77	78
900021	31	37	46	48	54	60	76	81
900022	29	37.5	43.5	49.5	54.5	58	74.5	78
900023	31	34	42	41	53	59	75	80
900024	33	38	49	49.5	56	59.5	76	79
900025	32	35.5	42.5	53.5	53	59.5	76	80

Table C3 Characteristics of Tagged rocks

Rock #		Rock Size (cm)			Tag Size	
Decimal	Hexadecimal	a-axis	b - axis	c-axis		
100001	186A1	4.2	3.1	1.9	SMALL	23 mm
100002	186A2	4.3	3.1	2.4		
100003	186A3	5.2	3.1	2.2		
100004	186A4	3.8	2.8	2		
100005	186A5	3.7	2.5	2		
100006	186A6	3.7	3.1	2.7		
200001	30D41	6	4.3	3.3		
200002	30D42	6	4.5	2.7		
200003	30D43	6.5	3.7	2.6		
200004	30D44	4.6	4.1	3.4		
200005	30D45	4.5	3.6	3.2		
200006	30D46	5.1	4.2	3.1		
300001	493E1	8.3	5.8	4.4	LARGE	32 mm
300002	493E2	7.1	5.3	3.3		
300003	493E3	7	6	3.7		
300004	493E4	6.7	5.7	4.8		
300005	493E5	6.1	5.6	2.6		
300006	493E6	6.1	5.7	4.1		
400001	61A81	10.9	7.8	6.3		
400002	61A82	9.2	6.6	6		
400003	61A83	8.4	6.4	3.9		
400004	61A84	8.4	6.8	4.4		
400005	61A85	7.3	6.9	5.4		
400006	61A86	7.3	7.2	6		
500001	7A121	14.1	10.6	7.6		
500002	7A122	11.1	9.3	5.7		
500003	7A123	11.2	9.5	6.8		
500004	7A124	11.5	10.9	8.4		
500005	7A125	12.8	9.5	8.3		
500006	7A126	11.7	9.1	4.8		
600001	927C1	16.9	13	9.5		
600002	927C2	16.1	14.2	8.5		
600003	927C3	17.6	14.3	10.3		
600004	927C4	18.4	14.3	9		
600005	927C5	16.6	13	7.3		
600006	927C6	20.7	15.5	2.4		

Table C4 Horizontal Tests for 4 sizes classes of rocks (Surface Tests)
Bins 3 and 4 contain tracers with 23 mm tags; Bins 5 and 6 contain tracers with 32 mm tags

Horizontal Tests		H-0	H-45	H-90	H-0b	H-45b	H-90b	H-0c	H-45c	H-90c	H-0a	H-45a	H-90a
Bin 3	Rock 1	25.0	6.5	25.5	24.0	7.5	25.0	76.0	32.5	60.0	27.7	26.8	18.4
	Rock 2	33.0	33.5	12.0	30.5	30.0	6.0	79.0	71.0	10.0	23.8	32.1	28.6
	Rock 3	40.5	31.5	9.0	37.0	32.0	13.0	76.0	37.0	62.0	36.6	36.6	30.4
	Rock 4	41.0	39.5	30.5	41.5	38.0	29.0	74.0	68.0	30.5	37.6	38.5	35.7
	Rock 5	40.0	38.0	26.5	40.0	33.0	22.0	75.0	62.0	29.0	35.3	33.9	34.8
	Rock 6	20.0	24.5	10.5	21.5	22.5	11.0	76.0	81.0	55.0	15.6	26.8	26.0
Bin 4	Rock 1	36.0	34.0	13.0	34.0	30.0	12.5	63.0	42.0	30.0	34.8	38.0	28.6
	Rock 2	37.0	34.5	4.0	37.0	30.5	12.0	74.0	34.5	17.5	33.9	34.8	29.5
	Rock 3	23.0	17.0	20.0	21.0	18.0	27.5	77.0	62.0	23.0	23.4	23.4	16.0
	Rock 4	37.5	38.0	27.0	39.5	34.0	22.0	62.0	56.0	10.0	37.6	34.8	27.7
	Rock 5	35.0	29.0	11.0	33.0	29.5	12.0	77.0	52.0	8.0	33.0	30.4	21.7
	Rock 6	35.5	35.5	14.0	35.0	36.0	23.0	75.0	63.5	10.5	28.6	34.8	29.5
Bin 5	Rock 1	23.0	21.0	28.0	29.0	18.0	31.5	80.0	75.0	23.5	18.8	23.4	16.8
	Rock 2	35.5	29.0	2.5	35.0	27.0	7.5	64.0	10.0	15.0	37.6	26.8	26.0
	Rock 3	29.0	26.5	12.0	28.0	22.0	10.0	67.0	41.0	25.0	33.5	23.8	22.5
	Rock 4	38.0	30.5	7.5	34.5	29.0	8.5	69.0	10.0	6.0	34.8	31.2	27.7
	Rock 5	30.5	25.0	3.5	30.0	27.0	4.0	75.0	43.0	17.0	31.2	29.9	22.5
	Rock 6	34.0	25.0	10.0	32.0	20.5	12.5	53.0	46.0	5.0	32.1	28.6	19.2
Bin 6	Rock 1	38.0	29.0	5.0	38.5	26.5	2.0	70.0	45.0	22.0	37.6	35.7	30.4
	Rock 2	38.0	34.0	21.0	40.0	36.0	19.0	76.0	60.5	12.0	29.0	33.0	31.2
	Rock 3	17.0	14.0	19.0	26.0	22.0	26.0	81.0	73.0	48.0	19.2	21.7	15.2
	Rock 4	35.0	35.0	20.5	33.0	32.0	20.5	74.0	73.5	30.0	22.5	29.5	25.1
	Rock 5	28.0	20.0	23.0	32.0	31.0	20.0	85.0	78.0	4.0	29.0	23.0	18.4
	Rock 6	29.0	24.0	24.0	34.0	22.0	21.5	84.0	66.0	14.0	25.5	26.8	20.0

Table C5 Vertical Tests for 4 sizes classes of rocks (Surface Tests)
Bins 3 and 4 contain tracers with 23 mm tags; Bins 5 and 6 contain tracers with 32 mm tags

Vertical Tests		V-0	V-45	V-90	V-0b	V-45b	V-90b	V-0c	V-45c	V-90c	V-0a	V-45a	V-90a
Bin 3	Rock 1	53.5	47.0	44.0	53.0	48.0	44.5	54.0	67.0	70.0	53.9	50.6	49.6
	Rock 2	55.0	55.0	59.0	56.0	54.0	57.0	67.0	64.0	59.5	52.4	53.4	60.0
	Rock 3	53.5	56.5	53.0	50.0	51.5	52.5	64.0	69.5	64.0	53.4	53.9	49.1
	Rock 4	55.0	55.0	54.0	51.0	54.0	55.0	63.0	66.0	60.5	54.8	54.3	54.8
	Rock 5	56.5	56.0	57.0	53.0	55.0	56.0	61.0	63.0	61.5	57.2	54.8	51.5
	Rock 6	59.5	60.0	56.0	59.0	58.0	58.5	58.0	59.0	61.0	58.1	61.0	61.9
Bin 4	Rock 1	59.0	58.0	56.0	58.5	56.5	52.0	62.5	66.0	63.0	56.2	58.1	54.3
	Rock 2	56.0	54.5	54.0	56.0	56.0	54.0	66.0	72.0	64.0	53.9	53.4	52.4
	Rock 3	57.5	53.0	54.0	55.0	53.0	59.0	67.0	70.0	65.0	53.4	50.6	53.4
	Rock 4	57.5	59.0	61.5	58.0	60.0	61.0	60.0	55.0	55.0	53.4	56.2	56.7
	Rock 5	54.0	55.5	54.0	57.0	53.0	55.0	67.0	70.0	61.0	53.4	55.3	54.3
	Rock 6	55.5	57.0	56.0	57.0	59.0	57.0	69.0	65.5	57.0	49.6	54.8	56.2
Bin 5	Rock 1	57.0	60.0	54.0	57.0	59.0	52.0	66.5	69.0	59.0	56.2	58.1	56.7
	Rock 2	54.0	56.5	56.0	56.0	56.0	58.0	64.0	67.0	62.0	49.6	53.4	56.2
	Rock 3	56.0	59.0	56.5	59.0	58.5	59.0	63.0	62.0	55.0	49.6	54.3	56.2
	Rock 4	55.0	55.0	58.0	58.5	58.0	57.0	65.0	71.0	65.0	57.2	56.2	56.2
	Rock 5	59.5	57.0	57.0	58.5	57.5	59.0	52.0	51.0	58.0	57.2	57.6	54.8
	Rock 6	56.0	56.5	57.5	57.0	57.0	59.0	66.0	65.0	60.0	53.4	53.4	55.3
Bin 6	Rock 1	59.0	55.5	59.0	59.0	56.0	59.0	73.0	62.0	57.0	56.2	57.6	57.6
	Rock 2	62.5	64.5	61.5	63.5	61.5	61.0	67.5	65.0	58.5	57.6	60.0	60.0
	Rock 3	59.0	59.5	54.0	62.0	56.5	56.0	49.0	54.0	59.0	58.1	59.1	56.2
	Rock 4	59.5	63.5	63.5	61.0	64.5	65.0	73.0	68.5	56.0	52.9	61.0	62.9
	Rock 5	57.0	58.0	57.0	56.0	60.0	58.5	68.0	71.5	62.0	53.9	56.2	55.3
	Rock 6	59.0	62.0	60.5	60.0	64.5	61.0	57.0	61.0	63.5	56.2	58.6	61.0

Table C6 Horizontal and Vertical Tests not parallel to the axis (Surface Tests)

Experiment Names		H-z	H-xyz	H-yz	H-xz	V-z	V-xyz	V-yz
Bin 3	Rock 1	46.5	25	58	54.5	74	29	39
	Rock 2	50.5	59	63.5	29	74	30	31
	Rock 3	43	45	64	44	76	26	23
	Rock 4	42	60	65	15	76.5	30	22.5
	Rock 5	45	50.5	63	11	71.5	28	38
	Rock 6	64	52.5	59.5	28	73	33	37
Bin 4	Rock 1	41	46.5	59	28.5	77.5	24	31.5
	Rock 2	39.5	50.5	62	18	76	18	24
	Rock 3	61.5	44.5	50.5	34	76	15	23
	Rock 4	50.5	54.5	59.5	26.5	63	43	38
	Rock 5	49.5	45.5	59	28	72	20	24
	Rock 6	54.5	53	62	20	73	31	28
Bin 5	Rock 1	59	47	62	31.5	75	34	24
	Rock 2	38	45	57	24.5	78	21	21.5
	Rock 3	53	46.5	57.5	8	72	43	36
	Rock 4	48	46.5	57	9	81	19	30
	Rock 5	56	50	55	9	74	51	47.5
	Rock 6	55	40.5	54	31.5	78	34	29
Bin 6	Rock 1	58	45	63	0.5	74	40	34
	Rock 2	46.5	49.5	58	7	76.5	48	43
	Rock 3	63	51	48	10	69	48	55
	Rock 4	53	53	55	27.5	77	39.5	33
	Rock 5	58	55	58	14	71.5	30	34
	Rock 6	58.5	50.5	56	31.5	79.5	47	50.5

Note: Bins 3 and 4 contain tracers with 23 mm tags; Bins 5 and 6 contain tracers with 32 mm tags

Table C7	Cluster Experiment Results for Dry Lateral Detection with Tracers at 0° axis																
		HH-0°	HH-45°	HH-90°	HH-xyz	HV-0°	HV-45°	HV-90°	HV-xyz	VH-0°	VH-45°	VH-90°	VH-xyz	VV-0°	VV-45°	VV-90°	VV-xyz
Position 1	0 cm	16.0	18.0	2.0	2.0	0.5	0.5	0.5	n/a ***	37.0	38.0	40.0	11.0	0.5	43.0	35.0	n/a ††
	Switch	n	n	n	y	y	y	y	n/a	n	n	n	y	y	n **	n **	n/a
Position 2	5 cm	-0.5	-3.5	-4.5	0.0	4.5	2.0	-2.5	2.0	40.0	40.0	39.0	n/a	3.0	2.0	0.5	0.0
	Switch	y	y	y	y *	y	y	y	y	n	n	n	n ***	y	y	y	y *
Position 3	10 cm	2.0	3.0	6.0	3.0	-54.5	6.0	-2.0	49.0	3.0	39.0	39.0	0.0	-55.5	4.0	-6.0	5.0
	Switch	y	y	n	y	y	y	y	n	y	n	n	y	y	y	y	y
Position 4	15 cm	5.0	4.0	9.0	4.0	14.5	7.5	-4.0	47.0	5.0	4.0	43.0	7.0	-37.0	12.0	2.0	6.0
	Switch	y	y	n	y	y	y	y	n	y	y	n	y	y	y	n	y
Position 5	20 cm	9.0	5.0	0.5	0.0	-62.0	-45.5	n/a	46.5	10.0	7.0	37.0	8.0	-32.0	4.0	9.0	10.0
	Switch	y	y	n	y *	y	y	n ***	n	y	y	n	y	y	y	n	y
Position 6	25 cm	4.0	2.5	-6.0	6.0	-26.0	-18.0	-1.0	-1.0	6.5	42.0	36.0	26.0	-27.0	12.0	3.0	n/a
	Switch	y	y	y	y	y	y	y	y	y	n	n	n	y	y †	n	n/a ***
Position 7	30 cm	14.0	10.0	0.5	17.0	-39.0	-40.0	-49.0	46.0	17.0	11.0	38.0	14.0	-22.0	4.0	23.0	n/a
	Switch	y	y	n	y	y	y	y	n	y	y	n	y	y	y	n	n ***
Position 8	35 cm	20.0	19.5	6.0	46.0	-18.0	9.5	-46.5	45.0	22.0	17.0	40.0	29.0	-17.0	-3.0	17.0	0.5
	Switch	y	y	n	n	y	y	y	n	y	y	n	y	y	y	n	y
Position 9	40 cm	3.0	19.5	7.0	47.0	-11.0	-33.5	3.5	47.0	26.0	24.0	40.0	9.0	-11.0	-14.0	18.0	5.0
	Switch	y	y	n	n	y	y	y	n	y	y	n	y	y	y	n	y
Position 10	45 cm	-14.0	22.0	6.0	44.0	-6.0	2.0	6.0	44.0	-11.0	40.0	37.0	12.0	-7.0	-9.0	22.0	6.0
	Switch	y	y	n	n	y	y	y	n	y	n	n	y	y	y	n	y
Position 11	50 cm	-10.0	-4.0	10.0	44.0	0.5	2.0	3.0	41.0	28.0	43.0	40.0	28.0	0.5	0.5	40.0	12.0
	Switch	y	y	n	y	y	y	y	n	y	n	n	n	y	y	n	y
Position 12	55 cm	1.0	18.0	11.5	43.0	2.0	8.0	10.0	46.0	-2.0	47.0	41.0	21.0	-5.0	7.0	32.0	9.0
	Switch	y	n	n	n	y	y	y	n	y	n	n	y	y	y	n	y
Position 13	60 cm	3.0	18.0	3.0	44.5	8.0	10.0	12.0	48.5	-1.5	34.0	32.0	23.0	6.0	11.0	37.0	14.0
	Switch	y	n	n	n	y	y	y	n	y	n	n	y	y	y	n	y
Position 14	65 cm	6.0	23.0	2.5	24.0	12.0	11.0	12.0	47.0	-1.0	36.0	34.0	25.0	-4.0	11.0	34.0	15.0
	Switch	y	n	n	n	y	y	n	n	y	n	n	y	y	y	n	y
Position 15	70 cm	8.0	23.0	0.5	27.0	6.0	12.0	1.0	46.0	8.0	46.0	43.0	21.0	5.0	18.0	39.0	14.0
	Switch	y	n	n	n	y	y	n	n	y	n	n	y	y	y	n	y
Position 16	75 cm	9.0	18.0	10.5	29.0	7.0	12.0	7.0	46.0	11.0	44.0	43.5	29.5	5.0	16.5	27.0	13.0
	Switch	y	y †††	n	n	y	y	n	n	y	n	n	n	y	y	n	y
Position 17	80 cm	15.0	25.0	7.0	35.5	11.0	13.0	9.5	44.0	14.0	36.0	35.0	24.0	25.0	22.0	38.0	15.0
	Switch	y	n	n	n	y	y	n	n	y	n	n	y	y	y	n	y
Position 18	85 cm	17.0	25.0	9.5	44.0	12.0	18.0	8.0	43.0	18.0	35.0	35.0	25.0	14.0	25.0	39.0	22.0
	Switch	y	n	n	n	y	y	n	n	y	n	n	n	y	y	n	y
Position 19	90 cm	15.5	25.0	8.0	43.0	14.0	22.0	10.0	41.0	20.0	37.0	35.0	28.0	13.0	24.0	32.0	24.0
	Switch	y	n	n	n	y	y	n	n	y	n	n	n	y	y	n	y
Position 20	95 cm	18.0	23.0	5.0	46.0	15.0	20.0	0.5	44.0	23.0	41.0	40.0	24.0	15.0	23.0	30.0	23.0
	Switch	y	n	n	n	y	y	n	n	y	n	n	n	y	y	n	n
Position 21	100 cm	24.0	20.0	9.0	44.0	12.0	17.0	8.0	41.0	25.0	44.0	44.0	30.0	16.5	26.0	27.0	28.0
	Switch	y	n	n	n	y	y	n	n	y	n	n	n	y	y	n	n
Position 22	At ∞	22.0	21.0	7.5	45.0	22.0	21.0	7.5	45.0	45.0	44.0	42.0	31.0	45.0	44.0	42.0	31.0

Notes: Rocks used: Rock#2 Bin#2 - stationary rock; Rock#4 Bin#2 movable rock
Tag was always facing north (0˚)
All distances are in cm.
Switch values:

- y = Signal switched from movable rock to stationary rock
- n = Signal did not switch from movable rock to stationary rock
- * = Stationary rock identified exactly on top of rock
- ** = Very tight range for stationary rock; no signal for a movable rock
- *** = No signal for stationary rock; consistent signal for movable rock
- † = Very tight range for stationary rock; dominant signal is for the movable rock
- †† = No reading at all!!
- ††† = Signal switches - with gaps (of no signal at all)

Table C8 Cluster Experiment Results for Dry Lateral Detection with Tracers at 45° axis

		HH-0°	HH-45°	HH-90°	HH-xyz	HV-0°	HV-45°	HV-90°	HV-xyz	VH-0°	VH-45°	VH-90°	VH-xyz	VV-0°	VV-45°	VV-90°	VV-xyz
Position 1	0 cm	16.0	18.0	2.0	2.0	0.5	0.5	0.5	n/a ***	37.0	38.0	40.0	11.0	0.5	43.0	35.0	n/a ††
	Switch	n	n	n	y	y	y	y	n	n	n	n	y	y	n **	n **	n/a
Position 2	5 cm	0.0	1.0	0.5	0.5	3.0	5.0	3.0	46.0	42.0	44.0	42.0	0.0	4.0	5.0	1.0	1.0
	Switch	y	y	y	y	y	y	y †††	n	n	n	n	y	y	y	y	y
Position 3	10 cm	3.0	4.0	2.0	4.0	7.5	11.0	8.0	n/a	45.0	41.0	44.0	3.0	8.0	10.0	2.0	0.0
	Switch	y	y	y	y	y	y	y	n/a ***	n	n	n	y	y	y	y	y
Position 4	15 cm	2.0	7.0	-45.0	8.0	11.0	-46.0	n/a	n/a	0.0	6.0	5.0	6.0	8.0	13.0	-42.5	1.0
	Switch	y	y	y	y	y	y	n/a ***	n/a ***	y	y	y	y	y	y	y	y
Position 5	20 cm	5.0	12.0	-42.5	13.0	12.0	-44.5	n/a	0.5	5.0	10.0	1.0	9.0	7.0	-32.0	-37.0	2.0
	Switch	y	y	y	y	y	y	n/a ***	y	y	y	y	y	y	y	y	y
Position 6	25 cm	1.0	10.0	0 *	14.0	12.5	-21.0	-25.0	0.5	15.5	10.0	40.0	10.5	13.0	26.0	10.0	0.5
	Switch	y	y	y	y	y †	y †	y	y	n	y	n	y	y †	y †	y †	y
Position 7	30 cm	5.0	18.0	-31.0	22.0	18.0	-21.0	-48.5	0.5	9.0	17.0	42.0	14.0	12.0	-18.0	-22.0	3.0
	Switch	y	y	y	y	y	y	y	y	y	y	n	y	y	y	y	y
Position 8	35 cm	10.0	21.0	28.0	23.0	2.0	-42.0	-6.0	0.5	10.0	22.0	42.0	10.0	13.0	-16.0	-22.0	2.0
	Switch	y	y	y	y	y	y	y	y	y	y	n	y	y	y	y	y
Position 9	40 cm	7.0	11.0	-22.0	39.0	12.0	-40.0	0.5	0.0	18.0	20.0	42.0	14.0	4.0	-9.0	-6.0	3.0
	Switch	y	y	y	n	y	y	y	y	y	y	n	y	y	y	y	y
Position 10	45 cm	10.0	-14.5	-15.5	45.0	3.0	-7.0	-44.5	n/a	21.0	28.0	40.0	6.0	20.0	-6.0	7.0	n/a
	Switch	y	y	y	n/a	y	y	y	n/a ***	y	y	n	y	y	y	y	n/a ***
Position 11	50 cm	18.0	-2.0	-2.0	34.0	8.5	-5.0	0.5	0.5	18.0	39.5	39.0	28.0	-1.0	-4.0	-2.0	0.5
	Switch	y	y	y	y	y	y	y	y	n **	y	n	y	y	y	y	y
Position 12	55 cm	20.0	1.0	5.0	46.0	6.0	4.0	3.0	4.0	28.0	35.0	41.0	0.0	8.0	4.0	11.0	5.0
	Switch	n	y	n	n	y	y	y	y	y	y	n	y	y	y	y	y
Position 13	60 cm	25.0	4.0	4.0	7.0	7.0	9.0	4.0	11.0	28.0	37.0	43.0	5.0	12.0	9.0	15.0	9.0
	Switch	n	y	n	y	y	y	y	y	y	y	n	y	y	y	n	y
Position 14	65 cm	25.0	7.0	8.0	10.0	8.0	5.0	5.0	18.0	38.0	7.0	41.0	5.0	14.0	17.0	15.0	5.0
	Switch	n	y	n	y	y	y	y	y	y	y	n	y	y	y	n	y
Position 15	70 cm	27.0	10.0	3.0	11.0	10.0	6.0	3.0	19.0	45.0	11.0	41.0	7.0	17.0	7.0	20.0	6.0
	Switch	n	y	n	y	y	y	y	y	n	y	n	y	y	y	n	y
Position 16	75 cm	20.0	10.0	6.0	13.0	11.5	7.0	2.0	27.0	43.0	12.0	33.0	14.0	18.5	9.0	26.0	13.0
	Switch	n	y	n	y	y	y	y	y †	n	y	n	y	y	y	y	y
Position 17	80 cm	27.0	15.0	11.0	18.0	14.0	9.0	5.0	29.0	42.0	18.0	42.0	12.0	21.0	11.0	25.0	11.0
	Switch	n	y	n	y	y	y	y	y	n	y	n	y	y	y	n	y
Position 18	85 cm	26.0	18.0	7.0	21.0	15.0	10.0	6.0	31.0	45.0	23.0	42.0	18.0	25.0	15.0	35.0	12.0
	Switch	n	y	n	y	y	y	y	y	n	y	n	y	y	y	n	y
Position 19	90 cm	30.0	22.0	11.0	25.0	18.0	11.0	7.0	45.0	43.0	23.0	41.0	17.0	26.0	17.0	36.0	18.0
	Switch	n	y	n	y	y	y	y	y	n	y	n	y	y	y	n	y
Position 20	95 cm	26.0	23.0	10.0	27.0	18.0	11.0	5.0	41.0	45.0	29.0	40.0	18.0	30.0	19.0	35.0	20.0
	Switch	n	y	n	y	y	y	n	y	n	y	n	y	y	y	n	y
Position 21	100 cm	12.5	11.0	7.0	27.0	18.0	16.0	7.0	24.0	43.0	32.0	41.0	23.0	38.5	18.0	36.0	18.5
	Switch	n	y	n	y	n	y	n	y	n	y	n	y	n	y	n	y
Position 22	At ∞	22.0	21.0	7.5	45.0	22.0	21.0	7.5	45.0	45.0	44.0	42.0	31.0	45.0	44.0	42.0	31.0

Notes: Rocks used: Rock#2 Bin#2 - stationary rock; Rock#4 Bin#2 movable rock
Tag was always facing north (0˚); tag was not parallel to the axis of measurement
All distances are in cm.
Switch values:

y = Signal switched from movable rock to stationary rock
n = Signal did not switch from movable rock to stationary rock
* = The back of the antenna hoop was directly over the tag tip at the first detection signal from stationary rock
** = Very tight range for stationary rock; no signal for a movable rock
*** = No signal for stationary rock; consistent signal for movable rock
† = Very tight range for stationary rock; dominant signal is for the movable rock
†† = No reading at all!!
††† = On the second trial: no signal for stationary rock and consistent signal for movable rock

Table C9 Cluster Experiment Results for Dry Lateral Detection with Tracers at 90° axis

		HH-0°	HH-45°	HH-90°	HH-xyz	HV-0°	HV-45°	HV-90°	HV-xyz	VH-0°	VH-45°	VH-90°	VH-xyz	VV-0°	VV-45°	VV-90°	VV-xyz
Position 1	0 cm	16.0	18.0	2.0	2.0	0.5	0.5	0.5	n/a ***	37.0	38.0	40.0	11.0	0.5	43.0	35.0	n/a ††
	Switch	n	n	n	y	y	y	y	n/a	n	n	n	y	y	n **	n **	n/a
Position 2	5 cm	-8.0	-4.0	0.0	-0.5	5.0	5.0	n/a	42.0	45.0	43.0	40.0	0.0	0.0	5.0	3.0	5.0
	Switch	y	y	y	y *	y	y	n ***	n	n	n	n	y	y	y	y	y
Position 3	10 cm	3.0	-2.0	4.0	0.0	3.0	6.0	-54.0	40.0	43.0	44.0	41.0	2.0	2.0	10.0	8.0	16.0
	Switch	n	y	y	y	y	y	y	n	n	n	n	y	y	y	y	n
Position 4	15 cm	7.0	-0.5	-4.0	0.0	5.0	6.0	-37.0	39.0	40.0	44.0	40.0	3.0	8.0	12.0	-37.0	-0.5
	Switch	n	y	y	y	y	y	y	n	n	n	n	y	n	y	y	y *
Position 5	20 cm	17.0	-1.0	2.0	-0.5	6.0	6.0	-48.0	40.0	43.0	42.0	25.0	3.0	15.0	11.0	-2.5	0.0
	Switch	n	y	y	y *	y	y	y	n	n	n	y	y	n	y	y	y
Position 6	25 cm	12.0	2.0	-26.0	4.0	13.0	16.0	0 †	n/a	41.0	41.0	42.0	0.5	8.0	19.0	-22.0	-0.5
	Switch	n	y	y	y	n	y †††	n/a	n/a ^	n	y †††	n	y	n	y †††	y	y
Position 7	30 cm	21.0	2.0	1.0	1.0	13.0	5.0	-22.0	36.0	45.0	0.0	22.0	0.0	40.0	16.0	2.0	n/a ***
	Switch	n	y	y	y	y	y	y	n	n	y	y	y	n	y	y	n
Position 8	35 cm	20.0	4.0	3.0	4.0	16.0	4.0	-17.0	40.0	44.0	2.0	27.0	0.0	34.0	11.0	-17.0	3.0
	Switch	n	y	y	y	y	y	y	n	n	y	y	y	n	y	y	y
Position 9	40 cm	20.0	4.0	10.0	7.0	15.0	4.0	-12.0	39.0	45.0	12.0	16.0	4.0	42.0	15.0	-12.0	15.0
	Switch	n	y	y	y	y	y	y	n	n	y	y	y	n	n	y	n
Position 10	45 cm	24.0	12.0	10.0	13.0	18.0	9.0	-7.0	41.0	43.0	38.0	21.0	8.0	45.0	8.0	-6.0	8.0
	Switch	n	y	y	y	n	y	y	n	n	n	y	y	n	y	y	y
Position 11	50 cm	16.0	4.0	-10.0	9.0	16.0	4.0	0.5	14.0	4.0	34.0	17.5	12.0	40.0	5.0	2.0	15.0
	Switch	n	y	y	y	n	y	y	y	n	n	y	y	n	y	y	y
Position 12	55 cm	17.0	13.0	17.0	15.0	20.0	11.0	-14.0	40.0	40.0	13.0	18.0	9.0	40.0	12.0	4.0	7.0
	Switch	n	y	y	n	n	y	y	n	n	y	y	y	n	n	y	n
Position 13	60 cm	17.0	12.0	17.0	22.0	18.0	10.0	-1.0	40.0	39.0	25.0	14.0	11.0	42.0	17.0	9.0	9.0
	Switch	n	n	y	n	n	y	y	n	n	y	y	y	n	y	y	y
Position 14	65 cm	17.0	16.0	7.0	24.0	15.0	9.0	0.0	37.0	42.0	43.0	40.0	16.0	41.0	22.0	5.0	11.0
	Switch	n	n	y	n	n	y	y	n	n	n	y	y	n	y	y	y
Position 15	70 cm	25.0	21.0	2.0	33.0	17.0	12.0	1.0	42.0	42.0	43.0	18.0	15.0	40.0	26.0	10.0	11.0
	Switch	n	n	y	n	n	y	y	n	n	n	y	n	n	y	y	y
Position 16	75 cm	20.0	14.0	5.0	27.0	16.0	10.0	0.5	24.0	39.0	42.0	18.0	24.0	38.0	17.0	7.0	12.0
	Switch	n	y	y	y	n	y	y	n	n	n	y	y	n	y	y	n
Position 17	80 cm	23.0	22.0	5.0	42.0	24.0	17.0	0.0	42.0	40.0	43.0	28.0	15.0	41.0	32.0	12.0	12.0
	Switch	n	n	y	n	n	n	y	n	n	n	y	n	n	n	y	y
Position 18	85 cm	24.0	22.0	10.0	38.0	23.0	22.0	0.0	42.0	40.0	39.0	34.0	18.0	40.0	37.0	15.0	14.0
	Switch	n	n	y	n	n	n	y	n	n	n	y	n	n	n	y	n
Position 19	90 cm	24.0	23.0	9.0	39.0	25.0	21.0	6.0	39.0	38.0	40.0	30.0	14.0	40.0	35.0	16.0	13.0
	Switch	n	n	y	n	n	n	y	n	n	n	y	n	n	n	y	n
Position 20	95 cm	28.0	24.0	3.0	38.0	23.0	20.0	3.0	39.0	-12.0	42.0	39.0	17.0	40.0	41.0	19.0	16.0
	Switch	n	n	y	n	n	n	y	n	n	n	y	n	n	n	y	n
Position 21	100 cm	19.0	14.0	1.0	26.0	17.0	11.0	6.5	24.0	44.0	46.0	43.0	31.0	37.0	36.0	18.0	24.0
	Switch	n	n	y	n	n	n	y	n	n	n	y	n	n	n	y	n
Position 22	At ∞	22.0	21.0	7.5	45.0	22.0	21.0	7.5	45.0	45.0	44.0	42.0	31.0	45.0	44.0	42.0	31.0

Notes: Rocks used: Rock#2 Bin#2 - stationary rock; Rock#4 Bin#2 movable rock

Tag was always facing north (0˚); tag was not parallel to the axis of measurement

All distances are in cm.

Switch values:

y = Signal switched from movable rock to stationary rock

n = Signal did not switch from movable rock to stationary rock

* = Detected stationary rock signal on the other side of the vertical rock face of the stationary rock

** = Very tight range for stationary rock; no signal for a movable rock

*** = No signal for stationary rock; consistent signal for movable rock

† = The back of the antenna hoop was directly over the tag tip at the first detection signal from stationary rock

†† = No reading at all!!

††† = tight detection interval for stationary rock; movable rock emits signals for a few tight intervals north and south of the stationary rock's signal

^ = no detection of stationary rock. Movable rock detected but stops being detected at +2 cm from stationary rock

Table C10	Burial Test Results (3" depth) Horizontal Tests												
Experiment A		Dry Lateral Detection (cm)											
		1	2	3	4	5	6	7	8	9	10	11	12
	Rock 1	37.5	31.5	6.5	37.0	36.0	-1.0	51.0	14.5	22.4	35.7	38.9	26.7
	Rock 2	39.5	32.0	22.5	43.5	33.5	30.2	50.0	56.5	60.0	44.0	34.7	33.9
Bin 1	Rock 3	38.2	35.0	23.5	39.0	39.2	28.0	24.0	19.5	13.0	31.2	36.6	33.0
	Rock 4	36.5	25.0	13.5	39.5	26.0	14.0	18.5	11.0	-3.0	33.0	33.5	18.4
	Rock 5	37.0	34.0	16.5	34.0	34.0	16.5	21.5	19.0	9.0	30.4	33.9	27.7
	Rock 6	13.5	28.5	28.0	10.0	23.5	23.0	10.0	15.0	15.0	28.2	22.5	28.6
	Rock 1	34.5	30.0	10.5	36.0	31.5	27.0	20.0	16.5	3.0	30.4	35.7	33.0
	Rock 2	32.5	31.0	15.0	35.0	34.5	12.0	54.5	58.0	37.0	31.2	37.6	31.2
Bin 2	Rock 3	45.0	36.0	8.0	37.0	31.0	7.0	25.0	21.0	14.0	44.0	44.9	31.2
	Rock 4	39.0	41.0	31.0	37.0	39.0	31.0	21.0	20.0	21.0	29.5	38.5	57.6
	Rock 5	32.0	32.0	16.0	34.0	33.5	10.0	20.0	16.5	5.0	32.1	33.0	26.0
	Rock 6	35.0	32.0	20.0	37.0	38.0	17.5	21.5	50.0	15.0	35.3	35.7	31.2
	Rock 1	38.0	20.0	28.0	47.0	7.0	35.0	69.0	7.0	23.0	42.2	32.1	12.9
	Rock 2	42.0	40.0	-1.0	51.5	44.0	2.0	84.0	77.0	8.0	40.3	43.1	33.0
Bin 3	Rock 3	48.0	46.0	32.0	55.0	51.0	9.0	28.0	28.0	29.0	49.6	46.8	44.0
	Rock 4	45.0	44.5	32.0	54.0	47.0	13.0	27.0	22.5	17.0	44.0	47.7	44.9
	Rock 5	48.0	47.0	40.0	49.0	48.0	38.0	28.0	24.0	27.0	36.6	45.9	44.9
	Rock 6	46.0	40.0	18.0	48.0	41.0	19.0	68.0	21.0	9.0	43.1	44.0	29.5
	Rock 1	50.5	47.0	11.0	52.0	46.0	33.5	28.0	30.0	36.0	50.1	49.1	38.9
	Rock 2	46.0	45.5	5.5	50.5	42.5	30.0	76.0	68.0	10.0	48.7	45.9	41.7
Bin 4	Rock 3	41.5	33.0	15.0	49.5	38.5	14.0	87.5	77.0	41.0	33.0	33.5	22.5
	Rock 4	36.5	33.5	11.5	40.5	38.5	25.0	86.5	79.0	55.0	32.6	35.7	26.8
	Rock 5	50.0	42.5	3.0	48.0	37.0	30.5	86.0	60.5	23.0	42.2	41.2	25.5
	Rock 6	45.0	43.0	1.0	57.0	42.0	9.0	76.0	71.0	25.0	40.3	43.5	40.3
	Rock 1	25.0	24.0	41.0	29.0	30.0	49.0	89.0	75.0	66.0	14.5	25.5	22.5
	Rock 2	38.0	32.0	21.0	42.5	32.0	25.0	82.0	60.0	29.0	36.6	38.5	26.8
Bin 5	Rock 3	40.0	39.0	23.0	36.0	36.0	14.0	80.0	67.0	42.0	33.0	33.9	18.4
	Rock 4	41.0	26.0	24.0	39.5	28.0	29.5	84.0	54.0	25.0	39.4	33.9	21.7
	Rock 5	23.0	16.0	39.0	23.0	18.0	45.0	82.0	73.0	55.0	12.2	20.9	29.5
	Rock 6	38.0	34.0	23.0	44.0	32.0	26.0	83.0	50.0	25.0	35.7	36.6	22.5
	Rock 1	50.0	38.0	19.0	47.0	37.0	12.0	69.0	19.5	6.0	46.8	38.5	31.2
	Rock 2	42.0	35.0	15.0	38.0	30.0	23.0	70.0	54.0	30.0	33.0	33.0	28.6
Bin 6	Rock 3	32.0	28.0	2.0	39.0	22.0	36.0	85.0	66.0	42.0	29.5	30.4	21.7
	Rock 4	43.0	37.0	25.0	41.0	36.0	4.0	65.0	50.0	9.0	35.7	39.4	33.0
	Rock 5	46.0	37.0	7.5	46.0	42.0	12.0	62.0	18.0	9.0	40.3	37.6	33.0
	Rock 6	44.0	32.0	6.0	43.4	34.0	24.0	75.0	47.0	13.0	38.5	36.6	23.4

Table C11 Burial Test Results (3" depth) Vertical Tests

Experiment B		Dry Lateral Detection (cm)											
		1	2	3	4	5	6	7	8	9	10	11	12
Bin 1	Rock 1	35.0	33.0	32.0	32.0	35.0	33.5	47.5	36.5	39.0	28.6	30.4	31.7
	Rock 2	40.5	35.0	33.0	39.0	31.0	30.0	45.0	33.0	39.5	30.8	30.8	32.6
	Rock 3	10.5	6.5	28.0	16.0	8.0	29.5	51.5	40.0	36.5	9.4	7.4	6.5
	Rock 4	34.0	33.0	30.5	32.5	33.0	30.5	40.0	33.0	33.5	33.9	31.2	31.2
	Rock 5	41.5	36.0	33.0	38.0	36.5	28.5	42.0	33.0	36.0	33.9	31.2	31.2
	Rock 6	25.0	30.0	35.5	10.5	28.0	36.5	53.0	38.5	34.5	6.8	20.5	33.9
Bin 2	Rock 1	39.0	36.0	36.0	29.5	22.0	29.5	44.0	34.0	38.5	33.9	33.9	33.9
	Rock 2	36.0	34.5	32.0	32.5	8.0	29.0	49.5	38.0	32.0	36.6	31.2	30.4
	Rock 3	31.0	34.0	35.0	33.5	29.0	34.0	48.0	32.0	30.5	6.8	27.7	33.0
	Rock 4	36.0	33.0	35.0	27.0	29.0	35.0	42.5	32.0	31.5	5.6	12.6	28.6
	Rock 5	35.0	35.0	34.5	33.0	35.0	34.0	51.0	39.0	38.0	16.8	6.2	34.4
	Rock 6	37.5	33.5	36.0	10.0	32.0	36.0	48.0	40.0	37.0	5.6	4.8	29.9
Bin 3	Rock 1	48.0	48.0	39.5	47.0	42.0	45.5	60.5	42.0	43.0	43.5	41.7	42.6
	Rock 2	51.0	51.0	35.5	48.0	40.5	36.0	63.0	46.0	48.5	53.9	47.7	40.3
	Rock 3	49.0	49.0	46.0	43.5	35.0	44.0	59.5	41.0	44.0	42.2	39.4	38.9
	Rock 4	52.0	52.0	44.0	49.5	43.0	46.0	58.0	48.0	49.0	50.6	48.7	46.8
	Rock 5	55.0	55.0	49.0	46.0	45.0	9.0	64.0	48.5	48.0	51.5	53.4	49.6
	Rock 6	50.0	50.0	39.0	47.5	36.0	13.5	49.0	43.0	49.0	45.9	44.9	38.0
Bin 4	Rock 1	52.5	52.5	53.5	53.5	51.5	47.5	56.0	54.0	54.5	49.6	50.6	49.6
	Rock 2	48.5	52.0	53.0	50.5	48.0	53.5	63.5	58.0	59.0	48.2	46.8	46.8
	Rock 3	43.0	44.5	52.0	44.0	44.0	54.0	70.0	56.0	48.0	41.2	35.7	47.3
	Rock 4	41.5	47.0	53.0	40.0	45.0	55.0	64.0	54.0	51.0	32.1	40.8	52.0
	Rock 5	53.5	52.0	51.0	52.0	51.0	53.5	61.0	54.0	55.5	48.2	51.5	50.6
	Rock 6	42.5	42.5	43.0	37.0	40.0	46.0	68.0	58.0	53.0	43.1	35.7	38.9
	Rock 1	51.0	48.0	52.0	48.0	47.0	49.0	62.5	56.0	58.0	47.7	44.9	47.7
	Rock 2	52.0	49.0	50.0	55.0	44.5	46.0	59.5	50.0	55.0	55.3	49.6	49.1

Bin 5	Rock 3	47.0	42.0	43.0	43.0	40.0	46.5	71.0	64.0	57.0	44.5	36.2	44.0
	Rock 4	52.0	52.0	56.5	54.0	52.0	58.0	66.0	56.0	59.0	52.0	52.0	54.3
	Rock 5	57.0	52.5	55.5	52.0	52.5	51.5	70.0	63.5	61.0	55.7	50.1	50.6
	Rock 6	54.0	55.5	61.5	52.5	56.0	60.5	63.0	57.0	59.0	52.0	55.3	57.6
Bin 6	Rock 1	49.5	49.0	53.0	48.5	49.0	50.0	58.0	58.0	58.0	47.3	49.1	51.0
	Rock 2	56.5	57.0	65.0	56.5	58.0	66.0	69.0	68.0	69.0	54.3	58.6	60.0
	Rock 3	51.0	50.5	55.0	52.0	48.5	55.5	49.0	68.0	80.0	46.8	49.6	51.5
	Rock 4	58.0	58.5	60.0	57.0	58.0	60.0	60.0	59.0	64.0	56.2	61.0	61.9
	Rock 5	55.0	55.0	56.0	54.0	67.0	58.5	57.0	55.5	61.0	51.5	52.4	52.9
	Rock 6	63.0	60.0	59.5	62.5	58.0	57.0	68.0	64.0	64.0	57.2	61.0	60.5

Table C12 Burial Test Results (3" depth) Other Horizontal and Vertical Tests

Experiment C,D		Dry Lateral Detection (cm)						
		C				D		
		1	2	3	4	1	2	3
Bin 1	Rock 1	18	29	37	0.5	46	0.5	13
	Rock 2	45	38.5	40.5	20	46.5	13	20
	Rock 3	36	37	43	12.5	48.5	8	27
	Rock 4	19.5	26	37.5	11.5	22	20.5	21
	Rock 5	33	33	41.5	15.5	24	27.5	33
	Rock 6	42.5	30.5	34.5	19	38	13.5	11.5
Bin 2	Rock 1	38	31	39	0.5	43	22	23
	Rock 2	21.5	29	40	1	46	10.5	6
	Rock 3	20	28	40	0.5	24	12	14.5
	Rock 4	27	34	40	18.5	45	15	5
	Rock 5	45	37	48	0.5	46.5	11	12
	Rock 6	23	31	40.5	9.5	43	9	7.5
Bin 3	Rock 1	32	0	44	39	54.5	15.5	13
	Rock 2	34	39	57.5	19	53	11	11.5
	Rock 3	35	31	52	23	51.5	13	23.5
	Rock 4	29	39	55	0	59	15.5	20
	Rock 5	39	43	53	3.5	60	10	14
	Rock 6	40	40.5	55	10	57.5	17	21
Bin 4	Rock 1	42	34.5	50	26.5	71.5	40.5	41
	Rock 2	45.5	39	55.5	19.5	61.5	22	24.5
	Rock 3	37.5	43	52	12.5	40	46.5	52
	Rock 4	44	56	57	42	53	36	20.5
	Rock 5	20.5	54	53	12	59.5	36	34
	Rock 6	40.5	49.5	56.5	14.5	66	19.5	12
Bin 5	Rock 1	31	47	53	26	69	17	30
	Rock 2	26	44	55	7	65.5	30.5	34
	Rock 3	53.5	48	57.5	24	67.5	10.5	28.5
	Rock 4	36.5	27.5	48.5	28	64	32	20
	Rock 5	29.5	43	55	20	61.5	5.5	14
	Rock 6	10	35	51.5	13	66.5	45.5	40
Bin 6	Rock 1	20	48.5	57	5	63	31	29
	Rock 2	32	50	53.5	12	76.5	31	36
	Rock 3	53	51	51.5	23	77	52.5	43
	Rock 4	36.5	56	56	43	72	30	36
	Rock 5	14	52	56.5	29	73.5	28	35
	Rock 6	33.5	53	57	18	82	22.5	43

Table C13 Burial Test Results (6" depth) Horizontal Tests

		Dry Lateral Detection (cm)						
		A1	A2	A3	A10	A11	A12	C2
Bin 1	Rock 1	34.0	30.0	-2.0	33.0	30.4	26.4	34.0
	Rock 2	37.0	33.0	-3.0	30.4	34.4	27.3	39.0
	Rock 3	35.0	33.0	13.0	29.5	33.0	29.0	38.0
	Rock 4	32.5	24.0	23.0	31.2	28.6	14.1	20.0
	Rock 5	38.0	33.0	19.0	30.8	34.8	33.5	40.0
	Rock 6	39.0	30.0	23.0	37.6	37.1	16.8	16.0
Bin 2	Rock 1	39.0	36.0	-13.0	30.4	35.7	33.9	41.0
	Rock 2	32.0	33.0	-11.0	30.4	31.2	22.5	34.0
	Rock 3	41.0	36.0	3.0	35.7	35.7	32.6	36.0
	Rock 4	38.0	40.0	19.0	36.6	36.6	26.8	38.0
	Rock 5	39.0	29.5	22.0	37.6	33.0	10.8	16.5
	Rock 6	39.0	31.0	-6.5	33.9	33.5	20.9	35.0
Bin 3	Rock 1	45.0	8.5	43.0	44.9	34.8	10.8	11.0
	Rock 2	51.5	43.0	11.0	41.7	43.1	32.1	48.0
	Rock 3	52.0	37.0	19.0	48.7	46.8	26.8	39.0
	Rock 4	55.5	54.0	7.0	47.7	53.4	39.4	53.5
	Rock 5	56.0	47.0	0.5	49.6	50.6	35.7	47.0
	Rock 6	40.0	35.0	5.0	34.4	38.5	29.5	46.5
Bin 4	Rock 1	50.5	46.0	15.5	49.6	49.6	29.5	42.0
	Rock 2	5.5	38.0	43.5	34.8	8.1	39.4	45.5
	Rock 3	40.5	26.0	27.0	35.7	32.1	19.2	30.5
	Rock 4	53.5	49.0	31.0	45.9	47.7	36.6	48.0
	Rock 5	52.5	41.0	17.0	47.7	46.3	27.7	39.5
	Rock 6	5.0	48.5	20.5	44.9	45.9	33.9	49.0

Table C14 Burial Test Results (6" depth) Vertical Tests

		Dry Lateral Detection (cm)						
		B1	B2	B3	B10	B11	B12	D2
Bin 1	Rock 1	39.5	39.0	32.0	37.1	36.6	34.8	18.0
	Rock 2	43.0	39.0	37.0	39.4	38.9	39.9	6.0
	Rock 3	37.0	32.0	43.5	25.1	31.2	41.7	17.0
	Rock 4	29.0	26.0	12.0	32.6	28.6	11.1	20.0
	Rock 5	27.0	36.0	40.0	14.1	27.3	37.6	2.0
	Rock 6	33.0	31.0	8.0	35.3	30.8	26.4	8.0
Bin 2	Rock 1	41.0	37.0	33.0	44.9	35.7	35.3	30.0
	Rock 2	40.0	40.5	37.0	40.3	39.4	35.7	2.5
	Rock 3	37.0	34.0	4.0	38.5	33.0	41.2	18.0
	Rock 4	15.5	36.5	37.0	31.2	34.8	35.7	17.5
	Rock 5	35.0	35.5	26.0	40.8	33.0	34.8	14.5
	Rock 6	37.0	35.0	37.0	39.4	34.4	38.5	5.0
Bin 3	Rock 1	57.5	51.0	48.5	57.6	54.3	48.7	24.0
	Rock 2	60.0	56.0	54.0	54.3	57.2	54.3	15.0
	Rock 3	51.0	50.5	54.5	53.4	49.6	50.1	15.0
	Rock 4	44.0	50.5	56.0	44.9	48.2	48.7	20.0
	Rock 5	57.0	53.0	55.5	53.4	55.3	53.4	12.0
	Rock 6	57.0	57.0	54.0	54.8	60.0	55.7	5.5
Bin 4	Rock 1	50.5	48.0	50.5	50.6	47.7	48.2	4.0
	Rock 2	62.0	63.0	57.0	57.2	62.9	58.1	22.5
	Rock 3	60.5	55.0	51.5	58.1	57.2	52.4	2.0
	Rock 4	54.0	56.0	57.5	54.3	54.8	55.3	4.0
	Rock 5	54.0	42.0	44.0	59.1	52.0	51.5	24.0
	Rock 6	57.0	60.5	60.5	52.4	57.6	60.0	12.0

Table C15 Burial Test Results (12" depth) Horizontal Tests

		Dry Lateral Detection (cm)						
		A1	A2	A3	A10	A11	A12	C2
Bin 1	Rock 1	43.0	18.5	-9.5	56.2	35.7	20.0	17.0
	Rock 2	40.0	31.0	n/a	19.2	35.7	23.8	26.0
	Rock 3	36.0	34.5	10.0	0.7	36.6	27.7	32.0
	Rock 4	32.0	20.5	3.0	20.0	26.8	7.4	7.0
	Rock 5	35.0	30.0	n/a	31.2	35.7	19.2	21.0
	Rock 6	35.0	25.0	n/a	34.8	31.2	13.7	12.0
Bin 2	Rock 1	39.0	33.0	-14.0	30.4	36.2	24.2	20.0
	Rock 2	36.0	33.0	n/a	31.2	38.5	23.0	22.5
	Rock 3	39.0	34.0	1.5	36.6	40.3	21.3	15.0
	Rock 4	37.0	34.0	n/a	32.1	35.7	23.4	24.5
	Rock 5	36.0	27.0	n/a	30.8	35.3	21.7	20.0
	Rock 6	38.0	24.0	n/a	36.6	35.7	17.6	20.0
Bin 3	Rock 1	45.0	33.0	21.5	47.7	44.0	21.3	33.0
	Rock 2	46.0	39.0	3.0	41.7	44.0	30.8	39.0
	Rock 3	50.0	49.0	-19.0	36.2	50.1	36.6	41.0
	Rock 4	48.0	48.0	4.0	41.2	48.2	34.8	48.0
	Rock 5	55.0	46.0	2.5	52.4	51.5	35.7	36.0
	Rock 6	49.0	44.5	0.0	35.7	46.8	34.8	43.0
Bin 4	Rock 1	47.0	30.0	27.5	45.4	39.4	24.7	34.0
	Rock 2	48.5	44.0	-25.0	41.2	45.9	29.9	40.0
	Rock 3	49.0	41.0	-17.0	48.7	45.9	29.5	37.0
	Rock 4	40.0	44.0	33.0	23.4	42.6	40.8	44.0
	Rock 5	54.0	40.0	24.0	49.6	49.6	21.7	20.0
	Rock 6	50.0	50.0	3.0	39.9	49.6	39.4	43.0

Table C16 Burial Test Results (12" depth) Vertical Tests

		Dry Lateral Detection (cm)						
		B1	B2	B3	B10	B11	B12	D2
Bin 1	Rock 1	18.0	16.5	14.0	5.6	12.2	13.7	18.0
	Rock 2	11.0	9.0	11.0	6.2	5.6	5.1	14.0
	Rock 3	9.0	9.5	11.0	6.2	6.8	8.1	10.5
	Rock 4	10.0	13.0	15.0	0.7	6.2	11.1	16.0
	Rock 5	4.0	3.0	10.0	5.1	1.9	2.2	4.0
	Rock 6	5.0	15.0	11.0	12.2	13.7	12.6	18.0
Bin 2	Rock 1	17.0	17.0	12.0	15.2	16.0	14.1	21.0
	Rock 2	17.5	18.0	14.0	11.5	16.0	16.8	24.0
	Rock 3	20.5	19.5	12.0	10.8	16.4	18.8	24.0
	Rock 4	21.5	20.0	12.0	11.8	17.6	16.8	25.0
	Rock 5	13.0	15.0	14.0	6.8	9.4	11.5	20.0
	Rock 6	14.5	10.5	8.0	14.5	12.9	10.4	14.0
Bin 3	Rock 1	21.0	21.0	17.5	13.7	19.2	19.2	33.0
	Rock 2	15.0	16.0	18.0	46.8	51.5	14.1	26.0
	Rock 3	23.0	23.0	18.0	14.5	21.7	22.1	34.0
	Rock 4	12.5	15.0	15.0	9.4	10.4	14.5	25.0
	Rock 5	23.0	24.0	20.5	10.8	20.0	24.7	38.0
	Rock 6	20.0	17.5	13.5	16.8	17.6	15.2	28.5
Bin 4	Rock 1	13.5	13.0	15.0	10.8	10.8	14.5	25.0
	Rock 2	14.0	15.0	15.5	35.7	38.5	14.1	30.0
	Rock 3	16.0	19.0	23.0	4.0	10.8	20.0	34.0
	Rock 4	15.0	14.0	13.0	13.7	13.3	11.5	21.0
	Rock 5	45.0	41.0	23.0	49.1	46.8	5.6	10.0
	Rock 6	21.0	20.0	17.0	15.2	20.0	18.0	32.0

Table C17 Burial Test Results (18" depth) Horizontal Tests

		Dry Lateral Detection (cm)						
		A1	A2	A3	A10	A11	A12	C2
Bin 1	Rock 1	32.0	24.5	n/a	n/a	32.1	10.4	11.0
	Rock 2	27.0	24.0	n/a	n/a	29.5	14.5	11.0
	Rock 3	23.0	25.0	7.0	n/a	23.8	18.4	18.0
	Rock 4	16.0	n/a	n/a	19.2	12.2	n/a	n/a
	Rock 5	27.0	27.0	n/a	n/a	21.7	19.2	14.0
	Rock 6	n/a	25.0	8.0	1.2	n/a	26.0	7.0
Bin 2	Rock 1	29.0	9.0	n/a	15.6	27.7	6.8	n/a
	Rock 2	30.0	16.0	n/a	n/a	29.9	6.8	n/a
	Rock 3	31.0	-41.0	n/a	n/a	26.0	n/a	n/a
	Rock 4	28.0	-32.0	n/a	n/a	26.0	n/a	n/a
	Rock 5	31.0	15.0	n/a	26.0	26.0	10.4	10.0
	Rock 6	29.0	27.0	n/a	n/a	32.1	14.8	6.0
Bin 3	Rock 1	41.0	n/a	29.0	50.1	30.8	2.6	n/a
	Rock 2	49.5	37.5	n/a	49.1	44.0	17.6	12.0
	Rock 3	43.0	20.0	n/a	45.4	36.2	10.4	5.0
	Rock 4	53.0	40.0	n/a	47.7	51.5	16.8	13.5
	Rock 5	55.0	41.5	n/a	39.9	49.6	16.0	16.0
	Rock 6	52.0	41.0	n/a	49.6	50.6	25.5	24.5
Bin 4	Rock 1	48.0	37.0	7.0	50.6	38.5	16.4	n/a
	Rock 2	47.0	33.0	-2.0	51.0	37.1	14.8	n/a
	Rock 3	47.0	35.0	n/a	48.7	41.2	17.6	18.5
	Rock 4	55.5	43.0	-10.0	51.0	53.9	21.7	17.0
	Rock 5	51.0	24.0	-10.0	49.1	44.0	10.4	n/a
	Rock 6	49.5	43.0	n/a	44.9	49.1	23.0	23.0

Table C18 Burial Test Results (18" depth) Vertical Tests

		Dry Lateral Detection (cm)						
		B1	B2	B3	B10	B11	B12	D2
Bin 1	Rock 1	14.0	18.0	14.0	n/a	9.0	14.8	18.0
	Rock 2	13.0	11.0	7.0	8.7	10.8	11.5	14.0
	Rock 3	14.0	16.0	10.0	2.0	11.1	12.2	15.0
	Rock 4	7.0	14.0	12.0	n/a	8.1	15.2	14.0
	Rock 5	7.0	5.0	4.0	8.7	3.5	3.5	5.0
	Rock 6	5.0	0.0	-1.0	9.0	3.1	0.3	0.0
Bin 2	Rock 1	13.0	11.5	7.0	8.1	10.8	10.1	11.0
	Rock 2	18.5	17.0	11.0	5.1	15.2	12.9	15.0
	Rock 3	14.0	12.0	12.0	2.6	8.7	10.8	13.0
	Rock 4	12.0	10.0	8.0	5.1	6.2	7.4	11.0
	Rock 5	17.0	16.0	10.0	5.1	12.2	15.2	16.0
	Rock 6	15.0	18.0	15.0	2.6	13.7	15.2	17.0
Bin 3	Rock 1	11.0	19.0	25.0	2.6	10.1	19.2	25.0
	Rock 2	18.0	14.0	11.0	16.0	14.5	12.2	18.0
	Rock 3	20.5	17.0	10.5	22.5	20.0	12.9	15.5
	Rock 4	17.0	16.0	16.0	14.1	15.6	14.1	19.0
	Rock 5	22.0	19.0	14.0	19.2	18.4	12.9	19.0
	Rock 6	10.0	10.0	13.0	9.4	6.8	8.1	13.0
Bin 4	Rock 1	16.0	18.0	19.0	11.5	14.8	14.1	20.0
	Rock 2	17.0	17.0	17.0	12.2	12.6	13.7	18.0
	Rock 3	17.5	20.0	20.0	11.5	16.8	18.0	23.0
	Rock 4	30.0	33.0	22.0	13.7	27.7	26.8	34.0
	Rock 5	18.0	15.0	10.0	16.8	17.2	11.1	16.0
	Rock 6	17.0	20.0	22.0	9.4	13.7	18.4	25.0

Table C19 Saturation Test Results (At Surface) Horizontal Tests

		Lateral Detection (cm)						
		A1	A2	A3	A10	A11	A12	C2
Bin 1	Rock 1	25.0	23.0	2.5	25.5	24.2	20.9	37.0
	Rock 2	19.0	17.5	12.0	16.4	20.0	17.6	40.5
	Rock 3	26.5	20.0	10.0	21.3	18.8	22.1	41.5
	Rock 4	20.0	14.0	14.5	24.2	22.5	15.2	30.5
	Rock 5	22.0	20.5	17.0	23.4	20.5	17.2	40.5
	Rock 6	25.0	24.0	11.0	23.4	23.8	22.5	40.0
Bin 2	Rock 1	28.0	25.0	7.5	26.8	24.7	24.2	39.0
	Rock 2	25.5	25.0	12.0	22.1	25.1	24.2	44.5
	Rock 3	31.0	29.0	17.5	26.0	27.7	27.3	42.5
	Rock 4	30.0	24.0	12.0	27.7	28.6	24.2	40.5
	Rock 5	23.5	20.0	17.5	18.8	18.8	14.5	36.5
	Rock 6	29.0	26.5	16.5	26.0	26.8	25.1	42.0
Bin 3	Rock 1	29.5	15.5	26.5	33.9	26.0	15.2	34.5
	Rock 2	31.5	30.0	12.5	26.4	29.5	28.2	51.0
	Rock 3	27.0	20.0	25.0	32.6	27.7	18.4	36.0
	Rock 4	34.0	31.5	17.0	33.0	34.4	31.2	48.5
	Rock 5	36.5	37.0	24.5	36.2	37.6	37.6	50.5
	Rock 6	23.5	21.5	25.5	15.2	20.0	20.0	53.5
Bin 4	Rock 1	42.0	43.0	37.0	35.7	13.3	37.6	60.0
	Rock 2	32.5	30.0	9.0	30.4	35.3	30.4	53.0
	Rock 3	27.5	20.5	23.5	26.4	26.8	21.3	50.5
	Rock 4	30.5	31.0	20.0	28.2	32.1	35.7	57.5
	Rock 5	36.0	30.5	15.0	38.9	32.6	27.7	51.0
	Rock 6	35.5	31.0	10.0	29.5	32.1	28.2	53.0

Table C20 Saturation Test Results (At Surface) Vertical Tests

		Lateral Detection (cm)						
		B1	B2	B3	B10	B11	B12	D2
Bin 1	Rock 1	38.0	39.0	44.5	41.2	37.1	45.4	20.5
	Rock 2	39.5	40.0	44.0	42.2	41.2	45.9	27.0
	Rock 3	40.0	39.5	46.0	38.5	36.6	44.0	28.0
	Rock 4	35.0	35.5	40.0	40.8	37.6	40.8	25.0
	Rock 5	41.5	40.5	46.0	40.8	39.4	44.9	28.0
	Rock 6	37.5	39.5	44.5	44.0	38.0	44.9	25.5
Bin 2	Rock 1	42.5	42.5	45.0	43.1	38.9	44.9	28.5
	Rock 2	39.0	40.0	47.5	41.2	39.9	44.5	29.0
	Rock 3	38.0	41.5	44.0	41.2	39.4	43.5	15.0
	Rock 4	36.0	36.0	42.5	39.4	47.7	43.1	11.0
	Rock 5	42.0	40.5	44.5	44.9	40.3	44.5	16.0
	Rock 6	43.0	43.5	46.0	43.1	41.7	44.0	25.0
Bin 3	Rock 1	38.5	25.0	39.5	49.1	40.3	39.4	42.0
	Rock 2	52.0	53.0	59.0	56.2	53.4	59.1	23.0
	Rock 3	54.0	52.0	59.0	57.6	53.9	58.1	10.5
	Rock 4	54.0	53.0	61.5	59.1	56.2	61.9	29.0
	Rock 5	52.0	51.0	60.0	57.6	54.3	56.7	19.5
	Rock 6	54.0	54.0	59.5	55.7	51.0	60.5	27.0
Bin 4	Rock 1	55.0	56.0	61.5	58.6	55.3	62.4	22.5
	Rock 2	55.0	54.0	62.5	58.6	53.4	63.4	20.5
	Rock 3	56.5	54.0	61.5	58.6	53.4	61.0	25.5
	Rock 4	55.0	56.5	62.0	57.6	54.3	60.0	27.5
	Rock 5	53.5	51.0	59.5	56.7	54.8	60.5	12.5
	Rock 6	58.5	55.5	60.0	62.9	57.2	59.1	15.0

Table C21 Saturation Test Results (6" depth) Horizontal Tests

		Lateral Detection (cm)						
		A1	A2	A3	A10	A11	A12	C2
Bin 3	Rock 1	39.0	20.0	31.0	43.1	38.5	14.1	7.5
	Rock 2	40.0	30.0	1.0	38.9	37.6	31.2	33.5
	Rock 3	40.5	30.0	27.0	42.6	38.9	26.4	25.0
	Rock 4	45.5	42.0	23.0	42.2	46.3	39.9	41.0
	Rock 5	45.0	33.0	13.0	44.0	40.3	33.0	32.0
	Rock 6	35.0	35.0	25.0	26.8	32.6	36.2	35.0
Bin 4	Rock 1	43.0	38.0	4.0	42.6	40.3	31.2	51.0
	Rock 2	44.0	34.0	9.0	44.9	40.8	29.5	40.5
	Rock 3	40.0	28.0	29.0	33.9	33.0	17.6	40.0
	Rock 4	39.0	34.0	9.0	33.5	36.6	26.8	47.0
	Rock 5	47.0	42.0	28.0	44.5	47.3	32.1	28.0
	Rock 6	40.5	39.5	14.5	33.5	37.6	33.9	52.0

Table C22 Saturation Test Results (6" depth) Vertical Tests

		Lateral Detection (cm)						
		B1	B2	B3	B10	B11	B12	D2
Bin 3	Rock 1	41.0	43.0	46.0	43.1	44.9	45.4	5.5
	Rock 2	52.0	47.0	47.0	49.6	54.3	48.7	15.0
	Rock 3	15.0	36.0	47.0	13.3	13.7	41.2	26.5
	Rock 4	45.0	49.0	50.0	50.6	48.7	48.7	16.0
	Rock 5	43.0	32.0	43.0	44.0	39.9	35.3	20.0
	Rock 6	45.5	45.0	49.0	49.1	46.8	43.1	10.0
Bin 4	Rock 1	58.0	58.0	62.0	58.1	60.0	59.1	36.0
	Rock 2	47.0	52.0	55.5	52.4	54.3	55.3	40.5
	Rock 3	58.0	55.0	47.0	59.1	58.1	55.3	32.0
	Rock 4	5.0	60.0	54.0	50.6	54.3	60.0	20.0
	Rock 5	46.0	46.0	52.0	52.0	52.9	56.2	42.0
	Rock 6	55.0	61.0	62.5	53.4	59.1	58.6	25.0

Table C23 Saturation Test Results (12" depth) Horizontal Tests

		Lateral Detection (cm)						
		A1	A2	A3	A10	A11	A12	C2
Bin 3	Rock 1	50.0	25.0	36.5	49.6	43.1	11.8	17.0
	Rock 2	51.0	45.0	n/a	43.1	48.2	31.7	31.5
	Rock 3	53.0	47.0	-25.5	49.6	51.5	35.7	35.0
	Rock 4	48.0	42.0	17.0	35.7	45.4	35.3	33.0
	Rock 5	54.0	36.0	22.0	54.3	46.8	16.8	13.0
	Rock 6	53.0	42.0	n/a	49.6	47.7	27.3	31.0
Bin 4	Rock 1	55.0	50.5	-8.0	52.0	54.3	37.6	35.0
	Rock 2	58.5	44.0	11.0	55.3	52.4	25.5	25.0
	Rock 3	52.0	40.0	n/a	52.4	44.0	24.7	34.0
	Rock 4	56.0	43.0	55.0	51.0	55.3	29.5	23.0
	Rock 5	52.5	12.0	29.5	54.3	41.2	10.8	n/a
	Rock 6	47.5	43.0	17.5	36.6	44.5	36.6	42.5

Table C24 Saturation Test Results (12" depth) Vertical Tests

		Lateral Detection (cm)						
		B1	B2	B3	B10	B11	B12	D2
Bin 3	Rock 1	18.5	21.0	21.0	11.8	17.6	18.0	29.5
	Rock 2	30.5	30.0	19.5	22.5	28.6	21.7	34.0
	Rock 3	9.5	10.5	16.0	9.7	7.7	9.7	17.5
	Rock 4	19.0	20.0	18.0	16.0	16.4	17.6	26.0
	Rock 5	26.0	21.0	13.0	26.0	20.9	16.8	25.0
	Rock 6	11.0	9.5	12.0	11.1	8.7	7.7	14.0
Bin 4	Rock 1	18.0	14.0	10.0	18.8	17.2	12.9	21.0
	Rock 2	15.5	13.5	14.0	14.5	14.1	13.7	24.0
	Rock 3	17.0	16.0	14.0	16.8	15.6	13.7	26.0
	Rock 4	17.0	15.5	14.5	16.0	13.7	13.3	24.0
	Rock 5	11.5	14.5	21.5	8.1	10.8	14.1	24.0
	Rock 6	11.5	11.0	14.0	11.8	44.9	10.8	19.0

Table C25 Submergence Test Results (At Surface) Horizontal Tests

		Lateral Detection (cm)						
		A1	A2	A3	A10	A11	A12	C2
Bin 3	Rock 1	35.0	15.0	30.0	32.1	33.0	17.6	32.0
	Rock 2	39.0	39.0	14.0	31.2	33.9	26.4	53.0
	Rock 3	45.0	34.0	19.0	36.2	30.4	23.8	59.0
	Rock 4	39.5	37.0	24.0	34.8	31.2	26.0	55.0
	Rock 5	46.0	366.0	32.0	39.4	44.9	27.3	49.0
	Rock 6	20.0	17.5	28.5	23.0	39.4	25.1	58.5
Bin 4	Rock 1	38.0	36.0	20.5	35.7	25.1	21.7	47.0
	Rock 2	26.0	36.0	26.0	31.2	26.0	23.4	49.0
	Rock 3	37.0	30.0	13.0	25.1	22.1	21.7	55.0
	Rock 4	32.0	38.5	31.0	29.9	31.7	29.9	59.0
	Rock 5	24.5	24.0	14.5	34.4	26.4	19.6	19.5
	Rock 6	35.0	35.0	12.0	29.5	30.4	27.3	54.5

Table C26 Submergence Test Results (At Surface) Vertical Tests

		Lateral Detection (cm)						
		B1	B2	B3	B10	B11	B12	D2
Bin 3	Rock 1	55.0	55.0	55.0	58.1	52.4	53.9	27.0
	Rock 2	40.0	39.0	30.0	36.2	34.8	31.2	38.0
	Rock 3	57.0	58.0	46.0	53.4	53.9	50.1	45.5
	Rock 4	60.0	58.5	57.0	54.3	56.2	58.1	42.0
	Rock 5	58.0	59.0	50.0	53.9	53.9	51.5	32.0
	Rock 6	56.5	56.0	54.0	54.3	54.3	50.6	51.0
Bin 4	Rock 1	56.0	60.5	50.0	46.8	47.7	44.9	55.0
	Rock 2	61.0	57.0	55.0	61.0	55.3	54.3	32.0
	Rock 3	51.0	56.0	55.0	55.7	56.7	54.3	38.0
	Rock 4	59.0	59.0	57.0	58.1	57.6	52.9	44.5
	Rock 5	57.5	52.0	55.0	61.5	53.4	54.3	37.0
	Rock 6	57.5	60.0	52.0	53.4	58.6	48.2	45.0

Table C27 Submergence Test Results (6" depth) Horizontal Tests

		Lateral Detection (cm)						
		A1	A2	A3	A10	A11	A12	C2
Bin 3	Rock 1	42.0	35.0	25.0	40.3	35.3	21.7	25.5
	Rock 2	35.0	27.0	5.0	19.2	32.1	23.4	30.0
	Rock 3	40.0	39.0	22.0	33.0	36.2	28.6	36.5
	Rock 4	46.0	20.0	17.0	32.1	34.8	30.8	33.0
	Rock 5	44.0	42.0	10.0	30.4	34.8	29.5	33.0
	Rock 6	41.0	50.0	14.0	33.0	44.9	34.8	39.0
Bin 4	Rock 1	40.5	30.0	7.0	34.8	32.1	11.5	24.0
	Rock 2	46.0	40.0	30.0	35.3	35.7	27.7	34.0
	Rock 3	42.5	37.0	n/a	36.6	35.7	33.9	36.5
	Rock 4	41.0	40.0	19.0	43.1	45.4	34.8	33.0
	Rock 5	45.0	35.0	8.0	43.1	37.6	22.5	21.0
	Rock 6	49.0	34.0	10.0	44.9	39.4	21.3	33.5

Table C28 Submergence Test Results (6" depth) Vertical Tests

		Lateral Detection (cm)						
		B1	B2	B3	B10	B11	B12	D2
Bin 3	Rock 1	18.0	20.0	16.0	13.7	10.8	13.7	33.0
	Rock 2	32.0	31.0	24.0	1.9	18.0	28.6	46.0
	Rock 3	29.0	27.0	23.0	10.1	14.5	17.6	44.0
	Rock 4	18.0	19.0	45.0	5.6	17.6	39.4	32.0
	Rock 5	30.0	47.0	53.0	13.7	35.7	42.2	7.5
	Rock 6	20.0	16.0	45.0	35.7	27.7	34.8	17.0
Bin 4	Rock 1	20.0	32.0	46.0	35.7	24.2	32.1	30.0
	Rock 2	50.0	45.0	14.0	48.7	44.0	40.3	37.0
	Rock 3	45.0	22.0	18.5	39.4	37.6	13.7	32.0
	Rock 4	15.0	41.0	35.0	13.7	10.8	36.6	27.0
	Rock 5	44.0	34.5	24.0	49.1	44.9	22.5	37.5
	Rock 6	43.0	15.0	38.0	35.7	36.2	24.7	23.0

Table C29 Antenna Range Tests (23 mm tags)

	F		G		H		I	
Tag#	F1	F2	G1	G2	H1	H2	I1	I2
800001	-12	77.5	-23.5	68	12	-63.5	-14	73.5
800002	-21.5	71	-17	72	7	-55	-17	67.5
800003	-16.5	74	-19	70	10	-53.5	-14.5	68.5
800004	-22	77	-17	63	6.5	-57	-15	70
800005	-16.5	72.5	-15.5	68	0.5	-56.5	-16	70.5
800006	-12	80	-17	67.5	5.5	-61	-18.5	63
800007	-20.5	71	-14.5	73	3.5	-57.5	-18.5	68
800008	-20	72	-12	66	4	-58.5	-16	66
800009	-18.5	76	-16.5	71	5	-54.5	-16.5	67
800010	-17	77	-17	69	-1	-53	-18	65
800011	-16	71	-14	76.5	8	-63.5	-15	62
800012	-16	78	-9	73.5	5	-54	-19.5	64.5
800013	-20	74	-16	73	-1	-53	-17.5	62.5
800014	-16.5	70.5	-17	70.5	2.5	-63	-15	68
800015	-18	72	-8.5	73	9	-57	-18	63
800016	-20	73.5	-8	73	7.5	-53.5	-19	64
800017	-15.5	77	-11.5	77.5	2	-58	-17	68
800018	-19	76	-9.5	76	7	-60	-20	65
800019	-18	72.5	-12	72	7	-63	-17.5	68
800020	-17	72	-15	71	3	-54	-18	68
800021	-16	72.5	-13	70.5	5	-53	-17	65
800022	-13	75.5	-8	74.5	11	-68	-18	59
800023	-15	72.5	-10	71	7	-54	-18	63
800024	-12	73	-13	76.5	10	-65	-19	59
800025	-15	76	-14	69.5	10	-55	-14	63

Table C30 Antenna Range Tests (32 mm tags)

	F		G		H		I	
Tag#	F1	F2	G1	G2	H1	H2	I1	I2
900001	-22	78.5	-18	79	5	-57	-22	64
900002	-19	80	-17	79	22	-53	-19.5	62
900003	-23	73	-15.5	78.5	6	-53	-22	65
900004	-19	74	-14.5	74	1	-63	-26	62
900005	-22	74	-19	76.5	9	-52	-18	68
900006	-25	72	-16	74	4	-51.5	-20	61
900007	-23	76	-15	77.5	11	-63	-20	67.5
900008	-21	75	-12	75	-2	-55	-19	67
900009	-26	74.5	-15	73	3.5	-49.5	-16	71
900010	-21.5	75	-15	74	1	-65	-21	71
900011	-22	75	-14	77	1	-55	-23	60
900012	-19.5	74	-14	79	0.5	-54	-19	63.5
900013	-19.5	76.5	-17	73	6	-56	-16	77
900014	-21	81	-23.5	74	12	-67	-15	70.5
900015	-18.5	76.5	-13.5	72	-1	-56	-19	67
900016	-20	78	-12	78.5	4.5	-61	-23	68.5
900017	-23.5	71.5	-15	77	0.5	-60.5	-19	66.5
900018	-25	72	-18	76	2	-57	-24.5	72
900019	-21	75.5	-18.5	76	3.5	-62	-21	65
900020	-20	76	-15	75	5	-60	-21	64
900021	-20.5	75	-24	67	7.5	-61.5	-17	75
900022	-19	82.5	-18	75.5	5	-61	-17	69.5
900023	-24.5	77.5	-19	74	2	-67.5	-17	68
900024	-23.5	80	-15	72	-1	-56	-13.5	61
900025	-18	73.5	-20.5	71	3	-59	-16	67

Table C31 Skip Zones Test Results

Direction	Skip Intervals (cm) for North Copper Tag Orientation								Skip Intervals (cm) for South Copper Tag Orientation							
Turn	0°		90°		180°		270°		0°		90°		180°		270°	
Tag																
800001	-4.5	-7.5	-2.5	-5	-5	-7	-4	-7	-5	1.5	-0.5	-4	-5	1.5	-0.5	-4.5
	-2	6	1	8	-1	6	0.5	5	7	8.5	7.5	9.5	6	9	6	7.5
800002	0.5	-4.5	1	6	1	-4	-4.5	-7.5	-4.5	-6	-4	-6	-1	-6	-3.5	-5.5
	4.5	7.5	3.5	6.5	6	8.5	0.5	7.5	1.5	6.5	1	6.5	4	7.5	2	6.5
900001	-6	-4.5	-4	0.5	-3.5	1	-7	-5	-3.5	0.5	-2	1	-3.5	-1.5	-4	-0.5
	1.5	4.5	4	7.5	4	7	1.5	6.5	5	7	6.5	8	3	6	1	6.5
900002	-5	-2.5	-4	3	-4	2.5	-3.5	4	-0.5	2.5	-3.5	-2.5	0.5	2.5	-4.5	-4
	1.5	7.5	5	7.5	6	8.5	6	8	5.5	8	1.5	8	7	8.5	2.5	6

Axes of Reference for the results shown

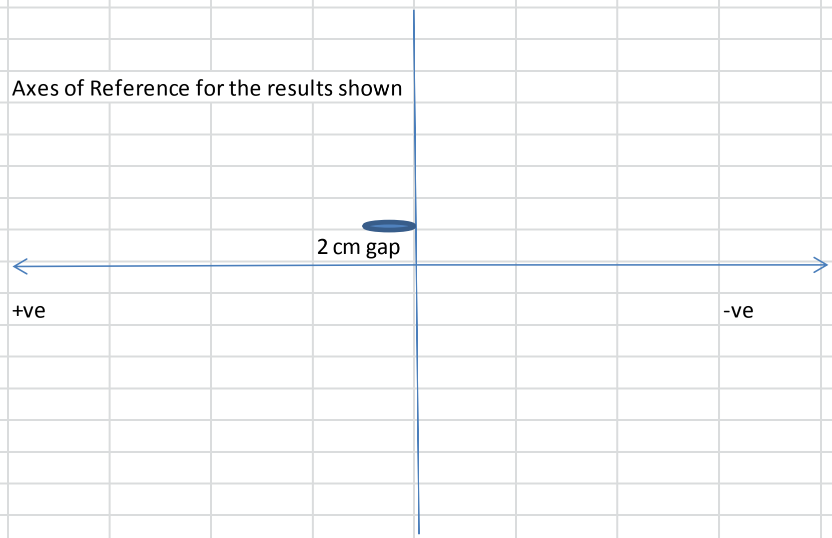

Legend

Table C32 Field Tests (Horizontal Tests) on the Surface of a Dry Point Bar of Laurel Creek

	Test	A1	A2	A3	A10	A11	A12	C2
Bin 2 (At surface)	Rock 1	30.5	27.5	16	23.8	31.2	23	49.5
	Rock 2	34	28	17.5	29	29	26.8	42.5
	Rock 3	34	31	26	30	32	28	45
	Rock 4	35	31	23	28	33	30	43
	Rock 5	24	16	18	21	22	15	36
	Rock 6	27	28.5	15	23	26.4	24	36
Bin 2 (Exposed)	Rock 1	11	4	9	5	7	8	44
	Rock 2	17	12	9	19	14	13	45
	Rock 3	15	21	17	16	16	21	46
	Rock 4	27	25	33	21	26	28	49.5
	Rock 5	12	9	12.5	5	7	9.4	41
	Rock 6	24	23	18.5	23	21	21.7	49
check--> Bin 3 (Exposed)	Rock 1	23	21	14	22	23	19	36
	Rock 2	10	15	21	21	20	21	54.5
	Rock 3	21	11	8	15	15	16	52.5
	Rock 4	17	26	26	15	19	25	49.5
	Rock 5	31	25.5	23	26	22.1	22	52
	Rock 6	27	22	7	22	18	21	56
Bin 4 (Exposed)	Rock 1	40.5	37	31.5	27.3	26	30.4	52.5
	Rock 2	11.5	8	4	10.1	8	8	48.5
	Rock 3	16	10.5	11	4	11.1	7	51
	Rock 4	30	28.5	23.5	25	28.6	27.3	65
	Rock 5	24	13.5	9.5	11	17.2	20.9	39.5
	Rock 6	20	14	8	11	13	5	54.5
Rod		66	75	45.5	58	44	33.9	157
Disc*		57	58	59	55	62	58	40
Wedge**		15.5	11.5	0.5	14.5	14.8	11.5	21

Notes

* lettering on top "TI"

** # inscribed on top; tag sitting on wooden ruler. Not on Aluminium. NO signal when on Aluminium

Saturation: On top of bar, Saturation = 0

Location: Bechtel Park, u/s of Site 4; point bar on right bank

Table C33 Field Tests (Vertical Tests) on the Surface of a Dry Point Bar of Laurel Creek

	Test	B1	B2	B3	B10	B11	B12	D2
Bin 2 (At surface)	Rock 1	43	41	42	40.3	41.2	42	31
	Rock 2	42	41	40	41	41	37.6	31
	Rock 3	41	40	40.5	38	38	43	31.5
	Rock 4	40.5	38	37	35	33	31	25
	Rock 5	36	37	29	38	34	36	18
	Rock 6	39	41	40	39	36.2	37	28
Bin 2 (Exposed)	Rock 1	41	41	39	40	40	37	35
	Rock 2	39	40.5	38	37	37	36	40.5
	Rock 3	40	39	37	38	41	39	28
	Rock 4	40.5	40	39.5	39	40	37	39.5
	Rock 5	41	40.5	40	40	42	42.2	29
	Rock 6	42	60	40	38	40	37.6	34
Bin 3 (Exposed)	Rock 1	47.5	51	50	41	50	50	40
	Rock 2	52	54	52.5	52	53	52	43.5
	Rock 3	50.5	51	51	48	48	49	43
	Rock 4	53	52.5	51.5	54	51	51	44.5
	Rock 5	52	51.5	51	51	50.6	53	43
	Rock 6	53.5	53	52	51	52	51	46
Bin 4 (Exposed)	Rock 1	53	54.5	56	49.6	54	54.8	39.5
	Rock 2	51	55	55	48.7	52	55	40.5
	Rock 3	53	53	54	51	49.6	51	47.5
	Rock 4	50	51.5	54	51	49.6	51.5	44.5
	Rock 5	56	55	53	55	54.8	51.5	41
	Rock 6	55	53	54	51	55	51	48.5
Rod		140	137	143	137	138	144.0	67
Disc		21	27	23	17	9	12	47
Wedge***		32	31.5	31.5	29.5	27.7	30.4	25.5

Notes:

*** On fat base; has groove on tag

Saturation: On top of bar, Saturation = 0

Location: Bechtel Park, u/s of Site 4; point bar on right bank

Table C34 Field Tests (Horizontal Tests) on the Edge of a Point Bar of Laurel Creek (under conditions of saturation)

	Test	A1	A2	A3	A10	A11	A12	C2
Bin 2 (At surface)	Rock 1	31.0	25.0	0.5	27.7	27.7	19.2	40.0
	Rock 2	37.0	24.5	15.0	24.2	28.6	21.7	37.0
	Rock 3	32.0	31.0	10.0	28.6	32.1	21.7	41.0
	Rock 4	28.0	25.0	19.0	20.5	26.8	23.8	42.0
	Rock 5	23.0	15.0	18.0	24.2	16.0	14.1	36.0
	Rock 6	24.0	25.0	13.5	24.2	30.4	16.0	35.0
Bin 2 (Exposed)	Rock 1	19.5	9.0	9.0	10.8	8.1	15.2	47.0
	Rock 2	18.0	13.0	14.0	14.5	14.5	20.0	34.0
	Rock 3	23.0	18.0	22.0	16.0	20.5	27.7	45.0
	Rock 4	19.0	25.0	20.0	20.9	26.8	30.4	44.0
	Rock 5	15.0	12.0	16.5	19.2	24.2	25.1	29.0
	Rock 6	25.0	12.0	3.0	22.5	13.7	11.5	46.0
Bin 3 (Exposed)	Rock 1	9.0	4.5	18.0	8.7	20.9	8.7	47.0
	Rock 2	28.0	26.0	3.5	18.8	27.7	17.6	51.0
	Rock 3	23.5	13.5	14.0	12.2	12.6	23.8	57.0
	Rock 4	37.0	39.0	26.0	32.1	38.5	35.7	54.0
	Rock 5	32.0	38.0	30.0	23.8	38.5	34.8	59.0
	Rock 6	29.0	11.0	8.0	24.2	11.5	13.7	55.0
Bin 4 (Exposed)	Rock 1	29.5	33.0	27.0	25.5	25.1	23.4	61.0
	Rock 2	17.5	15.5	6.0	17.6	8.1	22.5	61.0
	Rock 3	16.0	10.0	21.0	26.8	12.2	10.1	42.0
	Rock 4	30.0	24.0	31.0	14.5	18.4	29.9	44.0
	Rock 5	17.5	16.0	8.0	13.7	14.5	19.2	57.0
	Rock 6	12.0	9.0	13.0	12.2	23.0	21.3	58.5

Notes:

Saturation: At Water's Edge, Saturation = 1

Location: Bectel Park, u/s of Site 4; point bar on right bank

Table C35 Field Tests (Vertical Tests) on the Edge of a Point Bar of Laurel Creek (under conditions of saturation)

	Test	B1	B2	B3	B10	B11	B12	D2
Bin 2 (At surface)	Rock 1	34	40	35	35.7	43.1	36.6	34
	Rock 2	32	33	34	38.5	37.6	36.2	27
	Rock 3	39	35	34	38.0	41.2	40.8	25
	Rock 4	33	33.5	39	34.4	34.4	38.5	22
	Rock 5	41.5	39.5	39	39.4	41.2	38.9	28
	Rock 6	38	39	37	38.5	37.6	36.6	35
Bin 2 (Exposed)	Rock 1	41	41	40	39.9	40.3	41.2	35
	Rock 2	41	40	39.5	39.4	35.7	38.9	39
	Rock 3	40	39.5	40	39.4	39.9	40.8	32
	Rock 4	40	40	40	38.9	39.9	39.4	38
	Rock 5	42	40.5	41	38.9	38.5	35.7	37
	Rock 6	39	38	40	38.5	34.8	38.5	37
Bin 3 (Exposed)	Rock 1	49	49	49	48.7	52.4	54.3	34
	Rock 2	52	50.5	50	49.6	48.7	51.5	43
	Rock 3	51	52	53	50.6	52.4	50.6	36
	Rock 4	51	52	52.5	53.4	48.7	53.4	43
	Rock 5	51	50	50.5	50.6	49.1	52.0	41
	Rock 6	50.5	52	51	48.2	51.5	50.1	50
Bin 4 (Exposed)	Rock 1	53	54	52.5	53.4	52.4	51.5	44
	Rock 2	52.5	51	50.5	51.5	50.1	50.6	46
	Rock 3	52	52	53	50.6	52.4	52.9	42
	Rock 4	52	50.5	52	51.5	47.7	50.6	50
	Rock 5	53.5	50.5	50	50.6	51.5	48.7	48
	Rock 6	55	54	51	54.3	53.4	48.7	50.5

Table C36 Field Tests (Horizontal Tests) on the Centre of a Point Bar of Laurel Creek

	Test	A1	A2	A3	A10	A11	A12	C2
Bin 2 Depth: 12"	Rock 1 with backfill	33	34	8.5	27	37	27.3	24.5
	Rock 1	34	28.5	9	24	31.7	24	26.5
	Rock 2	33	33.5	-0.5	25	38.5	30.8	34
	Rock 3	32.2	31.5	-0.5	26.0	32.1	26.4	26.5
	Rock 4	32	37	26	0	34	34	27
	Rock 5	34	30.5	-3	22	31.2	21	25
	Rock 6	33	35	-1	21	38	30	23
Bin 2 Depth: 6"	Rock 1	40	33	-6	38	42	27	37
	Rock 2	30	29	9	26	30	25	37
	Rock 3	38.5	25	6	36.6	37	28	31.5
	Rock 4	35.5	37.5	23.5	27.7	35.7	35.7	42
	Rock 5	30.5	22	25	29.5	26	16	22
	Rock 6	36	38	11.5	29	37	33.9	39
Bin 2 Depth: 3"	Rock 1	36.5	31	3	29.5	30	28	39
	Rock 2	26	30	13	19	32	27	46
	Rock 3	35.5	31.5	17	32.6	39.4	30	40.5
	Rock 4	32	29	16	27	32	28	42
	Rock 5	20.5	15.5	17.5	24.2	19.2	15.6	32
	Rock 6	29.5	24	15.5	24.2	29	26.0	39.5

Notes:
· All tests were without backfill unless otherwise noted.
· Depth to water table = 27.5cm from top of bar
· For 12" test, approximately 4.5cm of water in bottom of hole

Table C37 Field Tests (Vertical Tests) on the Centre of a Point Bar of Laurel Creek

	Test	B1	B2	B3	B10	B11	B12	D2
	Rock 1	25	19	11	24	24	16	29.5
Bin 2	Rock 2	12.5	13.5	15	10.8	11.8	13	20
Depth: 12"	Rock 3	13.5	19	17	8.4	16	18	26.5
	Rock 4	17.5	18.5	14.5	15.6	15.2	16.8	22.5
	Rock 5	19	14.5	13	28	16.8	13	19.5
	Rock 6	13	14	14.5	11	11	11.5	19
	Rock 1	14	14.5	8	10	16.0	14	30.5
	Rock 2	31	36	27	36	9	31	10.5
Bin 2	Rock 3	7	10	27	4	8	12	13
Depth: 6"	Rock 4	12	7	35.5	15	12	30.4	13.5
	Rock 5	29	7	15	29	27	3	17
	Rock 6	11	11.5	34	11	11.8	11	23
	Rock 1	36	42	41	33	34	43	29
	Rock 2	35	37	36	33	31	33	3
Bin 2	Rock 3	30	30	32.5	31	23	23.8	16
Depth: 3"	Rock 4	36	43.5	44.5	31	41.7	45.9	11.5
	Rock 5	43	40	35	39	39	39	32.5
	Rock 6	39	36.5	35	37	37.6	36	12

Notes:

· All tests were without backfill unless otherwise noted.

· Depth to water table = 27.5cm from top of bar

· For 12" test, approximately 4.5cm of water in bottom of hole